



This is to certify that the

dissertation entitled

Mechanistic Studies and Inhibition of Dehydroquinase
Synthase and myo-Inositol 1-Phosphate Synthase

presented by

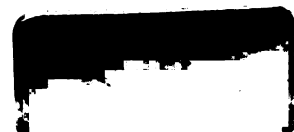
Jirong Peng

has been accepted towards fulfillment
of the requirements for

Ph.D. degree in Chemistry

Major professor

Date 9/27/86

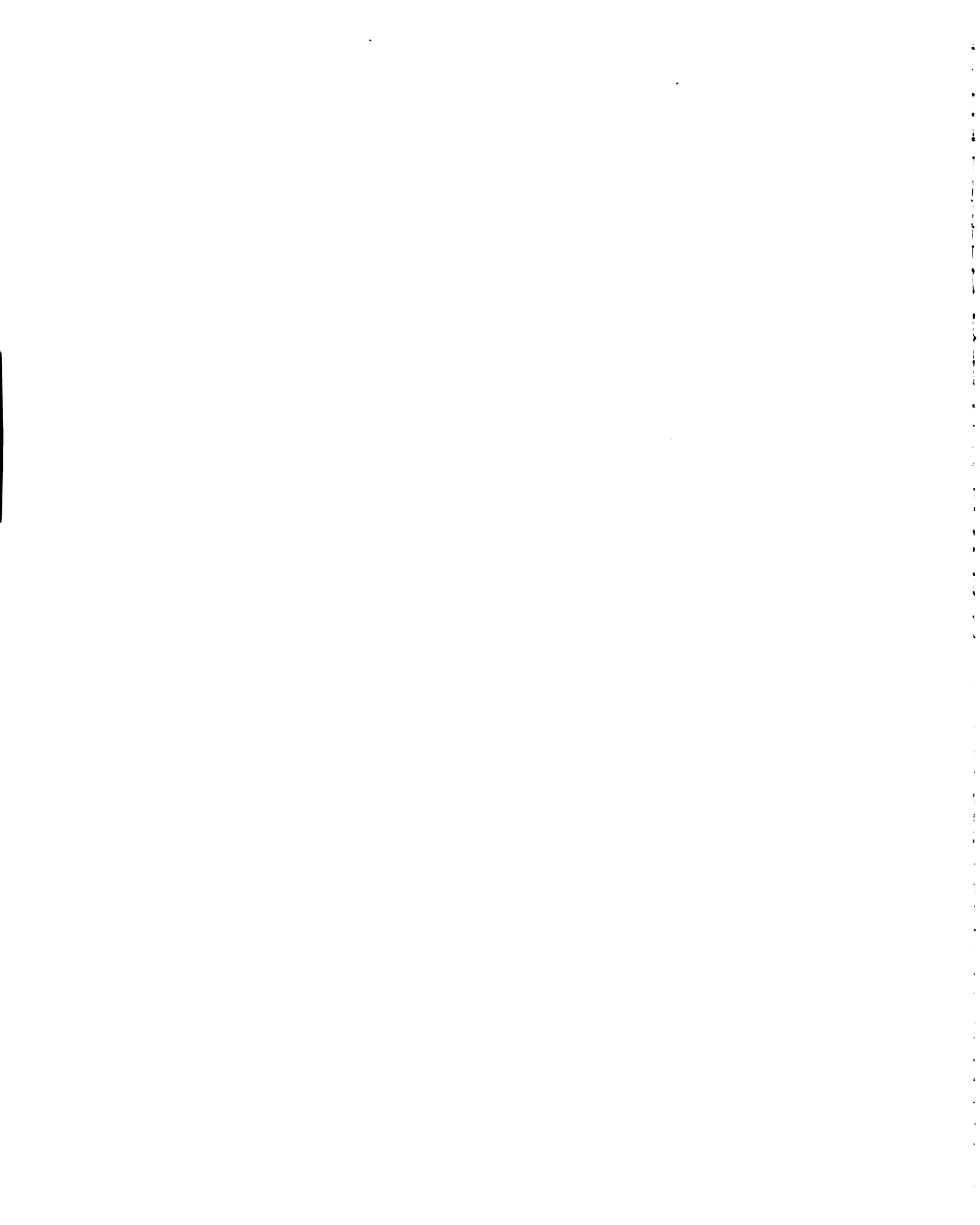


**PLACE IN RETURN BOX to remove this checkout from your record.
TO AVOID FINES return on or before date due.**

DATE DUE	DATE DUE	DATE DUE
OCT 16 2002	_____	_____
_____	_____	_____
_____	_____	_____
_____	_____	_____
_____	_____	_____
_____	_____	_____
_____	_____	_____

MSU is An Affirmative Action/Equal Opportunity Institution

ct/circ/datedue.pn3-p.1



**MECHANISTIC STUDIES AND INHIBITION OF DEHYDROQUINATE
SYNTHASE AND *myo*-INOSITOL 1-PHOSPHATE SYNTHASE**

by

Jirong Peng

A DISSERTATION

**Submitted to
Michigan State University
in partial fulfillment of the requirements
for the degree of**

DOCTOR OF PHILOSOPHY

Department of Chemistry

1996

ABSTRACT

MECHANISTIC STUDIES AND INHIBITION OF DEHYDROQUINATE SYNTHASE AND *myo*-INOSITOL 1-PHOSPHATE SYNTHASE

by

Jirong Peng

Both DHQ synthase and MIP synthase employ NAD as a catalyst rather than a cosubstrate. Challenging DHQ synthase with a series of carbocyclic substrate analogues possessing an inverted methine carbon relative to the same asymmetric center in substrate DAHP led to potent inhibition of DHQ synthase. The observed stereochemical and steric tolerance in active site binding is consistent with the hypothesis that the phosphate monoester of DAHP mediates its own elimination.

A series of substrate analogues, an actual reaction intermediate and its analogues were synthesized and examined for inhibition of MIP synthase. Isosteric homophosphonates were better inhibitors than nonisosteric phosphates. The α,α -gem-difluorohomo-phosphonates showed either weak or no inhibition. Removal of the C-3, C-4, or C-5 hydroxyl group resulted in weakened inhibition, while removal of the C-1 or C-2 functional group led to enhanced inhibition. Acyclic alditol analogues were consistently better inhibitors than predominantly cyclic aldose analogues. The actual oxidized reaction intermediate, 5-keto-D-glucose 6-phosphate, was a potent inhibitor of MIP synthase due to the formation of NAD-oxidized intermediate complex in the enzyme active site. Improved inhibition was obtained with intermediate analogues with pre-oxidized reaction centers.

Steady state NADH was detected by UV/vis spectroscopy during normal MIP synthase-catalyzed turnover. NADH formation was also observed when MIP synthase was incubated with substrate analogues. Inhibitory potency of the analogues correlated well with the rate of NADH formation, suggesting that the in situ generated reaction intermediates were responsible for the potent inhibition.

To my family

ACKNOWLEDGMENT

I would like to acknowledge my gratitude to many people who have made the completion of this dissertation possible. First and foremost, I am particularly appreciative of my advisor, Professor John Frost for his guidance, encouragement and support. His enthusiastic attitude toward science has deeply influenced me. My experience in his research lab means so much in my future career.

I would also like to acknowledge the support of my co-workers, the past and present members of Frost group, for their friendship, helpful discussion, and encouragement. They have created a pleasant atmosphere in which to work. I am grateful to Dr. Karen Frost for her kind and thoughtful help. I sincerely thank Dr. Jean-Luc Montchamp, who has provided me so much help, especially during the preparation of this manuscript. Feng Tian spent much time proofreading my poorly-spelled materials. Dr. Lars Piehler and Tim Ward taught me lab techniques with great patience during my early years in this group. Kai Li's sense of humor and friendly attitude brings more smiles on every one's face. Thanks are also due to my collaborators, Dr. Michael Hager, Dr. David Spear, and Dr. Marie Migaud, all of whom collaborated on the research projects.

Finally, I would like to thank my family, especially my parents, for their unlimited love and support. I am specially grateful to my wife, Xiumei, for her trust and understanding during all the years of my graduate career.

TABLE OF CONTENTS

LIST OF TABLES	vii
LIST OF FIGURES	viii
LIST OF ABBREVIATIONS.....	x
CHAPTER 1	
INTRODUCTION	1
Aromatic Amino Acid Biosynthesis and Herbicide Design.....	1
Mechanistic Aspects of DHQ Synthase.....	4
Cellular Signaling and Inositol 1,4,5-Trisphosphate Second Messenger.....	9
<i>myo</i> -Inositol 1-Phosphatase and Li ⁺ Inhibition.....	12
Mechanism of De novo Biosynthesis of <i>myo</i> -Inositol 1-Phosphate	14
Inhibition of MIP Synthase	17
CHAPTER 2	
<i>epi</i> -CARBOCYCLIC PHOSPHATE ANALOGUE AS A PROBE FOR THE MECHANISM OF SUBSTRATE MEDIATED <i>syn</i> -ELIMINATION.....	26
Design of the <i>epi</i> -Carbocyclic Phosphate Analogues	26
Synthetic Approaches to the <i>epi</i> -Carbaphosphate Analogues	28
Kinetic Evaluation.....	31
CHAPTER 3	
EXPLOITING THE ACTIVE SITE INTERACTIONS OF MIP SYNTHASE WITH SUBSTRATE ANALOGUES AND INTERMEDIATE ANALOGUES	42
Using Phosphonates as Phosphate analogues	42
Phosphonate and Homophosphonate Analogues of D-Glucose 6-Phosphate: Substrate Analogues Designed for the Inhibition of MIP Synthase	43
Syntheses of Phosphonate Analogues of D-Glucose 6-Phosphate	45
Enzymology Associated with the Phosphate and Homophosphonate Analogues	47
α,α - <i>gem</i> -Difluorohomophosphonate Analogues: An Attempt to Improve the Inhibition Properties	51
Synthesis of α,α - <i>gem</i> -Difluorohomophosphonate Analogues	53
Kinetic Evaluation of α,α - <i>gem</i> -Difluorohomophosphonate Analogues.....	54
The Deoxy Substrate Analogues: Probes for the Contribution of Individual Hydroxyl Groups to Active Site Binding.....	56
Synthetic Approaches to the Deoxy Substrate Analogues	57

Kinetic Evaluation of the Deoxy Substrate Analogues.....	62
Binding at the Enzyme active site: Cyclic vs. Acyclic.....	66
Intermediate B' and Analogues Possessing Oxidized Reaction Centers as Inhibitors	69
Synthesis of Intermediate B' and Some Analogues Possessing Oxidized Reaction Centers.....	70
Inhibition Studies of Intermediate B' and Analogues	75
Possessing An Oxidized Reaction Center	75
CHAPTER 4	
NADH FORMATION DURING MIP SYNTHASE-CATALYZED CONVERSION OF D-GLUCOSE 6-PHOSPHATE INTO <i>myo</i>-INOSITOL 1-PHOSPHATE.....	80
Determination of NADH Formation.....	80
Purification of MIP Synthase From <i>E. coli</i>	83
Detection of NADH Formation During MIP Synthase Catalysis	90
EXPERIMENTAL	96
General Information.....	96
General Chemistry	96
Reagents and Solvents.....	96
Chromatography.....	97
Spectroscopic and Physical Measurements.....	98
Assays	99
Synthetic Procedures.....	99
Enzymology.....	145
Enzyme Kinetics.....	147
BIBLIOGRAPHY.....	150

LIST OF TABLES

Table 1.	Phosphonate analogues used for probing the <i>syn</i> -elimination	8
Table 2.	Compounds tested for MIP synthase inhibition.....	18
Table 3.	Slow-binding inhibitors of DHQ synthase	34
Table 4.	Inhibition of DHQ synthase by <i>epi</i> -carbocyclic and carbocyclic reaction intermediate analogues	38
Table 5.	Inhibition of DHQ synthase by phosphonate and homophosphonate analogues	43
Table 6.	Phosphonate and homophosphonate substrate analogues of MIP synthase.....	44
Table 7.	Inhibition of MIP synthase by phosphonate and homophosphonate analogues	48
Table 8.	α,α - <i>gem</i> -difluorohomophosphonate analogues of D-glucose 6-phosphate	52
Table 9.	Deoxy substrate analogues	57
Table 10.	Compounds tested for formation of MIP synthase-bound NADH	64
Table 11.	Inhibition of MIP synthase by deoxy substrate analogues.....	65
Table 12.	Comparison of aldose analogues with alditol analogues.....	67
Table 13.	Intermediate B' and analogues possessing an oxidized reaction center.....	76
Table 14.	Purification of MIP synthase from <i>E. coli</i>	83
Table 15.	Inhibitors leading to the formation of enzyme-bound NADH.....	94

LIST OF FIGURES

Figure 1.	Shikimic acid pathway of aromatic acid biosynthesis	2
Figure 2.	Proposed mechanism of dehydroquinase synthase	5
Figure 3.	DHQ synthase-catalyzed <i>syn</i> -elimination of inorganic phosphate	6
Figure 4.	Non-enzymatic rearrangement of intermediate C to DHQ	7
Figure 5.	Phosphoinositol breakdown and resynthesis pathway	11
Figure 6.	Proposed mechanism of <i>myo</i> -inositol 1-phosphate synthase -catalyzed reaction.....	14
Figure 7.	Reaction intermediate analogues with an inverted C-5 chiral-center.....	27
Figure 8.	Synthesis of 5-[(phosphonoxy)methyl]-5-deoxyquinic acid 1	28
Figure 9.	Chahuua's synthesis of 3-(phosphonoxy)quinic acid 2	29
Figure 10.	Synthesis of 3-(phosphonoxy)quinic acid 2	30
Figure 11.	Competitive inhibition equilibria.....	31
Figure 12.	Progress curve for enzyme pre-incubated with a slow-binding inhibitor.....	35
Figure 13.	Progress curve in the presence of a slow-binding inhibitor	36
Figure 14.	Syntheses of intermediates 30 and 31	46
Figure 15.	Syntheses of phosphonate analogues	46
Figure 16.	Syntheses of difluorohomophosphonates	53
Figure 17.	Dahigard and Kaufmann's synthesis of 3-deoxy glucose 6-phosphate	58
Figure 18.	Szabo and Szabo's synthesis of 3-deoxy glucose 6-phosphate.....	58
Figure 19.	Synthesis of 3-deoxy glucose 6-phosphate.....	59
Figure 20.	Synthesis of 4-deoxy glucose 6-phosphate.....	60
Figure 21.	Synthesis of 5-deoxy glucose 6-phosphate.....	61

Figure 22.	Synthesis of D-erythritol 4-phosphate 50	62
Figure 23.	Barnett's synthesis of 5-keto-D-glucose 6-phosphate	71
Figure 24.	Kiely's synthesis of 5-keto-D-glucose 6-phosphate	72
Figure 25.	Synthesis of 5-keto-D-glucose 6-phosphate 70	73
Figure 26.	Synthesis of L-sorbose 1-phosphate 71	73
Figure 27.	Synthesis of 2-deoxy-L-sorbose 1-phosphate 72	74
Figure 28.	Syntheses of L-sorbose 1-(<i>E</i>)-vinylhomophosphonate 73 and L-sorbose 1-homophosphonate 74	75
Figure 29.	Interaction between enzyme, substrate, oxidized intermediate and product.....	77
Figure 30.	Redox reaction of NAD and NADH.....	80
Figure 31.	UV/vis spectra of NAD and NADH.....	81
Figure 32.	SDS-PAGE gel electrophoresis of MIP synthase preparations	84
Figure 33.	Enzymatic synthesis of D-glucose 6-phosphate	86
Figure 34.	¹³ C NMR time course of MIP synthase-catalyzed conversion of D-glucose 6-phosphate with 1 mM NAD	88
Figure 35.	¹³ C NMR time course of MIP synthase-catalyzed conversion of D-glucose 6-phosphate with 1 mM NAD in the presence of LDH and pyruvate.....	88
Figure 36.	¹³ C NMR time course of MIP synthase-catalyzed conversion of D-glucose 6-phosphate with 25 mM NAD in the presence of LDH and pyruvate.....	89
Figure 37.	Glucose 6-phosphate dehydrogenase activities, before and after Blue A affinity chromatography.....	90
Figure 38.	NADH formation during MIP synthase-catalyzed conversion of D-glucose 6-phosphate into <i>myo</i> -inositol 1-phosphate.....	91
Figure 39.	NADH formation during incubation of homophosphonate inhibitors with MIP synthase.....	92

LIST OF ABBREVIATIONS

Ac	acetyl
AIBN	2,2'-azobisisobutyronitrile
ADP	adenine diphosphate
ATP	adenine triphosphate
Bn	benzyl
BOM	benzyloxymethyl
Bu	butyl
Bz	benzoyl
CI	chemical ionization
DAHP	3-deoxy- <i>D-arabino</i> -heptulosonic acid 7-phosphate
DBU	1,8-diazabicyclo[5,4,0]undec-7-ene
DEAE	diethylaminoethyl
DHQ	3-dehydroquinate
DMF	<i>N,N</i> -dimethylformamide
DMSO	dimethyl sulfoxide
DTT	dithiothreitol
EI	electron impact
EPSP	5-enolpyruvylshikimate 3-phosphate
Et	ethyl
FAB	fast atom bombardment
h	hour
HPLC	high pressure liquid chromatography

HRMS	high resolution mass spectrometry
IPTG	isopropyl- β -D-thiogalactopyranoside
k	rate constant
<i>m</i> CPBA	<i>m</i> -chloroperbenzoic acid
Me	methyl
MIP	<i>myo</i> -inositol 1-phosphate
MOPS	4-morpholinepropanesulfonic acid
MS	mass spectrometry
min	minute
NAD	nicotinamide adenine dinucleotide, oxidized form
NADH	nicotinamide adenine dinucleotide, reduced form
NBS	<i>N</i> -bromosuccinimide
NMMO	<i>N</i> -methylmorpholine <i>N</i> -oxide
NMR	nuclear magnetic resonance
PEP	phosphoenolpyruvate
Ph	phenyl
PMSF	<i>p</i> -toluenesulfonyl fluoride
<i>i</i> Pr	isopropyl
pyr	pyridine
rt	room temperature
SDS PAGE	sodium dodecyl sulfate polyacrylamide gel electrophoresis
TBDMS	<i>t</i> -butyldimethylsilyl
TEAB	triethylamine bicarbonate
THF	tetrahydrofuran
TLC	thin layer chromatography
TMS	trimethylsilyl
TPAP	tetrapropylammonium perruthenate

Tr	triphenylmethyl
Ts	<i>p</i> -toluenesulfonyl
TSP	sodium 3-(trimethylsilyl)propionate-2,2,3,3-d ₄
Tf	trifluoromethanesulfonyl

CHAPTER 1

INTRODUCTION

Among the large group of pyridine nucleotide-dependent enzymes, there is a specific subgroup of enzymes employing NAD as a catalyst rather than as a cosubstrate.¹ During the complete turnover, there is no overall NAD reduction or NADH oxidation. NADH generated during the oxidation stage is oxidized back to NAD in the subsequent reduction step. Mechanistic studies reveal that these enzyme-catalyzed reactions share some common features. In order to cleave strong bonds which have no obvious chemical lability, the enzyme employs a pyridine nucleotide to transiently oxidize an alcohol group to the carbonyl concomitant with generation of NADH. The bond to be cleaved is then weakened by the carbonyl introduced at the nearby position. Upon completing the chemical transformation involving the weakened bond, the carbonyl group is then reduced back to alcohol by NADH. This subgroup of pyridine nucleotide-dependent enzymes catalyze such varied reactions as epimerization, the aldol reaction, cyclization, α,β -elimination, and decarboxylation. 3-Dehydroquinate synthase (DHQ synthase) and *myo*-inositol 1-phosphate synthase (MIP synthase) are two typical examples in this subgroup, and will be examined in detail in the following chapters.

Aromatic Amino Acid Biosynthesis and Herbicide Design

Aromatic amino acids and a range of primary and secondary metabolites in plants and microorganisms are biosynthesized from carbohydrates through the shikimic acid pathway.² The shikimic acid pathway is not found in animals but is essential to the metabolism of plants and microorganisms. Approximately 20% of the carbon fixed by

photosynthetic plants is processed via the shikimic acid pathway and converted to essential metabolic products which include aromatic amino acids, vitamins, lignins, alkaloids, and phenolics.

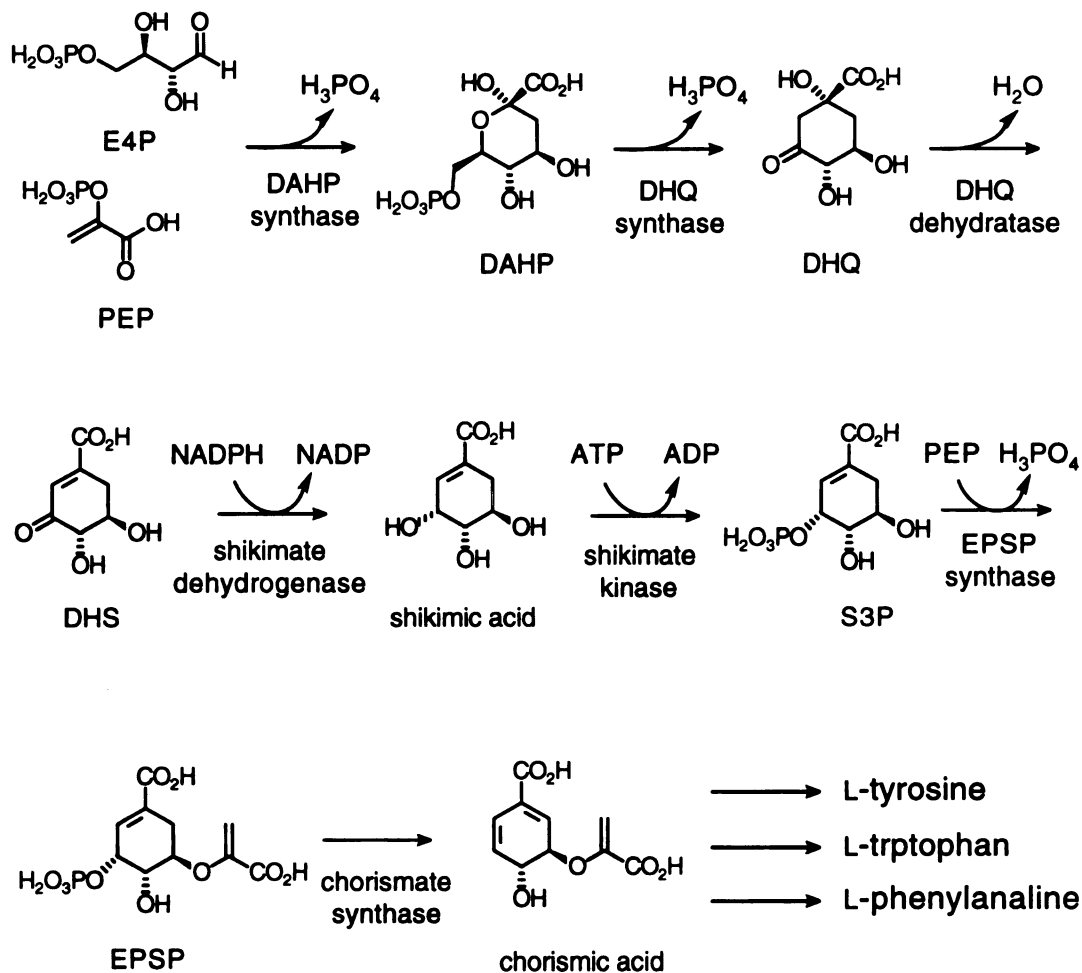


Figure 1. Shikimic acid pathway of aromatic acid biosynthesis.

There are seven enzymes involved in the pathway. The first enzyme, DAHP synthase, catalyzes the condensation of erythrose 4-phosphate (E4P) with phosphoenolpyruvate (PEP) to produce 3-deoxy-D-arabino-heptulosonic acid 7-phosphate (DAHP). The second enzyme, DHQ synthase, catalyzes the conversion of DAHP to 3-dehydroquinate (DHQ), which is the first carbocyclic metabolite in the biosynthesis of

aromatic compounds. DHQ is dehydrated by DHQ dehydratase to dehydroshikimate (DHS), which is then reduced by shikimate dehydrogenase to give shikimate. Shikimate kinase-catalyzed phosphorylation of shikimate with ATP leads to the formation of shikimate 3-phosphate (S3P). EPSP synthase catalyzes the condensation of S3P with PEP to produce 5-enolpyruvylshikimate 3-phosphate (EPSP), which then undergoes a chorismate synthase catalyzed 1,4-elimination of phosphate to give chorismate, which is the last common intermediate in the shikimic acid pathway.

Given the fact that the shikimic acid pathway is a critical route for plants to produce necessary metabolic products, a disruption to the pathway may result in significant herbicidal effects on plants. For this reason, herbicides that inhibit aromatic amino acid biosynthesis have been an attractive target for herbicidal studies to aim at.³ There may be numerous potential sites of herbicide action in this highly complex and normally well coordinated array of enzymes and processes. Because animals lack this pathway, targeting the pathway is potentially toxicologically safe for herbicide action. Glyphosate⁴ is an example of such a herbicide that blocks an enzymatic step of the shikimic acid pathway. Glyphosate is one of the most widely used herbicides and has very low mammalian toxicity. The herbicidal action of glyphosate is complex. Its primary site of action appears to be EPSP synthase. The inhibition of EPSP synthase consequently leads to deregulation of the shikimic acid pathway due to increased activity of DAHP synthase. Blockage and deregulation of the pathway cause an accumulation of very high levels of shikimate in the glyphosate-treated plants. The amount of shikimate that is phosphorylated by the deregulated pathway is an energy drain from other metabolic pathway. Uncontrolled flow of carbon into the shikimic acid pathway removes building blocks from other pathways, possibly disrupting other aspects of plant metabolism. Blockage and deregulation of the pathway also results in an accumulation of phenolics, which are toxic to plants.

DHQ synthase catalyzes the conversion⁵ of DAHP into DHQ and inorganic phosphate in the presence of both divalent metal (Co^{2+} or Zn^{2+}) and NAD. DHQ synthase is an appealing target for herbicide studies. DHQ synthase is located early in the pathway, and has only one substrate that is unique to the shikimic acid pathway. Effective inhibition of DHQ synthase would cut off the supplies for the whole pathway, thereby disrupting the biosynthesis of aromatic amino acid and related secondary metabolites and lead to herbicidal activity

Mechanistic Aspects of DHQ Synthase

DHQ synthase-catalyzed conversion of DAHP into DHQ begins from oxidation of the C-5 alcohol of DAHP to the carbonyl of intermediate A by enzyme-bound NAD. (Figure 2) Resulting acidification of the C-6 proton facilitates the β -elimination of inorganic phosphate to produce the enol ether B. The ketone group of C-5 is then reduced back to the alcohol of intermediate C by enzyme-bound NADH thereby regenerating NAD. Ring opening of intermediate C generates the enolate D, which then forms DHQ via an intramolecular aldol condensation.

DHQ synthase has been found to exhibit NAD and divalent metal dependency in all species in which it has been studied. Using homogeneous DHQ synthase purified from a over-producing strain⁶ of *E. coli*, Knowles found that the enzyme contains 1 equivalent of tightly bound Co^{2+} based on atomic absorption analysis.^{7a} Upon incubation with EDTA, the enzyme rapidly loses its activity to give an inactive apoenzyme. Activity of the apoenzyme is fully restored by addition of Co^{2+} and partially restored by Zn^{2+} . The enzyme also binds 1 equivalent of NAD with an apparent K_m of 80 nM. The presence of NAD is essential for catalytic activity of the enzyme.

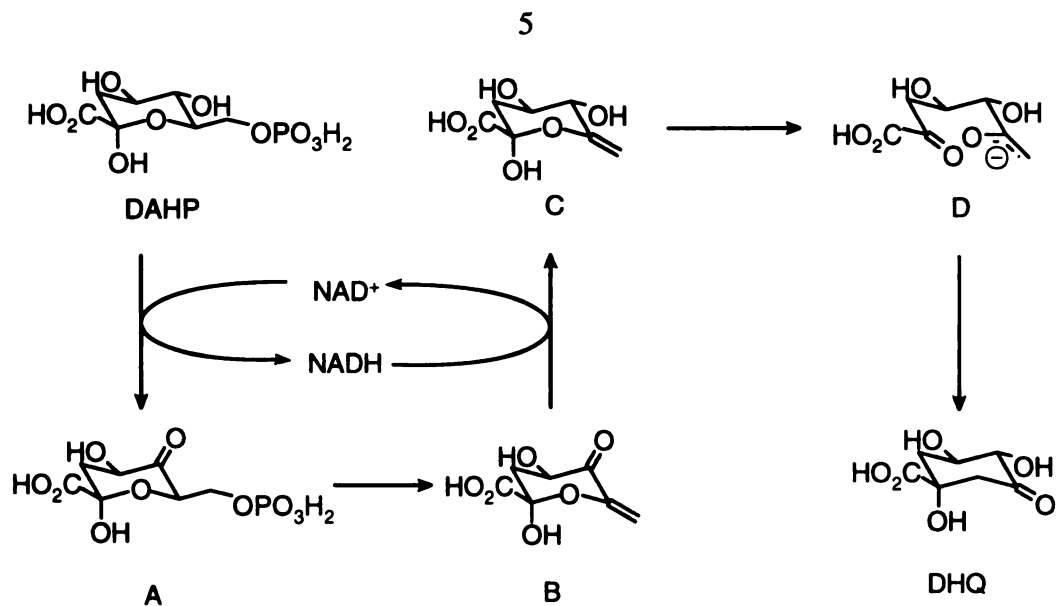


Figure 2. Proposed mechanism of dehydroquinase.

Rotenberg and Sprinson⁸ carried out a series of tracer experiments, in which, [4-³H], [5-³H] [6-³H], and [7-³H] DAHP were subjected to DHQ synthase-catalyzed conversion to DHQ. Analysis of resulting DHQ showed that tritium at the C-4, C-5, and C-7 position was conserved whereas tritium at the C-6 position was lost to the medium. A kinetic isotope effect k_H/k_T of 1.7 was observed at the C-5 position, consistent with a mechanism involving oxidation of the C-5 alcohol with NAD. A similar kinetic isotope effect k_H/k_T of 1.8 was also found at the C-6 position, owing to removal of a proton in elimination of phosphate. The reaction of [4-³H], and [7-³H] DAHP exhibited no kinetic isotope effect. Conservation of tritium at the C-7 position in the cyclization step of the reaction indicates that the enol formed in the phosphate elimination participates directly in an aldol condensation with the carbonyl at the C-2 position. The possible transient protonation of the enol intermediate to the methyl ketone during the rearrangement was ruled out. This conclusion is consistent with an observation in another experiment.⁹ Incubation of methyl ketone 3,7-dideoxy 6-ketoheptulosonic acid with DHQ synthase did not lead to the formation of DHQ. Sprinson also showed that a 5-dehydro-DAHP

intermediate is involved in the reaction with a trapping experiment.¹⁰ Reaction mixtures of DHQ synthase and DAHP were incubated for a short period of time and quenched with NaB^3H_4 . Degradation analysis of the resulting DAHP revealed that the tritium had been incorporated at the C-5 position. The amount of tritium found at the C-5 position corresponded to about 15% of the amount of enzyme present. This result was consistent with a 5-dehydro derivative of the substrate as an intermediate of the reaction.

Using a 2-deoxy substrate analogue, Knowles¹¹ investigated the stereochemical course of the postulated β -elimination of phosphate from the substrate. When the cyclic 2-deoxy substrate analogue 2,6-anhydro-DAHP, was incubated with the enzyme, inorganic phosphate and the enol ether are produced catalytically. The enol ether generated was released by the enzyme into solution. When the same reaction was carried out with the monodeuterated analogue, (7*S*)-[7-²H]-2,6-anhydro-DAHP, NMR analysis showed the product had deuterium in the *E* position. Thus it was established that DHQ synthase catalyzed the β -elimination of inorganic phosphate by a *syn* process. Since the overall reaction inverts the configuration at the C-7 position,⁸ consideration of steric effects and of minimal motion strongly favors the chairlike conformation, which can be easily reached by a rotation of only one bond. Further, the chairlike aldol transition state is the most reasonable in light of the preferred chair conformation of the final product DHQ.

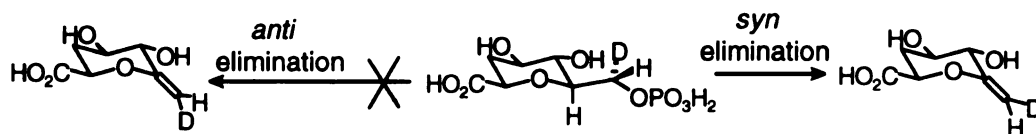


Figure 3. DHQ synthase-catalyzed *syn*-elimination of inorganic phosphate.

A model study by Bartlett and Satake^{12a} suggested that the conversion of enolpyranose, intermediate C (Figure 4), into product DHQ was nonenzymatic. When intermediate C was generated by photolysis of the C-2 O-nitrobenzyl ketal of intermediate

C in the absence of enzyme, examination of the products revealed complete conversion to DHQ rather than formation of intermediate C. Investigation with deuterated material showed the spontaneous rearrangement of intermediate C to DHQ was identical stereochemically with the biosynthetic transformation. Subsequent careful reexamination^{12b,c} of the product mixture did reveal the formation of 2-4% *epi*-DHQ. This result suggests that the enzyme is more than just a spectator during the intramolecular aldol condensation. At least, it serves as a template during the rearrangement.

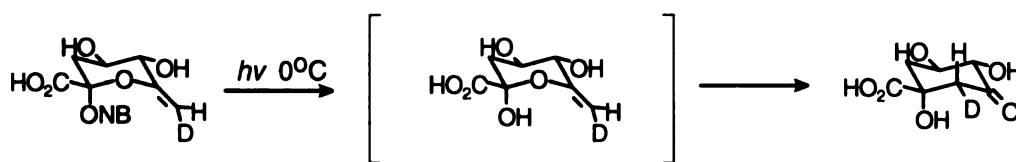
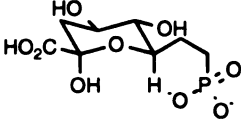
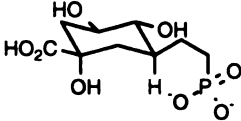
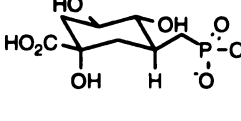
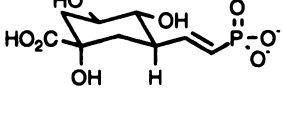
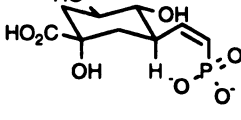


Figure 4. Non-enzymatic rearrangement of intermediate C to DHQ.

Le Marechal and Azerad⁶¹ reported the first synthesis of non-hydrolyzable phosphonate analogues of DAHP as inhibitors of DHQ synthase, and found that the nonisosteric phosphonate analogues were more potent inhibitors than the isosteric homophosphonate analogues. Later, Knowles synthesized a series of substrate phosphonate analogues and used them to probe the detailed mechanism of the phosphate elimination step.^{7c,13} (Table 1.) These phosphonate analogues were designed to be oxidized at the C-5 position and structurally allowed the abstraction of the C-6 proton. However the elimination reaction could not be completed due to substitution of a phosphonate for the phosphate monoester. When analogues were incubated with DHQ synthase in D₂O, the enzyme-catalyzed deuterium exchange was observed at the C-6 position of oxacyclic homophosphonate, carbocyclic homophosphonate, and *cis*-vinylhomophosphonate, but the nonisosteric carbaphosphonate and *trans*-vinylhomophosphonate showed no deuterium exchange. The *cis*-vinylhomophosphonate binds the enzyme more tightly than the *trans*-vinylhomophosphonate.

Table 1. Phosphonate analogues used for probing the *syn*-elimination.

Phosphonate Analogues		D ₂ O Exchange	NADH formation
Oxacyclic homophosphonate		yes	yes
carbocyclic homophosphonate		yes	yes
carcyclic phosphonate		no	yes
<i>trans</i> -vinyl homophosphonate		no	yes
<i>cis</i> -vinyl homophosphonate		yes	yes

All these results suggest that it is the peripheral oxygen of the phosphate group of the substrate DAHP itself that is responsible for removal of the C-6 proton. This proposal is consistent with all the experimental observations. If the phosphate oxygen is to serve as the base for proton abstraction, the elimination of phosphate will certainly be a *syn* process. *cis*-Vinylhomophosphonate binds more tightly to the enzyme than the corresponding *trans*-isomer, since it is constrained in the preferred conformation analogous to that of the bound substrate. The non-isosteric phosphonate analogue and *trans*-vinylhomophosphonate analogue do not enolize, because the oxygen base in these compounds can not achieve the preferred orientation with respect to the C-H bond at the C-6 position. A dianionic phosphate ester is the strongest base at physiological pH. Furthermore, by exploiting the

phosphate base, the enzyme avoids bringing an enzymic base close to the charged phosphate side chain to deprotonate a tertiary proton that is 1,3-diaxial to a hydroxyl group. Direct transfer of the C-6 proton to the phosphate oxygen of substrate DAHP would also make the phosphate group a better leaving group in the subsequent elimination step.

The first step in the conversion of DAHP to DHQ is the oxidation of the C-5 alcohol of DAHP by enzyme-bound NAD concomitant with generation of the oxidized intermediate and NADH. An attempt to detect steady-state NADH was not successful. However, when the carbacyclic homophosphonate analogue was added to DHQ synthase, Knowles^{7b} observed a new absorbance at 340 nm. Addition of lactate dehydrogenase and pyruvate to the solution did not change the absorbance at 340 nm, indicating the NADH is tightly bound to the enzyme. Similar rises in the absorbance at 340 nm were also observed with a number of other analogues,^{7b,14} suggesting that these analogues bind to the active site with similar orientation to the substrate and are consequently oxidized.

Cellular Signaling and Inositol 1,4,5-Trisphosphate Second Messenger

Complex organisms must sense what is happening in the extracellular environment in order to maintain life functions. The communication between individual cells involves the use of distinct chemicals to transmit messages from one cell to another. While some lipophilic steroid hormones can diffuse freely across cell membranes and bind to their target receptors within the cell, many chemical messengers are too hydrophilic to cross the bilayers of the cell membrane. A variety of extracellular signals are transmitted across the membranes by receptor-mediated signal transduction pathways.¹⁵ Several classes of receptors are involved in the signal transduction. The first class of cell surface receptors is linked to an ion channel. Stimulation of the receptor can trigger the ion channel to pump ions into or out of the cell. A change in the given ionic species inside the cell is perceived as an internal signal, evoking an ultimate response to the external signal. The second class of cell surface receptors is a tyrosine kinase based receptor. Binding of the extracellular

receptor by an agonist activates the intercellular tyrosine kinase and leads to the phosphorylation of tyrosine residues on the target proteins inside the cell, and cause the coordinate enzymes to respond. The third class receptors is coupled via a class of guanine nucleotide binding proteins (G-proteins) to the intracellular enzymes or ion channels, through which the receptors evoke their responses. The G-protein exists as heterotrimeric structures consisting of α , β , and γ subunit. In its inactive form, the G-protein trimeric complex is associated with the internal surface of the cell membrane with guanosine diphosphate (GDP) bound to the α subunit. Binding of the agonist molecule to the receptor causes a conformational change in the receptor protein, resulting in the formation of a ternary complex between the receptor protein and the GDP-protein complex. This complex then instantly releases GDP and binds guanosine triphosphate (GTP). The activated GTP-bound α subunit then dissociates from the complex. It is this GTP-bound α subunit that binds to the effector system to regulate the activity of associated enzymes, which act as amplifiers to generate so called second messengers on the cytosolic side of the cellular membrane.

Phosphoinositidase C, which is located on the cytosolic side of the membrane, is under the control of cell surface receptors via the intermediacy of a G-protein system. Upon activation, phosphoinositidase C cleaves the phosphodiester bond of phosphatidylinositol-4,5-bisphosphate (PIP₂) to give 1,2 diacylglycerol (DAG) and D-1,4,5-inositol trisphosphate (1,4,5-IP₃) (Figure 5). Both molecules act as messengers¹⁶ inside the target cell. The lipophilic DAG remains within the membrane of cell and activates a specific protein kinase C promoting phosphorylation of target proteins in the cell. The hydrophilic 1,4,5-IP₃ diffuses into the cytosol and binds to Ca²⁺ channel-linked 1,4,5-IP₃-specific receptors resulting in the release of Ca²⁺ from an internal store. This release of Ca²⁺ causes the increase of intracellular Ca²⁺ concentration, and thus leads to the overall cellular response by modulation of calcium dependent process.

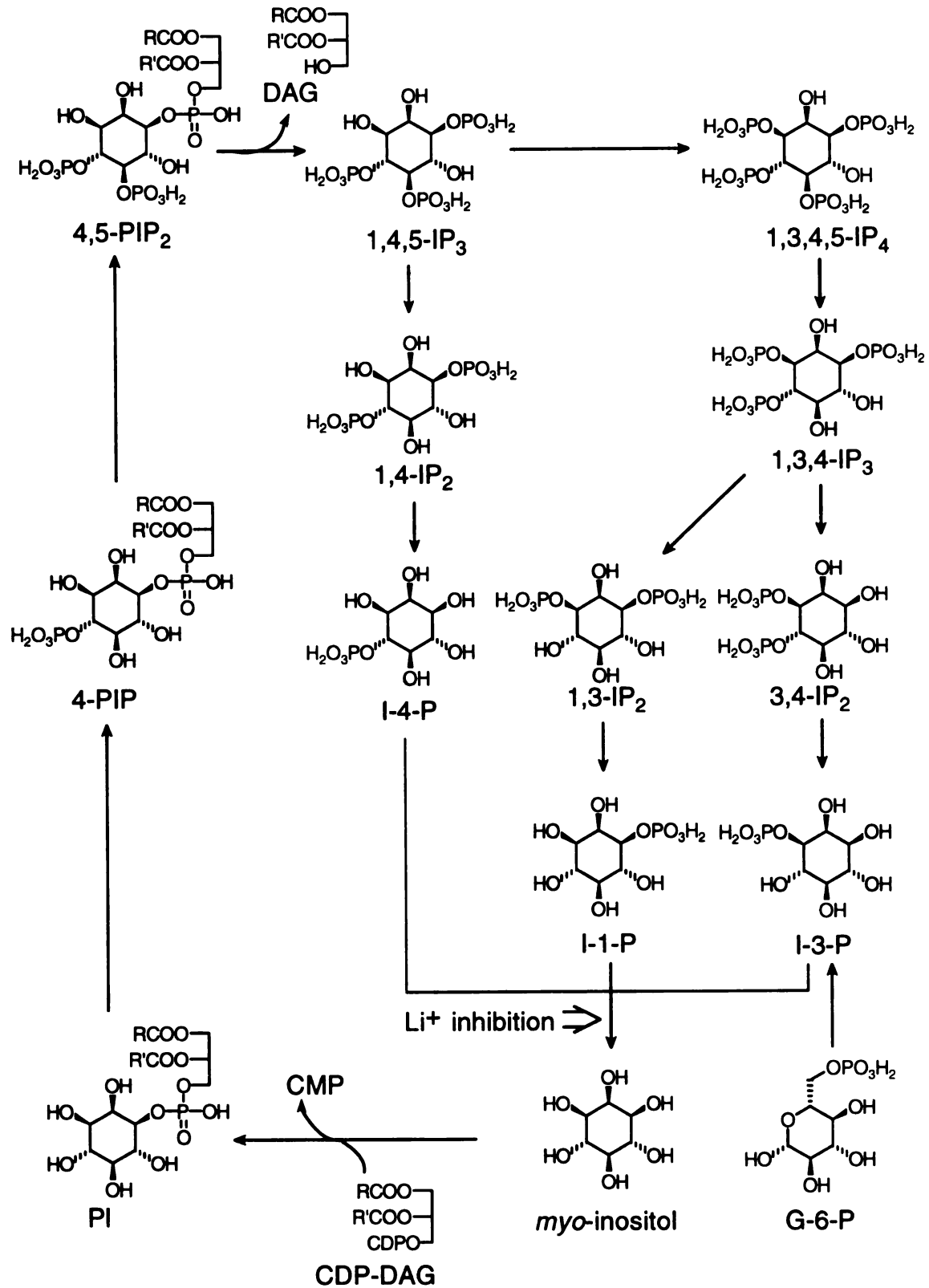


Figure 5. Phosphoinositide breakdown and resynthesis pathway.

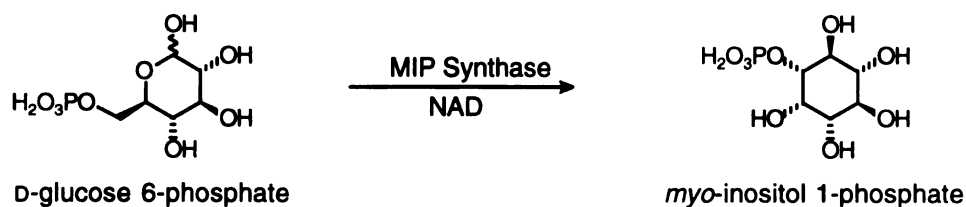
When the external signal is withdrawn, the internal signal must be effectively deactivated in order to terminate its actions and return the cell to a basal state in preparation for a new stimulus. The 1,4,5-IP₃ second messenger is terminated by the metabolism of 1,4,5-IP₃ through one of the two pathways. In the first pathway, the 5-phosphate group of 1,4,5-IP₃ is removed by a specific 5-phosphatase to give D-inositol 1,4-bisphosphate (1,4-IP₂). Further metabolism of 1,4 IP₂ by hydrolysis of the 1-phosphate group then gives D-inositol 4-phosphate, which is in turn hydrolyzed to free inositol by inositol monophosphatase. In the second pathway, 1,4,5-IP₃ is further phosphorylated to the 3-position by 1,4,5-IP₃ 3-kinase to give D-1,3,4,5-inositol tetrakisphosphate (1,3,4,5-IP₄), which is then dephosphorylated by the 5-phosphatase to D-1,3,4-inositol trisphosphate (IP₃). 1,3,4-IP₃ is then dephosphorylated either at the C-1 position to 3,4-IP₂ or at the C-4 position to 1,3 IP₂ by two separate phosphatases. Further metabolism of IP₂ gives D-*myo*-inositol 1-phosphate (I-1-P) and D-*myo*-inositol 3-phosphate (I-3-P or L-*myo*-inositol 1-phosphate). Both I-1-P and I-3-P are hydrolyzed to free *myo*-inositol by *myo*-inositol 1-phosphatase. The free *myo*-inositol generated is then used for the resynthesis of PIP₂. The incorporation of *myo*-inositol into phospholipids is achieved through the reaction with liponucleotide cytidine diphosphodiacylglycerol (CDP-DAG) to yield CMP and phosphatidylinositol (PI). PI is then phosphorylated via ATP and a PI 4-kinase to phosphatidylinositol 4-phosphate (4-PIP), which is in turn further phosphorylated by PIP 5-kinase to form phosphatidylinositol 4,5-bisphosphate (4,5-PIP₂).

myo-Inositol 1-Phosphatase and Li⁺ Inhibition

myo-Inositol 1-phosphatase is a key enzyme in the phosphatidylinositol cycle to generate free inositol, which is then used for the resynthesis of PIP₂. Since *myo*-inositol can not cross the blood-brain barrier, the brain does not have access to dietary *myo*-inositol.¹⁷ The regeneration of free inositol is therefore important in the brain. The

replenishing of free inositol in the brain is dependent on regeneration from the metabolism of inositol lipid and de novo synthesis from D-glucose 6-phosphate. Manic-depressive illness has been hypothesized to be caused by hyperactive neurons and their associated signal system, which overstimulate inositol lipid turnover. Li^+ salt has been successfully used for the treatment of manic-depressive illness for over 30 years.¹⁸ In the Li^+ therapy, *myo*-inositol 1-phosphatase is uncompetitively inhibited by the Li^+ .¹⁹ The enzyme catalyzes the hydrolysis of *myo*-inositol 1-phosphate via a ping-pong mechanism whereby phosphate is transferred from the substrate to the enzyme and then from enzyme to water. Li^+ blocks the transfer of phosphate from enzyme to water in the second step.^{19b} This inhibition reduces the supply of free *myo*-inositol for PIP_2 biosynthesis in stimulated cells, thus toning down receptor signaling via the 1,4,5- IP_3 second messenger pathway.

However, Li^+ is by no means an ideal drug. The major limitation of Li^+ therapy is the very low therapeutic ratio. To achieve the desired therapeutic effect, a plasma concentration of 0.5 to 1.0 mM Li^+ is required. But serious side effects occur at a plasma concentration of 2.0 mM. Plasma concentrations of over 3.0 mM may lead to severe toxic effects including coma and eventually death.^{15b,16c} Another approach to reduce the supply of *myo*-inositol in the brain might result from blocking the pathway of de novo biosynthesis of *myo*-inositol.



De novo biosynthesis of *myo*-inositol is achieved by isomerization of D-glucose 6-phosphate to *myo*-inositol 1-phosphate catalyzed by *myo*-inositol 1-phosphate synthase (MIP synthase) (EC 5.5.1.4) in the presence of nicotinamide adenine dinucleotide (NAD).^{1,20} *myo*-Inositol 1-phosphate is then hydrolyzed to *myo*-inositol by *myo*-inositol

1-phosphatase. De novo synthesis of *myo*-inositol 1-phosphate is the sole biosynthetic route to *myo*-inositol.

Mechanism of De novo Biosynthesis of *myo*-Inositol 1-Phosphate

MIP synthase has been isolated from wide verity of sources, such as yeast,^{21,22} mammalian tissues,²³⁻²⁷ fungi,²⁸⁻³⁰ and plant.³¹ Homogeneous enzyme has been purified from yeast, mammalian testes, and mammalian brain. The molecular weight of the native enzyme in yeast as determined by gel filtration is approximately 240,000. A single subunit of 62,000 is detected upon sodium dodecyl sulfate gel electrophoresis of the purified enzyme.²² The *INO1* locus was identified as the probable structural gene encoding the MIP synthase subunit in yeast.³² The sequence of the entire *INO1* gene revealed a peptide of 553 amino acids with a molecular weight of 62,842. Mechanism studies indicate that MIP synthase from various sources share the common mechanism originally proposed by Loewus and Kelly.³³

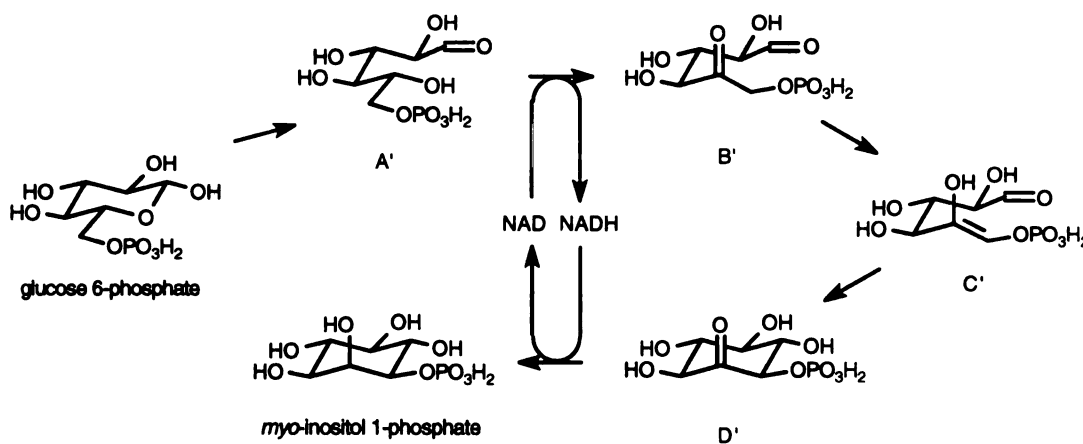


Figure 6. Proposed mechanism of *myo*-inositol 1-phosphate synthase-catalyzed reaction.

MIP synthase-catalyzed conversion of D-glucose 6-phosphate into *myo*-inositol 1-phosphate begins with the binding of D-glucose 6-phosphate to the active site. Oxidation

of the C-5 alcohol by enzyme-bound NAD forms 5-keto-glucose 6-phosphate, intermediate B'. Enolization and subsequent intramolecular aldol condensation of intermediate C' leads to 2-inosose 1-phosphate, intermediate D'. Reduction of the carbonyl of intermediate D' by NADH generated in the first step results in formation of *myo*-inositol 1-phosphate. D-Glucose 6-phosphate is converted into *myo*-inositol 1-phosphate without rearrangement of the carbon skeleton.

Most of the mechanistic studies were carried out with partially purified enzymes obtained from different sources. Most of the findings were similar with regard to mechanism, suggesting a similar reaction mechanism for all species. *myo*-Inositol 1-phosphate synthase requires NAD for its activity. Treatment with charcoal removes NAD from the rat testis enzyme, leaving a totally inactive apoenzyme.^{27,34} Reconstitution of the apoenzyme with added NAD restores 80% of the original activity. NADH generated during the reaction is tightly bound to the enzyme, and there does not seem to be exchange between the enzyme bound NADH and free NADH in the medium. Hydrogen on the C-5 of D-glucose-6-phosphate is transferred to the C-4 position of the dihydropyridine ring of NADH during the oxidation of D-glucose-6-phosphate, and the same hydrogen is delivered back to the product at the same position during the reduction of 2-inosose 1-phosphate. Adding NADH(³H) to an incubation medium of MIP synthase and D-glucose 6-phosphate failed to introduce tritium into the reaction substrate and product.^{27,35} None of the intermediates have been isolated, suggesting all intermediates are tightly bound and not released until the final reduction to *myo*-inositol 1-phosphate. When *myo*-inositol 1-phosphate synthase from bovine testis was incubated simultaneously with a mixture of deuterated D-glucose 6-phosphate-d₇ and nondeuterated D-glucose 6-phosphate-d₀, there was no crossover of the label from deuterated to nondeuterated product.³⁶

Incubation of partially purified apoenzyme from rat testis with 5-keto-D-glucose 6-phosphate and [RS-4-³H]-NADH led to the formation of D-glucose 5-³H 6-phosphate and trace levels of tritiated *myo*-inositol 1-phosphate.³⁴ This apoenzyme also catalyzed the

reduction of 5-keto-D-glucitol 6-phosphate by [RS-4-³H] NADH to form D-glucitol 5-³H 6-phosphate. Additional evidence for the involvement of 5-keto-D-glucose 6-phosphate was found in a chemical model study.³⁷ Base treatment of 5-keto-D-glucose 6-phosphate yielded two cyclose phosphates, which, after reduction with sodium borohydride, gave a mixture of two cyclitol monophosphates, L-*myo*-inositol 1-phosphate and *epi*-inositol 3-phosphate.

By the addition of NaB³H₄ to a solution containing homogeneous rat testis MIP synthase, glucose 6-phosphate and NAD, 2-inosose 1-phosphate was trapped as a mixture of tritiated *myo*-inositol and *scyllo*-inositol.³⁸ Iditol and glucitol, epimeric alditols representing 5-keto-D-glucose 6-phosphonate, were not significantly labeled. Rate of formation is coupled with rate of cyclization such that only very small steady state concentration are bound at the active site. Its cyclization to 2-inosose 1-phosphate occurs as soon as its formation. Its reduction by putative NADH in the enzymatic reaction must be the rate limiting step. *myo*-2-Imosose 1-phosphate has been chemically synthesized.⁴⁰ In the presence of apo-MIP synthase reconstituted with NADH, *myo*-2-inosose 1-phosphate is converted into *myo*-inositol 1-phosphate along with oxidation of enzyme bound NADH.

With [5-³H] glucose 6-phosphate as substrate, an isotope effect of 0.2 to 0.48 was observed.³⁵ An isotope effect in the reaction of D-[6-³H] glucose 6-phosphate was also reported⁴¹, suggesting that removal of the hydrogen at C-6 to be partially rate determining step. No isotope effects at C-1 C-2, C-3 and C-4 were detected.^{27,35,36}

When reactions were undertaken with D-[5-¹⁸O] glucose 6-phosphate in H₂O or with unlabeled substrate in H₂¹⁸O using enzyme from various sources, mass spectral analysis of the products showed no exchange of the C-5 oxygen with H₂O during reaction.⁴² This result is inconsistent with the involvement of a Schiff base between an active site amino residue and the C-5 keto group of intermediate B.

When reaction was carried out with both D-[(6S)-6-³H] glucose 6-phosphate and D-[(6R)-6-³H] glucose 6-phosphate as substrate, Floss⁴³ reported that the tritium was

preferentially removed from the pro-R position by all three enzymes purified from bovine testis, *Lilium longiflorum*, and *Streptomyces flavopericus*. Working with the charcoal treated partially purified rat testis and mammalian enzymes, Byun and Jenness⁴⁴ observed uptake of tritium in both D-glucose 6-phosphate and *myo*-inositol 1-phosphate from [(4S)-4-3H] NADH. No appearance of tritium in either D-glucose 6-phosphate or *myo*-inositol 1-phosphate was observed when [(4R)-4-3H] NADH was used. This result led to the conclusion that hydrogen transfer involves the pro-S hydrogen of NADH. However, this experimental result is not consistent with other experimental findings that NADH remains tightly bound to the enzyme throughout the reaction. Furthermore, whether the enzyme could process enzyme-NADH-D-glucose 6-phosphate complex is still questionable.

Inhibition of MIP Synthase

Early studies on MIP synthase inhibition are mainly focused on compounds similar in the structure to D-glucose 6-phosphate. Most of the compounds are commercially available and do not require chemical synthesis. Compounds that have been tested for the inhibition of MIP synthase are summarized in Table 2.

Since these data are collected from different research reports using enzymes from different sources, and most experiments were carried out with partially purified enzymes, the results are not always consistent with each other. Among carbohydrate analogues, only those having a phosphate group are inhibitory. However, not all the phosphorylated compounds are inhibitory. There is a disagreement in the literature on the inhibition effect of D-mannose 6-phosphate, which has a reversed stereochemistry at the C-2 position with respect to D-glucose 6-phosphate. Pina⁴⁵ observed no inhibition toward MIP synthase from fungi, while Wells²⁵ reported 29.6% inhibition at 5 mM toward MIP synthase from rat mammary gland. More recent work by Sherman^{26b} using bovine testis enzyme, showed D-mannose 6-phosphate to be not only a competitive inhibitor, but also a substrate for the MIP synthase. Incubation of D-mannose 6-phosphate with MIP synthase results in

Table 2. Compounds tested for MIP synthase inhibition.

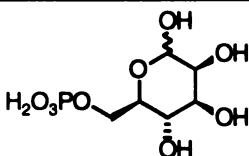
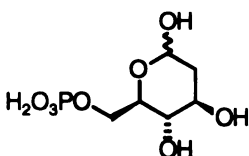
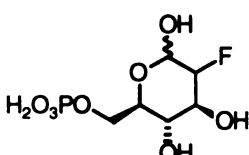
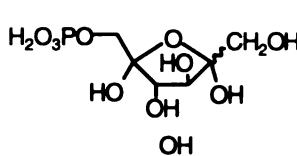
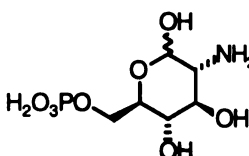
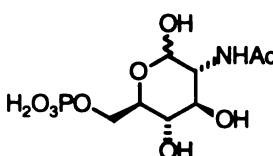
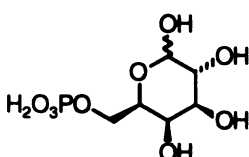
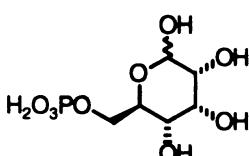
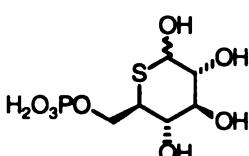
Compound	Enzyme source	Inhibition	Reference
	fungi rat mammary gland bovine testis	no inhibition 29.6% inhibition at 5 mM $K_i = 8.4 \text{ mM}$	45 25 20b
	rat testis yeast yeast plant	$K_i = 16 \text{ }\mu\text{M}$ 87% inhibition at 0.5 mM 82% inhibition at 0.5 mM $K_i = 8.7 \text{ }\mu\text{M}$	34 46 22 47
	bovine testis	$K_i = 330 \text{ }\mu\text{M}$	20b
	fungi rat mammary gland	47.5% inhibition at 5 mM 54% inhibition at 5 mM	45 25
	fungi	no inhibition	45
	rat testis	no inhibition	34
	fungi rat testis rat mammary gland bovine testis	3.7% inhibition at 5 mM no inhibition 31% inhibition at 5 mM no inhibition	45 34 25 20b
	bovine testis	39% inhibition at 14.1 mM	20b
	rat testis	$K_i = 330 \text{ }\mu\text{M}$	48

Table 2. (cont'd)

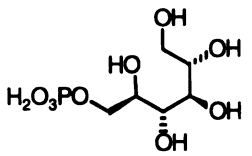
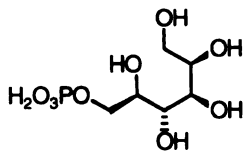
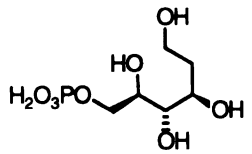
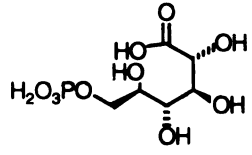
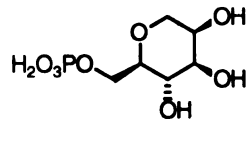
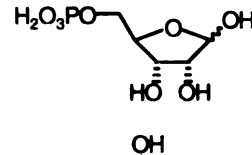
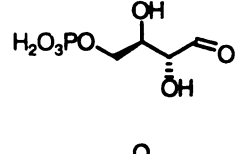
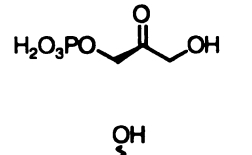
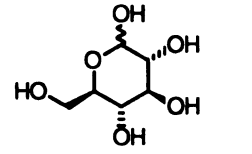
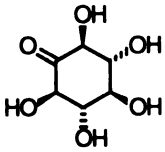
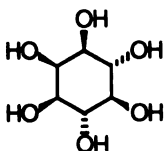
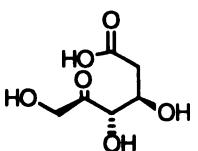
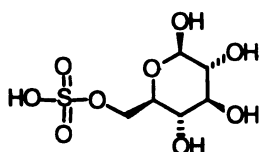
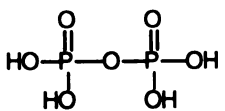
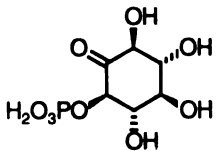
Compound	Enzyme source	Inhibition	Reference
	fungi	$K_i = 340 \mu\text{M}$	45
	rat testis	$K_i = 340 \mu\text{M}$	34
	yeast	68% inhibition at 0.5 mM	22
	rat testis	$K_i = 120 \mu\text{M}$	34
	rat testis	$K_i = 14 \mu\text{M}$	34
	fungi	23% inhibition at 5 mM	45
	rat testis	$K_i = 3.3 \text{ mM}$	34
	rat mammary gland	100% inhibition at 5 mM	25
	yeast	46% inhibition at 4 mM	46
	rat testis	no inhibition at 0.5 mM	34
	rat testis	10% inhibition at 20 mM	34
	fungi	50.7% inhibition at 5 mM	45
	rat testis	no inhibition	34
	yeast	80% inhibition at 5 mM	46
	yeast	60% inhibition at 4 mM	46
	plant	inhibitor	49
	yeast	$K_i = 700 \mu\text{M}$	40
	fungi	no inhibition	45

Table 2. (cont'd)

Compound	Enzyme source	Inhibition	Reference
	fungi	no inhibition	45
	rat mammary gland	no inhibition	35
	fungi	7% inhibition at 5 mM	45
	fungi	no inhibition	45
	fungi	$K_i = 4.6 \mu\text{M}$	45
NADH	fungi	$K_i = 68 \mu\text{M}$	45
	fungi	$K_i = 4.0 \mu\text{M}$	50
	rat mammary gland	30% inhibition at 1 mM	25
	yeast	$K_i = 3.6 \mu\text{M}$	40
		$K_i = 37 \mu\text{M}$	40
		$K_i = 170 \mu\text{M}$	40

the formation of *neo*-inositol 1-phosphate. Kinetic studies showed that D-mannose-6-phosphate and D-glucose 6-phosphate have similar K_m values and that D-mannose-6-phosphate is cyclized 31 times slower than D-glucose 6-phosphate.

It is noteworthy that when the C-2 hydroxyl group is removed, the resulting 2-deoxy D-glucose 6-phosphate becomes a very potent inhibitor. The results from all inhibition experiments^{22,34,46,47} on 2-deoxy D-glucose 6-phosphate are consistent with enzymes from various preparations (Table 2). Sherman and coworkers^{20b} also reported that when the C-2 hydroxyl group was replaced by a fluoro group, the derived 2-deoxy 2-fluoro D-glucose 6-phosphate was found to be a competitive inhibitor with inhibitory potency similar to that of 2-deoxy D-glucose 6-phosphate for the synthase. Both 2-deoxy D-glucose 6-phosphate and 2-deoxy 2-fluoro D-glucose 6-phosphate were also found to be substrates for the synthase, leading to the formation of 5-deoxy *myo*-inositol 1-phosphate and 5-deoxy 5-fluoro *myo*-inositol 1-phosphate respectively. D-fructose 6-phosphate, which has the carbonyl group located at the C-2 position instead of the C-1 position as in the case of D-glucose 6-phosphate, still retains its affinity for the enzyme. D-fructose 6-phosphate has been found to be a moderate inhibitor toward MIP synthase from fungi⁴⁵ and rat mammary gland.²⁵ Although the synthase seems to be reasonably tolerant of structural modification at the C-2 position, these modifications result in lowered rate of conversion to inositol phosphates as well as in reduced K_m values, or lead to the inhibition of the enzyme-catalyzed reaction. The tolerance to the C-2 modification is not a general phenomenon. When the C-2 hydroxyl group is replaced by an amino group or a *N*-acetylamino group, the resulting D-glucosamine 6-phosphate⁴⁵ and *N*-acetyl D-glucosamine 6-phosphate³⁴ showed no affinity for the enzyme at all.

There is also conflict in the literature on the inhibition of MIP synthase by D-galactose 6-phosphate, which has a hydroxyl group at the C-3 position with opposite orientation compared to that of D-glucose-6-phosphate (Table 2). Wells²⁵ observed inhibition of MIP synthase by D-galactose 6-phosphate similar to that by D-mannose 6-

phosphate. Pina⁴⁵ reported slightly reduced MIP synthase activity in presence of high concentrations of D-galactose 6-phosphate. Contrary to these reports, Barnett and coworkers³⁴ found no inhibition toward rat testis enzyme by D-galactose 6-phosphate. Sherman and coworkers^{20b} found D-galactose 6-phosphate to be neither an inhibitor nor a substrate for the bovine testis enzyme at concentration of 12.5 mM. It seems the C-3 hydroxyl group is more sensitive toward modification.

D-Allose 6-phosphate has also been examined.^{20b} No evidence for its conversion into the corresponding inositol phosphate could be found. However, it was found to be a weak inhibitor to the enzyme. At 14.1 mM, D-allose 6-phosphate inhibits the reaction of 1 mM D-glucose-6-phosphate with the MIP synthase by 39%. 5-Thio-D-glucose-6-phosphate, which substitutes the C-5 oxygen of D-glucose 6-phosphate with a sulfur group, was reported to be a competitive inhibitor in vitro. 5-Thio-D-glucose-6-phosphate could also be synthesized in vivo, and its inhibitory behavior has been reported.⁴⁸

Removal of the C-2 hydroxy group leads to the improved active site interaction. Whether similar phenomenon exists for the C-3, C-4, and C-5 hydroxy group is unknown. No studies on the C-3, C-4, and C-5 monodeoxy substrate analogues have been reported.

When D-glucose 6-phosphate and its aldose 6-phosphate analogues are reduced or oxidized at the C-1 position, the resulting derivatives exist exclusively in open chain forms, producing a series of potent inhibitors (Table 2). All the open chain phosphates tested including D-glucitol 6-phosphate, D-mannitol 6-phosphate, and 2-deoxy D-glucitol 6-phosphate, were potent inhibitors.^{22,25,34,45,46} By comparison, 1,5-anhydro D-glucose-6-phosphate, which is confined to the cyclic structure, is not a significant inhibitor.³⁴ 1,5-Anhydro-D-glucose-6-phosphate was not inhibitory at all at 0.6 mM, and showed 10% inhibition at 20 mM, which is ten times higher than the concentration of substrate used. All the tested substrate analogues that exert an inhibitory action exist either exclusively in acyclic form or are characterized by an equilibrium in solution consisting of acyclic and cyclic forms. The open chain alditol phosphate analogues are generally binding more

tightly than their aldose phosphate counterparts. These observations led Barnett to suggest that the enzyme might bind the substrate in a acyclic form before oxidation at C-5. The high affinity of the open chain analogues to the enzyme might arise because they could undergo oxidation at the C-5 position by NAD to form a stable enzyme-NADH-oxidized sugar analogue complex.

Beside D-glucose-6-phosphate and some of its hexose 6-phosphate analogues, MIP synthase also binds those carbohydrate phosphates with shorter carbon skeletons. D-ribose 5-phosphate, erythrose 4-phosphate, and dihydroxyacetone phosphate have been reported^{40,45,46} to be inhibitors for MIP synthase. The phosphate moiety is necessary for the interaction of substrate and analogues with the enzyme. D-Glucose, *myo*-inositol, and *myo*-inosose do not bind to the enzyme.^{25,45} Only a slight inhibition effect of 5-keto D-glucose on partially purified enzyme was reported.⁴⁵ Substituting the phosphate group of D-glucose-6-phosphate with a sulfate group leads to the loss of affinity for the enzyme.⁴⁵

Another interesting inhibitor is pyrophosphate.⁵⁰ Pyrophosphate acts as a strong competitive inhibitor with $K_i = 4.6 \mu\text{M}$ toward MIP synthase from fungi (Table 2). The inhibition of the enzyme by pyrophosphate occurs only in the presence of NH_4^+ , an activator of the enzyme, and the inhibition is pH dependent. The inhibition of MIP synthase by pyrophosphate is reversed by various cations, such as Mn^{2+} , Mg^{2+} *etc.* This finding was later confirmed by the work of Aradi and coworkers.⁵¹ The binding affinity of pyrophosphate for MIP synthase was successfully used in affinity chromatography for the purification of MIP synthase. Ethanolamine pyrophosphate was coupled to epoxy-activating Sepharose, and the resulting pyrophosphate-Sepharose possessed specific affinity to MIP synthase. The bound enzyme could not be eluted with NAD, suggesting that the binding site for NAD on the enzyme is different from the pyrophosphate binding site. The enzyme could be removed completely from pyrophosphate-Sepharose column by washing with Mg^{2+} . The enzyme purified by pyrophosphate-Sepharose column is free of

contaminating glucose 6-phosphate dehydrogenase, which is difficult to remove by other methods.

As mentioned earlier, MIP synthase catalyzed cyclization of D-glucose-6-phosphate into *myo*-inositol 1-phosphate is NAD-dependent. During the reaction, NADH is generated as a transient intermediate and tightly bound to the enzyme. Inhibition of MIP synthase by NADH has been reported using enzyme from fungi,^{45,50} rat mammary gland,²⁵ and plant⁴⁷ (Table 2). Kinetics with respect to both D-glucose 6-phosphate and NAD, as well as two inhibitors, 2-deoxy D-glucose 6-phosphate and NADH have been investigated using enzyme from plant.⁴⁷ The Michaelis constant for NAD and D-glucose 6-phosphate are 2.4 μM and 65 μM respectively. Inhibition by 2-deoxy D-glucose 6-phosphate is competitive with respect to D-glucose 6-phosphate with $K_i = 8.7 \mu\text{M}$, and is uncompetitive with respect to NAD with $K_i = 2.0 \mu\text{M}$. Inhibition by NADH is competitive with respect to both D-glucose 6-phosphate and NAD with $K_i = 3.9 \mu\text{M}$ and 4.7 μM respectively. Kinetic analysis suggested an ordered sequential mechanism in which NAD must react before D-glucose 6-phosphate. There is no evidence that NAD remains bound to the enzyme between reaction cycles.

Recently, Frost and coworkers⁴⁰ have synthesized *myo*-2-inosose 1-phosphate, the actual intermediate D' (Figure 6), and a series of carbocyclic intermediate analogues. Their inhibition behavior for MIP synthase from yeast has been investigated (Table 2). *myo*-2-Inosose 1-phosphate can be reduced by NADH in presence of charcoal treated synthase into *myo*-inositol 1-phosphate. In addition to being a reaction intermediate, *myo*-2-inosose 1-phosphate is a potent competitive inhibitor with $K_i = 3.6 \mu\text{M}$. 2-Deoxy-*myo*-inositol 1-phosphate, derived from removal of the oxidized reaction center from *myo*-2-inosose 1-phosphate, is also a competitive inhibitor with $K_i = 170 \mu\text{M}$. Substituting the phosphate monoester oxygen of *myo*-2-inosose 1-phosphate with a methylene group, results in 1-deoxy 1-(phosphonomethyl) *myo*-2-inosose, which exists in the neutral solution exclusively in the keto form. 1-Deoxy 1-(phosphonomethyl) *myo*-2-inosose is a

competitive inhibitor with $K_i = 37 \mu\text{M}$. Although it only contains 3 carbons in its carbon skeleton, dihydroxyacetone phosphate (DHAP) is a competitive inhibitor ($K_i = 700 \mu\text{M}$) with the minimum set of structural requirements for active site binding to the enzyme. Similar to 2-inosose 1-phosphate, both 1-deoxy 1-(phosphonomethyl) *myo*-2-inosose and DHAP can be reduced by NADH in presence of apoenzyme to 1-deoxy 1-(phosphonomethyl) *myo*-2-inositol and glycerol 3-phosphate respectively. Apparently, challenging MIP synthase with an oxidized reaction center leads to inhibition as a result of the enzyme's inability to process the oxidized center with NAD bound at the active site. Incorporation of a preoxidized reaction center into potential inhibitors may provide a general strategy for inhibition synthase.

CHAPTER 2

epi-CARBOCYCLIC PHOSPHATE ANALOGUE AS A PROBE FOR THE MECHANISM OF SUBSTRATE MEDIATED *syn*-ELIMINATION

Design of the *epi*-Carbocyclic Phosphate Analogues

DHQ synthase has been viewed as a catalytic marvel for most of the thirty-odd years since its existence was conclusively established. An enzyme of only MW = 40,000-44,000 appears to catalyze an unusually complicated series of chemical transformations. There are at least five reactions involved during each single turnover of the substrate DAHP to the product DHQ (Figure 2). These reactions include oxidation of the C-5 alcohol, elimination of inorganic phosphate, enolization, C-5 carbonyl reduction, and intramolecular aldol condensation. This view of DHQ synthase's catalytic prowess began to crumble under more recent scrutiny of the enzyme. Various experimental observations have raised doubts about the role DHQ synthase plays during the conversion. Bartlett¹² showed that intermediate C (Figure 2) generated photochemically from an *O*-nitrobenzyl ketal protected precursor spontaneously cyclized to DHQ as the only apparent diastereomer in the absence of DHQ synthase. Based on a series of experiments, Knowles^{7c,11,13} suggested that the β -elimination of inorganic phosphate is a *syn* process, and that the base involved for the deprotonation step may be the phosphate moiety of the substrate itself rather than a basic enzyme residue. However, a later examination of product mixture did reveal the formation of 2-4% of *epi*-DHQ. These results suggest DHQ synthase may not fully catalyze the enolization and the aldol condensation but may just play a minor role as a template for the last two reactions in the overall turnover series from substrate DAHP to product DHQ.

If DHQ synthase employs an active site residue to catalyze the elimination of inorganic phosphate, it is unlikely that the active site would tolerate the drastic repositioning

of the phosphoryl moiety of analogues relative to the location of these same moiety on previously synthesized carbocyclic analogues **3**, and **4**.^{7,52} However, if the phosphate monoester of DAHP mediates its own elimination, the active site might tolerate the stereochemical modification in these analogues. Inhibition of DHQ synthase by analogues **1** and **2** would then be possible. The *epi*-carbocyclic analogues might even be oxidized to their C-4 carbonyl forms with concomitant formation of enzyme-bound NADH. Improved inhibition of DHQ synthase might even be possible.

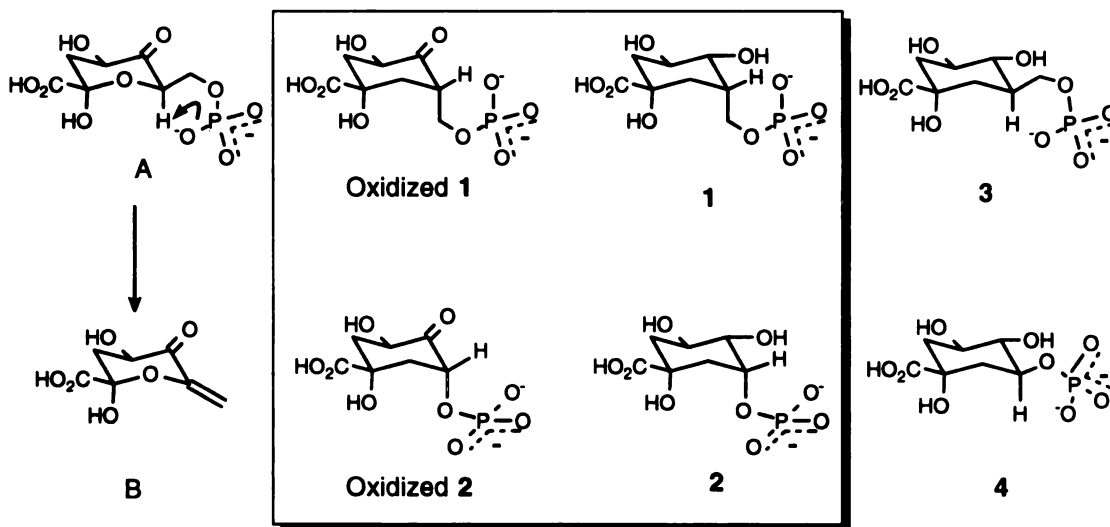
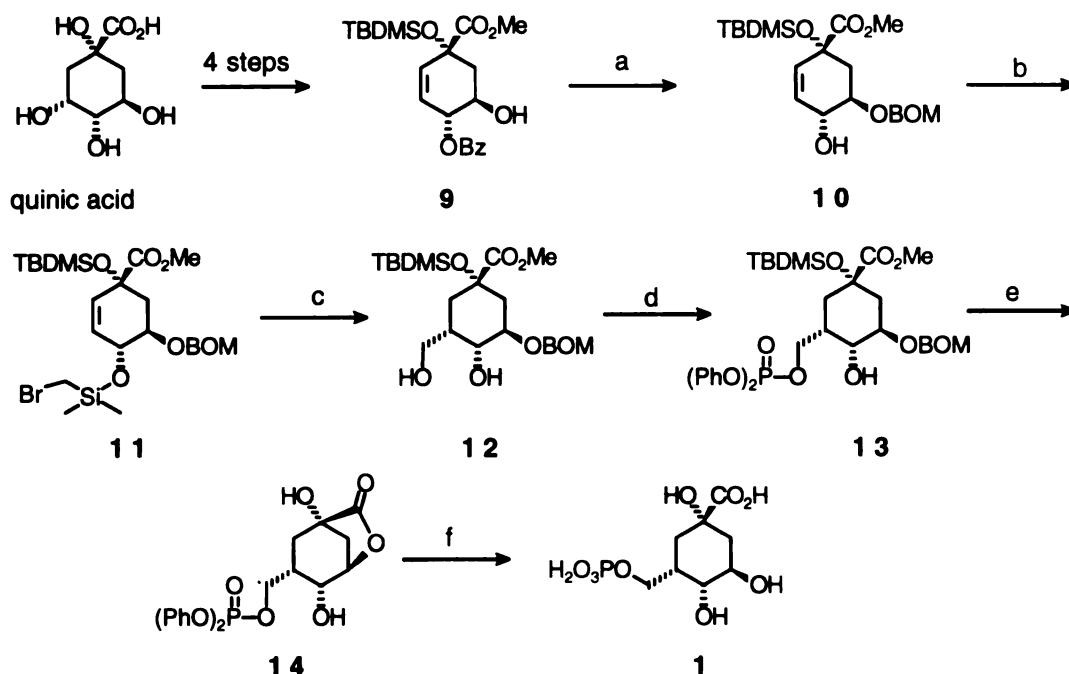


Figure 7. Reaction intermediate analogues with an inverted C-5 chiral-center.

To obtain additional insight into this hypothesis, we designed a new class of *epi*-carbocyclic analogues of the reaction intermediate to challenge the stereochemical and steric tolerance of DHQ synthase's active site. 5-[(Phosphonoxy)methyl]-5-deoxyquinates **1** and 3-(phosphonoxy)quinates **2** possess an asymmetric carbon atom which is inverted relative to the stereochemistry of the same carbon atom in the substrate DAHP.

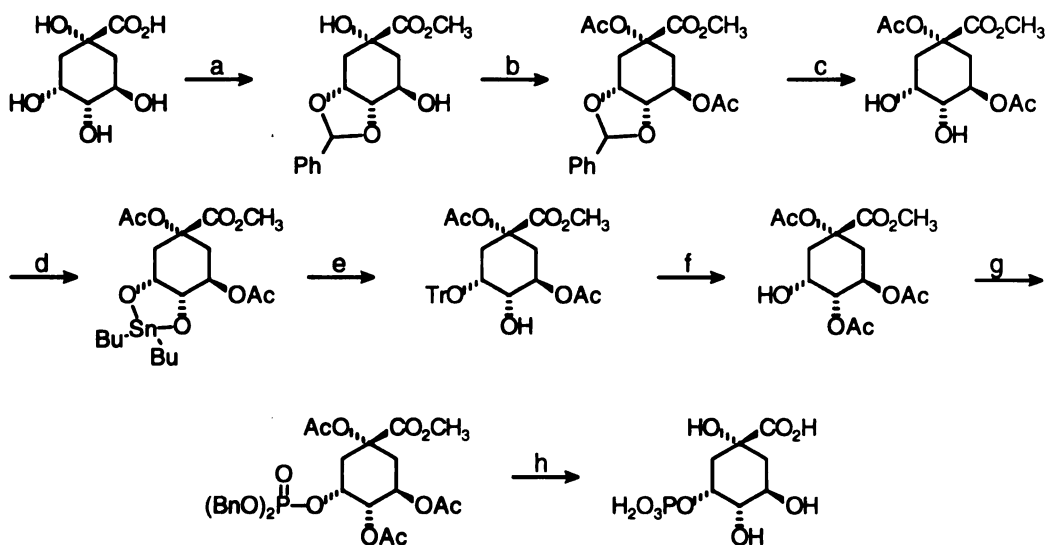
Synthetic Approaches to the *epi*-Carbaphosphate Analogues

(a) i) BOMCl, *i*-Pr₂EtN, CH₂Cl₂, 97%; ii) MeONa, MeOH, THF, 73%; (b) BrCH₂SiMe₂Cl, Et₃N, CH₂Cl₂, 0°C, 97%; (c) i) Bu₃SnH, AIBN, C₆H₆, reflux; ii) H₂O₂, NaHCO₃, 70%; (d) (PhO)₂POCl, pyr, 85%; (e) HF, H₂O, CH₃CN, 75%; (f) H₂, PtO₂, THF, H₂O, 61%.

Figure 8. Synthesis of 5-[(phosphonoxy)methyl]-5-deoxyquinate 1.

Quinic acid was used as starting material for synthesis of both 5-[(phosphonoxy)methyl]-5-deoxyquinate 1 and 3-(phosphonoxy)quinic acid 2. Intermediate 9 (Figure 8) can be routinely prepared in about 50% yield from quinic acid using a literature procedure.⁵³ Protecting the C-3 alcohol as a benzoxymethyl ether followed by deprotection of the C-4 benzoyl ester with sodium methoxide afforded allylic alcohol 10. Functionalization of allylic alcohol 10 with bromomethyl dimethylchlorosilane and triethylamine produced the precursor 11 needed for intramolecular radical cyclization. Nishiyama-Stork cyclization⁵⁴ was accomplished by slow addition of tributyltin hydride

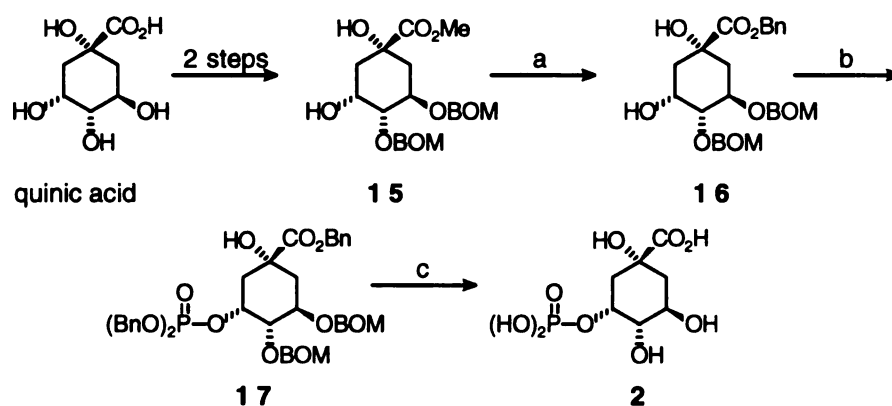
and AIBN to a refluxing benzene solution of bromomethylsilyl ether **11**. The resulting cyclic siloxane was submitted without purification to Tamao oxidation⁵⁵ using hydrogen peroxide and sodium bicarbonate to afford diol **12** with the desired stereocenter at C-5. The structure of diol **12** was confirmed by X-ray crystallography. The primary alcohol of **12** was then selectively phosphorylated with diphenyl phosphorochloridate to give the protected phosphate **13**. Subsequent removal of the *t*-butyldimethylsilyl group upon treatment with aqueous hydrogen fluoride in acetonitrile also resulted in hydrolysis of the benzyloxymethyl ether and spontaneous lactonization between the C-3 hydroxyl and the C-1 carbonyl groups. Lactone **14** was then hydrogenolyzed over platinum to remove the phenyl phosphate ester protecting groups. Treatment with base followed by neutralization opened the lactone to afford 5-[(phosphonoxy)methyl]-5-deoxyquinic acid **1**, which was purified by anion exchange chromatography.



(a) i) PhCHO, *p*-TsOH, benzene, reflux, 12 h, ii) NaOMe, MeOH, 72%; (b) (Ac)₂O, DMAP, CH₂Cl₂, 92%; (c) HOAc, H₂O, 92%; (d) Bu₂SnO, benzene, reflux; (e) i) TrCl, DMF, 45°C, ii) 4% dioxane, 45°C, 65%; (f) i) (Ac)₂O, DMAP, CH₂Cl₂, 50°C, 100%, ii) Cl₃CCO₂H, CH₂Cl₂, 87%; (g) i) (BnO)₂PN(*i*-Pr)₂, tetrazole, CH₂Cl₂, ii) *m*CPBA, CH₂Cl₂, -40°C, 79%; (h) TMSBr, CH₂Cl₂, 0°C, ii) NaOH, H₂O, 0°C, 80%.

Figure 9. Chahoua's synthesis of 3-(phosphonoxy)quinic acid **2**.

The first synthesis of 3-(phosphonoxy)quinic acid **2** has been recently reported⁵⁶ (Figure 9). However, the product we obtained from this procedure was contaminated with some impurities likely resulting from phosphate ester migrations. Attempted purification failed to give clean product suitable for the enzyme assay. So, a separate, more expeditious approach for its preparation has been elaborated. The selectively protected diol **15** (Figure 9) was obtained in two steps from quinic acid as previously described by Knowles.^{7b} To avoid the phosphate migration during base-catalyzed hydrolysis of the methyl ester, this carboxylate protection had to be changed. Hydrolysis of the methyl ester with sodium hydroxide was followed by re-protection of the carboxylate upon treatment with benzyl bromide and cesium carbonate.⁶² The resulting benzyl ester **16** was phosphorylated by reaction with *n*-butyllithium and tetrabenzylpyrophosphate to give fully protected phosphate **17**. One step deprotection was accomplished by hydrogenolysis over palladium on carbon. Product 3-(phosphonoxy)quinic acid **2** was thus obtained cleanly without any problematic phosphate ester migrations.



(a) i) NaOH, H₂O, THF, 90%; ii) BnBr, Cs₂CO₃, DMF, 69%; (b) i) *n*-BuLi, THF, -78°C; ii) [(BnO)₂P(O)]₂O, THF, -78°C to 0°C, 53%; (c) H₂, 10% Pd on C, H₂O, THF, 100%

Figure 10. Synthesis of 3-(phosphonoxy)quinic acid **2**.

Kinetic Evaluation

DHQ synthase was isolated from *E. coli* RB791(*pJB14*).^{6b} The assay of DHQ synthase inhibitors was carried out in a buffer solution at pH 7.5 consisting of 50 mM MOPS, 0.25 mM cobalt chloride and 0.25 mM NAD at 15°C. After the reaction was initiated, aliquots of reaction mixture were taken at time points and quenched with 20% trichloroacetic acid. The inorganic phosphate released during the conversion was then quantitated by colorimetric assay.⁷²

The kinetics⁵⁷ associated with a new enzyme inhibitor are usually the first indication as to whether a rationally designed inhibitor conforms to expectations. For most ground state or substrate analogues, the formation of a readily reversible complex with an enzyme is the basis for their inhibition. The primary distinction made between different types of rapidly reversible inhibition is whether binding of the inhibitor is mutually exclusive with (competitive, same binding site), dependent on (uncompetitive, second binding site), or independent of (noncompetitive, second binding site) the concentration of a varied substrate. If the inhibitor is structurally similar to a varied substrate, then the inhibitor and substrate should compete for the same binding site. The inhibition would be likely competitive. The equilibria for the simple competitive inhibition are shown in Figure 11:

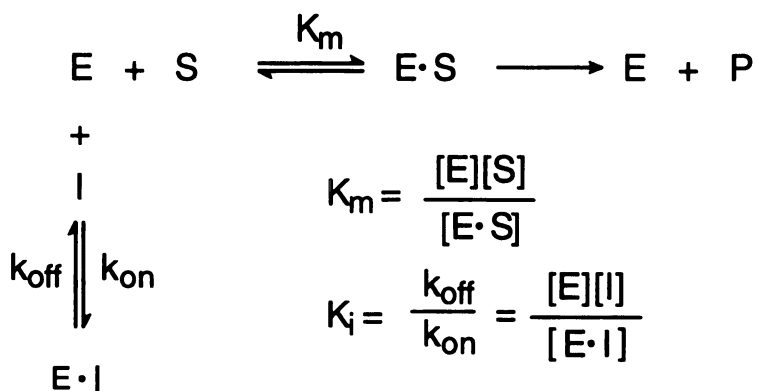


Figure 11. Competitive inhibition equilibria.

where E is the enzyme, S is the substrate, ES is the enzyme-substrate complex, P is the product, I is the inhibitor, and EI is the enzyme-inhibitor complex. The Michaelis constant K_m is expressed as $K_m = [E][S]/[ES]$, where [E], [S], and [ES] are the steady-state concentration of the enzyme, substrate, and enzyme-substrate complex, respectively. The Michaelis constant K_m is a measure of the enzyme's affinity for the substrate. A simple operational definition of K_m is the substrate concentration at which the reaction velocity is half-maximal. The inhibition constant is expressed in the equation: $K_i = k_{off}/k_{on} = [E][I]/[EI]$, where [I] and [EI] are the steady-state concentrations of the inhibitor and the enzyme-inhibitor complex respectively, k_{off} is the dissociation rate constant of the inhibitor from the enzyme, and k_{on} is the association rate constant of the inhibitor with the enzyme. The K_i is the primary basis for quantitating how tightly the inhibitor is bound by the enzyme. The relationship between the rate of reaction (v), maximum velocity (V_{max}), [S], [I], K_m , and K_i is described by the modified Michaelis-Menten equation (Equation 1).

$$v = \frac{V_{max} [S]}{K_m \left[1 + \frac{[I]}{K_i} \right] + [S]} \quad (1)$$

There are several methods for determining the values of the parameters of the Michaelis-Menten equation. Reaction velocity data are collected at varied substrate and varied inhibitor concentrations and plotted according to the equations rearranged from Michaelis-Menten equation.

For the Lineweaver-Burk plot (Equation 2), $1/v$ is plotted versus $1/[S]$ at different inhibitor concentration [I]. The plot is linear and has a slope of K_{mapp}/V_{max} (where $K_{mapp} = K_m(1+[I]/K_i)$), a $1/[S]$ intercept of $-1/K_{mapp}$, and a $1/v$ intercept of $1/V_{max}$. For a competitive inhibition, the lines at various concentrations of [I] intersect at $1/v$ axis = $1/V_{max}$. This is diagnostic for the competitive inhibition. Replotting of $K_{mapp} =$

$K_m(1+[I]/K_i)$ versus $[I]$ gives a linear line with a K_{mapp} intercept of K_m and an $[I]$ intercept of $-K_i$.

$$\frac{1}{v} = \frac{K_m \left[1 + \frac{[I]}{K_i} \right]}{V_{max}} \frac{1}{[S]} + \frac{1}{V_{max}} \quad (2)$$

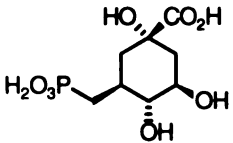
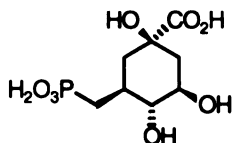
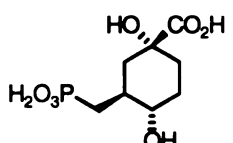
For the Hanes-Woolf plot (Equation 3), the $[S]/v$ is plotted versus $[S]$ at different inhibitor concentration $[I]$. The linear plot has a slope of $1/V_{max}$, a $[S]/v$ intercept of K_{mapp}/V_{max} and a $[S]$ intercept of K_{mapp} . For competitive inhibition, the lines at various concentration of $[I]$ are parallel with each other. This is another diagnostic for competitive inhibition. Similarly, the K_i is obtained by replotting K_{mapp} versus $[I]$.

$$\frac{[S]}{v} = \frac{K_m \left[1 + \frac{[I]}{K_i} \right]}{V_{max}} + \frac{1}{V_{max}} [S] \quad (3)$$

For most conventional substrate or ground state analogue inhibitors, the equilibrium between the enzyme, inhibitor, and the enzyme-inhibitor complex is established very rapidly, and reaches the steady-state within a very short period of time. However, for some inhibitors, the establishment of steady-state occurs slowly.⁵⁸ The lifetime of the resulting enzyme-inhibitor complex is dominated by the slow rate of dissociation (k_{off}) of inhibitor from the enzyme, while the rate of association (k_{on}) of inhibitor to the enzyme may be fast or slow. This type of time-dependent behavior is frequently observed in the inhibition associated with reaction intermediate analogues, especially the more potent

inhibitors. Frost¹⁴ and Knowles^{7b} have reported several carbaphosphonate substrate analogues to be slow-binding inhibitors for DHQ synthase (Table 3).

Table 3. Slow binding inhibitors of DHQ synthase.

Inhibitor	Type of Inhibition	k_{on} ($M^{-1}s^{-1}$)	k_{off} (s^{-1})	K_i (M)	Reference
	competitive slowly-reversible	1.0×10^6 1.4×10^6	7.5×10^{-4} 8×10^{-4}	5.4×10^{-9} 8×10^{-10}	14 7b
	competitive slowly-reversible	1.5×10^4	1.1×10^{-4}	7.3×10^{-9}	14
	competitive slowly-reversible	1.5×10^3	3.2×10^{-4}	2.2×10^{-7}	14

Unlike conventional inhibitors, for which the progress curve is a straight line as long as substrate depletion is insignificant, a slow-binding inhibitor produces a bent progress curve. For simple one-step, slow-binding inhibition, the enzyme is fully active at $t = 0$ and the initial velocity is the same as the velocity of the reaction in the absence of inhibitor. Along with the reaction, the enzyme slowly lose its activity due to slow formation of the enzyme-inhibitor complex. Although the K_i of a slow-binding inhibitor can be determined from the final steady-state linear portion of progress curves, the more convenient way to determine the K_i is to measure the dissociation rate constant (k_{off}) and the association rate constant (k_{on}), then calculate the inhibition constant from $K_i = k_{off}/k_{on}$.

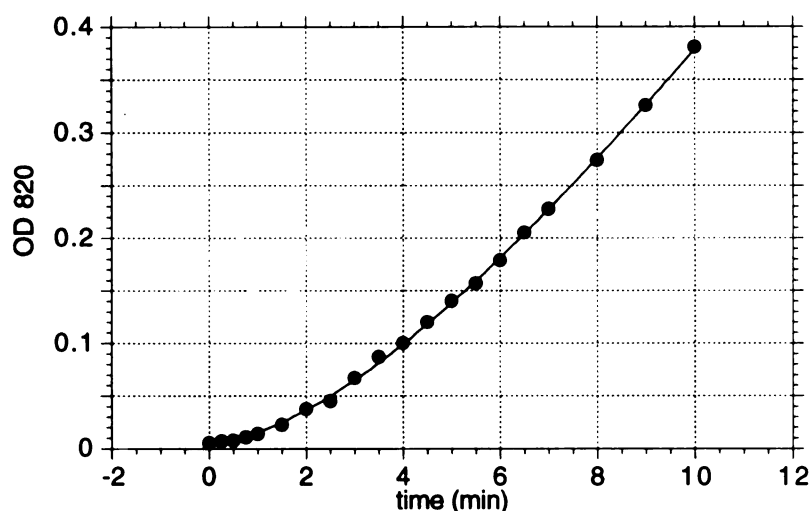


Figure 12. Progress curve for enzyme pre-incubated with a slow-binding inhibitor.

The dissociation rate constant (k_{off}) of the inhibitor from the enzyme can be obtained from an experiment where the enzyme is pre-incubated with the inhibitor to form an inactivated enzyme-inhibitor complex. A saturating amount of substrate is then added to the buffer containing the enzyme-inhibitor complex. The reaction progress curve is characterized by an initial zero enzyme activity followed by a slow recovery of enzyme activity until a final steady state rate is reached. The curve is fitted to $[P] = at + be^{-kt} + c$ where $[P]$ is the concentration of product, t is elapsed time, and a , b , c and k are the adjustable parameters. When $[I]$ is very low (close to $[E]$) and $[S]$ is much greater than K_m , the determined k is equal to k_{off} . Figure 12 is a representative progress curve for the recovery of enzyme activity. The reaction was initiated by adding substrate DAHP (700 μM) to a pre-incubated solution of DHQ synthase (10 nM) and 5-[(phosphonoxy)methyl]-5-deoxyquinic acid 1 (30 nM) at pH 7.5. Aliquots of the reaction solution were withdrawn at timed intervals and quenched with 20% trichloroacetic acid. The inorganic phosphate produced was then measured by colorimetric assay.⁷²

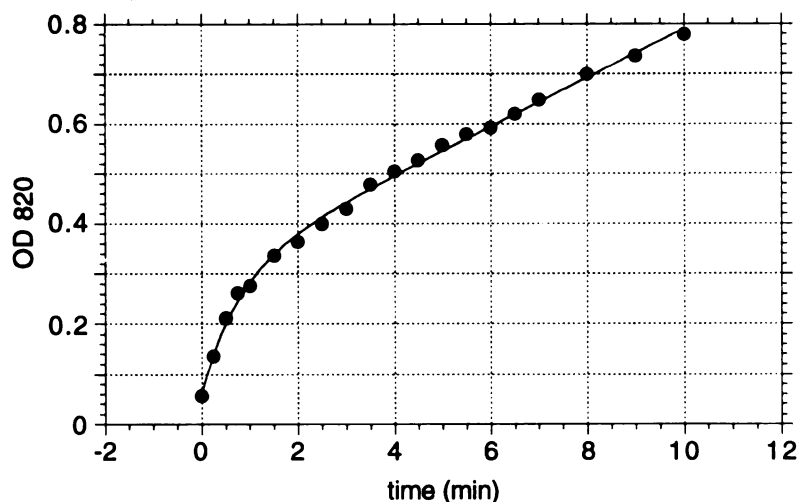


Figure 13. Progress curve in the presence of a slow-binding inhibitor

The associate rate constant (k_{on}) of the inhibitor with the enzyme can be obtained from another experiment where the reaction is initiated by adding the enzyme to the buffer containing inhibitor and substrate. The reaction progress curve is characterized by an initial burst followed by slow loss of enzyme activity until a final steady state rate is achieved. The curve is fitted to $[P] = at - be^{-kt} + c$. The rate constant (k) obtained is then used to derive k_{on} from the following equation (Equation 4).

$$K_{on} = \frac{(k - k_{off})(1 + [S]/K_m)}{[I]} \quad (4)$$

Figure 13 shows a representative progress curve for the inhibition of DHQ synthase with a slow-binding inhibitor, 5-[(phosphonoxy)methyl]-5-deoxyquinate **1**. The reaction was initiated by adding enzyme (50 nM) to a solution of substrate (400 μ M) and inhibitor (2 μ M) at pH 7.5, and the inorganic phosphate released was monitored.

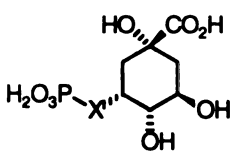
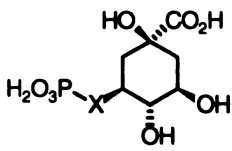
Incubating 5-[(phosphonoxy)methyl]-5-deoxyquinate **1** with DHQ synthase did not lead to detectable generation of inorganic phosphate. However, **1** was a slowly-reversible inhibitor with $K_i = 30$ nM, which can be compared to the $K_i = 120$ nM reported for C-5 epimer carbaDAHP 5.^{7,52} This makes 5-[(phosphonoxy)methyl]-5-deoxyquinate **1** the most potent phosphate monoester-containing inhibitor of DHQ synthase. An increase of absorbance at 340 nm indicative of analogue oxidation and formation of enzyme-bound NADH was also observed when 5-[(phosphonoxy)methyl]-5-deoxyquinate **1** was incubated with DHQ synthase. This indicated that **1** is positioned in the active site of DHQ synthase similarly to other carbocyclic substrate analogues, which are likewise preceded to undergo oxidation with formation of enzyme-bound NADH.

3-(Phosphonoxy)quinate **2** was a competitive inhibitor with $K_i = 53$ μ M. When 3-(phosphonoxy)quinate **2** was incubated with DHQ synthase, an increase in absorbance at 340 nm was not detected. By comparison, the corresponding carbaphosphate **4** (Figure 7) is reported to be a competitive inhibitor with $K_i = 1.7$ μ M.⁷ When bound to the enzyme, carbaphosphate **4** can be oxidized with concomitant formation of enzyme-bound NADH. One explanation for the lack of NADH formation when 3-(phosphonoxy)quinate **2** was incubated with DHQ synthase may be that its position in the active site of DHQ synthase differs significantly from that of carbaphosphate **4**. Another possible reason might be the increased redox potential of the C-4 alcohol. Unlike the other *epi*-carbocyclic phosphate and phosphonate **1**, **5**, and **6**, in which a methylene group is attached to the neighboring position, 3-(phosphonoxy)quinate **2** has an oxygen attached to the neighboring C-3 position. The electron-withdrawing effect of the neighboring oxygen might increase the redox potential of C-4 alcohol and make it more difficult to oxidize.

In addition to these two *epi*-carbocyclic phosphate analogues, two *epi*-carbocyclic phosphonate analogue **5**, and **6** (Table 4) have been synthesized and investigated by the Frost group.⁵⁹ 5-(Phosphonomethyl)-5-deoxyquinate **5**, which was a slow-binding inhibitor with $K_i = 55$ nM, exhibited almost the same behavior toward DHQ synthase

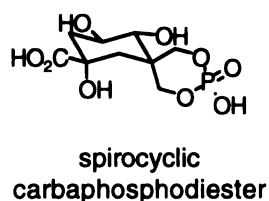
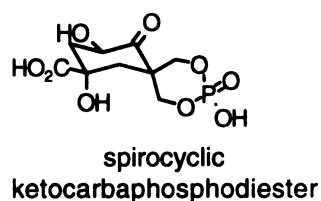
relative to the phosphate counterpart 5-[(phosphonoxy)methyl]-5-deoxyquinate **1**. The *epi*-carbocyclic homophosphonate, 5-(phosphonoethyl)-5-deoxyquinate **6**, was found to be a competitive inhibitor of DHQ synthase with $K_i = 30 \mu\text{M}$. An increase of absorbance at 340 nm was also observed when 5-(phosphonomethyl)-5-deoxyquinate **5** and 5-(phosphonoethyl)-5-deoxyquinate **6** was incubated with DHQ synthase. The results of kinetic studies of analogue **1**, **2**, **5**, and **6** along with that of previously reported counterpart epimers are summarized in Table 4.

Table 4. Inhibition of DHQ synthase by *epi*-carbocyclic and carbocyclic reaction intermediate analogues.

Inhibitor	Type of Inhibition	E-NADH Formation	k_{on} ($\text{M}^{-1}\text{s}^{-1}$)	k_{off} (s^{-1})	K_i (m)	Ref.	
	1. X=OCH ₂	slowly-reversible	+	1.4×10^5	4.3×10^{-3}	3.0×10^{-8}	
	2. X=O	competitive	-			5.3×10^{-5}	
	5. X=CH ₂ CH ₂	competitive	+			3.0×10^{-5}	59
	6. X=CH ₂	slowly-reversible	+	4.4×10^4	2.4×10^{-3}	5.5×10^{-8}	59
	3. X=OCH ₂	competitive	+			1.2×10^{-7}	7,52
	4. X=O	competitive	+			1.7×10^{-6}	7
	7. X=CH ₂ CH ₂	competitive	+/-			1.7×10^{-6}	7,13
	8. X=CH ₂	slowly-reversible	+	1.4×10^5	7.5×10^{-4}	5.4×10^{-9}	7

Detection of enzyme-bound NADH formation during incubation of these *epi*-carbocyclic analogues with DHQ synthase provided direct evidence that these *epi*-carbocyclic analogues were oxidized by enzyme-bound NAD in the enzyme active site. Comparison of these *epi*-carbocyclic analogues **1**, **2**, **5**, and **6** with corresponding carbocyclic analogues **3**, **4**, **7**, and **8** revealed that both *epi*-carbocyclic analogue and carbocyclic analogue could fit to the enzyme active site in a similar manner. DHQ synthase

is quite tolerant of the type of steric and stereochemical challenge presented to the active site. These experimental observations are consistent with the hypothesis that the elimination of inorganic phosphate is mediated by the phosphate moiety of substrate itself, rather than an active site residue of the enzyme.

**18****19**

Both the C-5 stereochemistry of *epi*-carbaphosphate analogue and carbaphosphate analogue were incorporated in spirocyclic carbaphosphodiester transition state analogues **18** and **19** by the Frost group.^{60e} To assist in defining as well as exploiting the role of DHQ synthase during the elimination of inorganic phosphate, the spirocyclic carbaphosphodiester transition state analogues were designed to be conformationally restrained mimics of the six-membered transition state wherein the methine proton in reaction intermediate A (Figure 7) is removed by the phosphate monoester. Spirocyclic carbaphosphodiester **18** was a modest competitive inhibitor of DHQ synthase with $K_i = 67 \mu\text{M}$, while spirocyclic ketocarbaphosphodiester **19** failed to show any inhibition of the enzyme. When DHQ synthase was incubated with spirocyclic carbaphosphodiester **18**, the accumulation of NADH was observed.

The modest inhibition of DHQ synthase by spirocyclic carbaphosphodiester **18** and failed inhibition by spirocyclic ketocarbaphosphodiester **19** indicate that active site conformational restriction of phosphorylmethyl group of intermediate A (Figure 7) plays a minor catalytic role during phosphate elimination. One reason for the modest inhibition of DHQ synthase by spirocyclic carbaphosphodiester **18** may be adverse steric interactions between the enzyme active site and cyclic phosphodiester of the spirocyclic

carbaphosphodiester **18**. However, this is not consistent with the tolerance by the enzyme active site of both epimer pairs **1** versus **5** and **4** versus **8**. What is the real reason that result in the potent inhibition of DHQ synthase by both epimers of carbocyclic phosphates or carbocyclic phosphonates, while spirocyclic carbaphosphodiester is a modest inhibitor? One explanation might be that the enzyme does not stabilize the transition state that spirocyclic carbaphosphodiester mimics. Instead, the enzyme may be stabilizing some other type of transition state. The observation of NADH formation for epimers of phosphate monoesters **1** and **3**, phosphonates **6** and **8**, and spirocyclic carbaphosphodiesters **18** and **19** indicates that they fit similarly into the active site and are consequently oxidized. Upon being oxidized, both epimers of phosphate monoesters **1** and **3** and phosphonates **6** and **8** can employ their phosphate or phosphonate to abstract the methine proton and generate the E1cb-like transition state analogues.⁹⁹ However, spirocyclic carbaphosphodiester **18** is restrained in a six-membered cyclic form, which makes it impossible to form a E1cb-like transition state analogue. If enzyme stabilizes the E1cb-like transition state, rather than the one that spirocyclic carbaphosphodiester mimics, then the analogues that can form E1cb-like transition state analogue in situ would be expected to show potent inhibition.

In summary, by challenging the DHQ synthase active site with this new class of *epi*-carbocyclic analogues of the reaction intermediate, new insights have been provided into the question of whether the phosphate monoester of DAHP catalyzes its own elimination and the attendant question as to whether DHQ synthase might display diastereomeric promiscuity in the C-5 region of carbocyclic DAHP substrate analogues. Such stereochemical and steric tolerance in active site binding has now been observed with the inhibition of DHQ synthase by 5-[(phosphonoxy)methyl]-5-deoxyquinate **1**, 3-(phosphonoxy)quinate **2**, 5-(phosphonomethyl)-5-deoxyquinate **5**, and 5-(phosphonoethyl)-5-deoxyquinate **6**. These observations, in turn, are consistent with the hypothesis that the phosphate monoester of DAHP mediates its own elimination.

Comparison of the inhibition behavior of these epimers with that of spirocyclic carbaphosphodiester **18** and **19** suggests that the enzyme active site does not stabilize the putative transition state that spirocyclic carbaphosphodiester mimics. However, this does not mean that the enzyme plays a minor role during the elimination of inorganic phosphate. The enzyme may play an important role to stabilize an E1cb-like transition state. The potent inhibition of DHQ synthase by both epimers of carbocyclic phosphates, or carbocyclic phosphonates might result from the in situ generated E1cb-like transition state analogues.

CHAPTER 3

EXPLOITING THE ACTIVE SITE INTERACTIONS OF MIP SYNTHASE WITH SUBSTRATE ANALOGUES AND INTERMEDIATE ANALOGUES

Using Phosphonates as Phosphate analogues

Phosphonates have been widely employed as analogues of naturally occurring phosphate esters.⁶³⁻⁶⁵ When used as analogues of phosphate esters, phosphonates possess intriguing possibilities for regulation or perturbation of the target biosystems. The rationale for the use of phosphonates as analogues of natural phosphates lies in the perceived isosteric relationship of the phosphate and its phosphonate mimic. Removal of the labile phosphate ester oxygen or substitution by a methylene group gives non-isosteric and isosteric phosphonate analogues respectively. The P-C bond is more stable and incapable of being hydrolyzed by the enzymes involved in phosphate cleavage.⁶⁶ As a substitute for a natural phosphate substrate, a phosphonate analogue may be capable of inhibiting or perturbing the regular activity of the target enzyme simply by not participating in the normal phosphate-involved process.

There are also significant differences between a phosphonate and phosphate ester. Upon substitution of the phosphate ester oxygen with an electron-donating alkyl group, there is a significant decrease in acidity of the phosphorus-containing acid function.⁶⁷ Another change is that of size and shape. Simply removing the phosphate ester oxygen would significantly decrease the overall size and shape of the resulting phosphonate relative to the parent phosphate ester. Substitution of the phosphate ester oxygen with a methylene group leads to a homophosphonate which is similar in size and shape relative to the parent phosphate ester. For most cases, it is true that an isosteric homophosphonate analogue is a

better mimic of the phosphate ester than the corresponding nonisosteric phosphonate analogue.⁶³

However, the isosteric analogue does not always lead to a better interaction with the enzyme active site when used as a substitute for a phosphate monoester. A series of phosphonate and homophosphonate analogues have been systematically studied as substrate analogues for the inhibition of DHQ synthase.^{7,60,61} For easy comparison, Table 5 lists the data reported by Knowles.⁷ Oxacyclic homophosphonate and carbocyclic homophosphonate, although isosteric to the native substrate DAHP, were poor inhibitors. By contrast, the nonisosteric oxacyclic phosphate and carbocyclic phosphate are much stronger inhibitors by more than three orders of magnitude than their homophosphonate counterparts.

Table 5. Inhibition of DHQ synthase by the phosphonate and homophosphonate substrate analogues.

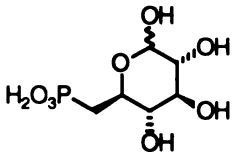
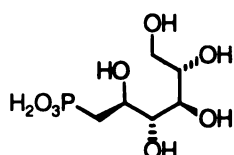
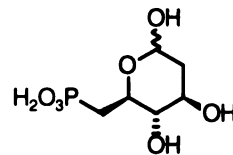
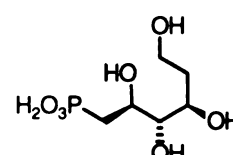
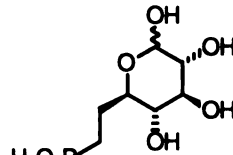
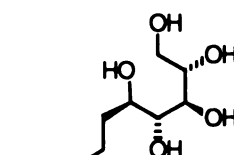
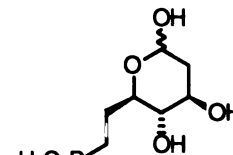
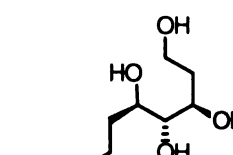
$K_i = 0.07 \mu\text{M}$	$K_i = 60 \mu\text{M}$	$K_i = 0.0008 \mu\text{M}$	$K_i = 2 \mu\text{M}$

Phosphonate and Homophosphonate Analogues of D-Glucose 6-Phosphate:
Substrate Analogues Designed for the Inhibition of MIP Synthase

The early stages of MIP synthase-catalyzed conversion of D-glucose 6-phosphate into *myo*-inositol 1-phosphate likely involve binding of the substrate to the active site and oxidation of the C-5 alcohol by enzyme bound NAD to generate 5-keto-D-glucose 6-phosphate (intermediate B', Figure 6). Mechanistic studies showed that these early stages are reversible. Intermediate B' could be reduced by NADH back to D-glucose 6-phosphate while incubated with apoenzyme-NADH complex.³⁴ Inhibition of MIP synthase with

substrate analogues revealed that removal of the C-2 hydroxyl group led to improved inhibition.^{34,46,47} The acyclic alditol phosphate analogues bind more tightly than the aldose counterparts.³⁴ However, there are some questions related to the early stages of the enzymatic reaction which are still not clear. These questions include whether isosteric or nonisosteric phosphonates are the best substrate analogues, and the contribution of each hydroxyl group to active-site binding.

Table 6. Phosphonate and homophosphonate substrate analogues of MIP synthase.

			
6-deoxy-D-glucose 6-phosphonate 20	6-deoxy-D-glucitol 6-phosphonate 21	2,6-dideoxy-D-glucose 6-phosphonate 22	2,6-dideoxy-D-glucitol 6-phosphonate 23
			
6-deoxy-D-glucose 6-homophosphonate 24	6-deoxy-D-glucitol 6-homophosphonate 25	2,6-dideoxy-D-glucose 6-homophosphonate 26	2,6-dideoxy-D-glucitol 6-homophosphonate 27

The first set of substrate analogues designed for initial screening of the inhibitors of MIP synthase was the series of phosphonate analogues of substrate D-glucose 6-phosphate listed in Table 6. In choosing the analogues to be examined, several factors were considered. Comparison of phosphonate versus homophosphonate inhibitors was intended to establish which of these nonhydrolyzable phosphate monoester analogues is the best mimic of the substrate's phosphate monoester bound in the enzyme active site. 2-Deoxy phosphonate analogues were chosen since the corresponding 2-deoxy phosphate analogues are among the best known inhibitors of MIP synthase. The glucitol phosphonate and

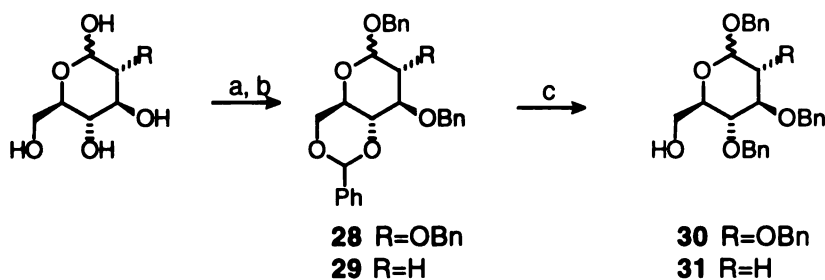
glucitol homophosphonate all exist exclusively in an acyclic form, The binding of these acyclic analogues was to be compared with substrate analogues which exist in solution as a mixture of acyclic and cyclic forms or exist in solution exclusively in a cyclic form. These comparisons would provide valuable clues to the puzzle of whether the acyclic form or the cyclic form of the substrate D-glucose 6-phosphate is bound to the active site of MIP synthase.

There are several possible phenomena that can result from the interaction of these organophosphonate analogues with MIP synthase. Analogues could bind to the enzyme, but the enzyme does not process the analogues into reaction intermediate analogues. This lack of C-5 alcohol oxidation would result in analogues which are just simply competitive inhibitors of D-glucose 6-phosphate binding to MIP synthase. Alternatively, the enzyme might partially process the bound phosphonate analogues by oxidation of the C-5 alcohol, thereby generating analogues of the reaction intermediates in situ at the enzyme active site. This scenario could lead to very potent inhibition of the enzyme, since the reaction intermediate analogues may bind the enzyme more tightly than the substrate analogues. Accompanying oxidation of the C-5 alcohol of the phosphonate analogues, NADH will be generated to form NADH-enzyme-intermediate analogue complexes detectable by UV-visible spectroscopy. Detection of NADH formation would provide the first direct evidence that NADH is involved in the catalysis. It is also possible that MIP synthase might process the phosphonate analogues all the way to inositol analogues. These inositol analogues, in vivo, could be used to perturb inositol metabolism.

Syntheses of Phosphonate Analogues of D-Glucose 6-Phosphate

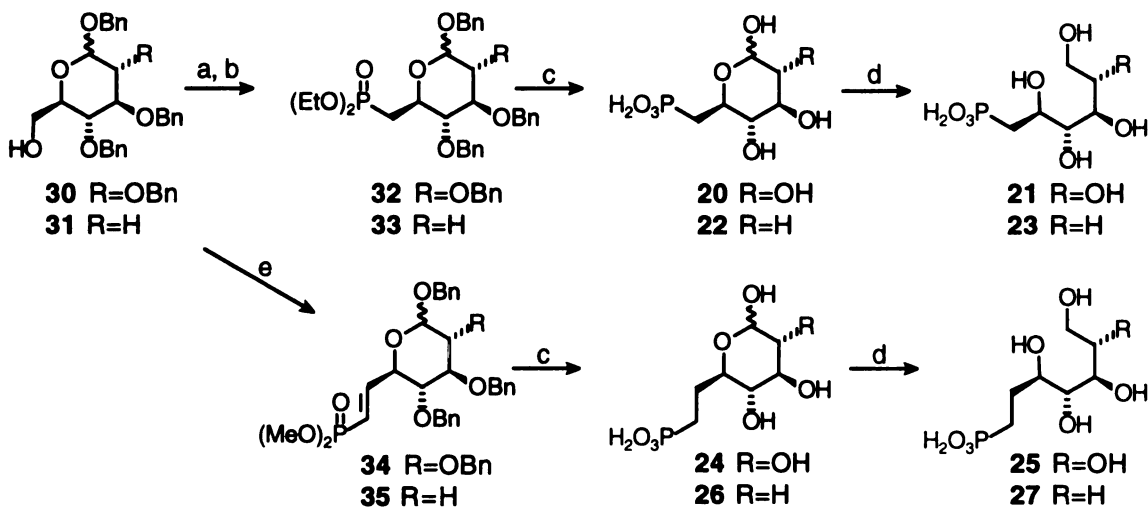
2,6-Dideoxy-D-glucose 6-phosphonate **22** was prepared using the procedure previously developed in our group for preparation of 6-deoxy-D-glucose 6-phosphonate **20**.⁶⁸ The synthesis of homophosphonate analogues was accomplished using a procedure modified from that previously reported by Le Marechal.⁶¹ All glucitol phosphonate

analogues were obtained by reducing their aldose precursors with sodium borohydride in water.



(a) For 2-deoxy D-glucose: i) BnOH, HCl(g); ii) PhCH(OCH₃)₂, TsOH, DMF, 60°C; for D-glucose: i) BnOH, TsOH, ii) PhCHO, ZnCl₂; (b) BnBr, NaH, DMF, THF; (c) LiAlH₄, AlCl₃, Et₂O, CH₂Cl₂, reflux.

Figure 14. Syntheses of intermediates **30** and **31**.



(a) NBS, PPh₃, DMF; (b) P(OEt)₃, reflux; (c) i) Me₃SiBr, CH₂Cl₂, Et₃N; ii) H₂, Pd/C, MeOH; (d) NaBH₄, H₂O, 0°C; (e) i) (COCl)₂, DMSO, Et₃N, CH₂Cl₂, -78°C; ii) [(MeO)₂P(O)]₂CH₂, *n*-BuLi, THF, -78°C.

Figure 15. Synthesis of phosphonate analogues.

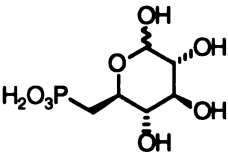
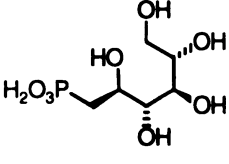
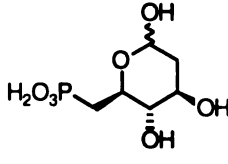
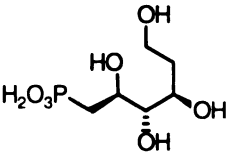
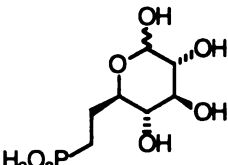
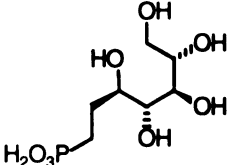
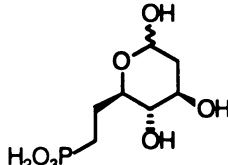
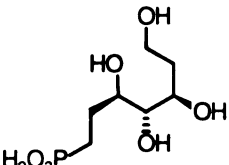
Sequential treatment of D-glucose with benzyl alcohol and benzaldehyde followed by benzylation with benzyl bromide and sodium hydride afforded fully protected D-glucose **28**. Cleavage of the benzylidene acetal with lithium aluminum hydride-aluminum trichloride generated a common intermediate **30**, subsequently used for synthesis of substrate analogues **20**, **21**, **24**, and **25**. Bromination of the primary alcohol of the common intermediate **30** followed by Arbuzov condensation with triethylphosphite produced fully protected phosphonate **32**. Deprotection of the ethyl esters with bromotrimethylsilane followed by hydrogenolysis over palladium afforded 6-deoxy-D-glucose 6-phosphonate **20**. Reducing **20** with sodium borohydride in water gave 6-deoxy-D-glucitol 6-phosphonate **21**. Synthesis of the homophosphonate series began with the same common intermediate **30**. Swern oxidation of the primary alcohol of the common intermediate **30** followed by the Wadsworth-Horner-Emmons reaction⁶⁹ of the resulting aldehyde with the anion of tetramethyl methylene diphosphonate formed the fully protected (*E*)-vinylphosphonate **34**. Removal of the benzyl protecting groups and reduction of the olefine gave the desired products 6-deoxy-D-glucose 6-homophosphonate **24** and 6-deoxy-D-glucitol 6-homophosphonate **25**. Using same procedure, 2,6-dideoxy-D-glucose 6-phosphonate **22**, 2,6-dideoxy-D-glucitol 6-phosphonate **23**, 2,6-dideoxy-D-glucose 6-homophosphonate **25**, 2,6-dideoxy-D-glucitol 6-homophosphonate **27** were prepared from 2-deoxy-D-glucose.

Enzymology Associated with the Phosphate and Homophosphonate Analogues

MIP synthase was purified from an *E. coli* strain recently constructed by the Frost group⁷⁰ to overproduce MIP synthase. The assay of inhibition for MIP synthase was performed in a buffer at pH 7.7 consisting of 50 mM Tris HCl, 2 mM ammonium chloride, 0.2 mM dithiothreitol and 1 mM NAD at 37 °C. After the reaction was initiated by adding enzyme into a buffer containing substrate and inhibitor, aliquots were withdrawn at timed intervals and quenched with 20% trichloroacetic acid. Selective oxidation of product MIP

in each quenched aliquot with sodium periodate at 37 °C for 1 h resulted in the quantitative release of inorganic phosphate.⁷¹ After quenching excess sodium periodate with sodium sulfite, the inorganic phosphate was measured by colorimetric assay.⁷²

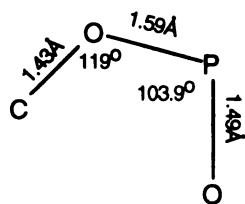
Table 7. Inhibition of MIP synthase by phosphonate and homophosphonate analogues.

 <p>20 no inhibition</p>	 <p>21 no inhibition</p>	 <p>22 no inhibition</p>	 <p>23 no inhibition</p>
 <p>24 $K_i = 4.9 \text{ mM}$</p>	 <p>25 $K_i = 0.11 \text{ mM}$</p>	 <p>26 $K_i = 0.071 \text{ mM}$</p>	 <p>27 $K_i = 0.0058 \text{ mM}$</p>

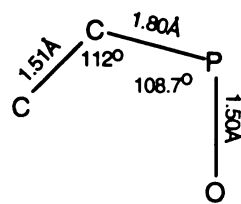
Among the phosphonate analogues tested, all of the isosteric homophosphonate analogues are inhibitors of MIP synthase. 6-Deoxy-D-glucose 6-homophosphonate **24**, 6-deoxy-D-glucitol 6-homophosphonate **25**, 2,6-dideoxy-D-glucose 6-homophosphonate **26**, and 2,6-dideoxy-D-glucitol 6-homophosphonate **27** were found to be competitive inhibitors with K_i values of 4.9 mM, 0.11 mM, 0.071 mM and 0.0058 mM, respectively (Table 7). None of the nonisosteric phosphonates inhibited MIP synthase at concentrations up to 1 mM. These results are very different from those observed with DHQ synthase.^{7,60,61} For DHQ synthase, the nonisosteric phosphonate analogues of substrate DAHP are better inhibitors than the isosteric homophosphonate analogues (Table 5). The

K_i values for nonisosteric phosphonate analogues of DAHP are three orders of magnitude lower than that of the isosteric homophosphonate analogues.

The lack of binding affinity of nonisosteric phosphonates to MIP synthase may result from the significant change in physical size and shape of these analogues relative to D-glucose 6-phosphate. This may consequently preclude binding interaction between the phosphonate moiety of the substrate analogues and the active site binding residues which normally interact with the phosphate monoester of D-glucose 6-phosphate. The homophosphonate analogues are better inhibitors. One possible explanation is that they can better fit the active site of MIP synthase. Using available crystallographic data⁷³ for the related compounds, 2-aminoethyl phosphate and 2-aminoethyl phosphonate, the relative positions, bond angles, the bond lengths, and overall size for a phosphate and its homophosphonate analogue are reasonably close.



2-aminoethyl phosphate



2-aminoethyl phosphonate

Phosphonic acids are also significantly weaker acids than phosphate monoesters. This can result in different ionization states in solution for phosphonates relative to phosphate monoesters at the same solution pH values. When the assay of MIP synthase inhibition was carried out at variable pH, we found the inhibition of MIP synthase by the homophosphonate analogues was enhanced as the pH increased. When MIP synthase was incubated with 2.5 mM of substrate D-glucose 6-phosphate, 0.25 mM 2,6-dideoxy-D-glucitol 6-homophosphonate **27** inhibited the reaction by 33%, 53%, 75%, and 82% at pH 6.4, 7.2, 7.6, and 8.4, respectively. The pK_a values of 2,6-dideoxy-D-glucose 6-homophosphonate **26**, 2,6-dideoxy-D-glucitol 6-homophosphonate **27**, and D-glucose 6-

phosphate were determined by titrimetric analysis. The second dissociation constant pK_a of 7.55 for **26** and 7.52 for **27** are significantly higher than the pK_a of 5.95 for D-glucose 6-phosphate.

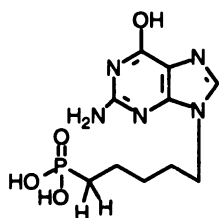
By comparing the K_i values of 6-deoxy-D-glucose 6-homophosphonate **24** ($K_i = 4.9$ mM), 2,6-dideoxy-D-glucose 6-homophosphonate **26** ($K_i = 0.071$ mM), 6-deoxy-D-glucitol 6-homophosphonate **25** ($K_i = 0.112$ mM) and 2,6-dideoxy-D-glucitol 6-homophosphonate **27** ($K_i = 0.0058$ mM), it is apparent that exclusively acyclic alditol homophosphonates **25** and **27** bind more tightly than the predominantly cyclic aldose homophosphonates **24** and **26**. These results are consistent with that of literature reports³⁴ that the acyclic alditol phosphate analogues are better inhibitors than predominantly cyclic aldose phosphate analogues. At this time, there is still not enough evidence to reach the final conclusion whether the enzyme initially binds the substrate in cyclic or acyclic form. However, it is clear that the enzyme can bind to the acyclic form of substrate and its analogues, and it seems the enzyme binds to the acyclic form more tightly. Removal of the C-2 hydroxyl group leads to more potent inhibitors. This result is also consistent with the observation made from the studies on the phosphate analogue inhibitors. Reduction of the aldose and removal of the C-2 hydroxyl group have an additive effect with 2,6 dideoxy-D-glucitol 6-homophosphonate **27** being the best inhibitor of MIP synthase among the phosphonate analogues tested.

When MIP synthase was incubated with homophosphonate analogues in the presence of NAD, an increase in absorbance at 340 nm was detected, which provided the first evidence for the formation of the enzyme-bound NADH during MIP synthase catalysis. Furthermore, this experiment also indicated that the rate of NADH formation correlates well with the inhibition potency of the analogues. The oxidation of homophosphonate substrate analogues by enzyme-bound NAD at the C-5 position suggests that these analogues bind to the active site in a conformation similar to that of the actual substrate D-glucose 6-phosphate. Barnett^{34b} suggested that the enzyme might bind

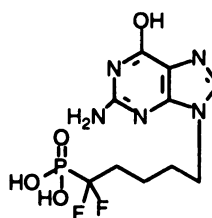
the substrate in acyclic form before oxidation at C-5 occurs, based on the observation that the acyclic phosphate analogues bind more tightly to MIP synthase than the corresponding cyclic phosphate analogues. Now the NADH formation during incubation of MIP synthase with the acyclic homophosphonate substrate analogues provide direct evidence that the acyclic form can bind to the enzyme active site and consequently be oxidized. More detail on NADH formation will be discussed later (Chapter 4).

*α,α -gem-Difluorohomophosphonate Analogues:
An Attempt to Improve the Inhibition Properties*

Our investigation showed that the inhibition of MIP synthase by homophosphonate substrate analogues improved with increasing pH. The determination of the second dissociation constants pK_a revealed that homophosphonates **26** and **27** exist as a monobasic/dibasic mixture while the native substrate D-glucose 6-phosphate predominantly exists in dibasic form under the assay conditions. The pH dependent behavior of the inhibition might result from the change in the monobasic/dibasic ratio at different pH. The pH-dependent behavior of the homophosphonate on inhibition of MIP synthase might be improved by reducing the pK_a value of the phosphonate analogue to increase the population of the dibasic form at physiological pH.



9-(5-phosphonopentyl)
guanine
 $K_i = 320 \text{ nM}$

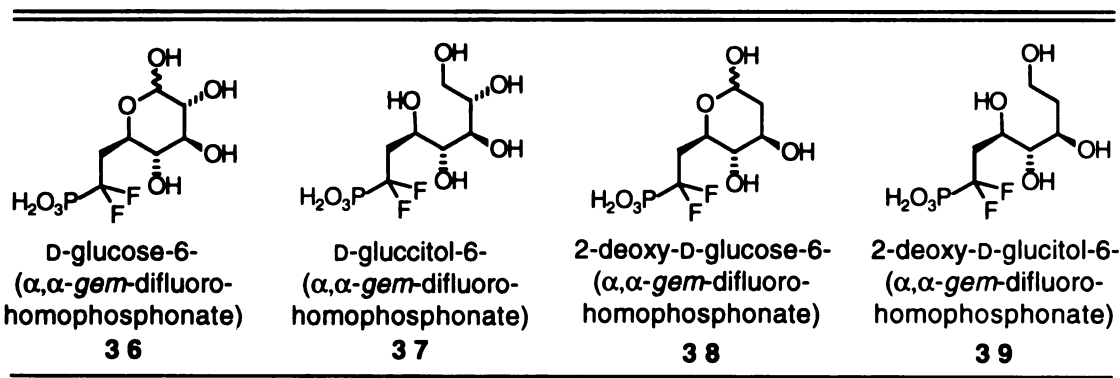


9-(5,5-difluoro-5-phosphonopentyl)
guanine
 $K_i = 18 \text{ nM}$

Blackburn and co-workers⁶⁴ suggested that mono and difluorinated phosphonates should have greater potential for biological activity than nonfluorinated phosphonates as

analogues of phosphate esters. Fluorinated phosphonates have been proposed to be isosteric and isopolar analogues of phosphate esters. Recently, Halazy and co-workers⁷⁴ reported the synthesis of 9-(5,5-difluoro-5-phosphonopentyl)guanine and compared it with the corresponding nonfluorinated phosphonate as inhibitors of purine nucleoside phosphorylase from four different origins. The result was that the difluorophosphonate derivative was a superior inhibitor relative to the phosphonate. The fluorinated phosphonate analogue had a K_i values 5- to 26-fold lower than that of the corresponding nonfluorinated phosphonate analogue. The difference between K_i values was even more pronounced when the inhibition study was performed at low pH. The marked difference was explained by the second dissociation constant of the fluorinated phosphonate ($pK_a = 5.3$), which is lower relative to the dissociation of the same proton in the nonfluorinated phosphonate ($pK_a = 7.2$). The fluorinated phosphonate analogue could also restore H-bonding which might be important with the phosphate monoester oxygen.

Table 8. α,α -gem-difluorohomophosphonate analogues of D-glucose 6-phosphate.

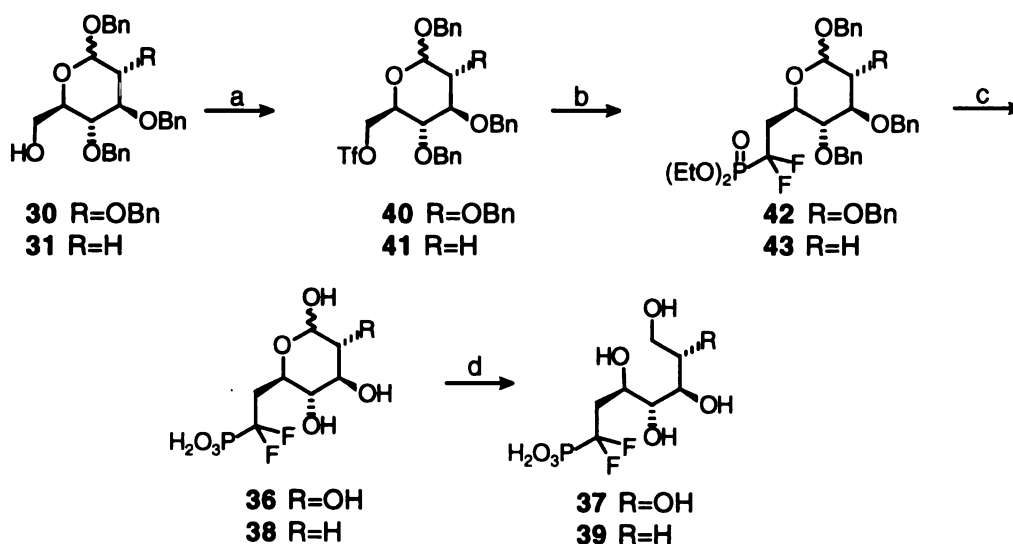


Based on the above reasoning, a difluorophosphonate series (Table 8, **36-39**) was designed in an attempt to improve inhibition properties of phosphonate analogues. These difluorophosphonate analogues differed from the homophosphonate analogues previously investigated by replacement of the methylene group immediately adjacent to the phosphonic acid with a *gem*-difluoromethylene group. Replacement of the electron-donating methylene

group by an electron withdrawing α,α -gem-difluoromethylene group was anticipated to cause significant increase in the acidity of the phosphonic acid. The fluorinated homophosphonates would therefore be predominantly in a dibasic form which is similar to the phosphate substrate at physiological pH.

Synthesis of α,α -gem-Difluorohomophosphonate Analogues

A variety of routes for the synthesis of fluorophosphonate have been developed.⁷⁵⁻⁷⁹ One of the most widely used synthetic approaches to the difluoroalkylphosphonates relies upon the construction of P-CF₂ bond via a Michaelis-Becker reaction.⁷⁵ Recently, Berkowitz⁷⁹ developed a synthetic methodology for the synthesis of (α,α -difluoroalkyl)phosphonates. Activating the primary alcohol of monosaccharides with a triflate and subsequently displacing the triflate by diethyl (lithiodifluoromethyl)phosphonate provides an expedient entry into a variety of (difluoroalkyl)phosphonate analogues of the monosaccharide phosphates.



(a) Tf₂O, pyr, CH₂Cl₂, -30°C; (b) (EtO)₂(O)PCF₂H, LDA, HMPA, THF, -78°C; (c) i) TMSI, Et₃N, CH₂Cl₂, H₂O, ii) for **42**: H₂, Pd/C, MeOH, HOAc, for **43**: H₂, Pd/C, THF, H₂O; (d) NaBH₄, H₂O.

Figure 16. Synthesis of difluorohomophosphonates.

The difluorohomophosphonate analogues **36**, **37**, **38**, and **39** were synthesized (Figure 16) from intermediates **30** and **31** using Berkowitz's methodology.⁷⁹ Treatment of **30** and **31** with triflic anhydride gave **40** and **41**, which were stable enough to be purified by silica gel chromatography. Subsequent displacement of the triflate with diethyl (lithiodifluoromethyl)phosphonate in HMPA-THF at -78 °C provided the fully protected α,α -gem-difluorohomophosphonate **42** and **43**. Diethyl phosphonate ester protection was then removed by treatment of **42** and **43** with TMSI and triethylamine in methylene chloride and subsequent hydrolysis with water. Hydrogenolysis of **42** in MeOH-HOAc yielded **36**. Although hydrogenolysis of **43** in MeOH-HOAc gave a mixture of several species, debenzylation of **43** in THF-water provided clean **38**. Both **36** and **38** were then separately purified by anion exchange chromatography using AG1-X8 resin. Reduction of **36** and **38** with sodium borohydride in water gave the glucitol derivatives **37** and **39**.

Kinetic Evaluation of α,α -gem-Difluorohomophosphonate Analogues

The interactions of these α,α -gem-difluorohomophosphonate analogues with MIP synthase were then examined. As expected, replacement of the methylene group of the homophosphonates by an α,α -gem-difluoromethylene group considerably decreased the second dissociation constant. Values of the pK_a for fluorinated homophosphonates **38** and **39** were found to be 5.20 and 5.05 respectively by titrimetric analysis. By comparison, the non-fluorinated homophosphonate counterparts **26** and **27** have a pK_a value of 7.55 and 7.52 respectively. However, the α,α -gem-difluorohomophosphonate analogues either failed to inhibit MIP synthase or were only weak inhibitors. When incubated with MIP synthase in the buffer containing 1.2 mM D-glucose 6-phosphate, 1 mM NAD at pH 7.7, **36**, **37**, **39** were not inhibitory at concentration up to 1 mM, and **38** was found to be a weak inhibitor with $K_i = 0.85$ mM (calculated from I_{50}). When incubated with the enzyme

in the presence of NAD, none of the α,α -*gem*-difluorohomophosphonate analogues caused an increase in absorbance at 340 nm.

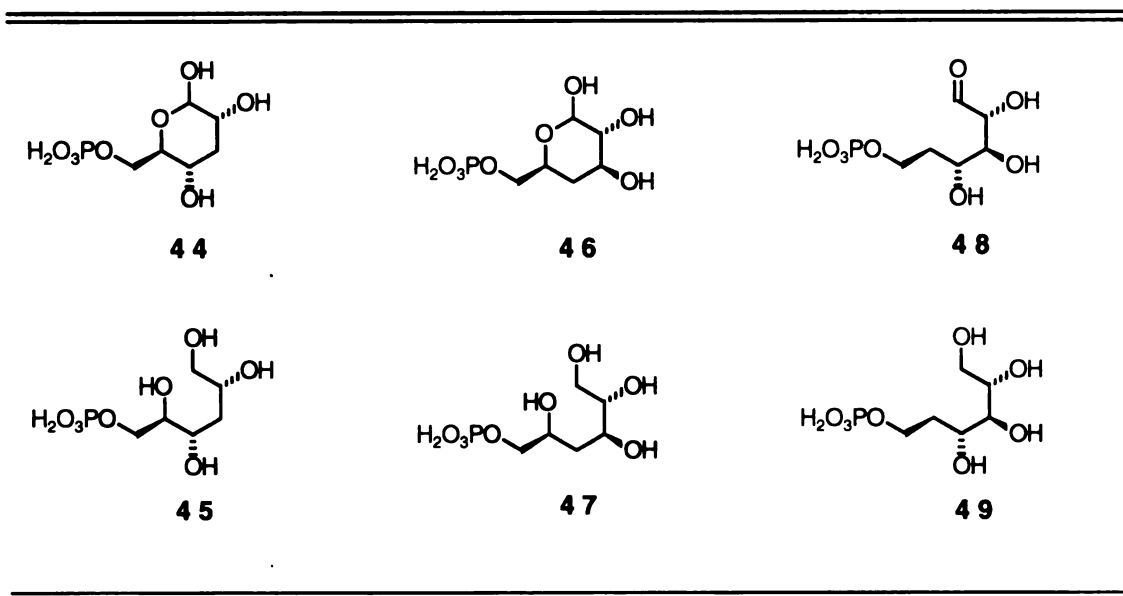
The failure of the α,α -*gem*-difluorohomophosphonate analogues to bind to the enzyme indicates that these analogues are poor mimics for the parent phosphate ester. Recently, Thatcher *et al*⁶⁵ explored the possibility of using fluorophosphonate as an analogue of native phosphate with *ab initio* SCF calculation. The results suggest that, despite the isopolar relationship of fluoromethyl phosphonate and the parent phosphate, binding at an active site may be considerably perturbed for the fluoromethyl phosphonate analogues. Replacement of divalent oxygen by tetracoordinate difluoromethylene group increases the steric requirement at this position. The C-F bonds are about 40% longer than the C-H bonds, and the van der Waals volume of -CF₃ is twice that of -CH₃. Thus steric perturbation alone may disrupt active site binding of the α,α -*gem*-difluorohomophosphonate analogues. A further effect of the bulky difluoromethylene linkage is the significantly increased barrier to rotation about the P-C bond as compared with the P-O bond of the phosphate.⁶⁵ From these calculations and consideration of the calculated molecular geometry, conformational preference, and electrostatic potential of α,α -*gem*-difluorophosphonates, Thatcher *et al*⁶⁵ suggested that ground-state active site binding may be significantly perturbed for the α,α -*gem*-difluorophosphonate thereby diminishing the ability of the analogue to mimic a phosphate monoester. Recently, Gross *et al* synthesized both *E*-fluorovinyl phosphonate and *Z*-fluorovinyl phosphonate analogues of D-glucose 6-phosphate as potential inhibitors of MIP synthase.⁸⁰ However, both analogues failed to show any inhibition at concentration > 5 mM toward partially purified MIP synthase from bovine testis. Although there have been some successful examples^{75,81} of using fluorinate phosphonates as analogues of phosphate monoesters, this work with MIP synthase and other reports in the literature suggest that it is questionable whether a α,α -*gem*-difluorophosphonate can be considered in general as isosteric and isopolar mimic to a phosphate monoester.

Another possible reason for the failure of inhibition of MIP synthase by the α,α -*gem*-difluorohomophosphonate analogues might be the increased redox potential at the C-5 position. Attaching a strong electron-withdrawing α,α -*gem*-difluoromethylene group to the carbon adjacent to the C-5 alcohol may make oxidation of this center more difficult. Oxidation of the C-5 alcohol and resulting generation of the C-5 oxidized reaction intermediate analogue may be responsible for potent inhibition of MIP synthase. Anything interfering with this oxidation might be expected to diminish the extent of enzyme inhibition.

The Deoxy Substrate Analogues:
Probes for the Contribution of Individual Hydroxyl Groups to Active Site Binding

In previous investigations, 2-deoxy derivative analogues of D-glucose 6-phosphate were found to be the most potent class of MIP synthase inhibitors.^{34,46,47} We also found that these 2-deoxy derivative analogues could bind to the active site of the enzyme and subsequently be oxidized. Beyond the C-2 secondary alcohol, the contribution to the active site binding for the remaining secondary alcohols of D-glucose 6-phosphate is unknown. The only information about the secondary alcohol's roles in binding is from the inhibition studies for galactose 6-phosphate, mannose 6-phosphate, and allose 6-phosphate (Chapter 1, Table 2). Each of these molecules possesses a secondary alcohol with inverted stereochemistry with respect to the same asymmetric center in D-glucose 6-phosphate.^{20b,25,34,45} Since the data were collected from different sources, it is difficult to draw definitive conclusions from the data. A possible way to clarify ambiguity was to evaluate a series of monodeoxy analogues (Table 9). In addition, investigation of the monodeoxy D-glucose 6-phosphate analogues would provide valuable insights into the minimum structure requirements necessary for binding of substrate analogues to the active site.

Table 9. Deoxy substrate analogues.

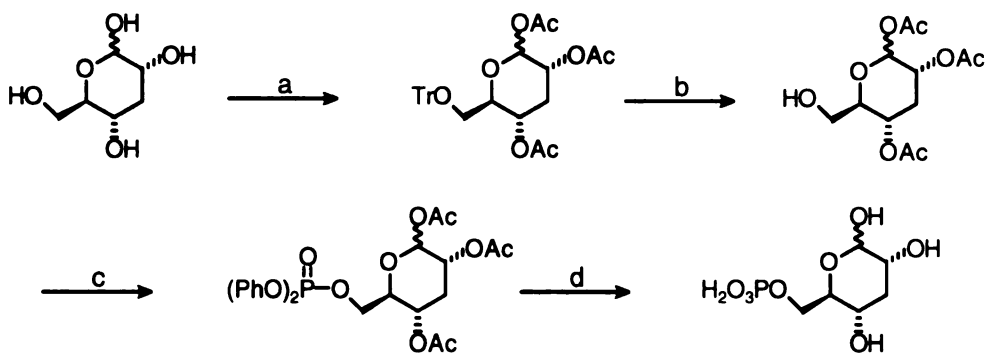


Synthetic Approaches to the Deoxy Substrate Analogues

Numerous synthetic methods have been developed for the preparation of deoxy saccharide derivatives. These methods are mainly based on reductive removal of the hydroxyl from the corresponding parent sugar precursors. The methods include hydrogenation of iodo or chloro sugar derivatives over Pd or Raney Ni, or radical deoxygenation with tributyltin hydride,⁸² reductive desulfurization of benzoylthio sugar derivatives with Raney Ni,⁸³ cleavage of an epoxide ring with hydrogen in the presence of Raney Ni⁸⁴, and reductive homolytic cleavage of a variety of thionocarbonyl derivatives with tributyltin hydride.^{85,86}

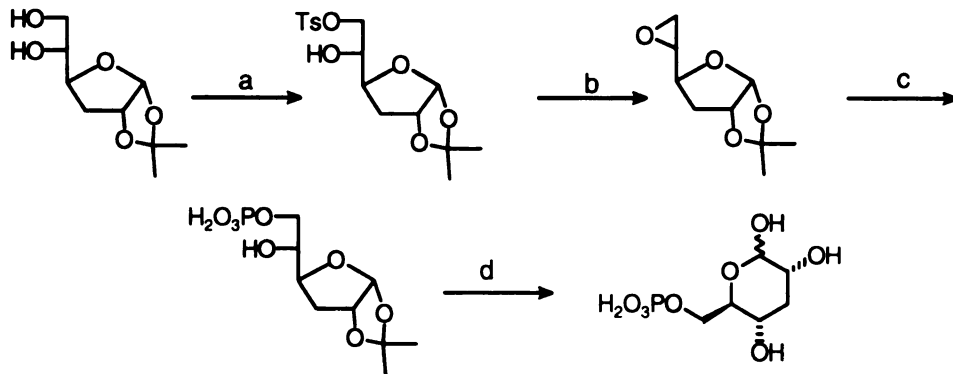
3-Deoxy-D-glucose 6-phosphate **44** has been previously synthesized by Dahigard *et al.*⁸⁷ and Szabo *et al.*⁸⁸ Dahigard's synthesis (Figure 17) began from 3-deoxy D-glucose, which was prepared from D-glucose.^{82b} 3-Deoxy D-glucose was treated with triphenylmethyl chloride and then with acetic anhydride in pyridine to afford a fully protected precursor. After removal of the trityl protecting group, the primary alcohol was

phosphorylated with diphenylphosphorochloridate. Hydrogenolysis over platinum and subsequent acid hydrolysis produced 3-deoxy-D-glucose 6-phosphate **44**.



(a) i) TrCl, Pyr, ii) Ac₂O, Pyr, 36%; (b) HBr, HOAc, 72%; (c) (PhO)₂P(O)Cl, Pyr, 84%; (d) i) H₂, PtO₂, 87%; ii) 0.6 N HBr (aq.), 100°C, 43%.

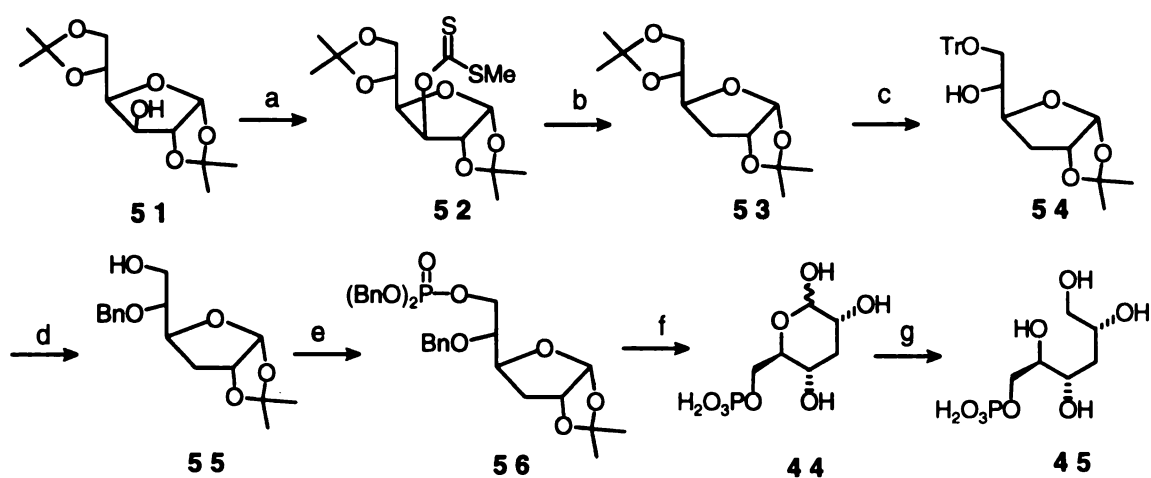
Figure 17. Dahigard and Kaufmann's synthesis of 3-deoxy glucose 6-phosphate.



(a) *p*-TsCl, Pyr, CHCl₃, 90%; (b) NaOMe, CHCl₃, -78°C, 62%; (c) K₂HPO₄, H₂O, 50°-60°C, 63%; (d) IR-120(H⁺), 100°C, 13 min. 95%.

Figure 18. Szabo and Szabo's synthesis of 3-deoxy glucose 6-phosphate.

In another approach, the known 3-deoxy-1,2-*O*-isopropylidene-D-glucofuranose^{82d,84} was used as starting material for the synthesis of 3-deoxy-D-glucose 6-phosphate **44** by Szabo *et al*⁸⁸ (Figure 18). Reaction of the starting material with *p*-toluene sulfonyl chloride yielded the C-6 tosylate, which upon treatment with sodium methoxide gave a 5,6-anhydro derivative. Reaction of the epoxide with inorganic phosphate selectively introduced the phosphate moiety to the C-6 position. 3-Deoxy-D-glucose 6-phosphate **44** was then obtained after acid hydrolysis.

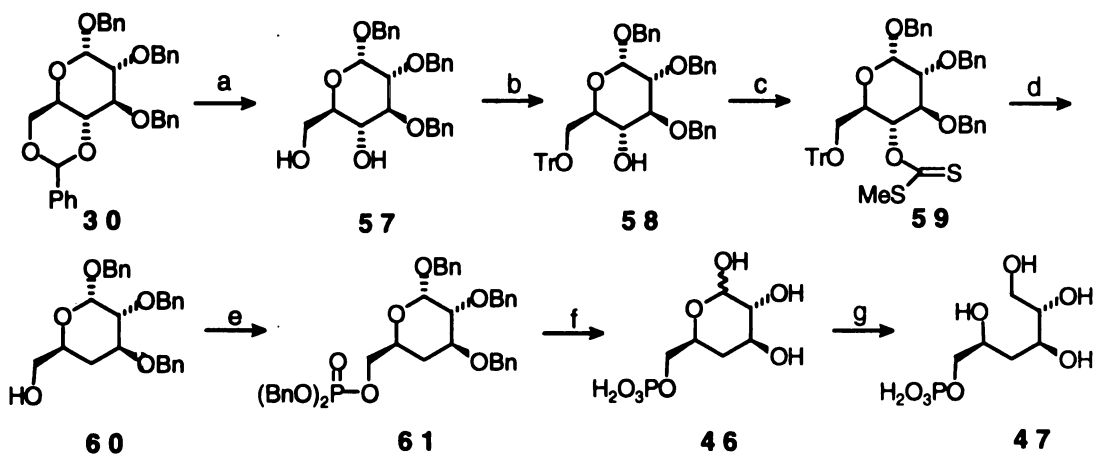


(a) NaH, CS₂, MeI, THF, reflux, 66%; (b) Bu₃SnH, AIBN, benzene, reflux, 82%; (c) i) 0.2 N HCl, ii) TrCl, Et₃N, CH₂Cl₂, 59%; (d) i) NaH, BnBr, THF, DMF, 90%; ii) HCO₂H, Et₂O, 64%; (e) i) (BnO)₂PN(*i*-Pr)₂, tetrazole, CH₂Cl₂, ii) *m*CPBA, CH₂Cl₂, -40°C, 90%; (f) i) H₂, Pd/C, THF, H₂O, ii) Dowex 50 (H⁺), 50°C, 45%; (g) NaBH₄, H₂O, 100%.

Figure 19. Synthesis of 3-deoxy glucose 6-phosphate.

Our synthesis of 3-deoxy-D-glucose 6-phosphate **44** used commercially available 1,2;5,6-diisopropylidene-D-glucofuranose **51** as the starting material (Figure 19). 3-Deoxy-1,2;5,6-diisopropylidene-D-glucofuranose **53** was prepared according to a literature procedure.⁸⁶ Careful hydrolysis of **53** with dilute acid selectively removed the 5,6-isopropylidene protecting group. Subsequent protection of the primary alcohol with a trityl ether gave **54**. The secondary hydroxyl group of **54** was protected with acetate.

However, the following hydrolysis of the trityl protecting group also resulted in migration of the acetate to the C-6 primary alcohol. To avoid the migration, a benzyl protecting group was used. After protecting the C-5 hydroxyl group with a benzyl ether and deprotecting the C-6 alcohol, the resulting intermediate **55** was phosphorylated with *N,N*-diisopropyl dibenzyl phosphoramidite and *m*CPBA⁸⁹ to provide fully protected product **56**. Hydrogenolysis over Pd/C in THF-water, and hydrolysis with Dowex 50 (H⁺) gave 3-deoxy-D-glucose 6-phosphate **44**, which was then purified by anion exchange chromatography using AG1-X8 resin.

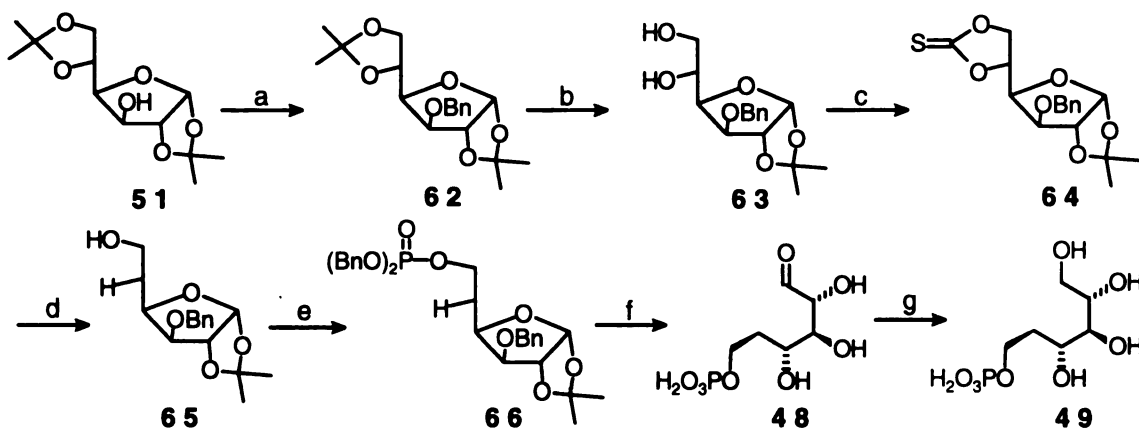


(a) *p*-TsOH, MeOH, (b) TrCl, Et₃N, CH₂Cl₂, 100%; (c) NaH, CS₂, MeI, THF, reflux, 90%; (d) i) Bu₃SnH, AIBN, benzene, reflux, ii) HCO₂H, Et₂O, 85%; (e) i) (BnO)₂PN(*i*-Pr)₂, tetrazole, CH₂Cl₂, ii) *m*CPBA, CH₂Cl₂, -40°C, 90%; (f) H₂, Pd/C, THF, H₂O, 70%; (g) NaBH₄, H₂O, 100%.

Figure 20. Synthesis of 4-deoxy glucose 6-phosphate.

Although 4-deoxy-D-glucose has been known for quite a long time,⁹⁰ the synthesis of 4-deoxy-D-glucose 6-phosphate **48** has not been reported. Benzyl 2,3-dibenzyl-6-triphenylmethyl-D-glucopyranoside **58** was prepared by acid hydrolysis of the benzylidene **30** (Figure 20).⁶⁸ Selective protection of the primary alcohol with trityl ether yielded **58** with a free C-4 hydroxyl group. Treating **58** with sodium hydride, carbon disulfide, and

methyl iodide⁸⁵ produced the methylthio thiocarbonate **59**. Refluxing **59** with tributyltin hydride and AIBN in benzene, and sequential treatment with formic acid in ether gave the 4-deoxy derivative **60**, which was then phosphorylated with *N,N*-diisopropyl dibenzyl phosphoramidite to give the fully protected 4-deoxy-D-glucose 6-phosphate **61**. Hydrogenolysis over palladium on carbon removed all protecting groups to provide 4-deoxy-D-glucose 6-phosphate **46**, which was then purified by anion exchange chromatography.

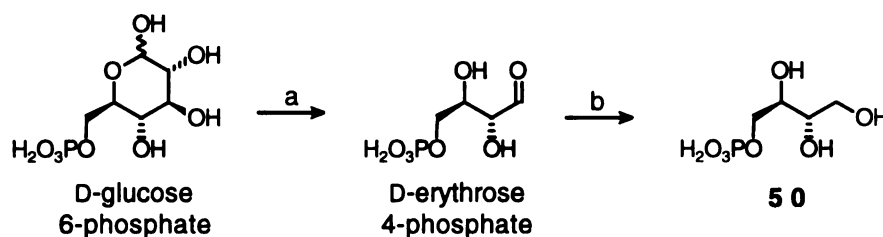


(a) NaH, BnBr, THF, DMF, 86%; (b) 60% aq. HOAc, 35°C, 82%; (c) Im₂CS, THF, reflux, 93%; (d) Bu₃SnH, AIBN, benzene, reflux, 63%; (e) i) (BnO)₂PN(*i*-Pr)₂, tetrazole, CH₂Cl₂, ii) *m*CPBA, CH₂Cl₂, -40°C, 86%; (f) i) H₂, Pd/C, THF, H₂O, ii) Dowex 50 (H⁺), 50°C, 100%; (g) NaBH₄, H₂O, 100%.

Figure 21. Synthesis of 5-deoxy glucose 6-phosphate.

5-Deoxy-D-glucose 6-phosphate **48** was also synthesized from 1,2;5,6-diisopropylidene-D-glucofuranose **51** (Figure 21). Thionocarbonate **64** was prepared according to the literature procedure.⁹⁷ Treatment of 1,2;5,6-diisopropylidene-D-glucofuranose **51** with sodium hydride, and benzyl bromide in THF-DMF gave intermediate **62**.⁹¹ Upon stirring with 60% aqueous acetic acid at 35 °C, the 5,6-isopropylidene was selectively removed to give diol **63**. Refluxing diol **63** with *N,N*-thiocarbonyl diimidazole in THF generated thionocarbonate **64**, which was then refluxed

with tributyltin hydride and small amount of AIBN as free radical initiator to yield the 5-deoxy intermediate **65**.⁸⁵ The regioselectivity is due to the higher stability of secondary relative to primary carbon radical. Phosphorylation of **65** gave the protected product. Sequential hydrogenolysis and hydrolysis gave 5-deoxy-D-glucose 6-phosphate **48**. 3-Deoxy-D-glucitol 6-phosphate **45**, 4-deoxy-D-glucitol 6-phosphate **47**, and 4-deoxy-D-glucitol 6-phosphate **49** were prepared from corresponding aldose precursors **44**, **46**, and **48**, respectively, by reduction with sodium borohydride in water.



(a) $\text{Pb}(\text{OAc})_4$, HOAc , H_2SO_4 ; (b) NaBH_4 , H_2O , 67% overall yield.

Figure 22. Synthesis of D-erythritol 4-phosphate **50**.

Erythritol 4-phosphate **50** was made from D-glucose 6-phosphate (Figure 22). Oxidation of D-glucose 6-phosphate with lead tetraacetate in acetic acid containing sulfuric acid, as described in the literature,⁹² gave erythrose 4-phosphate which was purified by anion exchange chromatography to remove unreacted D-glucose 6-phosphate. Erythrose 4-phosphate was reduced with sodium borohydride in water. After acidification and azeotropic removal of boric acid with methanol, erythritol 4-phosphate **50** was obtained in 67% overall yield.

Kinetic Evaluation of the Deoxy Substrate Analogues

The inhibitory behaviors of **44-50** toward MIP synthase were examined. All of the deoxy D-glucose 6-phosphate and deoxy D-glucitol 6-phosphate analogues were found to

be either weak inhibitors or inactive. 4-Deoxy-D-glucose 6-phosphate **46**, and 5-deoxy-D-glucose 6-phosphate **48** showed no inhibition at concentrations up to 1 mM, while 3-deoxy-D-glucose 6-phosphate **44**, 3-deoxy-D-glucitol 6-phosphate **45**, 4-deoxy-D-glucitol 6-phosphate **47**, and 5-deoxy-D-glucitol 6-phosphate **49** exhibited weak inhibition of the enzyme with $K_i = 0.59$ mM, 0.26 mM, 0.93 mM, and 1.5 mM respectively. Erythritol 4-phosphate **50** was found to be a surprisingly potent inhibitor of MIP synthase with $K_i = 0.047$ mM. When 3-deoxy-D-glucose 6-phosphate **44** or 3-deoxy-D-glucitol 6-phosphate **45** was incubated with MIP synthase in the presence of NAD, no increase in absorbance at 340 nm was detected (Table 10). On the other hand, incubation of 4-deoxy-D-glucose 6-phosphate **46**, 4-deoxy-D-glucitol 6-phosphate **47**, or erythritol 4-phosphate **50** with MIP synthase in the presence of NAD led to an increase in absorbance at 340 nm, indicating that the hydroxyl group corresponding to the C-5 alcohol of the substrate was oxidized. The rate of NADH formation for erythritol 4-phosphate **50** was much faster than that for 4-deoxy-D-glucitol 6-phosphate **47**. Although 4-deoxy-D-glucose 6-phosphate **46** did not show inhibition toward the enzyme at 1 mM concentration, a low level of NADH formation was detected when 4-deoxy-D-glucose 6-phosphate **46** was incubated with the enzyme and NAD. The rate of NADH formation associated with 4-deoxy-D-glucose 6-phosphate **46** was much slower than that of 4-deoxy-D-glucitol 6-phosphate **47**, and only reached about 20% of the level relative to **47**. Table 10 lists substrate analogues tested for formation of enzyme-bound NADH.

Along with the analogues **44-50** (Table 11), arabinitol 5-phosphate **67**, 1-deoxy arabinitol 5-phosphate **68**, and glycerol 1-phosphate **69** were also examined by the Frost group.⁹³ Arabinitol 5-phosphate **56** and 1-deoxy arabinitol 5-phosphate **68** were found to be competitive inhibitors with $K_i = 0.017$ mM and 0.008 mM respectively, while glycerol 1-phosphate **69** was not an inhibitor of MIP synthase.

Table 10. Compounds tested for formation of MIP synthase-bound NADH.

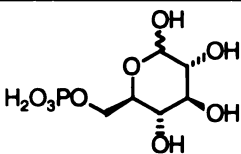
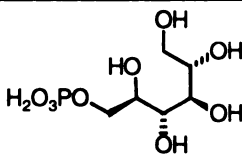
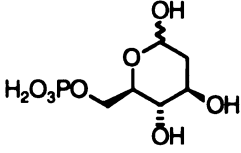
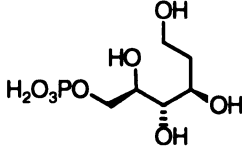
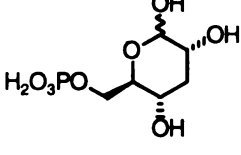
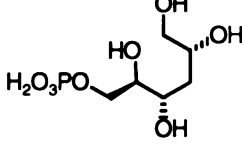
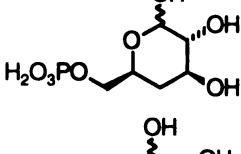
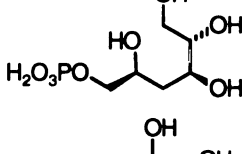
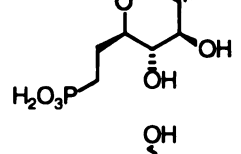
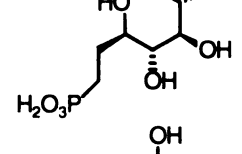
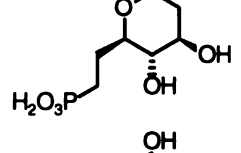
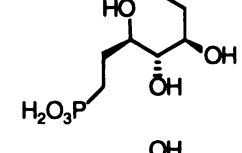
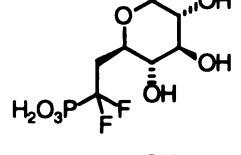
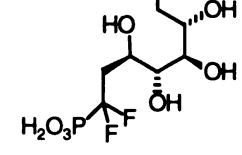
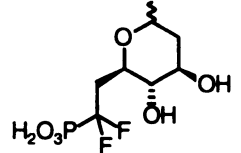
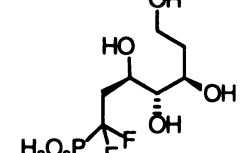
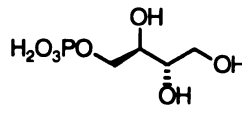
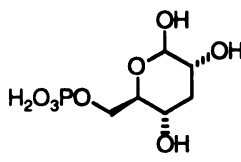
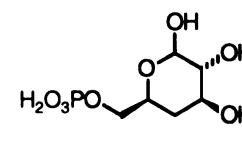
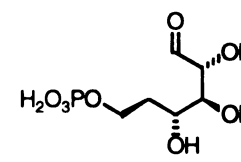
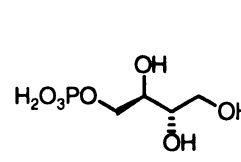
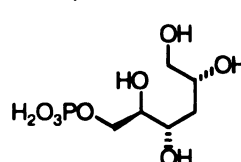
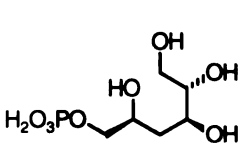
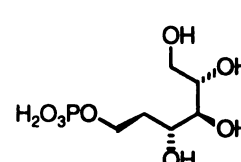
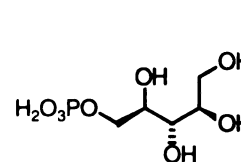
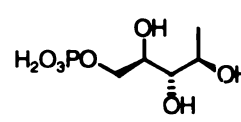
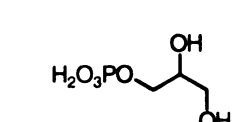
Compounds	K_i (mM)	NADH formation	Compounds	K_i (mM)	NADH formation
	$K_m = 1.2$	+		0.154	+
	0.0091	+		0.0023	+
	0.59	-		0.26	-
	no inhibition	+		0.93	+
	4.9	+		0.112	+
	0.071	+		0.0058	+
	no inhibition	-		no inhibition	-
	0.85	-		no inhibition	-
				0.047	+

Table 11. Inhibition of MIP synthase by deoxy substrate analogues.

			
44 $K_i = 0.59$ mM	46 no inhibition	48 no inhibition	50 $K_i = 0.047$ mM
			
45 $K_i = 0.26$ mM	47 $K_i = 0.93$ mM	49 $K_i = 1.5$ mM	67 $K_i = 0.017$ mM
			
68 $K_i = 0.008$ mM	69 no inhibition		

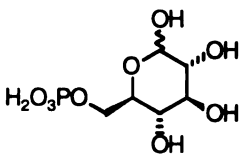
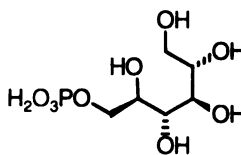
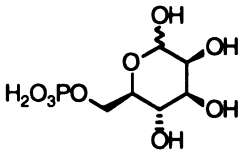
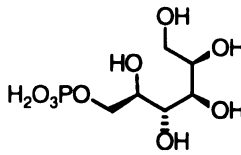
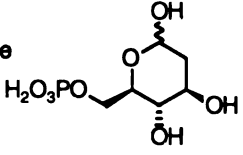
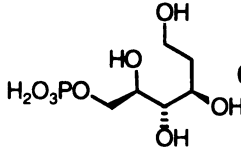
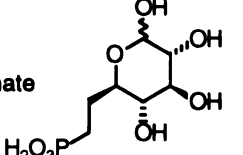
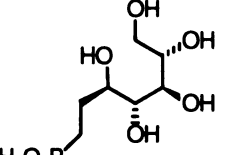
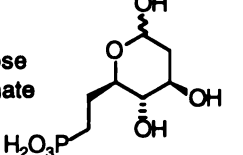
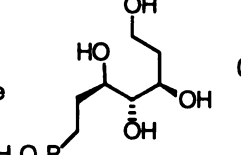
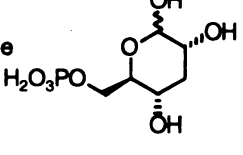
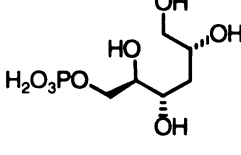
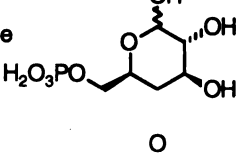
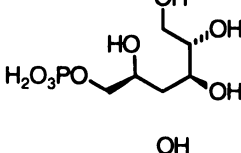
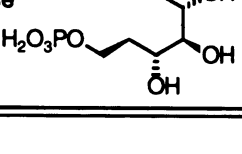
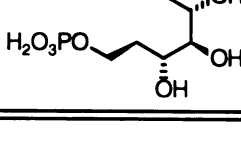
Examination of the C-3, C-4, and C-5 deoxy substrate analogue series revealed that, unlike removal of the C-2 hydroxyl group, which led to the enhanced inhibition of the enzyme, removal of the C-3, C-4, or C-5 hydroxyl group did not improve the binding to the enzyme. Instead, removal of the hydroxyl group at the C-3, C-4, or C-5 position consistently weakened the binding affinity to the enzyme. These experimental observations suggest that the C-3, C-4, and C-5 hydroxyl groups might play important roles in the active site binding. In contrast with the C-3, C-4, and C-5 deoxy substrate analogues, removal of the C-1 and C-2 functional groups led to a series of potent inhibitors including arabinitol 5-phosphate **67** ($K_i = 0.017$ mM), 1-deoxy arabinitol 5-phosphate **68** ($K_i = 0.008$ mM), and erythritol 4-phosphate **50** ($K_i = 0.047$ mM). It is noteworthy that erythritol 4-phosphate **50** bears only three hydroxyl groups corresponding to the C-3, C-4, and C-5

hydroxyl groups of the substrate D-glucose 6-phosphate. Although erythritol 4-phosphate **50** contains only four carbons in its skeleton, it is still a potent inhibitor for MIP synthase. This result is consistent with the suggestion that the C-3, C-4, and C-5 hydroxyl groups are important for active site binding. Comparison of erythritol 4-phosphate **50** ($K_i = 0.047$ mM), arabinitol 5-phosphate **67** ($K_i = 0.017$ mM), and 1-deoxy arabinitol 5-phosphate **68** ($K_i = 0.008$ mM) with D-glucitol 6-phosphate ($K_i = 0.154$ mM) and D-glucose 6-phosphate ($K_m = 1.2$ mM) showed that removal of the C-1 carbonyl or hydroxyl group and the C-2 hydroxyl group did not weaken the binding. Instead, the binding affinity to the enzyme was enhanced. It seems like that the C-1 and C-2 functional groups are not involved in active site binding, or at least they are not as important as the C-3, C-4, and C-5 hydroxyl groups for the binding. Possibly, active site interactions with the C-1 carbonyl group of the substrate might be important for the aldol condensation but may be much less important during substrate binding. Incubation of erythritol 4-phosphate **50** with MIP synthase in the presence of NAD led to an increase in absorbance at 340 nm. This observation is evidence that erythritol 4-phosphate **50** is bound to the active site in a conformation similar to that of the native substrate and was oxidized by enzyme-bound NAD. The relatively tight binding and ready oxidation of erythritol 4-phosphate **50** suggest that it possessed all the necessary structural requirement for initial binding and oxidation.

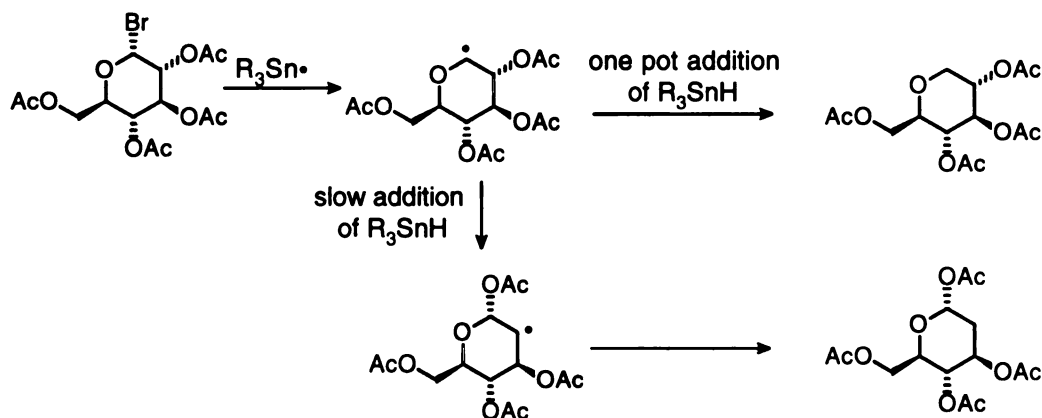
Binding at the Enzyme active site: Cyclic vs. Acyclic

Acyclic alditol substrate analogues were consistently stronger inhibitors than the corresponding cyclic aldose substrate analogues (Table 12). To date, all of the substrate analogues tested that exert an inhibitory action exist either exclusively in an acyclic form or can exist in solution as an equilibrium between cyclic and acyclic forms through equilibrium in the solution. A notable exception to this trend is 1,5-anhydro-D-glucose 6-phosphate.^{34b} No inhibition was observed for 1,5-anhydro-D-glucose 6-phosphate at a concentration of 0.6 mM, and only a 10% inhibition of rat testis enzyme was observed at a

Table 12. Comparison of aldose analogues with alditol analogues.

Aldose Analogues		Alditol Analogues	
Compounds	K_i (mM)	Compounds	K_i (mM)
D-glucose 6-phosphate 	$K_m = 1.2$	D-glucitol 6-phosphate 	0.154
D-mannose 6-phosphate 	8.4	D-mannitol 6-phosphate 	0.12
2-deoxy-D-glucose 6-phosphate 	0.0091	2-deoxy-D-glucitol 6-phosphate 	0.0023
D-glucose 6-homophosphonate 2 2 	4.9	D-glucitol 6-homophosphonate 2 3 	0.112
2-deoxy-D-glucose 6-homophosphonate 2 4 	0.071	2-deoxy-D-glucitol 6-homophosphonate 2 5 	0.0058
3-deoxy-D-glucose 6-phosphate 4 2 	0.59	3-deoxy-D-glucitol 6-phosphate 4 3 	0.26
4-deoxy-D-glucose 6-phosphate 4 4 	no inhibition	4-deoxy-D-glucitol 6-phosphate 4 5 	0.93
5-deoxy-D-glucose 6-phosphate 4 6 	no inhibition	5-deoxy-D-glucitol 6-phosphate 4 7 	1.5

concentration of 20 mM, which was 10 times higher than the concentration of substrate used. It should be noted, however, that 1-deoxy-D-glucose derivatives are usually made from the parent sugar via a free radical intermediate,^{101b} which can also generate the C-2 deoxy species depending on the conditions.^{101a} This raises the possibility that the inhibition observed for 1,5-anhydro-D-glucose 6-phosphate could be caused by a small amount of contaminating C-2 deoxy inhibitor which can exist in the acyclic form. All of these results strongly suggest that the enzyme binding site favors the acyclic form of substrate analogues.



Sherman^{20b} showed that MIP synthase had at least 5-fold preference for the β -anomer of substrate D-glucose 6-phosphate over the α -anomer. The α -anomer appeared to be an inhibitor as well as a substrate. He then suggested that the intact pyranose form was the substrate which binds to the enzyme. However, this experimental observation still can not exclude the possibility that the acyclic sugar phosphate is the substrate. The observation that acyclic alditol analogues were consistently better inhibitors than the cyclic aldose analogues indicates that the enzyme can bind the acyclic form and bind them more tightly than the cyclic form. It should also be noted that the enzyme requires the open chain

form of its substrate for the reactions which occur subsequent to formation of the Michaelis complex.

One question is whether the acyclic form of the substrate is readily available to the enzyme. There is only a small fraction (< 0.4%) of D-glucose 6-phosphate existing in its acyclic form in aqueous solution.⁹⁴ One possibility is that when the enzyme binds the acyclic form of the substrate, the rate of conversion of cyclic to acyclic substrate forms is rapid. In this fashion, the enzyme can displace the solution equilibrium in the direction of the acyclic form of substrate D-glucose 6-phosphate. Another possibility is that the enzyme binds the cyclic form of the substrate and then catalyzes ring opening at the active site. At present, there is still no conclusive evidence to confirm or rule out either possibility.

Intermediate B' and Analogues Possessing Oxidized Reaction Centers as Inhibitors

When incubated with MIP synthase in the presence of NAD, all potent inhibitors tested resulted in an increase in absorbance at 340 nm. It was also clearly shown that the inhibitory potency of inhibitors is well correlated with the rate of oxidation. The faster the oxidation, the stronger the inhibitor. From these experimental observations, we can hypothesize that it is the intermediate analogues generated in situ at the enzyme active site that are responsible for the potent inhibition of the enzyme. The binding of the enzyme with the unoxidized substrate analogues is weak. Because the analogues could not be oxidized, the simple substrate analogues are very weak inhibitors. Upon oxidation, the substrate analogue is transformed into a reaction intermediate analogue. The interaction between the reaction intermediate analogue and the enzyme is then significantly enhanced, and consequently could explain the potent inhibition.

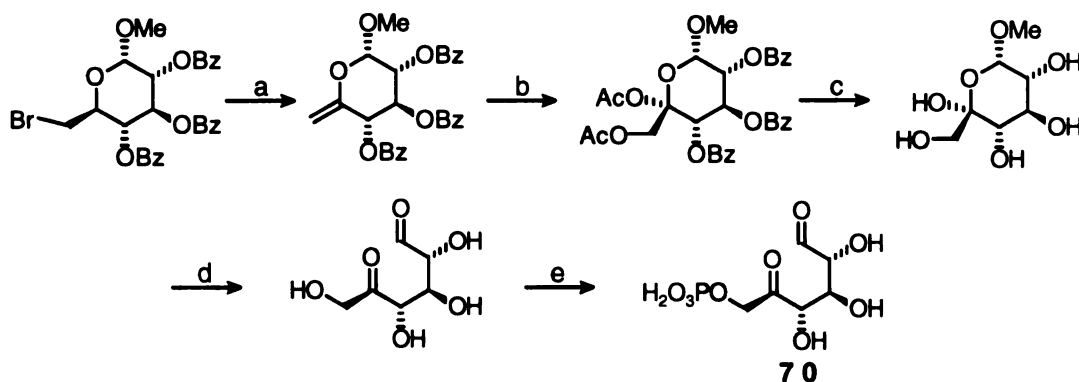
During the MIP-catalyzed conversion of D-glucose 6-phosphate into *myo*-inositol 1-phosphate, the substrate is first oxidized by NAD to 5-keto-D-glucose 6-phosphate (intermediate B', Figure 6) and tightly bound to the enzyme-NADH complex. Intermediate B' can either undergo aldol condensation and then be reduced to product or be reduced

back to D-glucose 6-phosphate. Our previous investigation on the interaction of MIP synthase with the substrate analogues revealed that all of the potent inhibitors tested were oxidized by enzyme-bound NAD. The potent inhibition might be the consequence of tight binding of the in situ generated carbonyl-containing intermediate analogue with the enzyme at the active site. Challenging the enzyme-NAD complex with the analogues possessing a pre-oxidized reaction center might therefore lead to the formation of enzyme-NAD-oxidized intermediate complex. But the enzyme could not process the inhibitor with both NAD and the intermediate in their oxidized state, and thus the normal turnover mechanism would be blocked. The enzyme can not reductively process the keto intermediate due to a lack of NADH. Indeed, this strategy has already been successfully used by the Frost group in inhibitor design for both DHQ synthase and MIP synthase.^{40,95,96} In one example, introduction of an oxidized reaction center into the inhibitor led to time-dependent, apparent irreversible inhibition of DHQ synthase.^{65,96} In another example, *myo*-2-inosose 1-phosphate (intermediate D', Figure 6) was found to be a potent inhibitors of MIP synthase ($K_i = 3.6 \mu\text{M}$). In fact, it is among the most potent inhibitor of MIP synthase thus far reported.⁴⁰ During the conversion of D-glucose 6-phosphate into *myo*-inositol 1-phosphate, there are three intermediates B', C', and D' existing in the oxidized state (Figure 6). In addition to intermediate D', another interesting target could be the intermediate 5-keto-D-glucose 6-phosphate **70** (intermediate B', Figure 6). Although intermediate B' has been previously reported in the literature,^{34,37} its potential use as an inhibitor of MIP synthase has not been examined.

Synthesis of Intermediate B' and Some Analogues Possessing Oxidized Reaction Centers

5-Keto-glucose 6-phosphate **70** (intermediate B', Figure 6) has been previously synthesized by Barnett³⁴ and Kiely,³⁷ respectively. Barnett's synthesis (Figure 23) began with methyl 2,3,4-tri-O-benzoyl-6-bromo-6-deoxy- α -D-glucopyranoside, which was treated with silver fluoride in pyridine for 80 h to gave the 5-enolpyranoside. Treatment of

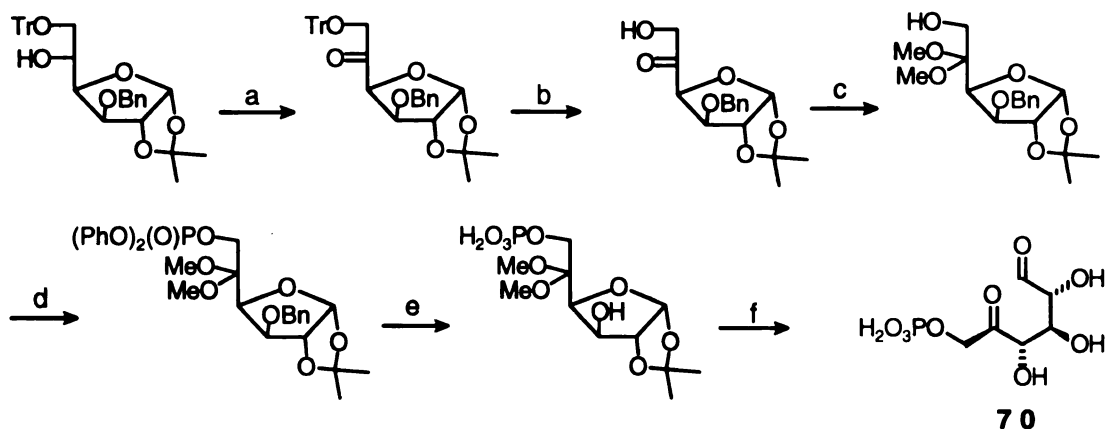
the 5-enolpyranoside with lead tetraacetate under UV light for 3 weeks yielded the fully protected 5-keto-D-glucose. Sequential base and acid hydrolysis, and paper chromatography purification yielded free 5-keto-D-glucose, which, upon enzymatic phosphorylation by hexokinase and ATP and repurification by paper chromatography, provided 5-keto-glucose 6-phosphate **70**.



(a) AgF, pyr, 80 h, 55%; (b) Pb(OAc)₄, benzene, *hν*, 3 weeks 30%; (c) NaOMe, -10°C, 40%; (d) i) 0.05 N H₂SO₄, ii) paper chromatography; (e) i) hexokinase, ATP, 1.0 M Tris-HOAc, 5 mM MgCl₂, pH 7.4, 35°C, 16 h, ii) paper chromatography.

Figure 23. Barnett's synthesis of 5-keto-D-glucose 6-phosphate.

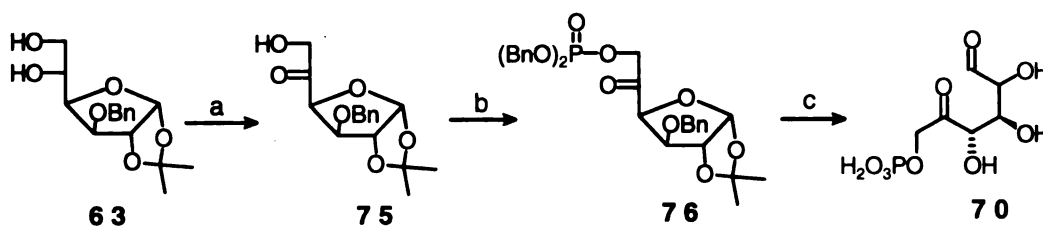
In Kiely's synthesis (Figure 24), Swern type oxidation of 3-*O*-benzyl-1,2-*O*-isopropylidene-6-*O*-trityl- α -D-glucopyranose with a mixture of methyl sulfoxide and acetic anhydride generated the 5-keto functional group. The trityl group was then cleaved with warm acetic acid. The carbonyl group was masked as its dimethyl acetal, and the C-6 hydroxyl group was then phosphorylated with diphenyl phosphorochloridate to afford the fully protected product. Sequential hydrogenolysis over palladium and then over platinum followed by acid hydrolysis gave a mixture containing three components by paper chromatography. The main component was obtained by paper chromatography and was found to be 5-keto-glucose 6-phosphate **70**.



(a) DMSO, Ac₂O, 91%; (b) HOAc, H₂O, 60°C, 57%; (c) HC(OCH₃)₃, NH₄Cl, 39°C, 5 days; (d) (PhO)₂P(O)Cl, pyr, 0°C, 91%; (e) i) H₂, Pd, MeOH, ii) H₂, PtO₂, MeOH, 36%; (f) Dowex 50-X8 (H⁺), 40°C, 42 h.

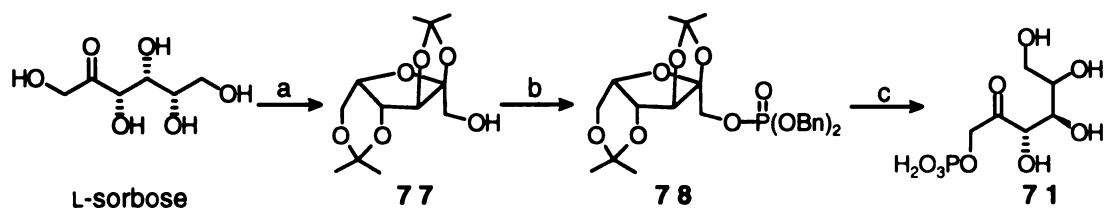
Figure 24. Kiely's synthesis of 5-keto-D-glucose 6-phosphate.

Both of the literature procedures were time consuming, and suffered from low yield, tedious workup and lack of reproducibility. Therefore, we designed a more expeditious route to prepare the desired 5-keto-glucose 6-phosphate **70** (Figure 25). 3-*O*-Benzyl-1,2-isopropylidene- α -glucofuranose **63** was oxidized with dibutyltin oxide and bromine⁹⁷ to give ketone **75**. The C-6 alcohol of **75** was then phosphorylated with *N,N*-diisopropyl dibenzyl phosphoramidite⁸⁹ to afford fully protected product **76**, which, upon hydrogenolysis, acid hydrolysis and purification by AG1-X8 anion exchange chromatography gave 5-keto-glucose 6-phosphate **70**. The dried sodium salt of **70** was a slightly colored brittle foam and could be stored at -20 °C for several month. Compared with the previously reported methods,^{34,37} this synthetic approach is short, convenient, and high-yielding. It has been successfully used to prepare ¹³C-labeled 5-keto-D-glucose 6-phosphate from ¹³C-labeled D-glucose in 20% overall yield.



(a) i) Bu_2SnO , MeOH , reflux, ii) Br_2 , CHCl_3 , 92%; (b) i) $(\text{BnO})_2\text{PN}(\text{i-Pr})_2$, tetrazole, CH_2Cl_2 , ii) $m\text{CPBA}$, CH_2Cl_2 , -40°C , 89%; (c) i) H_2 , Pd/C , THF , H_2O , ii) Dowex 50 (H^+), 50°C , 61%.

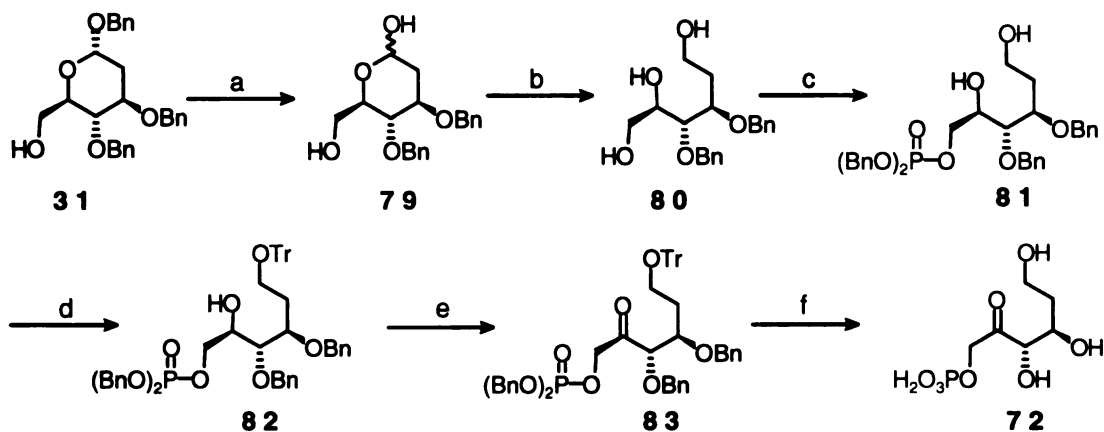
Figure 25. Synthesis of 5-keto-glucose 6-phosphate 70.



(a) ZnCl_2 , P_2O_5 , H_3PO_4 , acetone, 56%; (b) i) $(\text{BnO})_2\text{PN}(\text{i-Pr})_2$, tetrazole, CH_2Cl_2 , ii) $m\text{CPBA}$, CH_2Cl_2 , -40°C , 97%; (c) i) H_2 , Pd/C , THF , H_2O , ii) Dowex 50 (H^+), 65°C , 100%.

Figure 26. Synthesis of sorbose 1-phosphate 71.

5-Keto-D-glucitol 6-phosphate 71 (L-sorbose 1-phosphate) was prepared by a procedure (Figure 26) modified from a previously reported method.⁹⁸ Treating L-sorbose with zinc chloride, phosphorus pentoxide and phosphoric acid in acetone gave 2,3:4,6-diisopropylidene-L-sorbose 77, which was then phosphorylated with *N,N*-diisopropyl dibenzyl phosphoramidite⁸⁹ to give fully protected precursor 78. 5-Keto-D-glucitol 6-phosphate 71 was then obtained in quantitative yield upon deprotection of 78.



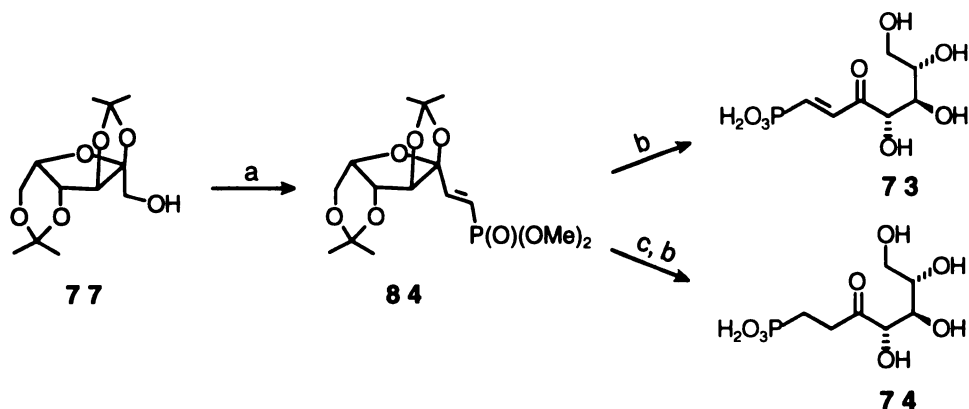
(a) 1 N aq. HCl, THF, H₂O, reflux, 61%; (b) NaBH₄, MeOH, 63%; (c) i) Bu₂SnO, MeOH, reflux, ii) (BnO)₂(O)POP(O)(OBn)₂, THF, 39%; (d) TrCl, Pyr, CH₂Cl₂, 74%; (e) cat. TPAP, NMMO, 4 Å molecular sieves, CH₂Cl₂, 72%; (f) H₂, Pd/C, THF, H₂O, 70%.

Figure 27. Synthesis of 2-deoxy L-sorbose 1-phosphate **72**.

2-Deoxy 5-keto-D-glucitol 6-phosphate **72** (2-deoxy-L-sorbose 1-phosphate) was prepared from benzyl 2-deoxy-3,4-dibenzyl glucopyranoside **31** (Figure 17). Refluxing **31** in 1 N hydrochloric acid gave pyranose **79** which, upon reduction with sodium borohydride, yielded triol **80**. Treating **80** with dibutyltin oxide followed by tetrabenzylpyrophosphate selectively introduced the phosphate moiety to the C-6 position of intermediate **81**. After protecting the C-1 primary alcohol, **80** was oxidized by tetra-*n*-propylammonium perruthenate¹⁰⁰ to give the precursor **83**. Hydrogenolysis over palladium on carbon removed all of the protecting groups to afford 2-deoxy-5-keto-D-glucitol 6-phosphate **72**. Purification by anion exchange chromatography using AG1-X8 resin removed a small amount of inorganic phosphate.

The readily available 2,3;4,6-diisopropylidene-L-sorbose **77** was also used for the synthesis of L-sorbose 1-(*E*)-vinylhomophosphonate **73** and L-sorbose 1-homophosphonate **74**. Swern oxidation of **77** converted the C-1 hydroxyl group into an aldehyde, which was then subjected to the Wadsworth-Horner-Emmons reaction⁶⁹ with tetramethyl methylene diphosphonate and *n*-butyllithium in THF at -78 °C to yield fully

protected (*E*)-vinylhomophosphonate **84**. Stepwise deprotection of **84** gave L-sorbose 1-(*E*)-vinylhomophosphonate **73**. Hydrogenolysis of **84** over palladium on carbon followed by the same deprotection yielded L-sorbose 1-homophosphonate **74**.



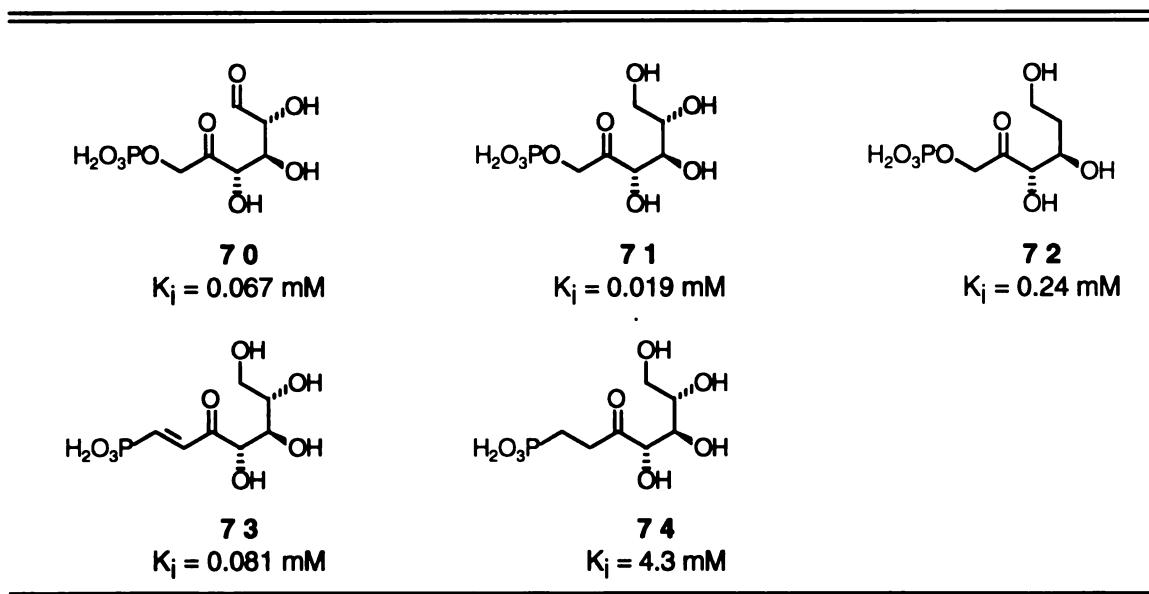
(a) i) $(\text{COCl})_2$, DMSO, CH_2Cl_2 , -78°C , ii) Et_3N , -78°C -RT, iii) $(\text{CH}_3\text{O})_2(\text{O})\text{PCH}_2\text{P}(\text{O})(\text{OCH}_3)_2$, *n*-BuLi, THF, -78°C , 60%; (b) i) TMSBr, CH_2Cl_2 , ii) Dowex 50 (H^+), **71**: 100%, **72**: 83%; (c) H_2 , Pd/C, MeOH,

Figure 28. Synthesis of L-sorbose 1-(*E*)-vinylhomophosphonate **73** and L-sorbose 1-homophosphonate **74**.

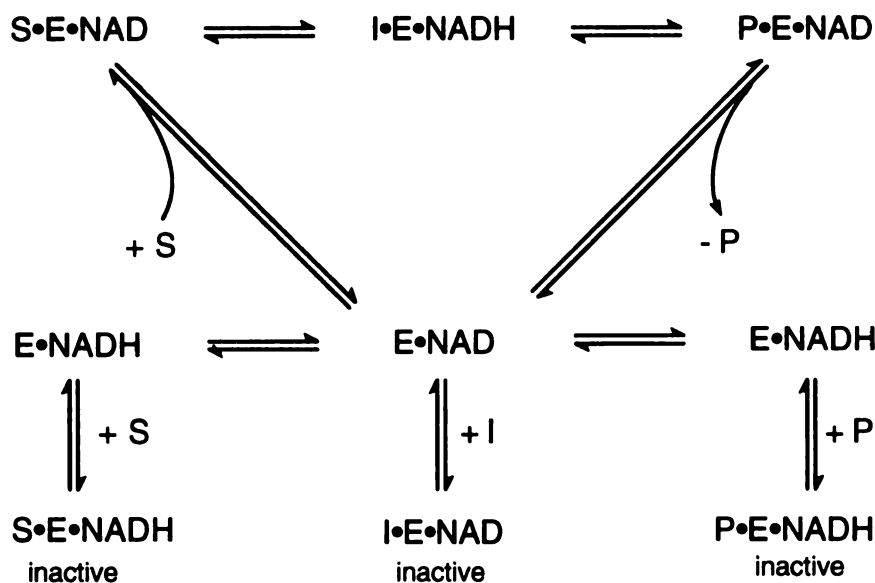
Inhibition Studies of Intermediate B' and Analogues Possessing An Oxidized Reaction Center

The inhibition behaviors of **70-74** toward MIP synthase were examined. 5-Keto-D-glucose 6-phosphate **70** (intermediate B', Figure 6) was found to be a competitive inhibitor with $K_i = 0.076$ mM (Table 12). 5-Keto-D-glucitol 6-phosphate **71** (L-sorbose 1-phosphate), which has a reduced C-1 hydroxyl group relative to 5-keto-glucose 6-phosphate **70**, was a potent inhibitor with $K_i = 0.019$ mM. This is another example that the alditol analogues are better inhibitors than the aldose counterparts. The K_i values of 2-deoxy-5-keto-D-glucose 6-phosphate **72**, L-sorbose 1-(*E*)-vinylhomophosphonate **73**, and L-sorbose 1-homophosphonate **74** were measured to be 0.24, 0.081, and 4.3 mM respectively.

Table 13. Intermediate B' and analogues possessing an oxidized reaction center.



During normal turnover of *D*-glucose 6-phosphate into *myo*-inositol 1-phosphate, the oxidized intermediate is generated along with accompanying formation of enzyme-bound NADH at the enzyme active site. Reduction of oxidized intermediate B' or intermediate C' (Figure 6) and oxidation of enzyme-bound NADH are necessary for the completion of the catalytic cycle. The reason behind the inhibition of MIP synthase by the actual reaction intermediate B' (Figure 6) lies in the formation of a postulated NAD-enzyme-intermediate B' complex. As discussed earlier, since both NAD and the intermediate B' were in their oxidized states, the enzyme could not process the pre-oxidized reaction intermediate in the absence of reducing equivalents. In addition, stabilizing interactions between the reaction intermediate and active site could make the release of the reaction intermediate more difficult, and result in potent inhibition.



S: substrate, I: oxidized intermediate, E: enzyme, P: product

Figure 29. Interaction between enzyme, substrate, oxidized intermediate and product.

Inhibition due to formation of a complex between enzyme with NAD bound at the active site and oxidized intermediate has been reported for both DHQ synthase and MIP synthase.^{40,95,96} In one experiment, challenging the DHQ synthase-NAD complex with ketocarbaphosphonate, an intermediate analogue bearing a pre-oxidized reaction center, led to potent, slowly-irreversible inhibition.^{95,96} In another experiment, *myo*-2-inosose 1-phosphate (intermediate D', Figure 6) was found to be one of the most potent inhibitors reported for MIP synthase.⁴⁰ Examples of inhibition due to formation of a complex with NADH bound at the active site and reduced reactive intermediate have not been reported. NADH was reported to be an inhibitor of MIP synthase from various sources.^{25,45,47,50} In this situation, the inhibition resulted from the formation of an enzyme-NADH-substrate complex, which blocked the normal reaction mechanism.

By comparing 5-keto-D-glucose 6-phosphate **70** ($K_i = 0.076$ mM) with D-glucose 6-phosphate ($K_m = 1.2$ mM), and 5-keto-D-glucitol 6-phosphate **71** ($K_i = 0.019$ mM) with D-glucitol 6-phosphate ($K_i = 0.154$ mM),⁹³ it appears that introduction of the C-5

preoxidized reaction center consistently improves the inhibition by an order of magnitude. One possible explanation is that the enzyme binds the intermediate analogues more tightly than the substrate analogues. The formation of a complex between enzyme with NAD bound at the active site and the oxidized intermediate analogues blocks the normal turnover pathway.

2-Deoxy-5-keto-D-glucitol 6-phosphate **72** was then prepared in hope of finding an even more potent inhibitor for MIP synthase. Surprisingly, 2-deoxy-5-keto-D-glucitol 6-phosphate **72** turned out to be a poor inhibitor ($K_i = 0.24$ mM) of MIP synthase. This result was opposite to the improved inhibition for previous substrate analogues (Table 2, Table 6) upon removal of the C-2 hydroxyl group. One possible explanation might follow from the inductive electron-withdrawing effect of the C-2 hydroxyl group. Previous investigations suggest that the enzyme favors the acyclic form of substrate or analogues. Relative to 5-keto-D-glucitol 6-phosphate **71**, the lack of the electron-withdrawing C-2 hydroxyl group in 2-deoxy-5-deoxy-D-glucitol 6-phosphate **72** would increase nucleophilicity of the neighboring C-1 hydroxyl group. This might result in a higher concentration of the cyclic form of **72** relative to **71**. Comparing 2-deoxy-D-glucose 6-phosphate ($K_i = 0.0091$ mM)⁹³ to D-glucose 6-phosphate ($K_m = 1.2$ mM), removal of the C-2 hydroxyl group would decrease the electrophilicity of the C-1 carbonyl group, thereby, increasing the tendency in favor of forming the acyclic form. A similar explanation might also be applied to the comparison of L-sorbose 1-(*E*)-vinylhomophosphonate **73** with L-sorbose 1-homophosphonate **74**. L-Sorbose 1-(*E*)-vinylhomophosphonate **71** ($K_i = 0.081$ mM) was a much more potent inhibitor than L-sorbose 1-homophosphonate **74** ($K_i = 4.3$ mM). As the C-5 carbonyl group was conjugated with the double bond of the vinylhomophosphonate, the electrophilicity of the conjugated carbonyl group would be significantly lower than the unconjugated carbonyl group of **74**. Decreased electrophilicity would then lower the energy barrier for forming the acyclic form of the analogue and consequently lead to tighter binding of L-sorbose 1-(*E*)-vinylhomophosphonate **73**. In

addition, the vinylhomophosphonate double bond might also restrain the conformation of **73** in a favored orientation for active-site binding and catalysis.

In summary, several conclusions can be drawn from the substrate analogue and intermediate analogue studies. Of the nonhydrolyzable phosphonate analogues, the isosteric homophosphonates are better substrate mimics than the nonisosteric phosphonate analogues for MIP synthase. Introducing the α,α -gem-difluoro group into the homophosphonate increased the acidity of the phosphonic acid, but the resulting α,α -gem-difluorohomophosphonates either failed to inhibit MIP synthase or were only weak inhibitors possibly due to steric factors or due to the increased difficulty in oxidizing the C-5 alcohol. The C-3, C-4, and C-5 hydroxyl groups are important for active-site binding, while the C-1 and C-2 functional groups may be not critical for binding. Removal of the C-1 and C-2 functional groups leads to improved inhibition of the enzyme for substrate analogues. MIP synthase favors acyclic substrate analogues over the cyclic ones. Acyclic substrate analogues are consistently better inhibitors than the cyclic ones. The potent inhibition of the enzyme results from the intermediate analogues generated in situ by enzymatic oxidation of the substrate analogues by NAD. The inhibitory potency of the substrate analogues is well correlated with the rate of oxidation. Challenging the enzyme-NAD complex with an actual reaction intermediate possessing a pre-oxidized reaction center also leads to the inhibition of the enzyme. The inhibition of the enzyme by the actual reaction intermediate is due to the formation of a complex between the enzyme with NAD bound to the active site and the oxidized intermediate that blocks the normal reaction mechanism.

CHAPTER 4

NADH FORMATION DURING MIP SYNTHASE-CATALYZED CONVERSION OF D-GLUCOSE 6-PHOSPHATE INTO *myo*-INOSITOL 1-PHOSPHATE

Determination of NADH Formation

Pyridine nucleotides are among the most important biochemical cofactors, and in fact, all known organisms require pyridine nucleotides to function. Together with the enzymes to which they bind, pyridine nucleotides perform many important oxidation-reduction reactions. The redox reaction site of the pyridine nucleotides is located at the nicotinamide moiety. The enzymatic oxidation-reduction occurs as if a hydride ion had been added at the C-4 position of the pyridine ring with concomitant neutralization of the positive charge of the oxidized NAD (Figure 30).¹⁰²

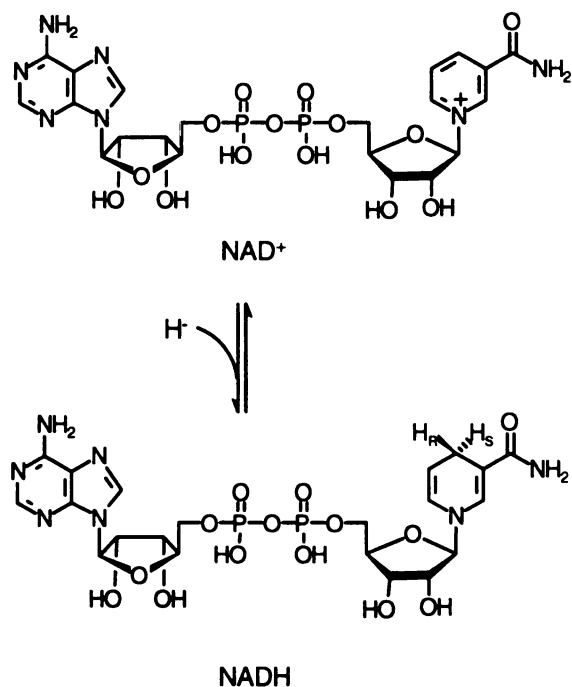


Figure 30. Redox reaction of NAD and NADH.

The optical absorption properties of the chromophores of NAD has considerably facilitated biochemical studies of systems requiring such cofactors. Different spectral properties of the oxidized and reduced forms of NAD have provided a direct analytical method for the study of enzymatic activity and kinetics. The UV/vis absorption spectrum of NAD cofactor is dominated by the properties of three chromophores: adenine for both NAD and NADH, nicotinamide for NAD, and 1,4-dihyronicotinamide for NADH. The absorption bands of adenine and nicotinamide are located at around 260 nm, while the absorption band of 1,4-dihyronicotinamide is located at around 340 nm.¹⁰³ The reduced form of NADH absorbs light at 340 nm ($\epsilon = 6300 \text{ M}^{-1}\text{cm}^{-1}$), but the oxidized form of NAD does not absorb at this wavelength. Based on this optical property, the activity of a large number of enzymes has been subsequently measured by determination of the rates of increases or decreases of absorbance at 340 nm.

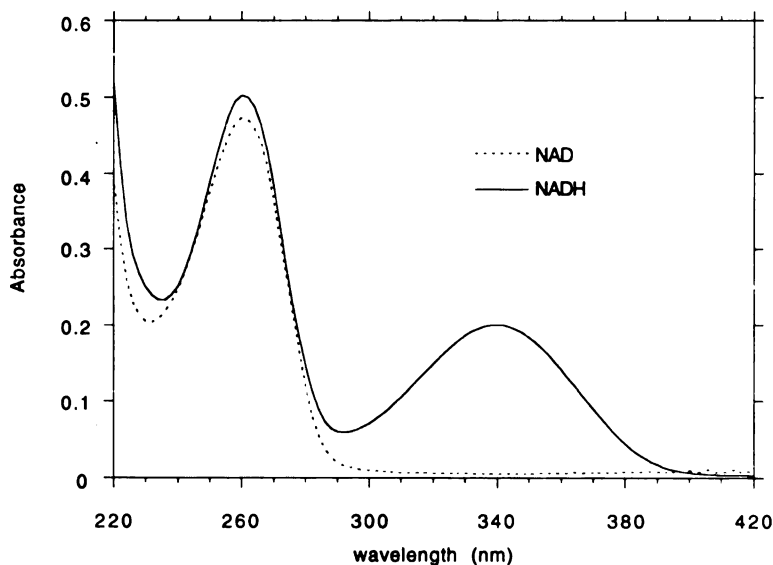


Figure 31. UV/vis spectra of NAD and NADH.

DHQ synthase and MIP synthase belong to a subgroup of pyridine nucleotide-dependent enzymes that employ NAD as a catalyst rather than a cosubstrate.¹ The reduction of enzyme-bound NAD to NADH is followed by oxidation of the enzyme-bound NAD back to NADH before the completion of catalytic cycle. NADH generated during the catalytic cycle is expected to be present at some steady state concentration that corresponds to the fraction of enzyme that has oxidized intermediate bound to it. Several experimental observations have been reported that when DHQ synthase was incubated with substrate analogues in the presence of NAD,^{7,14,59} an increase of absorbance at 340 nm was detected indicating the formation of NADH. Determination of absorbance at 340 nm provides a useful means to probe the interaction of the enzyme with substrate and its analogues at the enzyme active site.

In the proposed mechanism for MIP synthase-catalyzed conversion of D-glucose 6-phosphate into *myo*-inositol 1-phosphate, the enzyme employs NAD as a catalyst. However, no direct evidence for the formation of NADH during the conversion has been reported. Eisenberg³⁸ reported that an oxidized intermediate, *myo*-2-inosose 1-phosphate (intermediate D', Figure 6), was trapped as a mixture of tritiated *myo*-inositol and *scyllo*-inositol by adding NaB³H₄ to a system of homogeneous MIP synthase from rat testis, D-glucose 6-phosphate and NAD. It was estimated that 2 moles of *myo*-2-inosose 1-phosphate were bound per mole of enzyme. This experimental result implied that along with the oxidized intermediate, NADH should be also present in the enzyme active site. Determination of the steady state level of NADH might be possible as long as high concentrations of the enzyme are employed. UV/vis spectroscopic detection of NADH formation would provide the first direct evidence of the involvement of NADH during the catalysis. Detection of NADH formation could also used to monitor the interaction of the enzyme with substrate as well as its analogues. Insights would be provided into the mechanism of enzyme inhibition by determining if a substrate analogue is also oxidized by

enzyme-bound NAD. Formation of NADH would likely indicate that the inhibitor is bound in the active site similar to D-glucose 6-phosphate.

Purification of MIP Synthase From *E. coli*.

Detection of small, steady state concentrations of NADH requires large quantities of highly purified enzyme. Homogeneous MIP synthase has been previously purified from yeast, although only a small quantity of enzyme could be obtained from each purification. This problem was solved by using an overexpression of the *Saccharomyces cerevisiae* INO1 locus in *E. coli* (BL21(DE3)/pT7-7/MIPSYN) recently constructed in the Frost group⁷⁰ to overproduce MIP synthase. In a typical purification (Table 14), about 30 g of wet cell paste was obtained from 9 L of culture medium. Measurement of enzyme activity was based on quantitation of the inorganic phosphate⁷² selectively released from *myo*-inositol during oxidation by sodium periodate.⁷¹ The interfering phosphatase activity in crude lysate was measured similarly except sodium periodate was substituted with water. MIP synthase was purified about 30 fold after ammonium sulfate precipitation, DEAE anion exchange, and size exclusion chromatography on a Bio-Gel A 0.5 column. Phosphatase activity was totally removed upon DEAE column purification.

Table 14. Purification of MIP synthase from *E. coli*.

	total units ^a	specific activity ^b	x-fold purification	yield %
homogenate	18.9	0.0139	1	100
ammonium sulfate	18.2	0.0202	1.45	96
DEAE column	19.2	0.251	181	102
Bio-Gel column	17.9	0.413	29.7	95

^a 1 unit = 1 μ Mol MIP produced/min. at 37°C

^b units activity/mg protein

Examination of the purified enzyme by HPLC with both a DEAE analytical column and a size exclusion column monitored at 280 nm gave a single peak. Fully denatured SDS-PAGE gel electrophoresis gave a single band at 62 kd (Figure 32). The molecular weight of MIP synthase was determined to be 240 kd by size exclusion HPLC. The Michaelis constant (K_m) for substrate D-glucose 6-phosphate was 1.2 mM. The characteristics of MIP synthase purified from *E. coli* were identical to those obtained with the yeast enzyme.^{70,93}

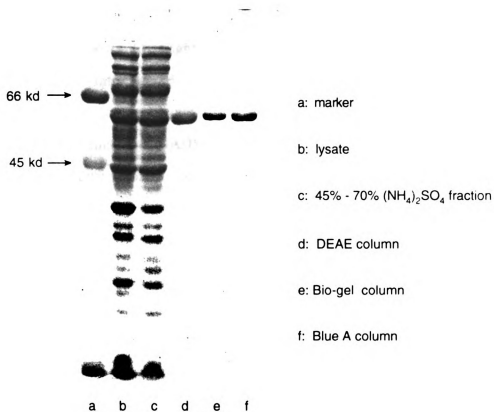


Figure 32. SDS-PAGE gel electrophoresis of MIP synthase preparations

When D-glucose 6-phosphate (5 mM) was incubated with MIP synthase in a buffer containing enzyme (2 units), NAD (1 mM) in buffer A (20 mM Tris HCl pH 7.2, 10 mM ammonium chloride, 10 mM β -mercaptoethanol), a steady increase in absorbance at 340 nm was detected. Examination at various enzyme concentrations and various NAD

concentrations revealed that the absorbance level was independent of enzyme concentration, but was dependent on NAD concentration. Upon adding lactate dehydrogenase and pyruvate into the reaction solution, the absorbance at 340 nm dropped to a level just above the background level. The fact that the NADH formed could be quenched with lactate dehydrogenase and pyruvate indicated that the NADH formed was free in the solution. One possible explanation might be that MIP synthase released some of its NADH during catalysis. If this is true, some oxidized intermediate must be also released to the solution along with NADH. However, this is in conflict with the literature reports that NADH and reaction intermediates were tightly bound to the enzyme during turnover of substrate into product.³⁶ Another possibility might be that some contaminating enzymes catalyzed the reduction of NAD into NADH. To find out the reason behind the free NADH concentrations in solution, an attempt was made to identify the free intermediate generated accompanying the formation of NADH.

There are several possible ways to identify the unknown intermediate. One is to isolate the unknown intermediate from the enzymatic reaction. It would provide conclusive evidence for the identity of the unknown species. However, the isolation would need large quantities of enzyme and tedious purification procedures. Successful isolation also depends heavily on the chemical stability of the species to be isolated. Another way is to spectroscopically analyze the enzymatic reaction products. ^1H NMR spectra would give valuable information about the species to be identified. However, since the enzymatic reaction needs to be carried out in a buffer solution, the interfering signals generated by the enzyme and buffer components would make the assignment of the ^1H NMR spectra difficult and purification of reaction mixture would be necessary before NMR analysis. The most convenient way would be monitoring the reaction with ^{13}C NMR spectroscopy with ^{13}C -enriched substrate D-glucose 6-phosphate. Employing the ^{13}C enriched substrate would significantly increase the relative intensity of ^{13}C resonances associated with the carbon atoms of the putative intermediate. This would not only facilitate spectroscopic

analysis of the unknown intermediate without isolation, but also allow direct monitoring of the enzymatic reactions.

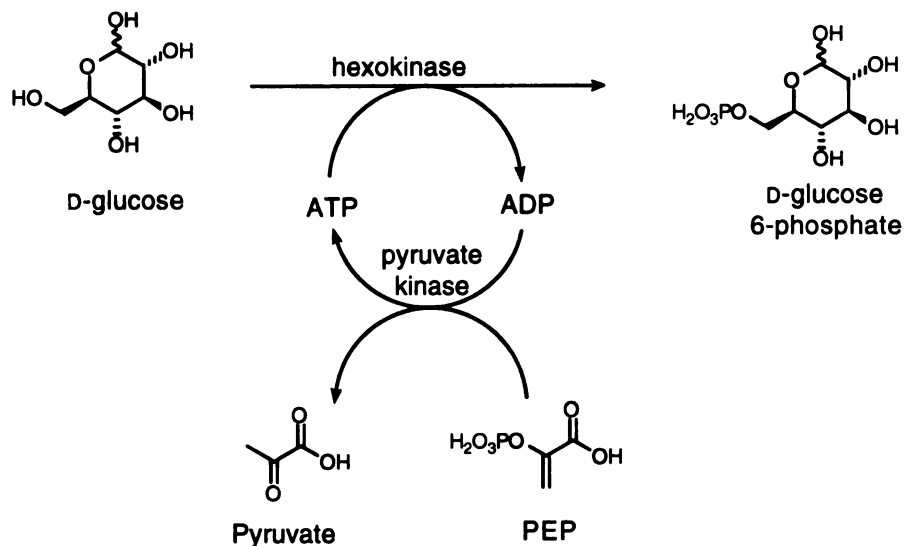


Figure 33. Enzymatic synthesis of D-glucose 6-phosphate.

D-glucose-d₆ 6-phosphate was prepared from commercially available D-glucose-d₆ using a procedure modified from literature.¹⁰⁴ Incubation of D-glucose-d₆ with 0.2 equivalents of ATP, 1.2 equivalents PEP, 3 units of hexokinase, and 3 units of pyruvate kinase led to the formation of D-glucose-d₆ 6-phosphate, which was then purified by anion exchange chromatography to give D-glucose-d₆ 6-phosphate in 65% yield.

¹³C NMR analysis was carried out at 37 °C. In one experiment (Figure 34), the enzymatic reaction was initiated by adding MIP synthase into an NMR tube containing 25 mM D-glucose-d₆ 6-phosphate and 1 mM NAD in a buffer containing 25% D₂O to lock the signal. NMR spectra were recorded at timed intervals. In another experiment (Figure 35), additional lactate dehydrogenase (LDH) and pyruvate was added to the reaction in an attempt to oxidize NADH back to NAD and increase the yield of unknown intermediate. Analysis of ¹³C NMR spectra revealed that in the absence of LDH and pyruvate, the reaction reached completion within about one hour. Almost all of D-glucose-d₆ 6-

phosphate was converted into *myo*-inositol- d_6 1-phosphate, which was compared with a synthetic sample. Only trace amounts of an unidentified species were produced. As expected, when LDH and pyruvate were added to the reaction, in addition to *myo*-inositol- d_6 1-phosphate, a significant amount of an unidentified species was generated. During the reaction, up to three unknown species were detected, two of which disappeared after about one hour. Reaction was slower in the presence of LDH and pyruvate than the reaction without LDH and pyruvate. At this point, the signals of unknown species were still too weak to be used for structural analysis. Earlier investigation with UV/vis analysis showed that the level of accumulated NADH depended on the concentration of NAD in the solution. This result implied that the level of unknown intermediate generated along with NADH should also depend on the concentration of NAD in the solution. In order to increase the signal of unknown intermediate for structural analysis, high concentrations of NAD were used. When a similar reaction was carried out with an NAD concentration at 25 mM rather than 1 mM (Figure 35), the major product was the same unidentified species in addition to *myo*-inositol 1-phosphate. The enhanced signals led to the identification of the unknown species as being 6-phosphogluconic acid.¹⁰⁵ The other two species generated during the reaction were identified as γ -(1-4) and δ -(1-5) 6-phosphogluconolactones. Indeed, the mixture of the three components has been reported in the literature as the products of D-glucose 6-phosphate dehydrogenase-catalyzed oxidation of D-glucose 6-phosphate.¹⁰⁵ Glucose 6-phosphate dehydrogenase catalyzes the oxidation of glucose 6-phosphate by NAD to generate NADH along with γ -(1-4) and δ -(1-5) 6-phosphogluconolactones, which are then hydrolyzed to 6-phosphogluconic acid.¹⁰⁵ These experiments revealed that the free NADH generated in the solution was associated with contaminating glucose 6-phosphate dehydrogenase. Since glucose 6-phosphate dehydrogenase has a much higher activity than MIP synthase, only a trace amount of contamination would result in spurious NADH formation not associated with MIP synthase activity.

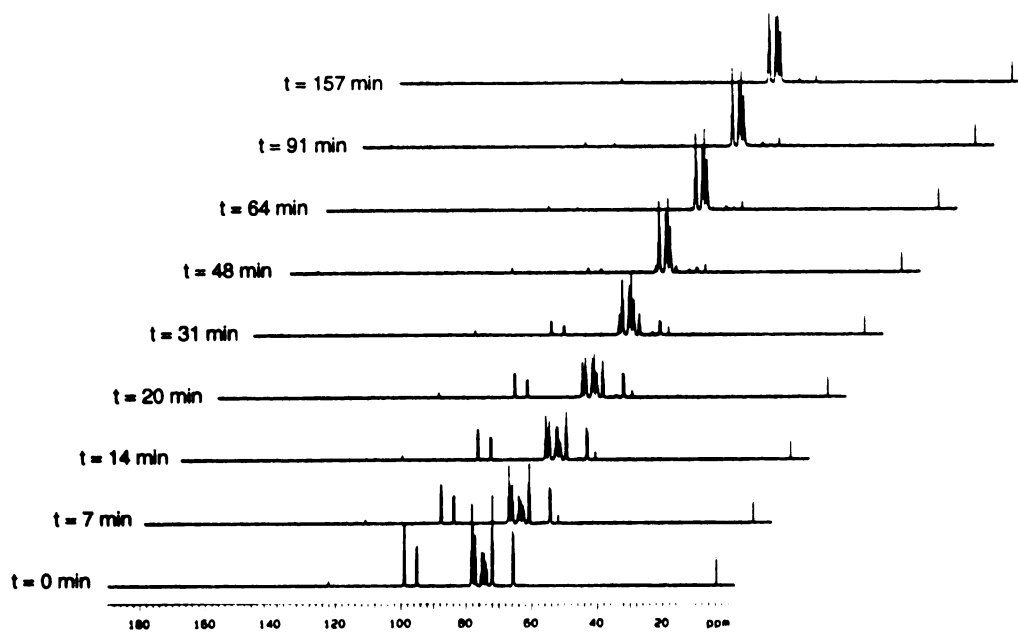


Figure 34. ^{13}C NMR time course of MIP synthase-catalyzed conversion of D-glucose 6-phosphate with 1 mM NAD.

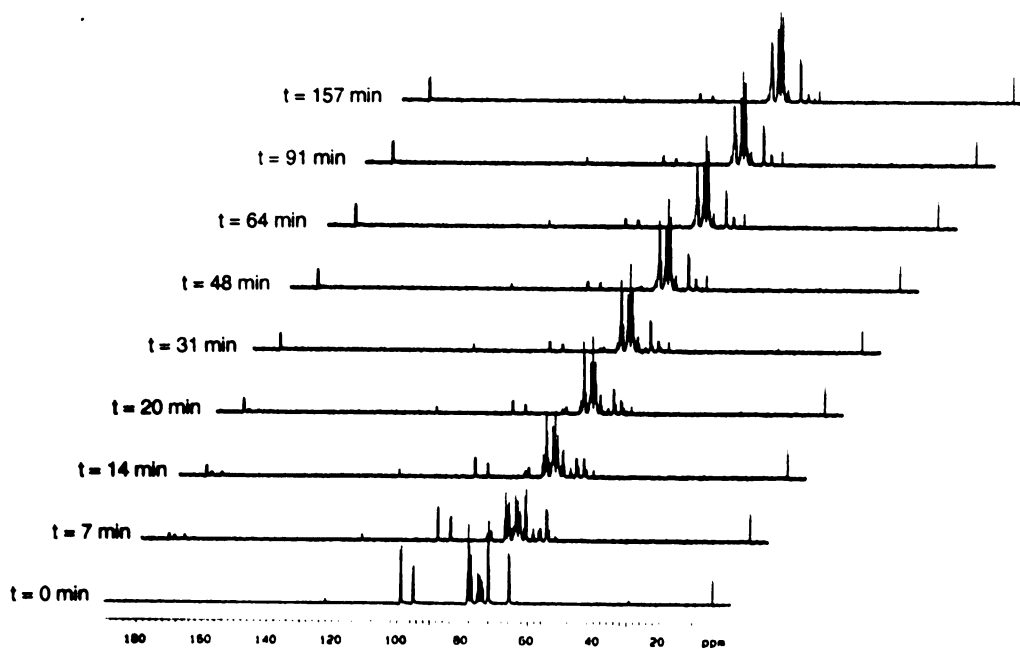


Figure 35. ^{13}C NMR time course of MIP synthase-catalyzed conversion of D-glucose 6-phosphate with 1 mM NAD in the presence of LDH and pyruvate.

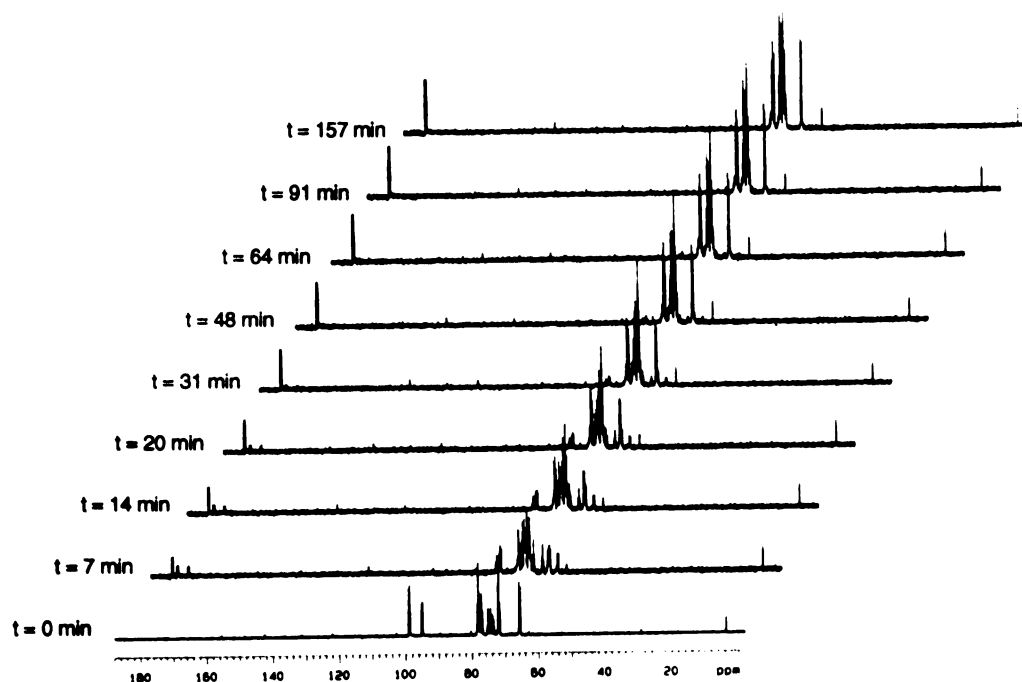


Figure 36. ^{13}C NMR time course of MIP synthase-catalyzed conversion of D-glucose 6-phosphate with 25 mM NAD in the presence of LDH and pyruvate

In order to remove the contaminating glucose 6-phosphate dehydrogenase, various purifications were performed. HPLC purification with both DEAE and size exclusion columns failed to remove the contaminating glucose 6-phosphate dehydrogenase. Both columns monitored at 280 nm gave only a single peak. A purification attempt using HTP hydroxylapatite chromatography also failed to separate MIP synthase from glucose 6-phosphate dehydrogenase. Careful examination of the literature indicated that other workers had faced the same problem.^{46,50} We also checked MIP synthase from yeast and found same D-glucose 6-phosphate dehydrogenase contamination. Aradi and coworkers reported that purification of *Neurospora crassa* MIP synthase by affinity chromatography on both pyrophosphate-sepharose and Blue sepharose-CL-6B successfully removed glucose 6-phosphate dehydrogenase from MIP synthase.⁵¹ In our case, the affinity chromatographic purification proved to be an effective method to remove the contaminating glucose 6-phosphate dehydrogenase when the Blue A affinity column was used. When the

contaminated enzyme was passed through the Blue A column, the eluant contained only MIP synthase with all glucose 6-phosphate dehydrogenase being absorbed by the Blue A column. Incubation of Blue A column purified enzyme with D-glucose 6-phosphate and NAD showed no glucose 6-phosphate dehydrogenase activity. Only a very low level of absorbance at 340 relative to that obtained with the enzyme without Blue A purification was detected.

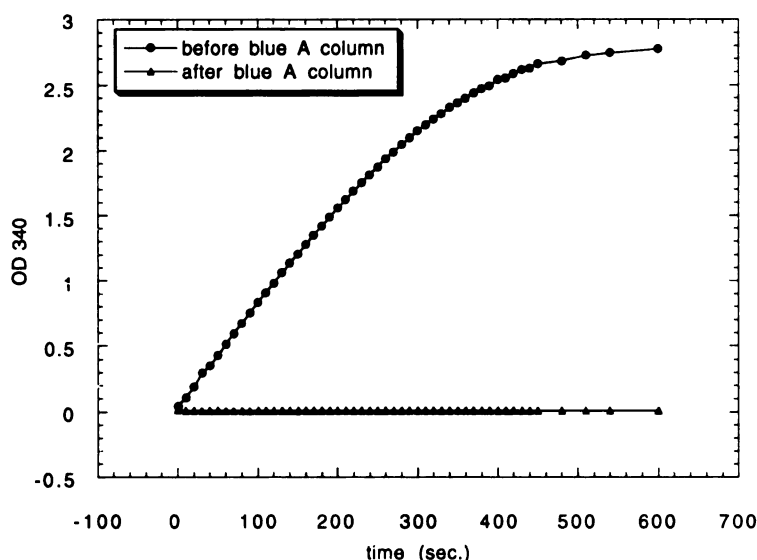


Figure 37. Glucose 6-phosphate dehydrogenase activities, before and after Blue A affinity chromatography

Detection of NADH Formation During MIP Synthase Catalysis

After removal of the contaminating glucose 6-phosphate dehydrogenase activity, it should become possible to detect the steady state formation of NADH during the MIP synthase-catalyzed conversion of D-glucose 6-phosphate into *myo*-inositol-phosphate. Indeed, when D-glucose 6-phosphate was incubated with the purified enzyme and NAD at 25 °C, an increase in absorbance at 348 nm corresponding to steady state NADH was detected (Figure 38). The increased absorbance associated with MIP synthase could not be quenched with LDH and pyruvate. The maximum absorbance of MIP synthase-bound

NADH shifted to 348 nm, while the free NADH had its maximum absorbance at 340 nm (Figure 31). The increase in absorbance corresponded to about 1 mole of NADH per mole of the enzyme. Although at high enzyme concentration, there was still some residual glucose 6-phosphate dehydrogenase activity, the interference associated with it could be eliminated by adding LDH and pyruvate to the solution. This experimental observation provided the first direct evidence of NADH formation during the MIP synthase-catalyzed conversion of D-glucose 6-phosphate into *myo*-inositol-phosphate.

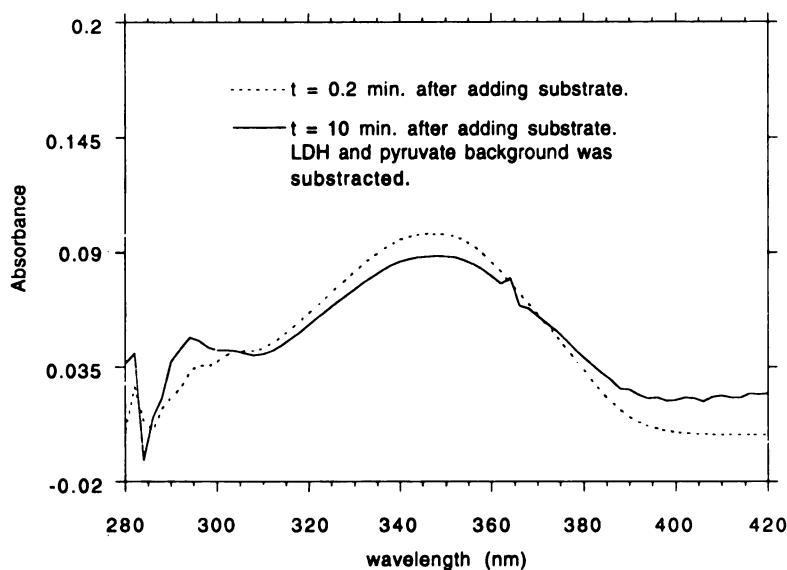


Figure 38. NADH formation during MIP synthase-catalyzed conversion of D-glucose 6-phosphate into *myo*-inositol 1-phosphate.

When each of the homophosphonate analogues **24-27** was added into a solution of MIP synthase purified to the Bio Gel step in the presence of NAD, a new absorbance at 348 nm was observed with all of the analogues. The rates of NADH formation correlated well with the potency of the inhibitors (Figure 39). The rate of NADH formation for a potent inhibitor was much faster than that of a weak one. Over a prolonged time of incubation, the level of NADH formed with all analogues reached a similar steady state level. A slight red-shift of the absorption band was also noticed. The maximum

absorbance shifted from 340 nm of free NADH (Figure 31) to about 346 - 348 nm of enzyme-bound NADH (Figure 38). Addition of lactate dehydrogenase (LDH) and pyruvate to the solution containing the complex of MIP synthase and the analogue did not change the absorbance at 348 nm for each of the analogues **24-27**, indicating that NADH was tightly bound to the enzyme. Similarly, NADH formation was also observed with some phosphate substrate analogues. These phosphate analogues included 2-deoxy D-glucose 6-phosphate, D-glucitol 6-phosphate, 4-deoxy D-glucose 6-phosphate **46**, 4-deoxy D-glucitol 6-phosphate **47**, and erythritol 4-phosphate **50**. When analogues showing weak or no inhibitory characteristics were added to MIP synthase, no formation of NADH was detected in most cases. These analogues tested include α, α -gem-difluorohomophosphonates **36, 37, 38, 39**, 3-deoxy D-glucose 6-phosphate **44**, and 3-deoxy D-glucitol 6-phosphate **45**. One exception is 4-deoxy-D-glucose 6-phosphate **46**. Although 4-deoxy-D-glucose 6-phosphate **46** showed no inhibition of MIP synthase at 1 mM, a low level of NADH formation was detected when 4-deoxy-D-glucose 6-phosphate **46** was incubated with MIP synthase and NAD.

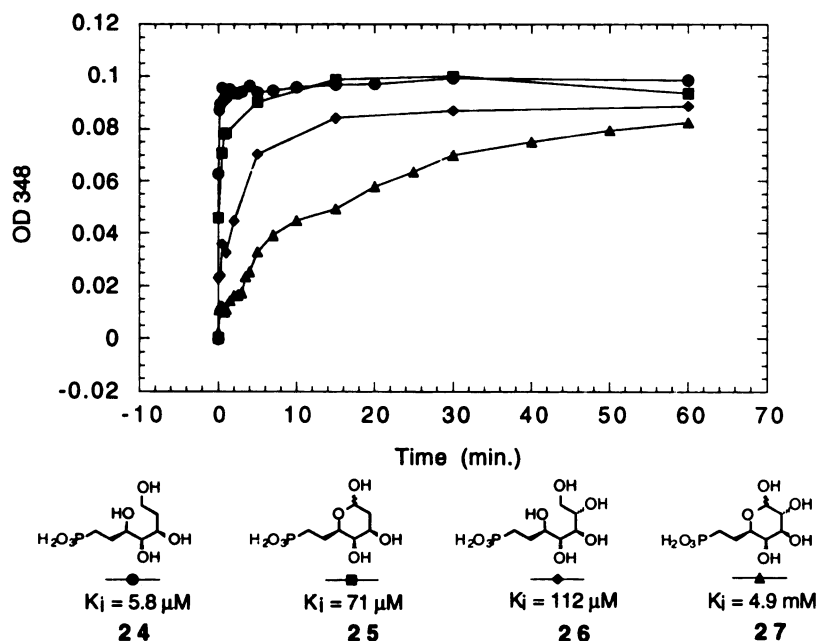
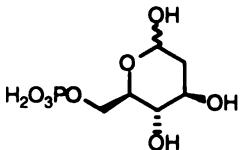
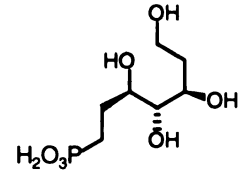
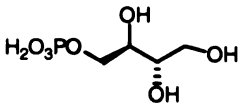
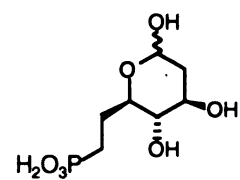
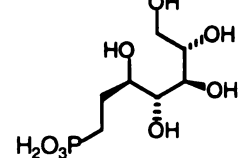
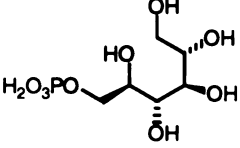
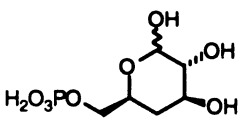
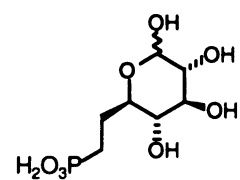
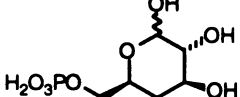


Figure 39. NADH formation during incubation of homophosphonate inhibitors with MIP synthase.

Observation of an increased absorbance at 348 nm provided the first direct evidence that NADH was formed during MIP synthase-catalyzed conversion of D-glucose 6-phosphate into *myo*-inositol 1-phosphate. Eisenberg previously reported³⁸ that *myo*-2-inositol 1-phosphate was trapped with NaB^3H_4 and hypothesized that the rate-limiting step was the reduction of *myo*-2-inositol 1-phosphate. High levels of steady state NADH were consistent with the hypothesis that the initial oxidation step was rapid, and that the rate-limiting step was located in a later stage of the turnover, likely the reduction of *myo*-2-inosose 1-phosphate.³⁸ High steady state levels of NADH also suggested that significant portions of enzyme existed as a complex with NADH and intermediates during the normal catalytic cycle.

Evidence supporting the formation of NADH during the catalysis was provided also by observation of an increase in absorbance at 348 nm during incubation of MIP synthase with substrate analogues. All of the potent inhibitors tested led to the formation of enzyme-bound NADH when incubated with MIP synthase in the presence of NAD, while most of those analogues that showed weak or no inhibition did not result in NADH formation. Table 12 lists the inhibitors that led to the formation of enzyme-bound NADH upon incubation with MIP synthase and NAD. For the potent inhibitors, the increase of absorbance at 348 nm rapidly reached the steady state level. The time needed for the NADH to accumulate to the maximum level was just a fraction of a minute for the potent inhibitors. For the weak inhibitors, the accumulation of NADH was much slower. The maximum level of NADH formation was not attained for an hour for some of the weaker inhibitors. These experimental results suggested that the potent inhibitors were bound in the enzyme active site similarly to the natural substrate, and were subsequently oxidized into reaction intermediate analogues. The inhibition potency of an analogue depended whether the analogue was readily oxidized. A lack of substrate analogue oxidation resulted in either weak or no inhibition of MIP synthase. From these experimental observations, we could draw some valuable clues about the interactions of enzyme and inhibitor at the

Table 15. Inhibitors leading to the formation of enzyme-bound NADH.

Inhibitors	K_i (mM)	Time (min) necessary to reach the maximum at Abs ₃₄₈
	0.0023	0.1
	0.0058	0.3
	0.047	0.5
	0.071	0.75
	0.112	15
	0.154	0.5
	0.93	15
	4.9	60
	no inhibition at 1 mM	> 60

enzyme active site. Unoxidized substrate analogues are likely weakly bound to the enzyme. If the substrate analogue can not be oxidized, then the weak binding of the unoxidized substrate analogue in the active site results in weak inhibition. For an oxidizable substrate analogue that may only be initially bound weakly to the enzyme active site, the analogue is subsequently oxidized by enzyme-bound NAD into a reaction intermediate analogue. The binding of reaction intermediates to the enzyme active site is apparently much tighter than the binding of the unoxidized substrate analogue. The potent inhibition of the enzyme by the oxidizable substrate analogues appeared to be the consequence of transforming a weak binding simple substrate analogue into a strong binding reaction intermediate analogue in the enzyme active site.

In summary, MIP synthase has been purified from an *E. coli* strain overexpressing the *Saccharomyces cerevisiae* INO1 locus. Small amounts of a contaminating enzyme were identified as glucose 6-phosphate dehydrogenase by ^{13}C NMR spectroscopy monitoring under MIP synthase turnover conditions with ^{13}C -labeled substrate. Glucose 6-phosphate dehydrogenase, which interfered with the measurement of enzyme-bound NADH, was removed by Blue A affinity chromatography. Subsequently, steady state NADH was detected for the first time during the normal MIP synthase-catalyzed conversion of D-glucose 6-phosphate into *myo*-inositol 1-phosphate. NADH formation was also observed when substrate analogues were incubated with MIP synthase in the presence of NAD. Analysis of the rate of formation of NADH revealed that it was likely the reaction intermediate analogue generated in situ that was responsible for the potent inhibition of MIP synthase.

EXPERIMENTAL

General Information

General Chemistry

All oxygen- or moisture-sensitive reactions were carried out in flame- or oven-dried glassware under a positive pressure of argon or nitrogen. Oxygen- or moisture-sensitive liquids and solutions were transferred to reaction flasks by syringe or cannula through rubber septa. Unless otherwise stated, reactions were carried out at room temperature. Concentration of solvents was accomplished using a Büchi rotary evaporator under vacuum (water aspirator or vacuum pump at 0.5 mm Hg) and followed by removal of residual solvents at 0.2 mm Hg on a vacuum line. Hydrogenation was carried out with a Parr hydrogenation apparatus at 50 psi hydrogen pressure.

Reagents and Solvents

Water used in reaction solution was deionized and glass-distilled. Ethyl acetate and hexane were distilled through a 500 mm Vigreux column from calcium hydride. Tetrahydrofuran (THF) was freshly distilled under nitrogen from sodium benzophenone ketyl. Dichloromethane and benzene were freshly distilled under nitrogen from calcium hydride. Pyridine, Et₃N and diisopropylamine were distilled from calcium hydride under nitrogen and stored over Linde 4 Å molecular sieves under nitrogen. Methanol was distilled from magnesium methoxide under nitrogen and stored over 3 Å molecular sieves. *N,N*-Dimethylformamide, dimethyl sulfoxide and acetonitrile were dried over Linde 4 Å molecular sieves under nitrogen. 2,2'-Azobis(2-methylpropionitrile) (AIBN) was

recrystallized from ethanol. *m*CPBA was purified by washing with phosphate buffer (1 N, pH 7.0), followed by extensive rinsing with water, and dried under vacuum. Triphenylphosphine was recrystallized from hexane. *N*-Bromosuccinimide (NBS) was recrystallized from water and dried under vacuum. All other solvents and reagents were used as received from commercial sources or purified according to literature procedure.¹⁰⁶

Chromatography

Flash chromatography was carried out on 230-400 mesh silica gel 60 (Whatman). Radial chromatography was carried out with a Harrison Model 7924 Chromatotron, using 1, 2, or 4 mm layers of silica gel 60 PF₂₅₄ containing gypsum (E. Merck). Analytical thin-layer chromatography (TLC) was performed on precoated glass-backed plates of silica gel 60 (0.25 mm thickness, Whatman or E.Merk). TLC plates were visualized by ultraviolet light (254 nm), exposure to iodine vapor, immersion in 5% phosphomolybdic acid in ethanol followed by heating, or immersion in anisaldehyde stain (by volume: 93% ethanol, 3.5% sulfuric acid, 1% glacial acetic acid, and 2.5% anisaldehyde) followed by heating. AG1-X8, Bio-gel A 0.5 and HTP hydroxylapatite were purchased from Bio-Rad, diethylaminoethyl (DEAE) cellulose (DE-52) from Whatman, Dyematrix Blue A from Amicon, and Dowex 50 (H⁺ form) from Sigma. AG1-X8 anion exchange columns were eluted with Et₃NH⁺HCO₃⁻ (TEAB) buffer. TEAB buffer was prepared by bubbling CO₂ gas through an aqueous solution of Et₃N until the pH reached 7.2. Dowex 50 (H⁺) was cleaned before use by the following procedure: a suspension of the gel was treated with bromine at pH 14, rinsed extensively with water, washed with 6 M aqueous hydrochloric acid followed by exhaustive rinsing with water until the filtrate was neutral. DEAE was routinely recycled and cleaned by eluting with 0.5 M ammonium chloride followed by exhaustive elution with water before use. All of the aqueous chromatographic purifications were carried out at 4 °C. High pressure liquid chromatography (HPLC) was carried out with a Rainin HPLC system using a 7.5 mm x 75 mm DEAE-5PW-TSK analytical HPLC

column (purchased from Beckman) and a 10 mm x 30 mm size exclusion HPLC column (obtained from Bio-Rad).

Spectroscopic and Physical Measurements

Proton nuclear magnetic resonance (^1H NMR) spectra and carbon nuclear magnetic resonance (^{13}C NMR) spectra were recorded on a Gemini 200, Gemini 300, or VXR 500S spectrophotometer. Chemical shifts for ^1H NMR spectra are reported in parts per million (ppm) relative to internal tetramethylsilane (Me_4Si , $\delta = 0.00$ ppm) when CDCl_3 was the solvent and to sodium 3-(trimethylsilyl)propionate-2,2-3,3- d_4 (TSP, $\delta = 0.00$ ppm) when D_2O was the solvent. The following abbreviations are used to describe spin multiplicity: s (singlet), d (doublet), t (triplet), m (unresolved multiplet), br (broad peak), dd (doublet of doublets). Chemical shifts for ^{13}C NMR spectra are reported in parts per million (ppm) relative to $^{\circ}\text{CDCl}_3$ ($\delta = 77.0$ ppm) or internal acetonitrile (CH_3CN , $\delta = 3.69$ ppm) in D_2O . Ultraviolet/visible spectra were recorded on a Hewlett Packard 8452A diode array spectrometer or a Perkin-Elmer Lambda 3B spectrometer. Infrared spectra were recorded in wavenumbers (cm^{-1}) on a Perkin-Elmer Model 1800 FTIR spectrometer. Low resolution mass spectra (MS) were recorded on a Finnigan 4000 mass spectrometer and high resolution mass spectra (HRMS) were recorded on a MS50 mass spectrometer. Fast atom bombardment (FAB) mass spectrometry was performed on a Kratos MS50 spectrometer employing glycerol as matrix. Combustion analysis were performed by Atlantic Microlab (Norcross, GA). All temperatures were reported in degrees Celsius, and are not corrected.

Assays

3-Deoxy-D-*arabino*-heptulosonic acid 7-phosphate (DAHP) was synthesized from methyl(methyl 3-deoxy-D-*arabino*-heptulopyranosid)onate according to the procedure of Frost and Knowles^{6a}. Methyl(methyl 3-deoxy-D-*arabino*-heptulopyranosid)onate was

prepared according to the procedure of Reimer et al.^{60a} DHQ synthase was purified from *E. coli* RB791 (*pJB14*) according to the procedure of Frost et al.^{6b} Enzyme was desalted into assay buffer using a Bio-Rad PD-10 desalting column prior to use. High purity nicotinamide adenine dinucleotide (NAD, grade V-C) was purchased from Sigma. D-Glucose 6-phosphate was obtained from Sigma. MIP synthase was isolated from an overexpression of the *Saccharomyces cerevisiae* *INO1* locus in *E. coli* BL12 (DE3)/*pT7-7/MIPSYN*⁷⁰ or from a yeast construct,^{40b} *Saccharomyces cerevisiae* MW 5.55. Protein solutions were concentrated by ultrafiltration (PM-10 Diaflo membranes or Centricon concentrators from Amicon). Protein concentrations were determined by Coomassie dye binding. Phosphorus was determined by the method of Ames.⁷² DAHP was measured using the thiobarbiturate assay. *myo*-Inositol 1-phosphate was determined by the method of Barnett.⁷¹ Least-squares curve fitting was carried out with the computer program KaleidaGraph 2.0 (Synergy Software)

Synthetic Procedures

Synthesis of C-5 epicarbaphosphate (1).

Methyl[1(R)-(1 α ,4 α ,5 β)]-5-[(benzyloxymethyl)oxy]-1-[[1,1-dimethylethyl) dimethylsilyl]oxy]-4-hydroxy-2-cyclohexene-1-carboxylate (10). Alcohol **9** (29.3 g, 72.1 mmol) was dissolved in anhydrous CH₂Cl₂ (100 mL), and anhydrous diisopropylethylamine (19.0 mL, 108 mmol) was added via syringe, under Ar. To the resulting colorless solution was added benzylchloromethyl ether (90%, 12.0 mL, 79.3 mmol) via syringe at rt. After 13 h, an additional amount of benzylchloromethyl ether (90%, 3.0 mL, 19 mmol) was added. Water was added 2 h later, and the aqueous layer was extracted with ether (3x). The combined organic layers were washed successively with dilute aqueous HCl (0.06 M, 2x), aqueous CuSO₄ (2x), saturated

aqueous NaHCO₃ (1x) and brine (1x). The organic layer was dried over MgSO₄ and concentrated to yield the benzoate ester (36.9 g, 97%) as a yellow oil: ¹H NMR (CDCl₃) δ 8.00-8.10 (m, 2 H), 7.45-7.60 (m, 1 H), 7.20-7.45 (m, 7 H), 6.00 (d, *J* = 10 Hz, 1 H), 5.87 (dd, *J* = 10, 2 Hz, 1 H), 5.70 (dd, *J* = 8, 2 Hz, 1 H), 4.83 (s, 2 H), 4.56 (s, 2 H), 4.40-4.60 (m, 1 H), 3.77 (s, 3 H), 2.30-2.50 (m, 1 H), 2.18 (dd, *J* = 12, 12 Hz, 1 H), 0.93 (s, 9 H), 0.15 (s, 3 H), 0.13 (s, 3 H); ¹³C NMR (CDCl₃) δ 173.6, 166.2, 137.8, 133.2, 130.8, 130.0, 129.7, 129.0, 128.5, 128.3, 127.6, 127.5, 93.1, 75.0, 73.8, 71.9, 69.1, 52.2, 38.8, 25.5, 18.0, -3.2, -3.5; MS *m/z* (rel inten) EI 105 (100), 91 (100); CI 395 (100); HRMS (CI) calcd for C₂₉H₃₈O₇Si (M+H⁺) 527.2465, found 527.2457.

A solution of sodium methoxide (3.75 g, 70.0 mmol) in CH₃OH (10 mL) was added to a solution of the benzoate ester (36.9 g, 70.1 mmol) in tetrahydrofuran (100 mL), at rt under nitrogen. After 15 min, the reaction mixture was cooled to 0 °C and quenched with 1N aqueous HCl. The aqueous layer was extracted with ether (1x) and the combined organic layers were successively washed with saturated aqueous NaHCO₃ (1x), water (1x), and brine (1x). The organic phase was dried over MgSO₄ and concentrated down to a colorless oil. Purification by flash chromatography (hexane, EtOAc/hexane, 1:5, v/v, v/v) afforded (along with a fraction overlapping with methyl benzoate which was not repurified) allylic alcohol **10** (21.4 g, 72%) as a colorless oil: ¹H NMR (CDCl₃) δ 7.25-7.40 (m, 5 H), 5.75-5.85 (m, 2 H), 4.92 (d, *J* = 7 Hz, 1 H), 4.83 (d, *J* = 7 Hz, 1 H), 4.75 (d, *J* = 12 Hz, 1 H), 4.60 (d, *J* = 12 Hz, 1 H), 4.05-4.15 (m, 1 H), 3.70-3.90 (m, 1 H), 3.72 (s, 3 H), 2.22 (ddd, *J* = 13, 4, 1 Hz, 1 H), 1.98 (dd, *J* = 13, 12 Hz, 1 H), 0.85 (s, 9 H), 0.08 (s, 3 H), 0.05 (s, 3 H); ¹³C NMR (CDCl₃) δ 174.1, 137.1, 132.4, 128.6, 128.1, 95.2, 79.9, 75.6, 71.8, 70.0, 52.2, 39.2, 25.5, 18.0, -3.2, -3.6; IR (film, NaCl) 3448 (br), 1742 (s); MS *m/z* (rel inten) EI 91 (100); CI 316 (19), 315 (100); HRMS (CI) calcd for C₂₂H₃₄O₆Si (M+H⁺) 423.2203, found 423.2198. Anal. Calcd for C₂₂H₃₄O₆Si: C, 62.58; H, 8.12. Found: C, 62.61; H, 8.08.

Methyl[1(R)-(1 α ,4 α ,5 β)]-5-[(benzyloxymethyl)oxy]-4-[[[(bromomethyl)dimethylsilyl]oxy]-[[[(1,1-dimethylethyl)dimethylsilyl]oxy]-2-cyclohexene-1-carboxylate (11). Allylic alcohol **10** (10.8 g, 25.6 mmol) was dissolved in anhydrous CH₂Cl₂ (150 mL) under Ar, and the solution was cooled to 0 °C. Anhydrous Et₃N (4.30 mL, 30.7 mmol) was added via syringe, followed by bromomethyldimethylchlorosilane (3.50 mL, 25.6 mmol). After 1 h at 0 °C, saturated aqueous NaHCO₃ was added and the aqueous layer was extracted with CH₂Cl₂ (3x). The combined organic layers were washed with cold water (1x), dried over MgSO₄ and concentrated to an oil. Purification by flash chromatography (EtOAc/hexane, 1:5, v/v, v/v) yielded the silyl ether **11** (14.3 g, 97%) as a colorless oil: ¹H NMR (CDCl₃) δ 7.25-7.40 (m, 5 H), 5.70-5.85 (m, 2 H), 4.86 (s, 2 H), 4.68 (d, *J* = 12 Hz, 1 H), 4.60 (d, *J* = 12 Hz, 1 H), 4.20-4.30 (m, 1 H), 3.99 (ddd, *J* = 11, 8, 4 Hz, 1 H), 3.72 (s, 3 H), 2.50 (s, 2 H), 2.25-2.40 (m, 1 H), 1.97 (dd, *J* = 12, 11 Hz, 1 H), 0.87 (s, 9 H), 0.32 (s, 3 H), 0.30 (s, 3 H), 0.10 (s, 3 H), 0.07 (s, 3 H); ¹³C NMR (CDCl₃) δ 173.9, 137.9, 133.3, 128.4, 128.3, 127.8, 127.6, 94.0, 75.4, 72.8, 69.1, 53.2, 52.1, 38.9, 25.4, 18.0, 15.9, -2.8, -3.0, -3.3, -3.6; IR (film, NaCl) 1743 (m); MS *m/z* (rel inten) EI 91 (100); CI 413 (100), 412 (20), 411 (96); HRMS (CI) calcd for C₂₅H₄₁O₆Si₂Br (M+H⁺) 573.1703, found 573.1692.

Methyl[1(S)-(1 α ,3 β ,4 α ,5 α)]-3-[(benzyloxymethyl)oxy]-1-[[[(1,1-dimethylethyl) dimethylsilyl]oxy]-4-hydroxy-5-(hydroxymethyl)-cyclohexane-1-carboxylate (12). Bromomethylsilyl ether **12** (7.52 g, 13.1 mmol) was dissolved in distilled benzene (100 mL, ca. 0.13 M) and Ar was bubbled through the solution for 15 min. The solution was heated to reflux under Ar, and a solution of AIBN (0.1 g) and tributyltin hydride (4.60 mL, 15.7 mmol) in benzene (45 mL) was added over 15 h via syringe pump (ca. 1.05 mmol Bu₃SnH/h), through the top of the reflux condenser. Once the addition was complete, the reaction mixture was refluxed for an

additional 2 h. Heating was stopped and the solvent removed under reduced pressure. The resulting colorless oil was dissolved in CH₃OH (40 mL) and THF (40 mL), and aqueous hydrogen peroxide (30%, 16 mL) was added via syringe. Sodium bicarbonate (2.21 g, 26.2 mmol) was then added as a solid, and the solution was heated to reflux under Ar. After 5 h at reflux, heating was stopped and 20% aqueous sodium thiosulfate was added. The aqueous layer was carefully saturated with solid sodium thiosulfate and then extracted with ether (3x). The combined organic layers were dried over MgSO₄, and concentrated to a yellow oil. This was taken up in technical grade (moist) ether, and iodine was added until the brown color persisted. DBU (2.5 mL, approx 1.2-1.5 eq, relative to the amount of tin hydride employed) was then added dropwise with a pipet, until no more precipitate formed. The suspension was then rapidly suction filtered through a short silica pad. The filtrate was washed with 10% sodium thiosulfate to destroy excess iodine. (Note: this DBU workup is often not necessary for a small scale reactions). Purification by radial chromatography (4 mm plate, hexane, EtOAc/hexane, 1:5, v/v, EtOAc/hexane, 1:1, v/v, v/v,) afforded diol **12** (3.6 g, 60%) as a colorless oil. An impure fraction was repurified by radial chromatography to afford more diol (0.58 g, 10%) and allylic alcohol **10** (0.49 g, 9%). Diol **12** (70 % total yield) slowly crystallized into a white solid: ¹H NMR (CDCl₃) δ 7.25-7.40 (m, 5 H), 4.74 (d, *J* = 7 Hz, 1 H), 4.67 (d, *J* = 7 Hz, 1 H), 4.60 (d, *J* = 12 Hz, 1 H), 4.52 (d, *J* = 12 Hz, 1 H), 3.65-4.00 (m, 4 H), 3.65 (s, 3 H), 2.15-2.40 (m, 2 H), 1.75-2.10 (m, 3 H), 0.84 (s, 9 H), 0.05 (s, 3 H), 0.02 (s, 3 H); ¹³C NMR (CDCl₃) δ 173.9, 137.5, 128.5, 127.9, 127.8, 93.3, 75.9, 75.5, 71.3, 69.6, 65.6, 51.6, 37.2, 36.2, 34.2, 25.4, 17.9, -3.5, -3.6; IR (film, NaCl) 3418 (br), 1736 (m); MS *m/z* (rel inten) EI 91 (100); CI 455 (M+H⁺, 5), 347 (100); HRMS (CI) calcd for C₂₃H₃₈O₇Si (M+H⁺) 455.2465, found 455.2461. Anal. Calcd for C₂₃H₃₈O₇Si: C, 60.76; H, 8.42. Found: C, 60.62; H, 8.37.

Methyl[1(S)-(1 α ,3 β ,4 α ,5 α)]-3-[(benzyloxymethyl)oxy]-1-[[1,1-dimethylethyl)dimethylsilyl]oxy]-5-[[bis(phenyloxy)phosphinyl]-oxymethyl]-4-hydroxycyclohexane-1-carboxylate (13). To a solution of the diol **12** (1.26 g, 2.77 mmol) in anhydrous pyridine (30 mL) was added diphenyl phosphorochloridate (0.86 mL, 4.2 mmol). The mixture was stirred at rt under nitrogen for 15 h. The solvent was then removed under vacuum. The residue was azeotroped with toluene (3x) and then dissolved in EtOAc, washed with brine (3x), dried over MgSO₄, and concentrated to a colorless oil. Purification by flash chromatography (EtOAc/hexane, 1:2, v/v) afforded **13** as a colorless oil (1.58 g, 85%): ¹H NMR (CDCl₃) δ 7.10-7.40 (m, 15 H), 4.66 (d, *J* = 7 Hz, 1 H), 4.32-4.48 (m, 3 H), 4.39 (dd, *J* = 10, 10 Hz, 1 H), 4.17 (ddd, *J* = 10, 10, 5 Hz, 1 H), 3.90-4.00 (m, 1 H), 3.70-3.75 (m, 1 H), 3.67 (s, 3 H), 3.30 (br, 1 H), 2.40-2.55 (m, 2 H), 1.85-2.00 (m, 2 H), 1.51 (dd, *J* = 12, 12 Hz, 1 H), 0.82 (s, 9 H), 0.04 (s, 3 H), 0.02 (s, 3 H); ¹³C NMR (CDCl₃) δ 173.9, 151.1, 150.9 (2), 138.0, 130.4 (2), 129.0, 128.4, 128.3, 126.1, 120.7, 120.6 (2), 120.5, 92.8, 75.4, 74.4, 69.8 (*J*_{POC} = 7 Hz), 65.6, 52.0, 36.3 (*J*_{POCC} = 5 Hz), 35.6, 32.1, 25.8, 18.3, -2.8, -3.2; MS *m/z* (rel inten) EI 91 (100), 92 (13); CI 365 (100), 366 (18), 687 (27, M+H⁺); HRMS calcd. 687.2754 (M+H⁺), found 687.2756; Anal. Calcd. for C₃₅H₄₇O₁₀PSi: C, 61.21; H, 6.90. Found: C, 61.05; H, 6.96.

1(S)-4-*exo*-1,4-Dihydroxy-3-*exo*-[[bis(phenyloxy)phosphinyl]-oxymethyl]-6-oxabicyclo-[3,2,1]octan-7-one (14). To a solution of compound **13** (0.67 g, 1.0 mmol) in acetonitrile (25 mL) was added 49% aqueous HF (5 mL). After 24 h at rt, the reaction mixture was quenched with saturated aqueous NaHCO₃ (100 mL), and extracted with EtOAc (3x). The combined organic layers were dried over MgSO₄ and concentrated to an oil. Purification by radial chromatography (2 mm plate, EtOAc/hexane, 1:1, v/v, EtOAc) gave **14** as a colorless oil (0.313 g, 75%): ¹H NMR (CDCl₃) δ 7.10-7.45 (m, 10 H), 4.73 (dd, *J* = 6, 6 Hz, 1 H), 4.48 (dd, *J* = 10, 10 Hz, 1 H), 4.25-4.30

(m, 1 H), 3.80-4.05 (m, 2 H), 2.72 (s, 1 H), 2.52 (d, $J = 11.5$ Hz, 1 H), 2.08-2.33 (m, 2 H), 1.58-1.63 (m, 2 H); ^{13}C NMR (CDCl_3) δ 178.1, 150.1, 150.0, 149.9, 149.8, 129.8, 125.7, 125.6, 120.0, 119.9, 119.8, 119.7, 76.6, 73.3, 68.0 ($J_{\text{POC}} = 6$ Hz), 62.1, 36.9 ($J_{\text{POCC}} = 6$ Hz), 36.5, 32.3; MS m/z (rel inten) EI 250 (37), 251 (100); CI 421 (100, $\text{M}+\text{H}^+$), 422 (16); HRMS calcd. 421.1052 ($\text{M}+\text{H}^+$), found 421.1051. Anal. Calcd. for $\text{C}_{20}\text{H}_{21}\text{O}_8\text{P}$: C, 57.15; H, 5.04. Found: C, 56.88; H, 5.08.

[1(S)-(1 α ,3 β ,4 α ,5 α)-5-[(Phosphonoxy)methyl]-1,3,4-trihydroxycyclohexane-1-carboxylic acid (1). Platinum oxide (0.1 g) was added to deionized water (10 mL) and reduced to platinum black with hydrogen (50 psi, 20 min) in a Parr hydrogenation apparatus. A solution of the diphenyl phosphate **14** (0.64 g, 1.5 mmol) in THF (10 mL) was hydrogenated at 50 psi hydrogen pressure over the platinum black catalyst. After 24 h, the platinum catalyst was filtered through Celite and the filtrate was concentrated to a brittle foam. The residue was dissolved in water and adjusted to pH 11.5 with dilute NaOH (0.5 N), then stirred at rt for 2 h, neutralized with dilute HCl (0.5 N) to pH 7.5. The crude product was loaded onto an AG1-X8 anion exchange column and eluted with water (50 mL) followed by a linear gradient (250 mL + 250 mL, 200 mM-500 mM) of triethyl ammonium bicarbonate (pH = 7.2). Fractions containing phosphorus were concentrated and azeotroped with 2-propanol (6x). The resulting residue was dissolved in water and passed down through a Dowex 50 (H^+ form) column, neutralized with a freshly prepared LiOH solution to pH 7.5. Removal of water under vacuum afforded white crystalsline solid (0.72 g, 61%): ^1H NMR (D_2O) δ 3.70-4.00 (m, 4 H), 2.10-2.35 (m, 1 H), 2.04 (dd, $J = 15, 4$ Hz, 1 H), 1.94 (dd, $J = 15, 4$ Hz, 1 H), 1.78 (dd, $J = 13, 4$ Hz, 1 H), 1.64 (dd, $J = 13, 11$ Hz, 1 H); ^{13}C NMR (D_2O) δ 185.1, 77.8, 72.5, 71.5, 67.5 ($J_{\text{POC}} = 5$ Hz), 39.1, 38.6 ($J_{\text{POCC}} = 7$ Hz), 35.9; MS m/z (relative intensity) EI 81 (100); CI 189 (100); HRMS (FAB) calcd for $\text{C}_8\text{H}_{15}\text{O}_9\text{P}$ ($\text{M}+\text{H}^+$): 287.0531, found 287.0530.

Synthesis of quinate 3-phosphate (2).

Benzyl[1(S)-(1 α ,3 α ,4 α ,5 β)-4,5-bis[(benzyloxymethyl)oxy]-1,3-dihydroxycyclohexane-1-carboxylate (16). To a solution of methyl ester **15** (1.22 g, 2.73 mmol) in THF (30 mL) was added NaOH (0.2 N, 30 mL). After 40 min at rt, aqueous NaHSO₄ (0.5 N, 100 mL) was added and the aqueous layer was extracted with EtOAc (3x). The combined organic layers were dried over Na₂SO₄ and concentrated to a white solid (1.06 g, 90%): ¹H NMR (CDCl₃) δ 7.25-7.40 (m, 10 H), 5.30 (br, 1 H), 4.98 (d, J = 7 Hz, 1 H), 4.93 (d, J = 7 Hz, 1 H), 4.88 (d, 7 Hz, 1 H), 4.83 (d, J = 7 Hz, 1 H), 4.66 (s, 2 H), 4.63 (s, 2 H), 4.34 (dd, J = 6, 3 Hz, 1 H), 4.10-4.25 (m, 1 H), 3.72 (dd, J = 9, 3 Hz, 1 H), 3.05 (br, 1 H), 2.33 (ddd, J = 13, 5, 3 Hz, 1 H), 1.95-2.25 (m, 3 H); ¹³C NMR (CDCl₃) δ 175.2, 137.4, 137.2, 128.5, 128.4, 127.9, 127.8, 127.7, 94.5, 94.1, 80.2, 75.5, 71.9, 70.0, 69.3, 39.6, 36.1; MS m/z (rel inten) EI 91 (100), 92 (66); CI 91 (100), 92 (13); HRMS (FAB) calcd for C₂₃H₂₈O₈ (M+Na⁺): 455.1682, found 455.1684.

To a solution of the above carboxylic acid (1.03 g, 2.38 mmol) in DMF (30 mL) was added Cs₂CO₃ (0.580 g, 1.79 mmol), followed by benzyl bromide (0.57 mL, 4.8 mmol). The reaction mixture was stirred at rt for 5 h, then diluted with EtOAc (100 mL), washed with brine (3x), dried over MgSO₄, and concentrated to a light yellow oil. Purification by radial chromatography (4 mm plate, EtOAc/hexane, 1:5, v/v, EtOAc/hexane, 1:1, v/v) afforded **16** as a colorless oil (0.86 g, 69%): ¹H NMR δ 7.25-7.40 (m, 15 H), 5.21 (s, 2 H), 4.98 (d, J = 7 Hz, 1 H), 4.93 (d, J = 7 Hz, 1 H), 4.89 (d, J = 7 Hz, 1 H), 4.83 (d, J = 7 Hz, 1 H), 4.55-4.75 (m, 2 H), 4.61 (s, 2 H), 4.20-4.35 (m, 2 H), 4.03 (s, 1 H), 3.67 (dd, J = 10, 6 Hz, 1 H), 3.35 (d, J = 6 Hz, 1 H), 2.32 (ddd, J = 13, 5, 3 Hz, 1 H), 2.16 (ddd, J = 15, 3, 3 Hz, 1 H), 2.04 (dd, J = 15, 3 Hz, 1 H), 1.90 (dd, J = 13, 11 Hz, 1 H); ¹³C NMR δ 173.8, 137.7, 137.4, 135.0, 128.6, 128.5, 128.4, 128.3, 128.1, 127.8, 127.7, 127.6, 94.5, 94.4, 80.4, 75.4, 72.0, 69.7,

69.5, 69.3, 67.6, 40.2, 36.8; MS m/z (rel inten) EI 91 (100); CI 91 (100); HRMS (FAB) calcd. for $C_{30}H_{34}O_8$ ($M+Na^+$): 545.2151, found 545.2154. Anal. Calcd for $C_{30}H_{34}O_8$: C 68.95, H 6.59. Found: C 69.06, H 6.63.

Benzyl[1(S)-(1 α ,3 α ,4 α ,5 β)-4,5-bis[(benzyloxymethyl)oxy]-3-[[bis(benzyloxy)phosphinyl]oxy]-1-hydroxycyclohexane-1-carboxylate (17). To a solution of the alcohol **16** (0.720 g, 1.38 mmol) in THF (10 mL) cooled at -78 °C was added a solution of *n*-butyl lithium in hexane (1.6 M, 0.95 mL 1.52 mmol). After 15 min, a solution of tetrabenzyl pyrophosphate (0.817 g, 1.52 mmol) in THF (10 mL) was added via cannula. The reaction mixture was stirred at -78 °C for 1 h, then at 0 °C for 2 h. The reaction was quenched with saturated aqueous NH_4Cl (100 mL). The reaction mixture was extracted with EtOAc (3x), and the combined organic layers were dried over $MgSO_4$, and concentrated to an oil. Purification by radial chromatography (4 mm plate, CH_2Cl_2 , 10:1 CH_2Cl_2 /acetone, v/v) gave **17** as a colorless oil (0.567 g, 53%). 1H NMR ($CDCl_3$) δ 7.25-7.40 (m, 25 H), 5.17 (s, 2 H), 5.09 (s, 2 H), 5.05 (s, 2 H), 4.95-5.10 (m, 1 H), 4.83 (s, 2 H), 4.72 (s, 2 H), 4.61 (s, 2 H), 4.54 (s, 2 H), 4.29 (ddd, $J = 9, 9, 4$ Hz, 1 H), 3.79 (ddd, $J = 9, 3, 3$ Hz, 1 H), 3.11 (s, 1 H), 2.15-2.30 (m, 3 H), 1.99 (dd, $J = 14, 9$ Hz, 1 H); ^{13}C NMR ($CDCl_3$) δ 174.1, 137.6, 137.5, 135.9, 135.8, 135.0, 128.6, 128.5, 128.4, 128.3, 128.2, 128.1, 127.9, 127.8, 127.7, 127.6, 93.9, 76.8 (d, $J_{POCC} = 4$ Hz), 74.8 (d, $J_{POCC} = 6$ Hz), 74.0, 71.5, 69.5, 69.3, 69.2 (d), 39.3, 36.4; HRMS (FAB) calcd. for $C_{44}H_{47}O_{11}P$ ($M+Na^+$): 805.2754, found 805.2790. Anal. Calcd for $C_{44}H_{47}O_{11}P$: C, 67.51; H, 6.05. Found: C, 67.36; H, 6.11.

[1(R)-(1 α ,3 α ,4 α ,5 β)]-3-(Phosphonoxy)-1,4,5-trihydroxycyclohexane-1-carboxylic acid (2). Water (7 mL) was added to a solution of the fully benzylated quinate phosphate **17** (0.41 g, 0.54 mmol) in THF (20 mL). The solution was then hydrogenated at 50 psi hydrogen pressure over 10%

palladium on carbon for 12 h. The catalyst was filtered through Celite. After removal of the solvent under vacuum, the final product was obtained as a brittle foam (0.170 g): ^1H NMR δ 4.72 (m, 1 H), 4.08 (ddd, $J = 10, 10, 4$ Hz, 1 H), 3.67 (ddd, $J = 9, 3, 3$ Hz, 1 H), 2.20-2.30 (m, 2 H), 2.16 (dd, $J = 14, 4$ Hz, 1 H), 1.97 (dd, $J = 14, 10$ Hz, 1 H); ^{13}C NMR δ 180.3, 78.0 (d), 77.3, 76.0 (d), 68.9, 42.3, 38.7; MS m/z (rel inten) EI 94 (100); CI 237 (100).

Syntheses of D-glucose 6-phosphonate (20) and D-glucitol 6-phosphonate (21)

Benzyl 2,3-di-O-benzyl-4,6-O-benzylidene- α -D-arabino-hexopyranoside (28).⁶⁸ A suspension of D-glucose (200 g, 1.11 mol) and *p*-toluenesulfonic acid monohydrate (10 g, 53 mmol) in BnOH (375 mL) was stirred at 85 °C for 5 h. After cooling, the solution was poured into ether (1 L), stirred for 15 min, and left standing at rt overnight. The supernatant was then decanted from the syrupy residue. The residue was mixed with ZnCl_2 (150 g, 1.11 mol) in benzaldehyde (375 mL, 5.55 mol), stirred at rt for 5 h, and poured into a mixture of water (1 L) and hexane (1 L). The mixture was stirred for 30 min, and the solid product was collected by filtration, dissolved in minimal volume of hot ethanol, and poured into cold water (1.2 L). The solid was collected and recrystallized from ethanol to afford the benzylidene intermediate as white crystals (32 g, 8%). To hexane washed NaH (60%, w/w in mineral oil, w/w in mineral oil, 6.7 g, 170 mmol) at 0 °C was added a solution of the above benzylidene (20.0 g, 55.8 mmol) in THF (120 mL) and DMF (30 mL) via cannula, and stirred at 0 °C for 30 min. BnBr (25.8 g, 151 mmol) was added dropwise and the solution was allowed to warm to rt and stirred for 3 h. After quenching excess NaH with CH_3OH , the reaction mixture was poured into cold water (1 L). The precipitate was collected and recrystallized from CH_3OH to yield benzyl ether **28** (22 g, 73%) as white crystals. ^1H NMR (CDCl_3) δ 7.23-7.52 (m,

20 H), 5.55 (s, 1H), 4.93 (d, $J = 11$ Hz, 1 H), 4.84 (d, $J = 11$ Hz, 1 H), 4.82 (d, $J = 4$ Hz, 1 H), 4.75 (d, $J = 12$ Hz, 1 H), 4.73 (d, $J = 12$ Hz, 1 H), 4.58 (d, $J = 12$ Hz, 2 H), 4.20 (dd, $J = 10, 5$ Hz, 1H), 4.11 (dd, $J = 9, 9$ Hz, 1 H), 3.91 (ddd, $J = 10, 10, 5$ Hz, 1 H), 3.50-3.74 (m, 3 H). ^{13}C NMR (CDCl_3) δ 138.8, 138.1, 137.4, 136.9, 128.9, 128.4, 128.3, 128.2, 128.1, 127.9, 127.8, 127.7, 127.5, 126.0, 101.2, 96.5, 82.1, 79.2, 78.7, 75.3, 73.4, 69.3, 69.0, 62.6. Anal. calcd. for $\text{C}_{27}\text{H}_{28}\text{O}_5$: C, 74.98; H, 6.53. found: C, 74.89; H, 6.57.

Benzyl 2,3,4-tri-*O*-benzyl- α -D-arabino-hexopyranoside (30).⁶⁸ To a solution of benzylidene **28** (22.0 g, 40.8 mmol) in CH_2Cl_2 (250 mL) and ether (250 mL) was added LiAlH_4 (7.74 g, 204 mmol) portionwise. The mixture was heated to reflux, and a solution of AlCl_3 (21.8 g, 163 mmol) in ether (250 mL) was added dropwise into the reaction mixture. After 3 h at reflux, the reaction was cooled to rt and quenched with EtOAc and water. The precipitate was removed by filtration and washed with ether. The filtrate was washed with brine (3x), dried over MgSO_4 , and concentrated. The crude product was recrystallized from hexane to afford **30** (18.1 g, 82%) as white crystals. ^1H NMR (CDCl_3) δ 7.25-7.40 (m, 20 H), 4.99 (d, $J = 11$ Hz, 1 H), 4.88 (d, $J = 11$ Hz, 1 H), 4.84 (d, $J = 11$ Hz, 1 H), 4.80 (d, $J = 4$ Hz, 1 H), 4.69 (d, $J = 11$ Hz, 2 H), 4.64 (d, $J = 11$ Hz, 1 H), 4.55 (d, $J = 12$ Hz, 1 H), 4.54 (d, $J = 12$ Hz, 1 H), 4.07 (dd, $J = 9, 9$ Hz, 1 H), 3.65-3.74 (m, 2 H), 3.53 (dd, $J = 10, 10$ Hz, 1 H), 3.49 (dd, $J = 10, 4$ Hz, 1 H), 1.56 (b, 1 H). ^{13}C NMR (CDCl_3) δ 138.8, 138.1, 137.0, 128.5, 128.4, 128.0, 127.9, 127.8, 127.6, 95.5, 81.9, 80.0, 77.4, 75.7, 75.0, 73.0, 71.0, 69.2, 61.7.

Benzyl 2,3,4-tri-*O*-benzyl-6-diethoxyphosphinoyl- α -D-arabino-hexopyranoside (32).⁶⁸ To a solution of alcohol **30** (3.60 g, 6.66 mmol) and NBS (2.37 g, 13.3 mmol) in DMF (50 mL) at 0 °C was added triphenylphosphine (3.49 g, 13.3 mmol) portionwise. The reaction mixture was stirred at 50 °C for 2 h, and then cooled to

rt. After addition of CH₃OH (10 mL), the reaction mixture was concentrated under vacuum to a wet solid, which was dissolved in CH₂Cl₂ (100 mL), washed with brine, dried over MgSO₄, and concentrated. Purification of crude product with flash chromatography (EtOAc/hexane, 1:5, v/v) yielded the bromide as a white solid (3.62 g, 90%). The bromide (4.88 g, 8.09 mmol) was dissolved in triethyl phosphite (40 mL) and refluxed for 24 h. After cooling to rt, excess triethylphosphite was removed under vacuum. The resulting residue was then purified by flash chromatography (EtOAc/hexane, 1:1, v/v) to yield fully protected phosphonate **32** (4.28 g, 80%) as a colorless oil, which crystallized upon standing. ¹H NMR (CDCl₃) δ 7.20-7.50 (m, 20 H), 5.02 (d, *J* = 11 Hz, 1 H), 4.94 (d, *J* = 11 Hz, 1 H), 4.89 (d, *J* = 12 Hz, 1 H), 4.80 (d, *J* = 12 Hz, 1 H), 4.78 (d, *J* = 4 Hz, 1 H), 4.58-4.70 (m, 3 H), 4.53 (d, *J* = 12 Hz, 1 H), 4.02-4.18 (m, 6 H), 3.53 (dd, *J* = 10, 4 Hz, 1 H), 3.22 (dd, *J* = 9, 9 Hz, 1 H), 2.29 (ddd, *J* = 20, 15, 2 Hz, 1 H), 1.79 (ddd, *J* = 16, 16, 11 Hz, 1 H), 1.20-1.37 (m, 6 H). ¹³C NMR (CDCl₃) δ 138.3, 137.6, 136.6, 128.1, 17.9, 127.4, 127.3, 127.1, 93.8, 81.5 (*J*_{PCC} = 21 Hz), 81.4, 79.5, 75.2, 74.6, 72.3, 76.8, 65.7 (*J*_{PCC} = 7 Hz), 60.9 (*J*_{POC} = 28 Hz), 27.9 (*J*_{PC} = 143 Hz), 15.6.

6-Deoxy-6-phosphono-D-glucopyranose (20).⁶⁸ To a solution of fully protected phosphonate **32** (4.18 g, 6.33 mmol) in CH₂Cl₂ (20 mL) at 0 °C was added TMSBr (9.69 g, 63.3 mmol). The mixture was warmed to rt and stirred for 1 h. Removal of solvent left a light yellow oil, which was stirred with water (20 mL) for 1 h. The reaction mixture was extracted with CH₂Cl₂ (4x). The combined organic layers were dried over Na₂SO₄, and concentrated to a white solid, and recrystallized from EtOAc/hexane to give a white powder. This solid was dissolved in CH₃OH and hydrogenated over 10% palladium on carbon for 12 h. The reaction mixture was filtered through a pad of Celite and the filtrate concentrated. The residue was dissolved in water, washed with CH₂Cl₂, and concentrated under vacuum to afford D-glucose 6-phosphonate **20** as a brittle foam

(1.12 g, 73%). ^1H NMR (D_2O) δ 5.20 (d, $J = 4$ Hz, 1 H), 4.65 (d, $J = 8$ Hz, 1H), 3.61-3.70 (m, 2 H), 3.53 (dd, $J = 10, 4$ Hz, 2 H), 3.46 (dd, $J = 9, 9$ Hz, 1 H), 3.21-3.28 (m, 3 H), 2.36 (dd, $J = 17, 2$ Hz, 2 H), 1.93-2.09 (m, 2 H). ^{13}C NMR (D_2O) δ 98.6, 94.6, 78.0 (2), 76.9, 76.8, 76.6 (2), 76.3, 75.2, 74.2, 74.1, 74.0, 69.5, ($J_{\text{PCCC}} = 6$ Hz), 31.8 ($J_{\text{PC}} = 138$ Hz).

6-Deoxy-6-phosphono-D-glucitol (21). D-Glucose 6-phosphonate **20** (0.10 g, 0.41 mmol) was dissolved in water (10 mL) at 0 °C, and NaBH_4 (0.046 g, 1.23 mmol) was added portionwise. The reaction was stirred for 1 h, quenched with Dowex 50 (H^+), passed through a short Dowex 50 (H^+) column, and concentrated to dryness. After azeotropic removal of boric acid with CH_3OH at reduced pressure (6x), D-glucitol 6-phosphonate **21** (0.1 g, 100%) was obtained as a white solid. ^1H NMR (D_2O) δ 4.02-4.09 (m, 1H), 3.84 (dd, $J = 3, 1$ Hz, 1H), 3.80 (ddd, $J = 4, 4, 2$ Hz, 1H), 3.72 (dd, $J = 5, 1$ Hz, 1 H), 2.27 (ddd, $J = 9, 9, 2$ Hz), 1.96 (ddd, $J = 9, 9, 6$ Hz, 1H). ^{13}C NMR (D_2O) δ 77.1, 76.8, 75.6, 72.2, 69.6 ($J_{\text{PCC}} = 5$ Hz), 65.2, 33.4 ($J_{\text{PC}} = 136$ Hz). HRMS (FAB) calcd for $\text{C}_6\text{H}_{15}\text{O}_8\text{P}$ (M-H^-) 245.0426, found 245.0492.

Syntheses of 2-deoxy-D-glucose 6-phosphonate (22) and 2-deoxy-D-glucitol 6-phosphonate (23)

Benzyl 3-O-benzyl-4,6-O-benzylidene-2-deoxy- α -D-arabino-hexopyranoside (29).⁶¹ HCl gas was bubbled into a suspension of 2-deoxy glucose (2.50 g, 15.2 mmol) in BnOH (50 mL) at 0 °C for 10 min, and stirred at 0 °C for 30 min. After bubbling with N_2 for 1 h, the reaction solution was diluted with EtOAc, neutralized with solid NaHCO_3 , and filtered. The filtrate was concentrated to an oil, which solidified upon treatment with hexane. Recrystallization of the solid from EtOAc gave the white crystalline benzyl pyranoside (2.22 g, 57%). This intermediate (2.22 g, 8.64 mmol) was

dissolved in DMF (10 mL) and stirred with benzaldehyde dimethyl acetal (1.32 g, 8.64 mmol) and *p*-toluenesulfonic acid (0.005 g, 0.03 mmol) at 60 °C for 2 h. The reaction was cooled to rt and concentrated under vacuum. The residue was dissolved in EtOAc, washed with saturated aqueous NaHCO₃ solution (3x), dried over MgSO₄, and concentrated to a solid, which was then recrystallized from isopropanol to yield the benzylidene derivative as white needles (2.05 g, 69%). NaH (60%, w/w in mineral oil, 0.96 g, 24 mmol) was washed with hexane (4x) under Ar and cooled to 0 °C, to which was added a solution of the benzylidene (5.5 g, 16 mmol) in THF (50 mL) and DMF (25 mL). After stirring at 0 °C for 15 min, BnBr (3.56 g, 20.8 mmol) was added. The reaction was warmed to rt and stirred for 3 h. After addition of CH₃OH (10 mL), the reaction mixture was poured into cold water. The precipitate was collected and recrystallized from isopropanol to afford **29** (6.52 g, 94%) as white needles. ¹H NMR (CDCl₃) δ 7.21-7.54 (m, 15 H), 5.63 (s, 1 H), 5.09 (d, *J* = 4 Hz, 1 H), 4.85 (d, *J* = 12 Hz, 1 H), 4.71 (d, *J* = 3 Hz, 1 H), 4.65 (d, *J* = 3 Hz, 1 H), 4.46 (d, *J* = 12 Hz, 1 H), 4.24 (dd, *J* = 10, 4, Hz, 2 H), 4.09 (ddd, *J* = 11, 9, 5 Hz, 1 H), 3.65-3.98 (m, 3 H), 2.32 (dd, *J* = 13, 5 Hz, 1 H), 1.83 (ddd *J* = 14, 11, 3 Hz, 1 H). ¹³C NMR (CDCl₃) δ 138.7, 137.6, 137.3, 128.8, 128.5, 128.3, 128.2, 128.0, 127.8, 127.6, 127.5, 126.0, 101.3, 97.3, 83.9, 73.0, 69.1, 63.2, 36.5.

Benzyl 3,4-di-*O*-benzyl-2-deoxy- α -D-arabino-hexopyranoside (31).⁶¹

To a solution of benzylidene **29** (6.5 g, 15 mmol) in CH₂Cl₂ (50 mL) and ether (50 mL) was added LiAlH₄ (2.9 g, 75 mmol) portionwise. The mixture was heated to reflux, and a solution of AlCl₃ (8.0 g, 60 mmol) in ether (50 mL) was added dropwise into the reaction mixture. After 3 h at reflux, the reaction was cooled to rt and quenched with EtOAc and water. The precipitate was removed by filtration and washed with ether. The filtrate was washed with brine (3x), dried over MgSO₄, and concentrated. The crude product was purified by flash chromatography (EtOAc/hexane, 1:2, v/v to afford alcohol **31** (4.22 g, 65%) as white crystals. ¹H NMR (CDCl₃) δ 7.21-7.39 (m, 15 H), 5.00 (d, *J* = 4 Hz, 1

H), 4.94 (d, $J = 11$ Hz, 1 H), 4.68 (d, $J = 11$ Hz, 1 H), 4.65 (s, 2 H), 4.64 (d, $J = 12$ Hz, 1 H), 4.42 (d, $J = 12$ Hz, 1 H), 4.00-4.13 (m, 1 H), 3.68-3.80 (m, 1 H), 3.53 (dd, $J = 9, 9$ Hz, 1 H), 1.68 (ddd, $J = 15, 11, 4$ Hz, 1 H). ^{13}C NMR (CDCl_3) δ 138.6, 138.3, 137.5, 128.4, 128.3, 128.1, 127.8, 127.7 (2), 127.6, 96.7, 78.2, 77.4, 75.0, 71.8, 71.5, 68.9, 62.1, 35.5.

Benzyl 3,4-di-*O*-benzyl-2,6-dideoxy-6-diethoxyphosphinoyl- α -D-arabino-hexopyranoside (33).⁶¹ To a solution of alcohol **31** (1.0 g, 2.3 mmol) and NBS (0.82 g, 4.6 mmol) in DMF (20 mL) at 0 °C was added triphenylphosphine (1.2 g, 4.6 mmol) portionwise. The reaction was stirred at 50 °C for 2 h, and then cooled to rt. After addition of CH_3OH (10 mL), the reaction mixture was concentrated under vacuum to a brown oil, which was dissolved in CH_2Cl_2 (100 mL), washed with brine (3x), dried over MgSO_4 , and concentrated. Purification of crude product with flash chromatography (EtOAc/hexane, 1:5, v/v) yielded the bromide as a white solid (1.12 g, 99%). The bromide (1.00 g, 2.01 mmol) was dissolved in triethyl phosphite (10 mL) and refluxed for 22 h. After cooling to rt, excess triethyl phosphite was removed under vacuum. The resulting residue was then purified by radial chromatography (EtOAc/hexane, 1:1, v/v) to yield fully protected phosphonate **33** (0.94 g, 84%) as a colorless oil. ^1H NMR (CDCl_3) δ 7.22-7.41 (m, 15 H), 4.99 (d, $J = 11$ Hz, 1 H), 4.96 (s, 1 H), 4.88 (d, $J = 12$ Hz, 1 H), 4.65 (d, $J = 10$ Hz, 1 H), 4.62 (d, $J = 4$ Hz, 1 H), 4.58 (d, $J = 11$ Hz, 1 H), 4.46 (d, $J = 12$ Hz, 1 H), 3.98-4.19 (m, 6 H), 3.22 (dd, $J = 9, 9$ Hz, 1 H), 2.30-2.52 (m, 2 H), 1.88 (ddd, $J = 16, 16, 10$ Hz, 1 H), 1.69 (ddd, $J = 13, 11, 4$ Hz, 1 H), 1.21-1.39 (m, 6 H). ^{13}C NMR (CDCl_3) δ 138.4, 138.2, 137.5, 128.3, 128.1, 127.8, 127.6, 127.5, 95.7, 82.4, 82.1, 77.4, 77.3, 74.9, 71.6, 68.4, 66.7, 61.6, 61.4, 61.3, 61.1, 35.3, 28.5 ($J_{\text{PC}} = 143$ Hz), 16.4, 16.3, 16.2, 16.1. Anal. calcd for $\text{C}_{27}\text{H}_{29}\text{O}_4\text{Br}$: C, 65.19; H, 5.88. found: C, 64.90; H, 5.89. Anal. calcd for $\text{C}_{31}\text{H}_{39}\text{O}_7\text{P}$: C, 67.13; H, 7.09. found: C, 67.25; H, 7.14.

2,6-Dideoxy-6-phosphono-D-arabino-hexopyranoside (22).⁶¹ To a solution of fully protected phosphonate **33** (1.0 g, 1.8 mmol) in CH₂Cl₂ (20 mL) at 0 °C was added Et₃N (1.8 g, 18 mmol), followed by TMSBr (5.5 g, 36 mmol). The reaction was warmed to rt and stirred for 1 h. Removal of solvent left a light yellow paste, which was stirred with water (20 mL) for 1 h. The reaction mixture was extracted with CH₂Cl₂ (3x). The combined organic layers were dried over Na₂SO₄, and concentrated to a yellow solid, which was dissolved in a mixture of THF (40 mL) and water (10 mL), and hydrogenated over 10% palladium on carbon for 12 h. The reaction mixture was filtered through a pad of Celite and the filtrate concentrated. The residue was dissolved in water, washed with CH₂Cl₂, passed through a Dowex 50 (H⁺) column, neutralized with aqueous NaOH to pH 7.0, and concentrated under vacuum to afford 2-deoxy-D-glucose 6-phosphonate **22** as a hygroscopic foam (0.562 g, 115%). ¹H NMR (D₂O) δ 5.33 (d, *J* = 2 Hz, 1 H), 4.93 (d, *J* = 6 Hz, 1H), 4.04 (ddd, *J* = 8, 8, 3 Hz, 1 H), 3.93 (ddd, 8, 7, 3 Hz, 1 H), 3.71 (ddd, *J* = 7, 5, 3 Hz, 1H), 3.57 (ddd, *J* = 8, 7, 3 Hz, 1 H), 3.20 (dd, *J* = 5, 5 Hz, 1 H), 3.16 (dd, *J* = 5, 5 Hz, 1 H), 2.26 (ddd, *J* = 7, 3, 1 Hz, 1 H), 2.02-2.14 (m, 3 H), 1.67-1.87 (m, 3 H), 1.51 (ddd, *J* = 7, 7, 6 Hz, 1 H). ¹³C NMR (D₂O) δ 96.1, 94.0, 79.3 (*J*_{PCCC} = 10 Hz), 78.7 (*J*_{PCCC} = 9 Hz), 75.3, 73.1, 71.3, 70.6, 42.2, 39.9, 35.2 (*J*_{PC} = 130 Hz), 34.9 (*J*_{PC} = 130 Hz). HRMS (FAB) calcd for C₆H₁₃O₇P (M+Na⁺) 251.0296, found 251.0298.

2,6-dideoxy-6-phosphono-D-arabino-hexitol (23). 2-Deoxy-D-glucose 6-phosphonate **22** (0.070 g, 0.26 mmol) was dissolved in water (15 mL) at 0 °C, and NaBH₄ (0.058 g, 1.5 mmol) was added portionwise. The reaction was stirred for 2 h, and quenched with Dowex 50 (H⁺), passed through a short Dowex 50 (H⁺) column, and concentrated to dryness. After azeotropic removal of boric acid with CH₃OH under reduced pressure (6x), 2-deoxy-D-glucitol 6-phosphonate **23** was obtained as a white solid. ¹H NMR (D₂O) δ 3.98-4.09 (m, 2 H), 3.73 (dd, *J* = 7, 7 Hz, 2 H), 3.34 (dd, *J* =

...the ... of ...

...the ... of ...

...the ... of ...

...the ... of ...

...the ... of ...

...the ... of ...

...the ... of ...

...the ... of ...

8, 2 Hz, 1 H), 2.29 (ddd, $J = 19, 16, 2$ Hz, 1 H), 1.75-2.05 (m, 3 H). ^{13}C NMR (D_2O) δ 79.2 ($J_{\text{PCCC}} = 15$ Hz), 69.7 ($J_{\text{PCC}} = 5$ Hz), 69.5, 61.3, 38.1, 34.6 ($J_{\text{PC}} = 136$ Hz). HRMS (FAB) calcd for $\text{C}_6\text{H}_{15}\text{O}_7\text{P}$ ($\text{M}+\text{Na}^+$) 253.0453, found 253.0450.

Syntheses of D-glucose 6-homophosphonate (24) and D-glucitol 6-homophosphonate (25)

Benzyl 2,3,4-tri-*O*-benzyl-6,7-dideoxy-7-diethoxyphosphinoyl- α -D-gluco-hept-6-*trans*-enopyranoside (34).⁶¹ Oxalyl chloride in CH_2Cl_2 (2 M, 2.3 mL, 4.6 mmol) was added to anhydrous CH_2Cl_2 (20 mL) at -78 °C, and anhydrous DMSO (0.44 g, 5.6 mmol) was added slowly under Ar. After 5 min, a solution of alcohol **30** (2.0 g, 3.7 mmol) in CH_2Cl_2 (30 mL) at -78 °C was cannulated into the reaction mixture. Triethylamine (0.76 g, 7.5 mmol) was added via a syringe 45 min later. After an additional 30 min at -78 °C, the reaction was warmed to rt and quenched with water. CH_2Cl_2 was added and the organic layer was washed successively with aqueous HCl (0.06 N, 1x), aqueous NaHCO_3 (2x), and brine (2x). Drying and concentration afforded the aldehyde. Without purification, the aldehyde was dissolved in THF (20 mL) and cooled to -78 °C. Tetramethyl methylenediphosphonate (1.29 g, 5.55 mmol) in THF (15 mL) was cooled to -78 °C under Ar, and *n*BuLi (1.6 M, 3.50 mL, 5.55 mmol) was then added. After 30 min, the above solution of aldehyde was added via a cannula. After stirring at -78 °C for 15 min, then at rt for 30 min, the reaction was diluted with ether, washed with brine, dried over MgSO_4 , and concentrated to an oil. Purification by flash chromatography (EtOAc/hexane, 1:1, v/v) yielded fully protected homophosphonate **34** as an oil (1.62 g, 68%). ^1H NMR (CDCl_3) δ 7.24-7.40 (m, 20 H), 6.90 (ddd, $J = 23, 21, 4$ Hz, 1 H), 5.96 (ddd, $J = 21, 17, 2$ Hz, 1 H), 5.00 (d, $J = 11$ Hz, 1 H), 4.85 (d, $J = 3$ Hz, 1 H), 4.84 (d, $J = 10$ Hz, 1 H), 4.83 (d, $J = 11$ Hz, 1 H), 4.68 (d, $J = 12$ Hz, 1 H), 4.67 (d, $J = 12$ Hz, 1 H), 4.57 (d, $J = 11$ Hz, 1 H), 4.56 (d, $J = 12$ Hz, 1 H), 4.54 (d, $J = 12$

Hz, 1 H), 4.26-4.33 (m, 1 H), 4.04-4.13 (m, 1 H), 3.72 (d, $J = 2$ Hz, 3 H), 3.68 (d, $J = 2$ Hz, 3 H), 3.51 (dd, $J = 10, 4$ Hz, 1 H), 3.24 (dd, $J = 10, 9$ Hz, 1 H). ^{13}C NMR (CDCl_3) δ 148.8 ($J_{\text{PCC}} = 6$ Hz), 138.5, 137.9, 137.5, 136.8, 128.4, 128.3 (2), 128.2, 128.1, 128.0, 127.9, 127.8, 127.6, 116.5 ($J_{\text{PC}} = 188$ Hz), 95.5, 81.7, 81.5, 79.7, 75.7, 75.3, 73.0, 70.2, 70.0, 69.4, 52.3 ($J_{\text{POC}} = 6$ Hz).

6,7-Dideoxy-7-phosphono- α -D-glucopyranose (24).⁶¹ To a solution of fully protected homophosphonate **34** (0.569 g, 1.02 mmol) in CH_2Cl_2 (10 mL), TMSBr (1.56 g, 10.2 mmol) was added at 0 °C. The reaction was stirred for 1 h and concentrated to a light yellow oil. Water (5 mL) and THF (5 mL) were then added and the mixture was stirred for 30 min. After the reaction mixture was diluted with water (50 mL) and extracted with CH_2Cl_2 (4x), the combined organic layers were dried over Na_2SO_4 and concentrated. The residue was dissolved in CH_3OH (20 mL) and hydrogenated over 10% palladium on carbon for 12 h. The suspension was filtered through a pad of Celite and the filtrate concentrated. The residue was dissolved in water, washed with CH_2Cl_2 , and concentrated under vacuum to afford D-glucose 6-homophosphonate **24** as a brittle foam (0.254 g, 96%). ^1H NMR (D_2O) δ 5.19 (d, $J = 2$ Hz, 1 H), 4.61 (d, $J = 5$ Hz, 1H), 3.79 (ddd, $J = 5, 5, 1$ Hz, 1 H), 3.66 (dd, $J = 6, 6$ Hz, 1H), 3.53 (dd, $J = 6, 2$ Hz, 1H), 3.44 (dd, $J = 6, 6$ Hz, 1 H), 3.40 (ddd, $J = 5, 5, 2$ Hz, 1,H), 3.20-3.26 (m, 3 H), 1.64-2.16 (m, 8 H). ^{13}C NMR (D_2O) δ 98.7, 94.8, 78.5, 78.0, 77.8, 77.1, 76.0, 75.8, 75.5, 74.5, 73.6, 73.4, 27.1 ($J_{\text{PCC}} = 3$ Hz), 27.0 ($J_{\text{PCC}} = 3$ Hz), 25.2 ($J_{\text{PC}} = 136$ Hz), 25.1 ($J_{\text{PC}} = 135$ Hz). HRMS (FAB) calcd for $\text{C}_7\text{H}_{15}\text{O}_8\text{P}$ ($\text{M}+\text{H}^+$) 259.0583, found 259.0578.

6,7-Dideoxy-7-phosphono- α -D-glucopyranitol (25). D-Glucose 6-homophosphonate **24** (0.14 g, 0.54 mmol) was dissolved in water (10 mL) at 0 °C, and NaBH_4 (0.12 g, 3.2 mmol) was added portionwise. The reaction was stirred for 1 h, and quenched with Dowex 50 (H^+), passed through a short Dowex 50 (H^+) column, and

concentrated to dryness. After azeotropic removal of boric acid with CH₃OH under reduced pressure (6x), D-glucitol 6-homophosphonate **25** was obtained as a brittle foam. ¹H NMR (D₂O) δ 3.82-3.88 (m, 2 H), 3.74 (dd, *J* = 7, 2 Hz, 1 H), 3.71 (dd, *J* = 5, 1 Hz, 1 H), 3.63 (dd, *J* = 7, 4 Hz, 1 H), 3.55 (dd, *J* = 5, 2 Hz, 1 H), 1.90-2.00 (m, 1 H), 1.59-1.76 (m, 2 H), 1.47-1.56 (m, 1 H). ¹³C NMR (D₂O) δ 76.3, 75.8, 74.3 (*J*_{PCCC} = 16 Hz), 72.7, 65.3, 29.8 (*J*_{PCC} = 3 Hz), 27.2 (*J*_{PC} = 134 Hz). HRMS (FAB) calcd for C₇H₁₇O₈P (M-H)⁻ 259.0583, found 259.0606.

Syntheses of 2-deoxy-D-glucose 6-homophosphonate (26) and 2-deoxy-D-glucitol 6-homophosphonate (27)

Benzyl 3,4-di-O-benzyl-2,6,7-trideoxy-7-diethoxyphosphinoyl- α -D-arabino-hept-6-trans-enopyranoside (35). Oxalyl chloride in CH₂Cl₂ (2 M, 0.60 mL, 1.2 mmol) was added to anhydrous CH₂Cl₂ (15 mL) at -78 °C, and anhydrous DMSO (0.12 g, 1.5 mmol) was added slowly under Ar. After 5 min, a solution of alcohol **31** (0.44 g, 1.0 mmol) in CH₂Cl₂ (15 mL) at -78 °C was cannulated into the reaction mixture. Triethylamine (0.2 g, 2 mmol) was added via a syringe 45 min later. After an additional 30 min at -78 °C, the reaction was warmed to rt and quenched with water. CH₂Cl₂ was added and the organic layer was washed successively with aqueous HCl (0.06 N, 1x), saturated aqueous NaHCO₃ (2x), and brine (2x). Drying and concentration afforded the aldehyde. Without purification, the aldehyde was dissolved in THF (20 mL) and cooled to -78 °C. Tetramethyl methylenediphosphonate (0.35 g, 1.5 mmol) in THF (10 mL) was cooled to -78 °C under Ar, and *n*BuLi (1.6 M, 0.94 mL, 1.5 mmol) was then added. After 30 min, the above solution of aldehyde was added via a cannula. After stirring at -78 °C for 15 min, then at rt for 30 min, the reaction was diluted with ether, washed with brine, dried over MgSO₄, and concentrated to an oil. Purification by flash chromatography (EtOAc/hexane, 1:1, v/v) yielded fully protected homophosphonate **35** (0.22 g, 41%) as

an oil. ^1H NMR (CDCl_3) δ 7.20-7.30 (m, 15 H), 7.01 (ddd, $J = 23, 21, 4$ Hz, 1H), 6.04 (ddd, $J = 21, 17, 2$ Hz, 1H), 5.03 (d, $J = 4$ Hz, 1H), 4.88 (d, $J = 12$ Hz, 1H), 4.55-4.70 m, 4 H), 4.42 (d, $J = 4.42$ Hz, 1H), 4.25-4.33 (m, 1 H), 4.00-4.12 (m, 1 H), 3.72 (d, $J = 2$ Hz, 3 H), 3.69 (d, $J = 2$ Hz, 3 H), 3.23 (dd, $J = 9, 9$ Hz, 1H), 2.32 (dd, $J = 13, 5$ Hz, 1H), 1.68 (ddd, $J = 13, 11, 4$ Hz, 1H). ^{13}C NMR (CDCl_3) δ 149.3 ($J_{\text{POC}} = 7$ Hz), 138.1, 137.6, 137.1, 128.1, 128.0, 127.8, 127.5, 127.4, 127.3, 115.8 ($J_{\text{PC}} = 188$ Hz), 96.3, 81.6, 77.0, 74.9, 71.5, 70.5 (m), 68.9, 52.0, 35.1. HRMS (FAB) calcd for $\text{C}_{30}\text{H}_{36}\text{O}_7\text{P}$ ($\text{M}+\text{H}^+$) 539.2199, found 539.2208.

2,6,7-Trideoxy-7-phosphono- α -D-arabino-heptose (26).⁶¹ To a solution of **35** (0.49 g, 0.91 mmol) in CH_2Cl_2 (20 mL) at 0 °C was added Et_3N (0.92 g, 9.1 mmol), followed by TMSBr (2.8 g, 18 mmol). The reaction was warmed to rt and stirred for 4 h. Removal of solvent left a light yellow paste, which was stirred with water (20 mL) for 30 min. The reaction mixture was then extracted with CH_2Cl_2 (3x). The combined organic layers were dried over Na_2SO_4 , and concentrated to a light yellow wet solid, which was dissolved in a mixture of THF (8 mL) and water (2 mL), and hydrogenated over 10% palladium on carbon for 12 h. The reaction mixture was filtered through a pad of Celite and the filtrate concentrated. The residue was dissolved in water, washed with CH_2Cl_2 , passed through a Dowex 50 (H^+) column, neutralized with aqueous NaOH to pH 7.2, and concentrated under vacuum to afford a solid. This crude product was purified with AG1-X8 anion exchange chromatography eluted with a linear gradient (250 mL + 250 mL, 100-300 mM) of $\text{Et}_3\text{NH}^+\text{HCO}_3^-$ (pH 7.2). Fractions containing organic phosphate were combined, passed through Dowex 50 (H^+) column, degassed, and neutralized with dilute aqueous NaOH . Concentration under vacuum afforded the disodium salt of 2-deoxy-D-glucose 6-homophosphonate **26** (0.159 g, 61%) as a light yellow flakes. ^1H NMR (D_2O) δ 5.35 (d, $J = 2$ Hz, 1 H), 4.91 (dd, $J = 6, 1$ Hz, 1 H), 3.90 (ddd, $J = 7, 6, 3$ Hz, 1 H), 3.76 (ddd, $J = 5, 5, 2$ Hz, 1 H), 3.68 (ddd, $J = 7, 5, 3$

Hz, 1 H), 3.30 (ddd, $J = 5, 5, 2$ Hz, 1 H), 3.23 (dd $J = 6, 6$ Hz, 1 H), 3.17 (dd, $J = 6, 6$ Hz, 1 H), 2.26 (ddd, $J = 7, 3, 1$ Hz, 1 H), 2.14 (dd, $J = 8, 3$ Hz, 1H), 2.01-2.10 (m, 2 H), 1.61-1.74 (m, 5 H), 1.38-1.54 (m, 3 H). ^{13}C NMR (D_2O) δ 96.2, 94.0, 78.9, 78.7, 77.5, 77.0, 75.1, 74.9, 73.2, 70.8, 42.5, 40.2, 28.5 ($J_{\text{PCC}} = 13$ Hz), 28.4 ($J_{\text{PCC}} = 13$ Hz), 27.1 ($J_{\text{PC}} = 132$ Hz), 27.0 ($J_{\text{PC}} = 132$ Hz). HRMS (FAB) calcd for $\text{C}_7\text{H}_{15}\text{O}_7\text{P}$ ($\text{M}+\text{Na}^+$) 265.0453, found 265.0460.

2,6,7-Trideoxy-7-phosphono- α -D-arabino-heptol (27). 2-Deoxy-D-glucose 6-homophosphonate **26** (0.11 g, 0.38 mmol) was dissolved in water (15 mL) at 0 °C, and NaBH_4 (0.086 g, 2.3 mmol) was added portionwise. The reaction was stirred for 1 h, and quenched with Dowex 50 (H^+), passed through a short Dowex 50 (H^+) column, and concentrated to dryness. After azeotropic removal of boric acid with CH_3OH under reduced pressure (6x), 2-deoxy-D-glucitol 6-homophosphonate **27** was obtained as a light yellow solid (0.067 g, 61%). ^1H NMR (D_2O) δ 4.03 (ddd, $J = 6, 3, 1$ Hz, 1 H), 3.73-3.76 (m, 2 H), 3.70 (ddd, $J = 5, 5, 2$ Hz, 1 H), 3.33 (dd, $J = 5, 2$ Hz, 1 H), 1.93-2.00 (m, 1 H), 1.70-1.88 (m, 3 H), 1.54-1.70 (m, 2 H). ^{13}C NMR (D_2O) δ 78.3, 74.0 ($J_{\text{PCCC}} = 16$ Hz), 69.9, 61.4, 38.1, 29.6, 26.6 ($J_{\text{PC}} = 133$ Hz). HRMS (FAB) calcd for $\text{C}_7\text{H}_{17}\text{O}_7\text{P}$ ($\text{M}+\text{Na}^+$) 267.0609, found 267.0615.

Syntheses of D-glucose 6- α,α -gem-difluorohomophosphonate (36) and D-glucitol 6- α,α -gem-difluorohomophosphonate (37)

Benzyl 2,3,4-tri-O-benzyl-6-O-trifluoromethylsulfonyl- α -D-arabino-hexopyranoside (40).⁷⁹ To a solution of alcohol **30** (2.0 g, 3.7 mmol) and pyridine (0.44 g, 5.5 mmol) in CH_2Cl_2 (40 mL) at -30 °C was added triflic anhydride (1.2 g, 4.1 mmol). After 30 min at -30 °C, the reaction was quenched with aqueous NaHSO_4 (0.5 M), diluted with CH_2Cl_2 , washed with aqueous NaHSO_4 (0.5 M, 3x), dried over MgSO_4 , and

concentrated to a light oil. Purification by radial chromatography (EtOAc/hexane, 1:5, v/v) afforded triflate **40** as a colorless oil (2.44 g, 98%). ^1H NMR (CDCl_3) δ 7.19-7.41 (m, 20 H), 5.04 (d, $J = 11$ Hz, 1 H), 4.92 (d, $J = 11$ Hz, 1 H), 4.84 (d, $J = 4$ Hz, 1 H), 4.81 (d, $J = 11$ Hz, 1 H), 4.67 (d, $J = 12$ Hz, 1 H), 4.65 (d, $J = 12$ Hz, 1 H), 4.56 (d, $J = 12$ Hz, 1 H), 4.55 (d, $J = 11$ Hz, 1 H), 4.53 (d, $J = 12$ Hz, 1 H), 4.41-4.45 (m, 2 H), 4.07 (dd, $J = 9, 9$ Hz, 1 H), 3.88 (ddd, $J = 10, 4, 3$ Hz, 1 H), 3.53 (dd, $J = 10, 4$ Hz, 1 H), 3.44 (dd, $J = 10, 9$ Hz, 1 H). ^{13}C NMR (CDCl_3) δ 138.4, 137.8, 137.4, 136.7, 128.5 (2), 128.4, 128.2, 128.1, 128.0, 127.8, 127.7, 118.5 (ddd, $J_{\text{CF}} = 320, 320, 320$ Hz), 95.4, 81.8, 79.7, 76.4, 75.7, 75.1, 74.8, 73.0, 69.6, 68.4.

Benzyl 6-deoxy-6-[(diethoxyphosphinyl)difluoromethyl]-2,3,4-tri-*O*-benzyl- α -D-arabino-hexopyranoside (42).⁷⁹ To a solution of diisopropylamine (1.23 g, 12.1 mmol) and HMPA (2.17 g, 12.1 mmol) at -78 °C was added *n*BuLi (1.6 M, 7.6 mL, 12 mmol) and the mixture was stirred at -78 °C for 10 min. A solution of diethyl difluoromethylphosphonate (2.28 g, 12.1 mmol) in THF (20 mL) was added and stirred for 10 min at -78 °C. A solution of the triflate **40** obtained above in THF (20 mL) was then added via cannula. After another 15 min, reaction was quenched with saturated aqueous NH_4Cl . The aqueous layer was extracted with ether (2x), and the combined organic layers were washed with brine (3x), dried over MgSO_4 , and concentrated to a light yellow oil. Purification of the crude product with flash chromatography (EtOAc/hexane, 1:1, v/v) afforded **42** (1.68 g, 64%). ^1H NMR (CDCl_3) δ 7.21-7.45 (m, 20 H), 5.02 (d, $J = 11$ Hz, 1 H), 4.95 (d, $J = 11$ Hz, 1 H), 4.81 (d, $J = 12$ Hz, 1 H), 4.80 (d, $J = 11$ Hz, 1 H), 4.75 (d, $J = 4$ Hz, 1 H), 4.63 (d, $J = 12$ Hz, 1 H), 4.60 (d, $J = 11$ Hz, 1 H), 4.53 (d, $J = 12$ Hz, 1 H), 4.52 (d, $J = 12$ Hz, 1 H), 4.17-4.32 (m, 5 H), 4.08 (dd, $J = 9, 9$ Hz, 1 H), 3.52 (dd, $J = 10, 4$ Hz, 1 H), 3.22 (dd, $J = 9, 9$ Hz, 1 H), 2.50-2.71 (m, 1 H), 2.01-2.25 (m, 1 H), 1.38 (dd, $J = 7, 7$ Hz, 1 H). ^{13}C NMR (CDCl_3) δ 138.5, 137.8, 137.7, 136.6, 128.6, 128.3, 128.2, 128.0, 127.9, 127.8, 127.7 (2), 127.6, 127.5, 124.7, 121.8, 119.8

(ddd, $J_{CP} = 116$ Hz, $J_{CF} = 260, 260$ Hz), 114.9, 93.9, 81.9, 80.6, 79.6, 75.6, 75.0, 72.6, 68.2, 64.3, 64.2, 35.0 (m), 16.2 (2).

6-Deoxy-6-(phosphonodifluoromethyl)-D-glucopyranose (36). To a solution of **42** (1.15 g, 1.63 mmol) in CH_2Cl_2 (25 mL) at 0 °C was added TMSI (1.31 g, 6.54 mmol). After stirring for 30 min, the reaction mixture was concentrated to a brown oil, which was then stirred with water for 1 h. Removal of water under vacuum yielded a yellow solid, which was dissolved in a mixture of CH_3OH (10 mL) and HOAc (1 mL) and hydrogenated over 10% palladium on carbon for 18 h. The catalyst was replaced and hydrogenolysis was continued for 12 h. The suspension was filtered through a pad of Celite, and the filtrate was concentrated. The crude product was dissolved in water, neutralized to pH 6.5 with dilute aqueous NaOH and purified by AG1-X8 anion exchange chromatography eluted with a linear gradient (250 mL + 250 mL, 100-300 mM) of $\text{Et}_3\text{NH}^+\text{HCO}_3^-$ (pH 7.2). Fractions containing organic phosphate were combined, passed through Dowex 50 (H^+) column, degassed, and neutralized with dilute aqueous NaOH. Concentration under vacuum yielded D-glucose 6- α,α -gem-difluorohomophosphonate **36** (0.354 g, 64%) as white crystals. ^1H NMR (D_2O , pH 6.5) δ 5.19 (d, $J = 4$ Hz, 1 H), 4.68 (d, $J = 8$ Hz, 1 H), 4.27 (dd, $J = 9, 9$ Hz, 1H), 3.86 (dd, $J = 9, 9$ Hz, 1 H), 3.71 (dd, $J = 9, 9$ Hz, 1H), 3.55-3.57 (m, 1 H), 3.48 (dd, $J = 9, 9$ Hz, 1H), 3.24-3.30 (m, 3 H), 2.54-2.68 (m, 2 H), 2.10-2.25 (m, 2 H). ^{13}C NMR (D_2O) δ 98.5, 94.6, 78.4, 76.8, 75.7, 75.6, 75.4, 74.2, 73.1, 68.7, 37.9 (m). HRMS (FAB) calcd for $\text{C}_7\text{H}_{13}\text{O}_8\text{F}_2\text{P}$ ($\text{M}+\text{Na}^+$) 317.0214, found 317.0216.

6-Deoxy-6-(phosphonodifluoromethyl)-D-glucitol (37). D-Glucose 6- α,α -gem-difluorohomophosphonate **36** (0.10 g, 0.30 mmol) was dissolved in water (20 mL) at 0 °C, and NaBH_4 (0.067 g, 1.77 mmol) was added portionwise. The reaction was stirred for 1 h, and quenched with Dowex 50 (H^+), passed through a short

Dowex 50 (H⁺) column, and concentrated to dryness. After azeotropic removal of boric acid with CH₃OH under reduced pressure (6x), the residue was dissolved in water, neutralized with aqueous NaOH to pH 6.5, and concentrated to afforded D-glucitol 6- α,α -gem-difluorohomophosphate **37** (0.10 g, 100%) as a white flakes. ¹H NMR (D₂O) δ 4.19 (dd, $J = 5, 5$ Hz, 1H), 3.80-3.88 (m, 2 H), 3.72 (dd, $J = 7, 2$ Hz, 1 H), 3.61 (dd, $J = 7, 4$ Hz, 1 H), 3.57 (dd, $J = 5, 1$ Hz, 1H), 2.46-2.58 (m, 1 H), 2.16-2.24 (m, 1H). ¹³C NMR (D₂O) δ 76.3, 75.6, 72.3, 68.3, 65.2, 39.4 (m). HRMS (FAB) calcd for C₇H₁₅O₈F₂P (M+Na⁺) 319.0370, found 319.0370.

Syntheses of 2-deoxy-D-glucose 6- α,α -gem-difluorohomophosphate (38) and 2-deoxy-D-glucitol 6- α,α -gem-difluorohomophosphate (39)

Benzyl 3,4-di-O-benzyl-2-deoxy-6-O-trifluoromethylsulfonyl- α -D-arabino-hexopyranoside (41). To a solution of alcohol **31** (1.34 g, 3.08 mmol) and pyridine (0.37 g, 4.6 mmol) in CH₂Cl₂ (30 mL) at -30 °C was added triflic anhydride (0.96 g, 3.4 mmol). After 30 min at -30 °C, the reaction was quenched with aqueous NaHSO₄ (0.5 M), diluted with CH₂Cl₂, washed with aqueous NaHSO₄ (0.5 M, 3x), dried over MgSO₄, and concentrated to a light oil. Purification by radial chromatography (EtOAc/hexane, 1:5, v/v) afforded triflate **41** as a colorless oil (2.59 g, 84%). ¹H NMR (CDCl₃) δ 7.17-7.35 (m, 15 H), 4.99-5.01 (m, 1 H), 4.98 (d, $J = 11$ Hz, 1 H), 4.65 (d, $J = 11$ Hz, 1 H), 4.61 (d, $J = 12$ Hz, 1 H), 4.60 (d, $J = 11$ Hz, 3 H), 4.57 (d, $J = 12$ Hz, 1 H), 4.55 (d, $J = 3$ Hz, 1 H), 4.45 (d, $J = 12$ Hz, 1 H), 4.05 (ddd, $J = 9, 5, 5$ Hz, 1 H), 3.88 (ddd, $J = 10, 3, 3$ Hz, 1 H), 2.33 (dd, $J = 13, 5$ Hz, 1 H), 1.68 (ddd, $J = 13, 11, 3$ Hz, 1 H). ¹³C NMR (CDCl₃) δ 138.2, 137.7, 137.2, 128.5, 128.4, 128.1, 128.0, 127.8, 127.6, 127.5, 118.5 (ddd, $J = 320, 320, 320$ Hz) 96.6, 77.3, 76.8, 75.3, 74.9, 71.5, 69.2, 69.0, 35.0.

Benzyl 2,6-dideoxy-3,4-di-*O*-benzyl-6-[(diethoxyphosphinyl)-difluoromethyl]- α -D-arabino-hexopyranoside (43). To a solution of diisopropylamine (0.92 g, 9.08 mmol) and HMPA (1.63 g, 9.08 mmol) at -78 °C was added *n*BuLi (1.6 M, 5.7 mL, 9.1 mmol) and the mixture was stirred at -78 °C for 10 min. A solution of diethyl difluoromethylphosphonate (1.72 g, 9.08 mmol) in THF (15 mL) was added and stirred for 10 min at -78 °C. A solution of the triflate **41** obtained above in THF (15 mL) was then added via cannula. After another 15 min, the reaction was quenched with saturated aqueous NH₄Cl. The aqueous layer was extracted with ether (2x), and the combined organic layers were washed with brine (3x), dried over MgSO₄, and concentrated to a light yellow oil. Purification of the crude product with flash chromatography (EtOAc/hexane, 1:1, v/v) afforded **43** (0.98 g, 63%). ¹H NMR (CDCl₃) δ 7.20-7.40 (m, 20 H), 5.00 (d, *J* = 11 Hz, 1 H), 4.94 (d, *J* = 3 Hz, 1 H), 4.75 (d, *J* = 11 Hz, 1 H), 4.64 (d, *J* = 12 Hz, 1 H), 4.63 (d, *J* = 11 Hz, 1 H), 4.57 (d, *J* = 12 Hz, 1 H), 4.42 (d, *J* = 12 Hz, 1 H), 4.16-4.31 (m, 5 H), 4.02-4.11 (m, 1 H), 3.22 (dd, *J* = 9, 9 Hz, 1 H), 2.60-2.81 (m, 1 H), 2.34 (dd, *J* = 13, 5 Hz, 1 H), 2.10-2.30 (m, 1 H), 1.70 (ddd, *J* = 13, 13, 4 Hz, 1 H), 1.30-1.42(m, 6 H). ¹³C NMR (CDCl₃) δ 138.4, 138.0, 137.3, 128.2, 128.1, 127.8, 127.5 (2), 127.4, 120.0 (ddd, *J*_{PC} = 215 Hz, *J*_{CF} = 259, 259 Hz), 95.6, 80.7, 77.5, 74.8, 71.4, 68.4, 65.0 (*J*_{PCCC} = 5 Hz), 64.2 (m), 35.3 (m), 35.2, 16.2 (2). HRMS (FAB) calcd for C₃₂H₃₉O₇F₂P (M+H⁺) 605.2480, found 605.2464.

2,6-Dideoxy-6-(phosphonodifluoromethyl)-D-arabino-pyranose (38).

To a solution of **43** (1.00 g, 1.65 mmol) in CH₂Cl₂ (30 mL) at 0 °C was added TMSI (1.32 g, 6.62 mmol). After stirring for 30 min, the reaction mixture was then concentrated to a brown oil, which was then stirred with water for 1 h. The reaction mixture was then extracted with CH₂Cl₂ (3x). The combined organic layers were washed with aqueous NaHSO₄ solution (0.5 M, 3x), dried over MgSO₄, and concentrated to dryness under

vacuum. The resulting residue was dissolved in a mixture of THF (10 mL) and water (2.5 mL) and hydrogenated over 10% palladium on carbon for 18 h. The catalyst was replaced and hydrogenolysis was continued for 12 h. The reaction mixture was filtered through a pad of Celite, and the filtrate was concentrated. The crude product was dissolved in water, neutralized to pH 6.5 with aqueous NaOH and purified by AG1-X8 anion exchange chromatography eluted with a linear gradient (250 mL + 250 mL, 100-300 mM) of $\text{Et}_3\text{NH}^+\text{HCO}_3^-$ (pH 7.2). Fractions containing organic phosphate were combined, passed through Dowex 50 (H^+) column, degassed, and neutralized with dilute aqueous NaOH. Concentration under vacuum afforded 2-deoxy-D-glucose 6- α,α -gem-difluorohomophosphonate **38** (0.278 g, 52%) as a light yellow brittle foam. ^1H NMR (D_2O) δ 5.33 (s, 1H), 4.95 (d, $J = 5$ Hz, 1 H), 4.25 (dd, $J = 6, 6$ Hz, 1H), 3.90-3.96 (m, 1 H), 3.78 (dd, $J = 6, 6$ Hz, 1 H), 3.68-3.74 (m, 1H), 3.22 (dd, $J = 6, 6$ Hz, 1 H), 3.16 (dd, $J = 6, 6$ Hz, 1H), 2.56-2.72 (m, 2H), 2.13-2.30 (m, 4 H), 1.72 (ddd, $J = 8, 8, 2$ Hz, 1 H), 1.52 (ddd, $J = 6, 6, 6$ Hz, 1 H). ^{13}C NMR (D_2O) δ 130.8, 128.3, 127.3, 124.9, 123.9, 121.4, 96.0, 93.9, 77.2, 76.7, 73.1 70.7, 69.3, 42.2, 40.0, 37.4-38.2 (m). HRMS (FAB) calcd for $\text{C}_7\text{H}_{13}\text{O}_7\text{F}_2\text{P}$ ($\text{M}+\text{Na}^+$) 301.0265, found 301.0266.

2,6-Dideoxy-6-(phosphondifluoromethyl)-D-arabino-hexitol (39).

2-Deoxy-D-glucose 6- α,α -gem-difluorohomophosphonate **38** (0.097 g, 0.30 mmol) was dissolved in water (20 mL) at 0 °C, and NaBH_4 (0.068 g, 1.8 mmol) was added portionwise. The reaction was stirred for 1 h, and quenched with Dowex 50 (H^+), passed through a short Dowex 50 (H^+) column, and concentrated to dryness. After azeotropic removal of boric acid with CH_3OH under reduced pressure (6x), the residue was dissolved in water, neutralized with aqueous NaOH to pH 6.5, and concentrated to afford 2-deoxy-D-glucitol 6- α,α -gem-difluorohomophosphonate **39** (0.11 g, 119%) as a yellowish hygroscopic foam. ^1H NMR (D_2O) δ 4.11 (dd, $J = 5, 5$ Hz, 1 H), 4.03 (ddd, $J = 6, 4, 2$ Hz, 1 H), 3.73-3.79 (m, 2 H), 3.37 (dd, $J = 4, 1$ Hz, 1 H), 2.39-2.52 (m, 1 H), 2.12-

2.15 (m, 1 H), 1.72-1.88 (m, 2 H). ^{13}C NMR (D_2O) δ 78.3, 69.6, 68.8, 61.3, 40.9 (m), 38.0. HRMS (FAB) calcd for $\text{C}_7\text{H}_{15}\text{O}_7\text{F}_2\text{P}$ ($\text{M}+\text{Na}^+$) 303.0421 found 303.0420.

Syntheses of 3-deoxy-D-glucose 6-phosphate (44) and 3-deoxy-D-glucitol 6-phosphate (45)

1,2;5,6-Di-*O*-isopropylidene-3-*O*-(*S*-methyldithiocarbonate)- α -D-glucofuranose (52).⁸⁶ NaH (60%, w/w in mineral oil, 4.0 g, 100 mmol) was washed with hexane (6x) and suspended in THF (50 mL), to which was added a solution of 1,2;5,6-diisopropylidene glucofuranose **51** (13 g, 50 mmol) in THF (150 mL). The reaction was then brought to reflux and CS_2 (20 mL) was added dropwise. After 30 min, MeI (20 mL) was added dropwise. The reaction was refluxed for 2 h and then cooled to rt. The reaction mixture was diluted with EtOAc, washed with brine (3x), and dried over Na_2SO_4 . A brown oil was obtained upon concentration, which was then purified by flash chromatography (4:1 hexane/EtOAc) to yield a light yellow oil (11.7 g, 66%) ^1H NMR (CDCl_3) δ 5.91 (d, $J = 6$ Hz, 1 H), 5.90 (d, $J = 4$ Hz, 1 H), 4.67 (d, $J = 4$ Hz, 1 H), 4.25-4.34 (m, 2 H), 4.10 (dd, $J = 9, 5$ Hz, 1 H), 4.04 (dd, $J = 9, 5$ Hz, 1 H), 2.59 (s, 3 H), 1.53 (s, 3 H), 1.41 (s, 3 H), 1.32 (s, 6 H). ^{13}C NMR (CDCl_3) δ 214.5, 112.1, 109.0, 104.8, 84.0, 82.5, 79.5, 72.1, 66.7, 26.6, 26.4, 26.0, 25.0, 19.1.

3-Deoxy-1,2;5,6-di-*O*-isopropylidene- α -D-ribo-hexofuranose (53).⁸⁶ To a refluxing solution of Bu_3SnH (0.82 g, 2.8 mmol) in benzene (15 mL), a solution of **52** (0.663 g, 1.89 mmol) and AIBN (10 mg) in benzene (10 mL) was added dropwise. After refluxing for 2 h, the reaction was cooled to rt and concentrated to an oil, which was then purified by radial chromatography (hexane, EtOAc) to give **53** as a colorless oil. (0.38 g, 82%). ^1H NMR (CDCl_3) δ 5.82 (d, $J = 4$ Hz, 1 H), 4.75 (dd, $J = 5, 5$ Hz, 1 H), 4.07-4.19 (m, 3 H), 3.82 (ddd, $J = 8, 8, 4$ Hz, 1 H), 2.19 (dd, $J = 13, 4$ Hz, 1 H), 1.76

(ddd, $J = 13, 10, 5$ Hz, 1 H), 1.50 (s, 3 H), 1.42 (s, 3 H), 1.35 (s, 3 H), 1.32 (s, 3 H). ^{13}C NMR (CDCl_3) δ 111.1, 109.4, 105.4, 80.2, 78.5, 76.7, 67.0, 35.1, 26.6, 26.3, 26.0, 25.0.

3-Deoxy-1,2-*O*-isopropylidene-6-triphenylmethyl- α -D-ribo-

hexofuranose (54). Diisopropylidene **53** (1.5 g, 6.2 mmol) was stirred with aqueous HCl (0.2 N, 40 mL) at rt for 30 min. The reaction was then neutralized with Amberlite IRA-400 (OH^-). After removal of the resin, the solution was concentrated and dried azeotropically with toluene. The dried residue was then dissolved in CH_2Cl_2 and stirred with TrCl (2.6 g, 9.3 mmol) and Et_3N (1.25 g, 12.4 mmol) at rt for 3 h. The reaction mixture was then washed with saturated aqueous NH_4Cl (3x) and dried over MgSO_4 . Removal of solvent afforded an oil, which was then purified by radial chromatography ($\text{EtOAc}/\text{hexane}$, 1:5, 1:1, v/v). **54** (1.5 g, 59%) was obtained as a white solid. ^1H NMR (CDCl_3) δ 7.20-7.45 (m, 15 H), 5.77 (d, $J = 4$ Hz, 1 H), 4.69 (dd, $J = 4, 4$ Hz, 1 H), 4.29 (ddd, $J = 11, 5, 5$ Hz, 1 H), 4.03 (m, 1 H), 3.24 (dd, $J = 9, 6$ Hz, 1 H), 3.15 (dd, $J = 10, 5$ Hz, 1 H), 2.38 (br, 1 H), 1.93 (dd, $J = 13, 4$ Hz, 1 H), 1.78 (ddd, $J = 13, 11, 5$ Hz, 1 H), 1.50 (s, 3 H), 1.30 (s, 3 H). ^{13}C NMR (CDCl_3) δ 143.6, 128.6, 127.8, 127.1, 111.1, 105.2, 86.8, 80.5, 78.5, 70.8, 64.6, 33.2, 26.7, 26.1. Anal. calcd for $\text{C}_{28}\text{H}_{30}\text{O}_5$: C, 75.31; H, 6.77. found: C, 75.06; H, 6.85.

5-*O*-Benzyl-3-deoxy-1,2-*O*-isopropylidene- α -D-ribo-hexofuranose

(55). NaH (60%, w/w in mineral oil, 0.16 g, 3.9 mmol) was washed with hexane and stirred at 0 °C under Ar, and a solution of **54** (0.80 g, 2.0 mmol) in THF (24 mL) and DMF (6 mL) was then added. BnBr (0.40 g, 2.3 mmol) was added 15 min later and stirring was continued at rt for 8 h. The mixture was then quenched with brine and extracted with ether (3x). The combined organic layers were washed with brine (3x), dried over MgSO_4 , and concentrated. Upon purification by radial chromatography, **55** was

obtained as a foaming syrup (0.88 g, 90%). ^1H NMR (CDCl_3) δ 7.25-7.39 (m, 5 H), 5.76 (d, $J = 4$ Hz, 1 H), 4.70 (d, $J = 12$ Hz, 1 H), 4.66-4.72 (m, 1 H), 4.65 (d, $J = 12$ Hz, 1 H), 4.30 (ddd, $J = 11, 4, 4$ Hz, 1 H), 3.66-3.72 (m, 2 H), 3.58 (dd, $J = 13, 7$ Hz, 1 H), 2.42 (br, 1 H), 2.10 (dd, $J = 13, 5$ Hz, 1 H), 1.80 (ddd, $J = 13, 11, 5$ Hz, 1 H), 1.49 (s, 3 H), 1.30 (s, 3 H). ^{13}C NMR (CDCl_3) δ 138.2, 128.3, 127.7, 127.6, 111.1, 104.9, 80.3, 79.7, 78.5, 73.1, 62.3, 34.5, 26.6, 26.0. Anal. calcd for $\text{C}_{16}\text{H}_{22}\text{O}_5$: C, 65.29; H, 7.53. found: C, 65.38; H, 7.56.

5-*O*-Benzyl-3-deoxy-6-dibenzoxyphosphinoyl-1,2-*O*-isopropylidene- α -D-ribo-hexofuranose (56). Alcohol **55** (0.20 g, 0.69 mmol), tetrazole (0.097 g, 1.4 mmol) and *N,N*-diisopropyl dibenzyl phosphoramidate (0.26 g, 0.76 mmol) in CH_2Cl_2 (20 mL) were stirred at rt for 2 h. The reaction mixture was then cooled to -40 °C (dry ice-acetonitrile bath), and a solution of *m*CPBA (0.238 g, 1.38 mmol) in CH_2Cl_2 (10 mL) was added via cannula. After stirring for 20 min, the reaction mixture was diluted with CH_2Cl_2 and washed with saturated aqueous Na_2SO_3 (2x), saturated aqueous NaHCO_3 (2x), and dried over MgSO_4 . Removal of the solvent left an oil, which was purified by radial chromatography (1:2 -EtOAc/hexane, 1:1, v/v) to give product **56** (0.35 g, 91%) as a colorless oil. ^1H NMR (CDCl_3) δ 7.20-7.37 (m, 15 H), 5.73 (d, $J = 4$ Hz, 1 H), 4.95-5.08 (m, 4 H), 4.67 (d, $J = 12$ Hz, 1 H), 4.65 (dd, $J = 4, 4$ Hz, 1 H), 4.57 (d, $J = 12$ Hz, 1 H), 4.26 (ddd, $J = 10, 5, 5$ Hz, 1 H), 4.18 (ddd, $J = 11, 6, 4$ Hz, 1 H), 4.01 (ddd, $J = 13, 7, 6$ Hz, 1 H), 3.70 (ddd, $J = 9, 5, 5$ Hz, 1 H), 2.07 (dd, $J = 13, 5$ Hz, 1 H), 1.73 (ddd, $J = 13, 12, 5$ Hz, 1 H), 1.46 (s, 3 H), 1.28 (s, 3 H). ^{13}C NMR (CDCl_3) δ 137.8, 135.5, 135.4, 128.4, 128.3, 128.2 (2), 128.0, 127.7, 127.6 (2), 127.5, 127.4, 110.9, 105.0, 80.1, 77.9 ($J_{\text{POCC}} = 8$ Hz), 77.2, 72.9, 69.0 ($J_{\text{POC}} = 3$ Hz), 66.9 ($J_{\text{POC}} = 6$ Hz), 66.8 ($J_{\text{POC}} = 6$ Hz), 34.3, 26.5, 25.9. HRMS (FAB) calcd for $\text{C}_{30}\text{H}_{35}\text{O}_8\text{P}$ ($\text{M}+\text{H}^+$) 555.2148 found 555.2159.

3-Deoxy-D-ribo-hexose 6-phosphate (44). Intermediate **56** (0.347 g, 0.626 mmol) was dissolved in a mixture of THF (8 mL) and water (2 mL), and hydrogenated over 10% palladium on carbon for 4 h. The catalyst was replaced and hydrogenolysis was continued for 12 h. The suspension was filtered through a pad of Celite and the filtrate concentrated to dryness. The crude product was redissolved in water, neutralized with aqueous NaOH, and loaded onto an AG1-X8 column equilibrated with 0.1 M $\text{Et}_3\text{NH}^+\text{HCO}_3^-$ (pH 7.2) buffer, and eluted with a linear gradient (250 mL + 250 mL, 100-300 mM) of $\text{Et}_3\text{NH}^+\text{HCO}_3^-$ (pH 7.2). Fractions containing organic phosphorus were pooled, concentrated, and residual Et_3N azeotropically removed with isopropanol (3x). The residue was redissolved in water and passed through a short Dowex 50 (H^+) column. The filtrate was degassed, neutralized to pH 7 with aqueous NaOH, and concentrated to give 3-deoxy-D-glucose 6-phosphate **44** as a white solid (0.081 g, 45%). Because **44** existed in solution as a complex mixture, ^1H NMR and ^{13}C NMR characterization was best achieved after reduction to **45**. HRMS (FAB) calcd for $\text{C}_6\text{H}_{13}\text{O}_8\text{P}$ ($\text{M}+\text{Na}^+$) 267.0246 found 267.0242.

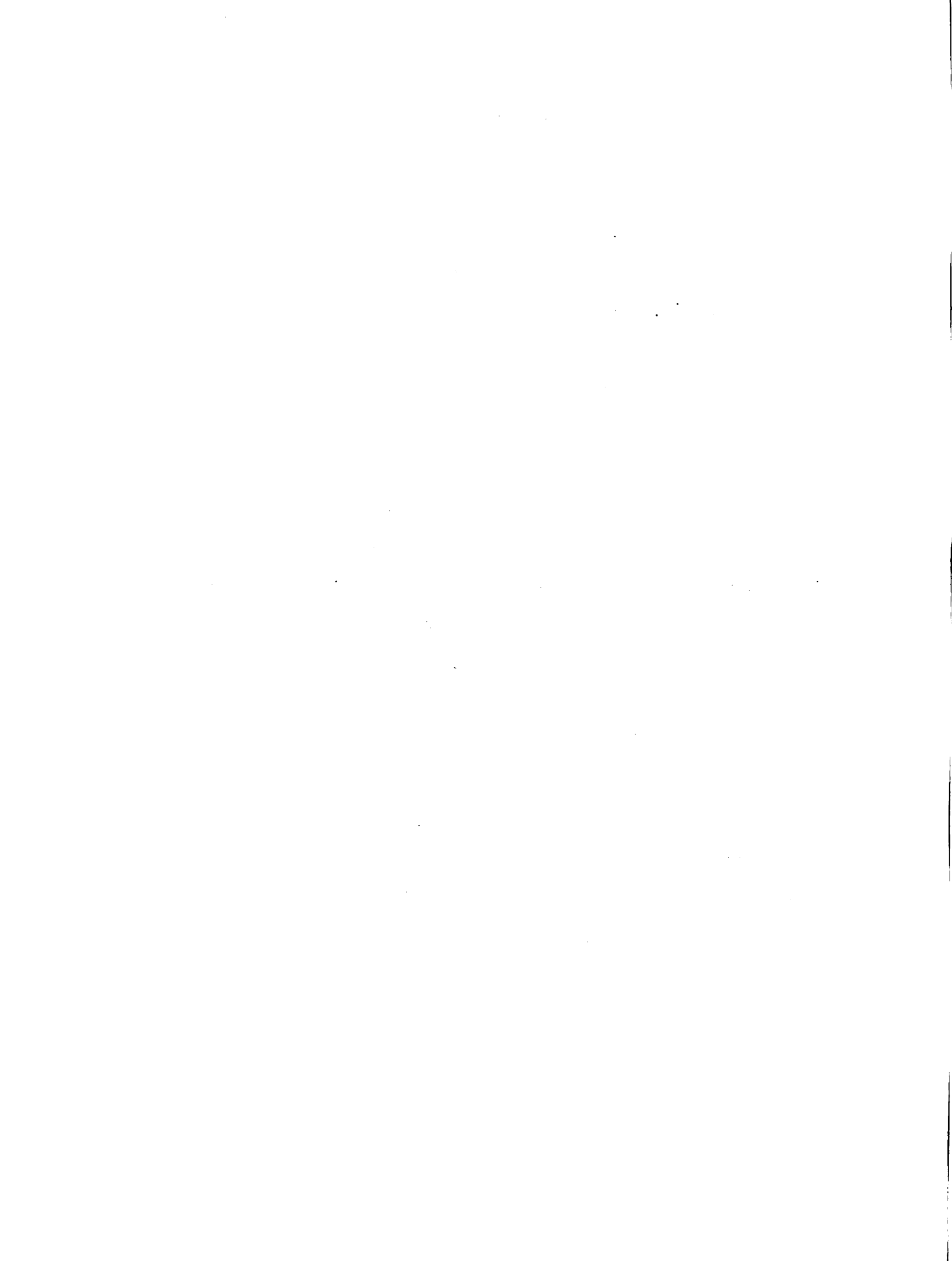
3-Deoxy-D-ribo-hexitol 6-phosphate (45). 3-Deoxy-D-glucose 6-phosphate **44** (32 mg, 0.11 mmol) was dissolved in water (5 mL), and NaBH_4 (0.026 g, 0.67 mmol) was added portionwise. The reaction was stirred for 1 h, and quenched with Dowex 50 (H^+), passed through a short Dowex 50 (H^+) column, and concentrated to dryness. After removing boric acid as an azeotrope with CH_3OH (6x), the residue was dissolved in water, neutralized with aqueous NaOH, and concentrated to give 3-deoxy-D-glucitol 6-phosphate **45** (0.027 g, 85%). ^1H NMR (D_2O) δ 4.08 (ddd, $J = 11, 6, 3$ Hz, 1 H), 3.91-4.02 (m, 2 H), 3.82 (ddd, $J = 10, 6, 3$ Hz, 1 H), 3.74 (ddd, $J = 6, 6, 3$ Hz, 1 H), 3.66 (dd, $J = 12, 3$ Hz, 1 H), 3.52 (dd, $J = 12, 7$ Hz, 1 H), 1.88 (ddd, $J = 14, 7, 3$ Hz, 1 H), 1.63 (ddd, $J = 16, 9, 7$ Hz, 1 H), ^{13}C NMR (D_2O) δ 76.1 ($J_{\text{POCC}} = 8$ Hz),

72.8, 71.9, 69.3 ($J_{\text{POC}} = 5$ Hz), 67.7, 38.0. HRMS (FAB) calcd for $\text{C}_6\text{H}_{15}\text{O}_8\text{P}$ ($\text{M}+\text{Na}^+$) 269.0402 found 269.0408.

Syntheses of 4-deoxy-D-glucose 6-phosphate (46) and 4-deoxy-D-glucitol 6-phosphate (47)

Benzyl 2,3-di-O-benzyl- α -D-arabino-hexopyranoside (57). To a suspension of benzylidene **30** (5.0 g, 9.3 mmol) in CH_3OH (100 mL) was added $\text{TsOH}\cdot\text{H}_2\text{O}$ (0.1 g) and the mixture was stirred at rt for 16 h. The reaction was then quenched with water (20 mL) and concentrated to a white paste, which was dissolved in CH_2Cl_2 , washed with saturated aqueous NaHCO_3 , dried over MgSO_4 , and concentrated to a white solid. After trituration of the solid with hexane and filtration, diol **57** was obtained as a white solid (3.38 g, 81%). ^1H NMR (CDCl_3) δ 7.24-7.55 (m, 15 H), 5.03 (d, $J = 12$ Hz, 1 H), 4.83 (d, $J = 4$ Hz, 1 H), 4.71 (d, $J = 12$ Hz, 1 H), 4.70 (d, $J = 12$ Hz, 1 H), 4.63 (d, $J = 12$ Hz, 1 H), 4.54 (d, $J = 12$ Hz, 1 H), 4.53 (d, $J = 12$ Hz, 1 H), 3.86 (dd, $J = 9, 9$ Hz, 1 H), 3.68-3.74 (m, 2 H), 3.66 (dd, $J = 4, 4$ Hz, 1 H), 3.54 (dd, $J = 9, 9$ Hz, 1 H), 3.48 (dd, $J = 9, 4$ Hz, 1 H). ^{13}C NMR (CDCl_3) δ 138.7, 137.9, 137.0, 128.6, 128.4, 128.3, 127.9 (2), 127.8, 95.5, 81.3, 79.7, 75.3, 72.7, 71.0, 70.4, 69.2, 62.3. Anal. calcd for $\text{C}_{27}\text{H}_{30}\text{O}_6$: C, 71.98; H, 6.71. found: C, 72.09; H, 6.80.

Benzyl 2,3-di-O-benzyl-6-O-triphenylmethyl- α -D-arabino-hexopyranoside (58). A solution containing **57** (2.7 g 6.0 mmol), trityl chloride (22.0 g, 7.2 mmol), and Et_3N (1.25 mL, 9.0 mmol) in CH_2Cl_2 (30 mL) was stirred at rt for 3 h. The reaction was then diluted with CH_2Cl_2 and washed with aqueous CuSO_4 (2x), brine (2x), and dried over MgSO_4 . Solvent removal afforded **58** (4.25 g, 100%) as a white foam. ^1H NMR (CDCl_3) δ 7.18-7.48 (m, 30 H), 4.99 (d, $J = 11$ Hz, 1 H), 4.89 (d, $J = 4$ Hz, 1 H), 4.79 (d, $J = 11$ Hz, 1 H), 4.75 (d, $J = 11$ Hz, 1 H), 4.65 (d, $J = 12$ Hz, 1 H),



4.61 (d, $J = 12$ Hz, 1 H), 4.56 (d, $J = 12$ Hz, 1 H), 3.83 (dd, $J = 10, 10$ Hz, 1 H), 3.78-3.85 (m, 1 H), 3.57 (dd, $J = 9, 9$ Hz, 1 H), 3.54 (dd, $J = 11, 4$ Hz, 1 H), 3.33 (dd, $J = 10, 3$ Hz, 1 H), 3.27 (dd, $J = 10, 5$ Hz, 1 H). ^{13}C NMR (CDCl_3) δ 143.8, 138.7, 138.1, 137.0, 129.6, 128.6, 128.4, 128.3, 128.2, 128.1 (2), 127.9, 127.8 (2), 127.7, 127.1, 127.0, 94.8, 86.7, 81.7, 79.6, 75.5, 72.6, 71.4, 70.3, 68.6, 63.6. Anal. calcd for $\text{C}_{46}\text{H}_{44}\text{O}_6$: C, 79.74; H, 6.40. found: C, 79.60; H, 6.48.

Benzyl 2,3-di-*O*-benzyl-3-*O*-(*S*-methyldithiocarbonate)-6-*O*-triphenylmethyl- α -D-*arabino*-hexopyranoside (59). A solution of **58** (2.00 g, 2.89 mmol) and imidazole (0.013 g) in THF (30 mL) was added via cannula to NaH (60%, w/w in mineral oil, 0.23 g, 5.8 mmol) that had previously been washed with hexane (3x) under Ar. The reaction was then brought to reflux and CS_2 (5 mL) was added dropwise. After 2 h, MeI (5 mL) was added dropwise. The reaction was refluxed for 2 h and then cooled to rt. The reaction mixture was diluted with ether, washed with brine (3x), dried over MgSO_4 , and concentrated to a yellow brittle foam. Purification by radial chromatography (hexane, EtOAc/hexane, 1:5, v/v) afforded **59** (2.0 g, 90%) as a light-yellow, brittle foam. ^1H NMR (CDCl_3) δ 7.17-7.50 (m, 30 H), 5.93 (dd, $J = 9, 9$ Hz, 1 H), 4.90 (d, $J = 4$ Hz, 1 H), 4.88 (d, $J = 12$ Hz, 1 H), 4.78 (d, $J = 11$ Hz, 1 H), 4.71 (d, $J = 12$ Hz, 1 H), 4.68 (d, $J = 11$ Hz, 1 H), 4.64 (d, $J = 11$ Hz, 1 H), 4.56 (d, $J = 12$ Hz, 1 H), 4.12 (dd, $J = 9, 9$ Hz, 1 H), 4.03-4.12 (m, 1 H), 3.65 (dd, $J = 10, 6$ Hz, 1 H), 3.10-3.16 (m, 2 H), 2.37 (s, 3 H). ^{13}C NMR (CDCl_3) δ 214.9, 146.8, 143.7, 138.2, 138.1, 136.7, 128.7, 128.5, 128.4, 128.3, 128.2, 128.1, 128.0, 127.8, 127.7 (2), 127.6, 127.5, 127.2, 126.8, 94.5, 86.5, 79.8, 79.6, 78.9, 75.5, 73.2, 69.4, 68.6, 62.7, 19.1.

Benzyl 2,3-di-*O*-benzyl-4-Deoxy- α -D-*arabino*-hexopyranoside (60). To a boiling solution of Bu_3SnH (0.65 mL, 2.6 mmol) in benzene (20 mL) was added

slowly (over 2 h) a solution of **59** (2.0 g, 2.6 mmol), Bu₃SnH (0.65 mL, 2.6 mmol), and AIBN (0.01 g) in benzene (20 mL). Reflux was continued for 4 h after addition. The reaction was cooled and concentrated to an oil. The oil was redissolved in ether (50 mL), and 58% aqueous HCO₂H (10 mL) was added and stirred for 1 h. Solvent was then removed and the residue was stirred with aqueous NaOH (1 N, 20 mL) for 2 h. The reaction mixture was then extracted with ether (3x). The combined organic layers were washed with brine (3x), dried over MgSO₄, and concentrated to an oil, which was then purified by radial chromatography (hexane/EtOAc, 1:2, v/v) to give **60** (0.96 g, 85%) as an oil. ¹H NMR (CDCl₃) δ 7.23-7.42 (m, 15 H), 4.89 (d, *J* = 4 Hz, 1 H), 4.77 (d, *J* = 12 Hz, 1 H), 4.75 (d, *J* = 12 Hz, 1 H), 4.71 (d, *J* = 10 Hz, 1 H), 4.67 (d, *J* = 9 Hz, 1 H), 4.59 (d, *J* = 9 Hz, 1 H), 4.57 (d, *J* = 12 Hz, 1 H), 4.03 (ddd, *J* = 10, 10, 5 Hz, 1 H), 3.85-3.93 (m, 1 H), 3.54-3.63 (m, 1 H), 3.48-3.54 (m, 1 H), 3.45 (dd, *J* = 9, 4 Hz, 1 H), 2.00 (ddd, *J* = 13, 5, 2 Hz, 1 H), 1.84 (br, 1 H). ¹³C NMR (CDCl₃) δ 138.9, 138.5, 137.4, 128.4, 128.3, 128.2, 127.8, 127.6, 127.5, 96.4, 80.5, 75.1, 73.0, 72.4, 69.0, 68.3, 65.2, 33.0.

Benzyl 2,3-di-O-benzyl-4-deoxy-6-dibenzoxyphosphinoyl- α -D-xylohexopyranoside (61). Alcohol **60** (0.80 g, 1.8 mmol), tetrazole (0.26 g, 3.7 mmol) and *N,N*-diisopropyl dibenzyl phosphoramidate (0.70 g, 2.0 mmol) in CH₂Cl₂ (40 mL) was stirred at rt for 2 h. The reaction mixture was then cooled to -40 °C (dry ice-acetonitrile bath), and a solution of *m*CPBA (0.64 g, 3.7 mmol) in CH₂Cl₂ (20 mL) was added via cannula. After 1 h, the reaction mixture was washed with saturated aqueous Na₂SO₃ (2x), saturated aqueous NaHCO₃ (2x), and dried over MgSO₄. Removal of the solvent left an oil, which was purified by radial chromatography (EtOAc/hexane, 1:2, v/v) to give product **61** (1.22 g, 95%) as an oil. ¹H NMR (CDCl₃) δ 7.24-7.4 (m, 25 H), 4.99-5.12 (m, 5 H), 4.83 (d, *J* = 4 Hz, 1 H), 4.74 (d, *J* = 12 Hz, 1 H), 4.71 (d, *J* = 12 Hz, 1 H), 4.65 (d, *J* = 12 Hz, 1 H), 4.64 (d, *J* = 12 Hz, 1 H), 4.55 (d, *J* = 12 Hz, 1 H),

4.49 (d, $J = 12$ Hz, 1 H), 3.88-4.01 (m, 4 H), 3.41 (dd, $J = 10, 4$ Hz, 1 H), 1.99 (dd, $J = 12, 5$ Hz, 1 H). ^{13}C NMR (CDCl_3) δ 138.8, 138.4, 137.2, 135.8 (m), 128.6, 128.5, 128.3, 128.2 (2), 128.0 (2), 127.8, 127.7, 127.5 (2), 96.0, 80.2, 74.9, 72.9, 72.4, 69.3 ($J_{\text{POC}} = 6$ Hz), 69.1 ($J_{\text{POC}} = 6$ Hz), 67.2 ($J_{\text{POC}} = 6$ Hz), 66.4 ($J_{\text{POCC}} = 8$ Hz), 33.0. HRMS (FAB) calcd for $\text{C}_{41}\text{H}_{43}\text{O}_8\text{P}$ ($\text{M}+\text{H}^+$) 695.2774, found 695.2777.

4-Deoxy-D-xylo-hexose 6-phosphate (46). Perbenzylated precursor **61** (0.50 g, 0.72 mmol) was dissolved in THF (12 mL) and water (3 mL), and hydrogenated over 10% palladium on carbon for 6 h. The catalyst was replaced and hydrogenolysis was continued for 6 h. The suspension was filtered through a pad of Celite and the filtrate concentrated. The residue was dissolved in water and neutralized to pH 7 with aqueous NaOH. The crude product was loaded onto an AG1-X8 column and eluted with a linear gradient (250 mL + 250 mL, 100-300 mM) of $\text{Et}_3\text{NH}^+\text{HCO}_3^-$ (pH 7.2). Fractions containing organic phosphate were combined and concentrated. Residual Et_3N was removed by azeotropic distillation with isopropanol (3x). The residue was redissolved in water, passed down a short Dowex 50 (H^+) column, degassed, neutralized with aqueous NaOH to pH 7 with aqueous NaOH, and concentrated to yield white flakes (0.17 g, 70%). ^1H NMR (D_2O) α -anomer δ 5.27 (d, $J = 2$ Hz, 1 H), 4.22 (d, $J = 7$, Hz, 1 H), 3.97 (ddd, $J = 7, 7, 3$ Hz, 1 H), 3.73-3.85 (m, 2 H), 3.49 (dd, $J = 6, 2$ Hz, 1 H), 2.02-2.06 (m, 1 H), 1.45-1.56 (m, 1 H). β -anomer δ 4.59 (d, $J = 5$ Hz, 1 H), 3.73-3.85 (m, 4 H), 3.18 (dd, $J = 5, 5$ Hz, 1H), 2.02-2.06 (m, 1 H), 1.45-1.56 (m, 1 H). ^{13}C NMR (D_2O) α -anomer δ 95.5, 75.9, 74.3, 70.5, 69.2, 37.1, β -anomer δ 99.0, 78.7, 73.1, 69.7, 69.0, 37.2. HRMS (FAB) calcd for $\text{C}_6\text{H}_{13}\text{O}_8\text{P}$ ($\text{M}+\text{Na}^+$) 267.0246, found 267.0239.

4-Deoxy-D-xylo-hexitol 6-phosphate (47). 4-Deoxy-D-xylo-hexose 6-phosphate **46** (0.026 g, 0.090 mmol) was dissolved in water (5 mL) at 0 °C, and NaBH_4 (0.020 g, 0.54 mmol) was added portionwise. The reaction was stirred for 1 h, and then

quenched with Dowex 50 (H⁺), filtered, and concentrated to dryness. After azeotropic removal of boric acid with CH₃OH under reduced pressure (6x), the residue was dissolved in water, neutralized with aqueous NaOH to pH 7, and concentrated to give **47** (0.024 g, 92%) as a white brittle foam. ¹H NMR (D₂O) δ 3.92-4.08 (m, 2 H), 3.80-3.88 (m, 2 H), 3.55-3.74 (m, 3 H), 1.55-1.75 (m, 2H). ¹³C NMR (D₂O) δ 77.5, 72.8 (*J*_{POC} = 5 Hz), 70.4, 69.8 (*J*_{POCC} = 8 Hz), 65.5, 38.4. HRMS (FAB) calcd for C₆H₁₅O₈P (M+Na⁺) 269.0402, found 269.0398.

Syntheses of 5-deoxy-D-xylo-hexose 6-phosphate (48) and 5-deoxy-D-xylo-hexitol 6-phosphate (49).

3-O-Benzyl-1,2;5,6-di-O-isopropylidene- α -D-glucofuranose (62).

NaH (60%, w/w in mineral oil, 1.15 g, 28.8 mmol) was washed with hexane (3x) under Ar and cooled to 0 °C. A solution of 1,2;5,6-di-O-isopropylidene- α -D-glucofuranose **51** (5.00 g, 19.2 mmol) in THF (80 mL) and DMF (20 mL) was added to NaH suspension via cannula. After 20 min at 0 °C, benzyl bromide (3.94 g, 23.0 mmol) was added, and the ice-bath was removed. The reaction was stirred at rt for 3 h and quenched with water. The reaction mixture was concentrated to about 30 mL, and then diluted with ether (100 mL). The solution was washed with brine (3x), dried over MgSO₄, and concentrated to a yellow oil. Purification by flash chromatography (EtOAc/hexane, 1:4, v/v) afforded **62** (5.66 g, 84%) as a light yellow oil. ¹H NMR (CDCl₃) δ 7.25-7.36 (m, 5 H), 5.90 (d, *J* = 4 Hz, 1 H), 4.67 (d, *J* = 12 Hz, 1 H), 4.64 (d, *J* = 12 Hz, 1 H), 4.58 (d, *J* = 5 Hz, 1 H), 4.32-4.42 (m, 1 H), 4.06-4.16 (m, 2 H), 3.98-4.04 (m, 2 H), 1.48 (s, 3 H), 1.43 (s, 3 H), 1.37 (s, 3 H), 1.31(s, 3 H). ¹³C NMR (CDCl₃) δ 137.6, 128.4, 128.2, 127.8, 127.6, 127.5 (2), 127.4, 111.7, 108.9, 105.3, 82.6, 81.6, 81.3, 72.5, 72.3, 67.4, 26.8, 26.7, 26.2, 25.4.

3-O-Benzyl-1,2-O-isopropylidene- α -D-glucofuranose (63).⁹⁷

Diisopropylidene **62** (2.00 g, 5.71 mmol) was partially dissolved in aqueous acetic acid (60%, v/v, 10 mL) and stirred at 35 °C for 24 h. The reaction was then concentrated to a thick oil, which was then purified by radial chromatography (EtOAc/hexane, 1:2, v/v, EtOAc) to yield an oil (1.46 g, 82%). ¹H NMR (CDCl₃) δ 7.26-7.40 (m, 5 H), 5.93 (d, J = 4 Hz, 1 H), 4.72 (d, J = 12 Hz, 1 H), 4.62 (d J = 3 Hz, 1 H), 4.56 (d, J = 12 Hz, 1 H), 4.08-4.15 (m, 2 H), 4.00-4.05 (m, 1 H), 3.81 (dd, J = 12, 4 Hz, 1H), 3.68 (dd, J = 12, 5 Hz, 1H), 1.48 (s, 3 H), 1.32 (s, 3 H). ¹³C NMR (CDCl₃) δ 137.1, 128.6, 128.2, 127.8, 111.8, 105.1, 82.0, 81.9, 79.9, 72.1, 69.2, 64.3, 26.6, 26.1. Anal. calcd for C₁₆H₂₂O₆: C, 61.92; H, 7.15. found: C, 62.04; H, 7.19.

3-O-Benzyl-1,2-O-isopropylidene-5,6-O-thiocarbonyl- α -D-

glucofuranose (64). A solution of **63** (0.50 g, 1.6 mmol) and thiocarbonyldiimidazole (0.326 g, 1.77 mmol) in THF (15 mL) was refluxed under Ar for 6 h. The reaction was cooled to rt and concentrated to a yellow paste, which was then purified by radial chromatography (EtOAc/hexane, 1:2, v/v). Thionocarbonate **64** (0.53 g, 93%) was obtained as a yellow solid. ¹H NMR (CDCl₃) δ 7.24-7.42 (m, 5 H), 5.97 (d, J = 4 Hz, 1 H), 5.05 (ddd, J = 9, 8, 4 Hz, 1 H), 4.75 (dd, J = 9, 8 Hz, 1H), 4.68 (d, J = 12 Hz, 1 H), 4.55-4.65 (m, 3 H), 4.10 (d, J = 4 Hz, 1 H), 1.49 (s, 3 H), 1.33 (s, 3 H). ¹³C NMR (CDCl₃) δ 191.2, 136.2, 128.5, 128.1, 127.6, 112.2, 105.4, 81.3, 81.2, 79.7, 78.5, 71.9, 70.0, 26.6, 26.0. Anal. calcd for C₁₇H₂₀O₆S: C, 57.94; H, 5.72. found: C, 57.77; H, 5.69.

3-O-Benzyl-5-deoxy-1,2-O-isopropylidene- α -D-xyllo-hexofuranose

(65). A solution of **64** (0.20 g, 0.57 mmol) in benzene was brought to reflux, and a solution of tributyltin hydride (0.33 g, 1.1 mmol) and AIBN (0.015 g) in benzene (20 mL) was added via a syringe pump (over 3 h). Reflux was continued for 2 h. The reaction was

then cooled to 40 °C and aqueous NaOH (10%, 20 mL) was added and stirred at 40 °C overnight. The aqueous layer was separated and extracted with ether. The combined organic layers were washed with brine (3x), dried over MgSO₄, and concentrated to an oil. Purification by radial chromatography (EtOAc/hexane, 5:1, v/v, EtOAc) gave **65** (0.106, 63%). ¹H NMR (CDCl₃) δ 7.26-7.38 (m, 5H), 5.92 (d, *J* = 5 Hz, 1 H), 4.70 (d, *J* = 12 Hz, 1 H), 4.62 (d, *J* = 4 Hz, 1 H), 4.49 (d, *J* = 12 Hz, 1 H), 4.33 (ddd, *J* = 9, 5, 3 Hz, 1 H), 3.82 (d, *J* = 3 Hz, 1 H), 3.75 (d, *J* = 6 Hz, 1 H), 3.73 (d, *J* = 6 Hz, 1 H), 2.00-2.13 (m, 1 H), 1.79-1.85 (m, 1 H), 1.49 (s, 3 H), 1.32 (s, 3 H). ¹³C NMR (CDCl₃) δ 137.4, 128.4, 127.8, 127.6, 111.3, 104.6, 82.4, 82.1, 78.4, 71.6, 60.1, 30.8, 26.5, 26.1. Anal. calcd for C₁₆H₂₂O₅: C, 65.29; H, 7.53. found: C, 65.35; H, 7.60.

3-*O*-Benzyl-5-deoxy-6-dibenzoxyphosphinoyl-1,2-*O*-isopropylidene- α -D-xyllo-hexofuranose (66). A solution of **65** (0.33 g, 1.1 mmol), *N,N*-diisopropyl dibenzyl phosphoramidate (0.567 g, 1.64 mmol), and tetrazole (0.192 g, 2.73 mmol) in CH₂Cl₂ was stirred at rt for 5 h. The reaction was then cooled to -40 °C and a solution of *m*CPBA (0.378 g, 2.19 mmol) in CH₂Cl₂ (10 mL) was added and stirred at -40 °C for 3 h. The reaction was warmed to rt, washed with saturated aqueous Na₂SO₃ (2x), saturated aqueous Na₂CO₃ (2x), dried over MgSO₄, and concentrated to an oil. Purification by radial chromatography afforded **66** (0.512 g, 86%). ¹H NMR (CDCl₃) δ 7.24-7.39 (m, 15 H), 5.89 (d, *J* = 4 Hz, 1 H), 4.98-5.12 (m, 6 H), 4.65 (d, *J* = 12 Hz, 1 H), 4.60 (d, *J* = 4 Hz, 1 H), 4.44 (d, *J* = 12 Hz, 1 H), 4.28 (ddd, *J* = 8, 5, 3 Hz, 1 H), 4.12 (dd, *J* = 7, 7 Hz, 1 H), 4.09 (d, *J* = 7, 7 Hz, 1 H), 3.78 (d, *J* = 3 Hz, 1 H), 2.02-2.14 (m, 1 H), 1.88-2.00 (m, 1 H), 1.45 (s, 3 H), 1.30 (s, 3 H). ¹³C NMR (CDCl₃) δ 137.3, 135.8, 135.7, 128.6 (2), 128.5, 128.4, 128.0, 127.8, 127.5, 111.3, 104.6, 82.1, 76.5, 71.6, 69.1 (*J*_{POC} = 5 Hz), 69.0 (*J*_{POC} = 5 Hz), 65.1 (*J*_{POC} = 6 Hz), 29.0 (*J*_{POCC} = 7 Hz), 26.6, 26.1. HRMS (FAB) calcd for C₃₀H₃₅O₈P (M+H⁺) 555.2148, found 555.2169.

5-Deoxy-D-xylo-hexose 6-phosphate (48). Precursor **66** (0.15 g, 0.27 mmol) in THF (12 mL) and water (3 mL) was hydrogenated over 10% palladium on carbon for 20 h. The reaction mixture was filtered and concentrated. The residue was dissolved in water (10 mL) and stirred with Dowex 50 (H⁺) (5 mL) at 50 °C for 20 h. The reaction mixture was filtered, neutralized with aqueous NaOH, and concentrated to yield **48** (0.095 g, 100%). ¹H NMR (D₂O) δ 5.45 (d, *J* = 2 Hz, 1 H), 5.17 (s, 1H), 4.37 (ddd, *J* = 4, 4, 2 Hz, 1H), 4.33 (ddd, *J* = 4, 4, 2 Hz, 1 H), 4.24 (dd *J* = 2, 2 Hz, 1 H), 4.17 (dd, *J* = 2, 1 Hz, 1 H), 4.12 (dd, *J* = 2, 2 Hz, 1 H), 4.10 (s, 1 H), 3.88-3.99 (m, 2 H), 3.81-3.88 (m, 2 H), 2.06-2.14 (m, 1 H), 1.91-2.02 (m, 2 H), 1.79-1.87 (m, 1 H). ¹³C NMR (D₂O) δ 104.4, 98.5, 83.6, 82.7, 79.8, 79.0, 78.9, 78.1, 64.3, 64.1, 33.1 (*J*_{POCC} = 6 Hz), 32.5 (*J*_{POCC} = 7 Hz). HRMS (FAB) calcd for C₆H₁₃O₈P (M+Na⁺) 267.0246, found 267.0242.

5-Deoxy-D-xylo-hexitol 6-phosphate (49). 5-Deoxy-D-xylo-hexose 6-phosphate **48** (0.027 g, 0.94 mmol) was dissolved in water (10 mL), and NaBH₄ (0.035, 9.4 mmol) was added portionwise. The reaction was stirred at rt for 2 h, and then quenched with Dowex 50 (H⁺), filtered through a short Dowex 50 (H⁺) column, and concentrated. After azeotropic removal of boric acid with CH₃OH (6x), the residue was dissolved in water, neutralized with aqueous NaOH to pH 7, and concentrated to afford **49** (0.027 g, 100%). ¹H NMR (D₂O) δ 4.11 (dd, *J* = 6, 6 Hz, 1H), 4.06 (dd, *J* = 6, 6 Hz, 1H), 3.99 (ddd, *J* = 9, 4, 4 Hz, 1H), 3.83 (ddd, 6, 5, 5 Hz, 12 H), 3.72 (dd, *J* = 12, 5 Hz, 1 H), 3.63 (dd, *J* = 12, 7 Hz, 1H), 3.52 (dd, *J* = 4, 4 Hz, 1 H), 1.79-1.98 (m, 2 H). ¹³C NMR (D₂O) δ 76.2, 74.8, 71.1, 65.9, 65.6, 36.3 (*J*_{POCC} = 7 Hz). HRMS (FAB) calcd for C₆H₁₅O₈P (M+Na⁺) 269.0402, found 269.0405.

Synthesis of D-erythritol 4-phosphate (50).

D-Erythritol 4-phosphate (50). D-Glucose 6-phosphate (0.66 g, 2.0 mmol) was dissolved in water (4 mL), and the resulting solution was added to acetic acid (500 mL). A solution of $\text{Pb}(\text{OAc})_4$ (1.5 g, 3.4 mmol), and H_2SO_4 (6 N, 1.2 mL, 3.5 mmol) in acetic acid (50 mL) was then added via a syringe pump (0.5 mL/min). Once the addition was complete, the reaction mixture was partially concentrated and repeatedly redissolved then evaporated with water under vacuum (3x). The residue was dissolved in water, passed through a Dowex 50 (H^+) column, and the filtrate was concentrated to about 15 mL and stored at 4 °C. Half of the solution was loaded onto an AG1-X8 column equilibrated with HCO_2H (0.2 M), and eluted with a linear gradient (400 mL + 400 mL, 0.05-0.2 M) of $\text{NH}_4^+\text{HCO}_2^-$ in HCO_2H (0.2 M). Fractions were assayed for organic phosphate. The slower running band corresponding to the dimer of erythrose 4-phosphate was collected. The combined fractions were passed through Dowex 50 (H^+), concentrated to dryness and repeatedly redissolved then evaporated with water under vacuum (3x). The residue was then dissolved in water and neutralized with NaHCO_3 to pH 7. After cooling to 0 °C, NaBH_4 (0.38 g 10 mmol) was added and the reaction stirred for 1 h. The reaction was quenched with Dowex 50 (H^+) and filtered through a short Dowex 50 (H^+) column. The filtrate was concentrated to dryness. After azeotropic removal of boric acid with CH_3OH (6x), the residue was dissolved in water, neutralized with aqueous NaOH , and concentrated to afforded **50** as white crystals (0.136 g, 67%). ^1H NMR (D_2O) δ 4.12 (dddd, $J = 16, 16, 5, 3$ Hz, 1 H), 4.07 (ddd, $J = 11, 11, 6$ Hz, 1 H), 3.76-3.83 (m, 2 H), 3.73 (ddd, $J = 7, 7, 2$ Hz, 1 H), 3.64 (ddd, $J = 5, 5, 5$ Hz, 1 H). ^{13}C NMR (D_2O) δ 73.9, 73.1 ($J_{\text{POCC}} = 8$ Hz), 70.1 ($J_{\text{POC}} = 5$ Hz), 65.3. HRMS (FAB) calcd for $\text{C}_4\text{H}_{11}\text{O}_7\text{P}$ ($\text{M}+\text{Na}^+$) 225.0140, found 225.0138.

Synthesis of D-xylo-hexose-5-ulose 6-phosphate (70).**3-O-Benzyl-1,2-O-isopropylidene- α -D-xylo-hexofuranose-5-ulose**

(75).⁹⁷ A suspension of **63** (1.36 g, 4.38 mmol) and dibutyltin oxide (2.18 g, 8.76 mmol) in CH₃OH (50 mL) was refluxed for 3 h. The resulting homogeneous reaction solution was then cooled to rt and concentrated. This residue was then dissolved in CHCl₃ (30 mL) and a solution of Br₂ (0.84 g, 5.2 mmol) in CHCl₃ was added dropwise until the brown color persisted. The reaction mixture was then poured directly onto a silica gel column. A column washing followed by elution (CHCl₃/EtOAc, 2:1, v/v) afforded **75** (1.24 g, 92%). ¹H NMR (CDCl₃) δ 7.18–7.34 (m, 5 H), 6.05 (d, J = 4 Hz, 1 H), 4.82 (d, J = 4 Hz, 1 H), 4.61 (d, J = 4 Hz, 1 H), 4.58 (d, J = 12 Hz, 1 H), 4.51 (d, J = 3 Hz, 1 H), 4.49 (d, J = 4 Hz, 1 H), 4.47 (d, J = 12 Hz, 1 H), 4.31 (d, J = 4 Hz, 1 H), 2.96 (dd, J = 5, 5 Hz, 1 H), 1.47 (s, 3 H), 1.33 (s, 3 H). ¹³C NMR (CDCl₃) δ 208.0, 136.5, 128.4, 128.0, 127.9, 127.5, 112.5, 105.9, 84.4, 83.3, 81.6, 72.4, 68.0, 26.8, 26.1.

3-O-Benzyl-6-dibenzoylphosphinoyl-1,2-O-isopropylidene- α -D-xylo-hexofuranose-5-ulose (76). Compound **75** (0.79 g, 2.6 mmol), tetrazole (0.36 g, 5.1 mmol) and *N,N*-diisopropyl dibenzyl phosphoramidate (0.97 g, 2.8 mmol) in CH₂Cl₂ (30 mL) was stirred at rt for 3 h. The reaction mixture was then cooled to -40 °C (dry ice-acetonitrile bath), and a solution of *m*CPBA (0.884 g, 5.12 mmol) in CH₂Cl₂ (20 mL) was added via cannula. After stirring for 20 min, the reaction mixture was diluted with CH₂Cl₂, washed with saturated aqueous Na₂SO₃ (2x), saturated aqueous NaHCO₃ (2x), and dried over MgSO₄. Removal of the solvent left an oil, which was purified by radial chromatography (EtOAc/hexane, 1:2, v/v) to give product **76** (1.3 g, 89%) as an oil. ¹H NMR (CDCl₃) δ 7.35–7.19 (m, 15 H), 6.01 (d, J = 3.6 Hz, 1 H), 5.12 (s, 1 H), 5.09 (s, 1 H), 5.07 (s, 1 H), 5.06 (s, 1 H), 4.98 (dd, J = 18, 9 Hz, 1 H), 4.87 (dd, J = 18, 10 Hz, 1 H), 4.74 (d, J = 4 Hz, 1 H), 4.56 (d, J = 4 Hz, 1 H), 4.53 (d, J = 12 Hz, 1 H), 4.46 (d,

$J = 12$ Hz, 1 H), 4.29 (d, $J = 3.6$ Hz, 1 H), 1.45 (s, 3 H), 1.31 (s, 3 H). ^{13}C NMR (CDCl_3) δ 200.7, 200.6, 136.5, 135.7, 135.6, 128.6, 128.4, 128.3, 128.0, 127.9, 127.6, 112.5, 105.9, 84.6, 83.2, 81.6, 72.5, 70.7, 70.8, 69.4, 26.8, 26.2. Anal. calcd for $\text{C}_{30}\text{H}_{33}\text{O}_9\text{P}$: C, 63.38; H, 5.85. found: C, 63.24; H, 5.90.

D-xyllo-Hexose-5-ulose 6-phosphate (70). Precursor **76** (0.19 g, 0.33 mmol) was dissolved in THF (10 mL) and water (2.5 mL), and hydrogenated over 10% palladium on carbon for 6 h. The catalyst was replaced and hydrogenation was continued for 12 h. The reaction mixture was filtered and concentrated. The residue was dissolved in water (5 mL) and stirred with Dowex 50 (H^+) (5 mL) at 50 °C for 8 h. The reaction mixture was filtered, neutralized, and concentrated to a light yellow solid, which was then purified by AG1-X8 anion exchange chromatography eluted with a linear gradient (250 mL + 250 mL, 100-300 mM) of $\text{Et}_3\text{NH}^+\text{HCO}_3^-$ (pH 7.2). Fractions containing organic phosphate were combined, passed through Dowex 50 (H^+) column, degassed, and neutralized with dilute aqueous NaOH. Removal of water under vacuum afforded the disodium salt of **70** (0.060 g, 61%) as a light yellow solid. ^1H NMR (D_2O) δ 5.01 (d, $J = 8$ Hz, 1 H), 3.78-3.86 (m, 2H), 3.74 (dd, $J = 9, 10$ Hz, 1 H), 3.63 (d, $J = 9$ Hz, 1 H), 3.33 (dd, $J = 9, 9$ Hz, 1 H). ^{13}C NMR (D_2O) δ 99.6 ($J_{\text{POCC}} = 8$ Hz), 94.4, 77.0, 74.5, 73.2, 68.8. HRMS (FAB) calcd for $\text{C}_6\text{H}_{11}\text{O}_9\text{P}$ ($\text{M}+\text{Na}^+$) 281.0038, found 281.0042.

Synthesis of L-sorbose 1-phosphate (71).

2,3;4,6-Di-O-isopropylidene-L-sorbose (77).^{98b} To a suspension of L-sorbose (10.0 g, 55.5 mmol) in dry acetone (200 mL) was added anhydrous ZnCl_2 (12 g), P_2O_5 (2 g) and concentrated H_3PO_4 (2.5 mL). The reaction was stirred at rt for 1 h, and then poured into a saturated aqueous Na_2CO_3 solution. After being filtered and partially concentrated, the mixture was extracted with ether (3x). The combined organic layers were

washed with brine (3x), dried over MgSO₄, and concentrated to a light yellow solid. Recrystallization of the crude product from cyclohexane yielded **77** as white crystals (7.6 g, 53%). ¹H NMR (CDCl₃) δ 4.49 (s, 1 H), 4.34 (d, *J* = 2 Hz, 1 H), 4.11 (ddd, *J* = 2, 2, 2 Hz, 1 H), 4.08 (d, *J* = 2 Hz, 1 H), 4.07 (d, *J* = 2 Hz, 1 H), 3.88 (d, *J* = 12 Hz, 1 H), 3.80 (d, *J* = 12 Hz, 1 H), 1.07 (br, 1 H), 1.52 (s, 3 H), 1.45 (s, 3 H), 1.39 (s, 3 H), 1.38 (s, 3 H). ¹³C NMR (CDCl₃) δ 114.3, 111.9, 97.5, 85.0, 73.3, 72.3, 63.6, 60.3, 28.9, 27.3, 26.5, 18.6.

1-Dibenzoxyphosphinoyl-2,3;4,6-di-*O*-isopropylidene-L-sorbose

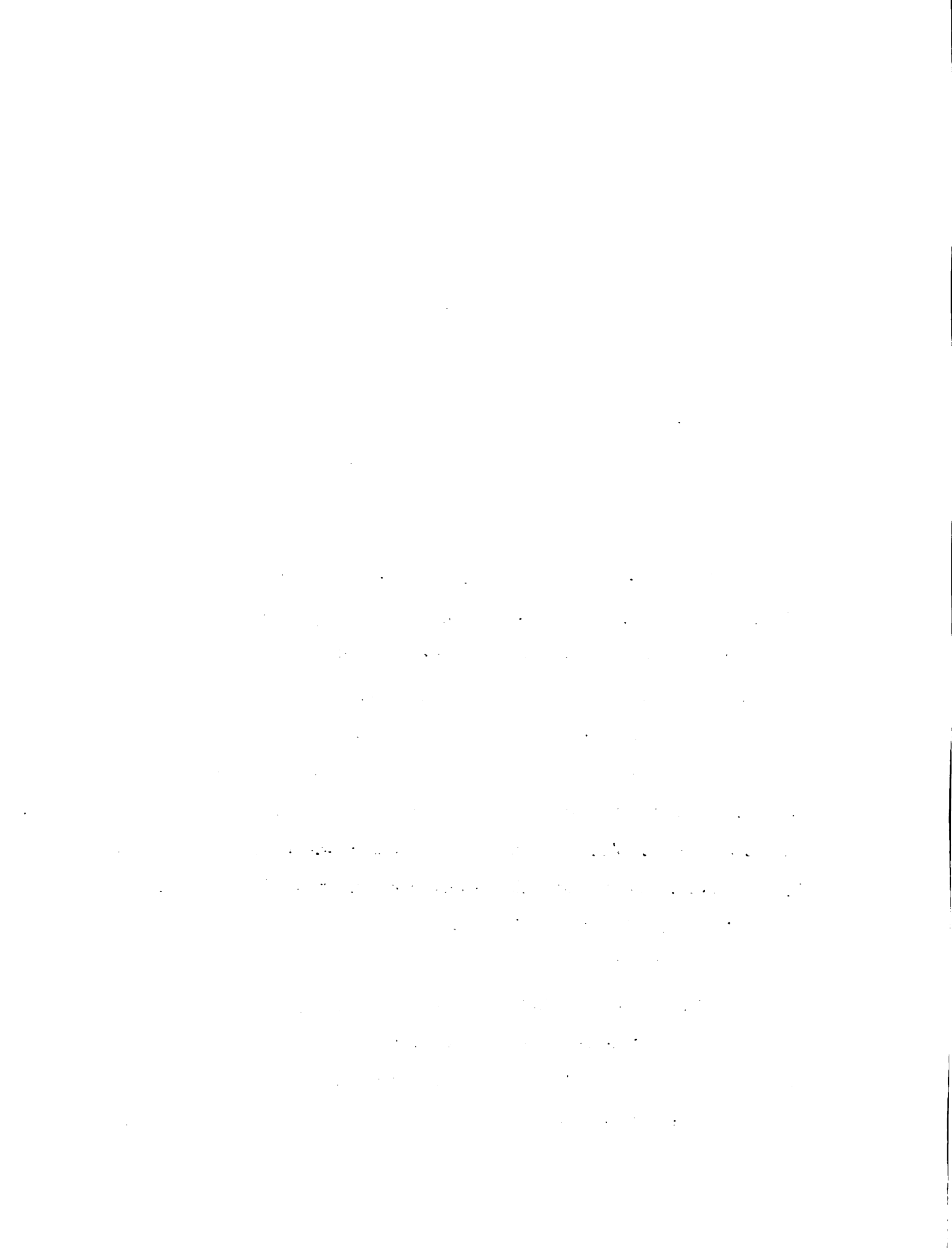
(78).^{98a} A solution of **77** (0.50 g, 1.9 mmol), tetrazole (0.27 g, 3.8 mmol) and *N,N*-diisopropyl dibenzyl phosphoramidate (0.73 g, 2.2 mmol) in CH₂Cl₂ (20 mL) was stirred at rt for 3 h. The reaction mixture was then cooled to -40 °C and a solution of *m*CPBA (0.66 g, 3.8 mmol) in CH₂Cl₂ (20 mL) was added via cannula to the cooled reaction mixture. After stirring for 20 min, the reaction mixture was washed with saturated aqueous Na₂SO₃ (2x), saturated aqueous NaHCO₃ (2x), and dried over MgSO₄. Removal of the solvent left an oil, which was purified by radial chromatography (EtOAc/hexane, 1:2, v/v, EtOAc/hexane, 2:1, v/v) to give product **78** (0.97 g, 97%) as an oil. ¹H NMR (CDCl₃) δ 7.28-7.36 (m, 10 H), 5.09 (s, 1 H), 5.08 (s, 1 H), 5.07 (s, 1H), 5.06 (s, 1 H), 4.46 (s, 1 H), 4.31 (d, *J* = 3 Hz, 1 H), 4.29 (dd, *J* = 11, 6 Hz, 1 H), 4.20 (dd, *J* = 11, 5 Hz, 1 H), 4.10 (d, *J* = 2 Hz, 1 H), 4.03 (dd, *J* = 13, 2 Hz, 1 H), 3.90 (d, *J* = 13 Hz, 1 H), 1.49 (s, 3 H), 1.40 (s, 3 H), 1.35 (s, 3 H), 1.32 (s, 3 H). ¹³C NMR (CDCl₃) δ 135.6, 135.5, 128.5, 128.3, 128.2, 127.8, 127.7, 127.6, 112.5, 112.4, 97.1, 83.9, 72.8, 72.4, 69.0 (2), 65.7, 65.8, 59.9, 28.6, 27.3, 26.2, 18.4.

L-Sorbose 1-phosphate (71). A solution of **78** (0.30 g, 0.58 mmol) in THF (10 mL) and water (2.5 mL) was subjected to hydrogenolysis over 10% palladium on carbon for 10 h. The reaction mixture was filtered and concentrated. The residue was then

redissolved in water (5 mL) and stirred with Dowex 50 (H⁺) (5 mL) at 65 °C for 16 h. After removal of the resin, the solution of crude product was neutralized with aqueous NaOH to pH 7.2, partially concentrated and purified by AG1-X8 anion exchange chromatography eluted with a linear gradient (250 mL + 250 mL, 100-300 mM) of Et₃NH⁺HCO₃⁻ (pH 7.2). Fractions containing organic phosphate were combined, passed through Dowex 50 (H⁺) column, degassed, and neutralized with dilute aqueous NaOH. Concentration under vacuum yielded the disodium salt of **71** (0.18 g, 100%) as white crystals. ¹H NMR (D₂O) δ 3.84 (dd, *J* = 11, 8 Hz, 1 H), 3.76 (dd, *J* = 11, 5 Hz, 1 H), 3.59-3.78 (m, 4 H), 3.53-3.59 (m, 1 H). ¹³C NMR (D₂O) δ 100.6 (*J*_{POCC} = 7 Hz), 76.1, 73.4, 72.2, 68.8, 64.5. HRMS (FAB) calcd for C₆H₁₃O₉P (M+Na⁺) 283.0195, found 283.0195.

Synthesis of 5-deoxy-L-sorbose 1-phosphate (**72**).

3,4-Di-O-benzyl-2-deoxy-D-arabino-hexose (79). Intermediate **31** (3.4 g, 7.8 mmol) was refluxed in THF (40 mL) and aqueous HCl (1 N, 40 mL) for 2 days. The biphasic mixture was then cooled to rt and concentrated to an oil. The crude product was kept under high vacuum overnight, and then purified by radial chromatography (EtOAc/hexane, 1:2, v/v, EtOAc) to give **79** (1.65 g, 61%) as a syrup. ¹H NMR (CDCl₃) δ 7.24-7.37 (m, 20 H), 5.33 (d, *J* = 3 Hz, 1 H), 4.95 (d, *J* = 6 Hz, 1 H), 4.91 (d, *J* = 6 Hz, 1 H), 4.58-4.79 m, 9 H), 4.06 (ddd, *J* = 11, 8, 5 Hz, 1 H), 3.94 (ddd, *J* = 11, 8, 5 Hz, 1 H), 3.60-3.88 (m, 3 H), 3.30-3.48 (m, 3 H), 2.36 (ddd, *J* = 13, 5, 2 Hz, 1 H), 2.29 (ddd, *J* = 13, 5, 3 Hz, 1 H), 1.49-1.68 (m, 2 H). ¹³C NMR (CDCl₃) δ 138.4, 138.0, 128.3 (2), 128.0 (2), 127.7, 127.6 (2), 127.5, 93.9, 61.6, 79.0, 78.6, 77.7, 76.9, 75.5, 74.8 (2), 71.6, 71.4, 71.3, 62.3, 61.8, 37.8, 35.6.



3,4-Di-*O*-benzyl-2-deoxy-D-arabino-hexitol (80). Pyranose **79** (1.65 g, 4.79 mmol) was dissolved in CH₃OH (50 mL), and NaBH₄ (1.81 g, 47.9 mmol) was added portionwise. The reaction mixture was stirred at rt for 1 h, quenched with CH₃OH-washed Dowex 50 (H⁺), and then filtered through a CH₃OH-washed Dowex 50 (H⁺) column. The filtrate was then concentrated to dryness. After azeotropic removal of boric acid with CH₃OH (3x), the residue was purified by radial chromatography to give triol **80** (1.05 g, 63%). ¹H NMR (CDCl₃) δ 7.25-7.39 (m, 10 H), 4.63 (d, *J* = 11 Hz, 1 H), 4.62 (d, *J* = 11 Hz, 1 H), 4.59 (d, *J* = 11 Hz, 1 H), 4.49 (d, *J* = 11 Hz, 1 H), 3.80-3.90 (m, 2 H), 3.61-3.81 (m, 5 H), 3.10 (b, 2 H), 1.78-2.05 (m, 2 H). ¹³C NMR (CDCl₃) δ 137.6, 137.3, 128.5, 128.4, 128.1, 128.0, 127.9, 77.0, 76.7, 73.5, 72.6, 71.5, 63.3, 59.5, 32.5.

3,4-Di-*O*-benzyl-2-deoxy-6-dibenzoxyphosphinoyl-D-arabino-hexitol (81). A suspension of triol **80** (0.078 g, 0.23 mmol) and dibutyltin oxide (0.067 g, 0.27 mmol) in CH₃OH was refluxed for 4 h. The reaction mixture was cooled to rt and concentrated to white paste. The paste was then dissolved in CH₂Cl₂ (20 mL), cooled to -40 °C (dry ice-acetonitrile bath), and a solution of tetrabenzyl pyrophosphate (0.15 g, 0.27 mmol) in CH₂Cl₂ (10 mL) was added via cannula. The reaction was then warmed to rt, stirred for 3 h, and quenched with water. The aqueous layer was separated and extracted with CH₂Cl₂. The combined organic layers were washed with brine (3x), dried over MgSO₄, and concentrated. Purification by radial chromatography (EtOAc/hexane, 2:1, v/v) afforded **81** (0.053 g, 39%). ¹H NMR (CDCl₃) δ 7.20-7.39 (m, 20 H), 5.01-5.06 (m, 4 H), 4.59 (d, *J* = 11 Hz, 1 H), 4.57 (d, *J* = 11 Hz, 1 H), 4.52 (d, *J* = 11 Hz, 1 H), 4.45 (d, *J* = 11 Hz, 1 H), 4.10-4.25 (m, 2 H), 3.95-4.01 (m, 1 H), 3.89 (ddd, *J* = 8, 5, 5 Hz, 1 H), 3.58-3.70 (m, 3 H), 1.75-1.95 (m, 2 H). ¹³C NMR (CDCl₃) δ 137.6, 137.4, 135.7, 135.6, 128.6, 128.5, 128.4 (2), 128.3, 128.1 (2), 128.0, 127.9, 76.7, 76.6, 73.5, 72.6, 70.5 (*J*_{POCC} = 7 Hz), 69.4 (*J*_{POC} = 6 Hz), 69.1 (*J*_{POC} = 6 Hz), 59.6, 32.6.

3,4-Di-*O*-benzyl-2-deoxy-6-dibenzoxyphosphinoyl-1-*O*-triphenylmethyl-*D*-arabino-hexitol (82). Diol **81** (0.29 g, 0.47 mmol) was stirred with TrCl (0.20 g, 0.70 mmol) and pyridine (0.074 g, 0.94 mmol) in CH₂Cl₂ (20 mL) at rt for 16 h. The reaction mixture was then washed with brine (3x), dried over MgSO₄, concentrated, and purified by radial chromatography (EtOAc/hexane, 1:2, v/v) to afford **82** (0.295 g, 74%). ¹H NMR (CDCl₃) δ 7.05-7.48 (m, 35 H), 5.07, (s, 1 H), 5.06 (s, 1 H), 5.04 (s, 1 H), 5.03 (s, 1 H), 4.52 (d, *J* = 11 Hz, 1 H), 4.47 (d, *J* = 11 Hz, 1 H), 4.41 (d, *J* = 11 Hz, 1 H), 4.28 (d, *J* = 11 Hz, 1 H), 4.11-4.32 (m, 2H), 3.90-4.01 (m, 2 H), 3.56 (δd, *J* = 8, 4 Hz, 1 H), 3.23 (ddd, *J* = 9, 5, 5 Hz, 1 H), 3.13 (ddd, *J* = 9, 9, 5 Hz, 1 H), 2.00-2.15 (m, 1 H), 1.77-1.90 (m, 1 H). ¹³C NMR (CDCl₃) δ 144.1, 137.6, 137.4, 135.8, 135.7, 128.6, 128.5, 128.4 (2), 128.3, 128.2, 128.1, 128.0, 127.9, 127.8, 127.7, 127.6, 126.9, 86.4, 76.3, 75.8, 73.2, 72.8, 70.6, 70.5, 69.3, 69.2, 59.7, 30.3.

5-Deoxy-3,4-di-*O*-benzyl-1-dibenzoxyphosphinoyl-6-*O*-triphenylmethyl-*L*-sorbose (83). To a suspension of **82** (0.14 g, 0.16 mmol), *N*-methylmorpholine *N*-oxide (0.038 g, 0.32 mmol), and 4 Å sieves (0.2 g) in CH₂Cl₂ (10 mL) was added tetrapropylammonium perruthenate (0.003 g, 0.008 mmol) and the reaction mixture stirred at rt for 4 h. The reaction mixture was then poured onto a short silica gel column, rinsed with CH₂Cl₂, and eluted with EtOAc. The filtrate was concentrated, and then purified by radial chromatography (EtOAc/hexane, 1:2, v/v) to yield **83** (0.098 g, 72%). ¹H NMR (CDCl₃) δ 7.06-7.54 (m, 35 H), 5.13 (s, 1H), 5.11 (s, 1 H), 5.07 (s, 1 H), 5.05 (s, 1H), 4.86 (d, *J* = 3 Hz, 1 H), 4.82 (d *J* = 4 Hz, 1 H), 4.54 (d, *J* = 12 Hz, 1 H), 4.38 (d, *J* = 11 Hz, 1H), 4.34 (d, 11 Hz, 1 H), 4.21 (d, *J* = 12 Hz, 1H), 4.04 (ddd, *J* = 6, 6, 3 Hz, 1 H), 3.85 (d, *J* = 4 Hz, 1 H), 3.05 (ddd, *J* = 9, 6, 6 Hz, 1, H), 2.93 (ddd, *J* = 9, 6, 6 Hz, 1 H), 1.86 (dd, *J* = 13, 6 Hz, 1H). ¹³C NMR (CDCl₃) δ 204.9, 204.8, 143.9, 137.4, 136.4, 135.7, 128.6, 128.5, 128.4, 128.3, 128.2, 128.1, 128.0, 127.9, 127.7, 126.9, 86.5, 84.0, 77.1, 73.8, 72.9, 70.9, 69.5, 59.3, 30.5.

5-Deoxy-L-sorbose 1-phosphate (72). Precursor **83** (0.20 g, 0.12 mmol) was dissolved in THF (8 mL) and water (2 mL), and hydrogenated over 10% palladium on carbon for 12 h. The reaction mixture was filtered through a pad of Celite, and the filtrate was concentrated. The crude product was purified with AG1-X8 anion exchange chromatography eluted with a linear gradient (250 mL + 250 mL, 100-300 mM) of $\text{Et}_3\text{NH}^+\text{HCO}_3^-$ (pH 7.2). Fractions containing organic phosphate were combined, passed through Dowex 50 (H^+) column, degassed, and neutralized with dilute aqueous NaOH. Concentration under vacuum afforded the disodium salt of **72** (0.046 g, 70%). ^1H NMR (D_2O) δ 3.65-3.94 (m, 5 H), 3.5 (d, $J = 10$ Hz, 1 H), 1.97 (dd, $J = 13, 4$ Hz, 1 H), 1.66 (dddd, $J = 13, 13, 13, 5$ Hz, 1 H). ^{13}C NMR (D_2O) δ 101.1 ($J_{\text{POCC}} = 8$ Hz), 75.3, 70.6, 69.0, 61.5, 35.6. HRMS (FAB) calcd for $\text{C}_6\text{H}_{13}\text{O}_8\text{P}$ ($\text{M}+\text{Na}^+$) 267.0246, found 267.0252.

Syntheses of (73) and 1-deoxy-1-phosphonomethyl-L-sorbitol (74).

1-Deoxy-1-(E)-dimethoxyphosphinylmethylidene-2,3;4,6-di-O-isopropylidene-L-sorbose (84). Oxalyl chloride (0.293 g, 2.31 mmol) was added to CH_2Cl_2 (20 mL) at -78 °C, and DMSO (0.225 g, 2.88 mmol) was added slowly under Ar. After 5 min, diacetone sorbose **77** (0.500 g, 1.92 mmol) in CH_2Cl_2 (20 mL) was cannulated into the reaction mixture. Triethylamine (0.388 g, 3.84 mmol) was added via a syringe 45 min later. After an additional 30 min at -78 °C, the reaction was warmed to rt and quenched with water. The reaction mixture was washed with aqueous HCl (1 N, 1x), aqueous NaHCO_3 (2x), and brine (2x). Drying and concentration afforded the aldehyde, which was dissolved in THF (20 mL), cooled to -78 °C, and directly used for the following reaction. Tetramethyl methylenediphosphonate (0.669 g, 2.88 mmol) in THF (20 mL) was cooled to -78 °C under Ar, and *n*BuLi (1.6 M, 1.80 mL, 2.88 mmol) was then added. After 30 min, the above solution of aldehyde was added via cannula. After stirring at -78

°C for 15 min and then at rt for 30 min, the reaction was diluted with ether, washed with brine (3x), dried over MgSO₄, and concentrated to an oil. Purification by radial chromatography (EtOAc/hexane, 2:1, v/v) yielded an oil, which upon standing under vacuum, gave a crystalline needle of **84** (0.42 g, 60%). ¹H NMR (CDCl₃) δ 6.83 (dd, *J* = 21, 17 Hz, 1 H), 6.36 (dd, *J* = 21, 17 Hz, 1 H), 4.33-4.35 (m, 2 H), 4.14-4.16 (m, 2 H), 4.08-4.11 (m, 2 H), 3.76 (d, *J* = 1 Hz, 3 H), 3.72 (d, *J* = 1 Hz, 3 H), 1.53 (s, 3 H), 1.44 (s, 3 H), 1.38 (s, 3 H), 1.34 (s, 3 H). ¹³C NMR (CDCl₃) δ 148.9 (*J*_{PCC} = 7 Hz), 118.5 (*J*_{PC} = 184 Hz), 112.4, 111.5 (*J*_{PCCC} = 24 Hz), 97.1, 87.4, 72.8, 59.9, 52.1, 28.5, 26.7, 25.9, 18.3. Anal. calcd for C₁₅H₂₅O₈P: C, 49.45; H, 6.92. found: C, 49.52; H, 6.88.

1-Deoxy-(E)-phosphonomethylidene-L-sorbose (73). To a solution of **84** (0.207 g, 0.544 mmol) in CH₂Cl₂ (15 mL) at 0 °C under Ar was added TMSBr (0.833 g, 5.44 mmol). The reaction was stirred for 1 h and concentrated to a light yellow paste, which was then stirred with water (5 mL) for 15 min. Dowex 50 (H⁺) (10 mL suspension in water) was added and stirred at 65 °C for 18 h. The reaction mixture was filtered, neutralized with aqueous NaOH, and purified by AG1-X8 anion exchange chromatography eluted with a linear gradient (250 mL + 250 mL, 100-300 mM) of Et₃NH⁺HCO₃⁻ (pH 7.2). Fractions containing organic phosphate were combined, passed through Dowex 50 (H⁺) column, degassed, and neutralized with dilute aqueous NaOH. Concentration under vacuum afforded **73** (0.169 g, 100%). ¹H NMR (D₂O) δ 6.35 (dd, *J* = 17, 17 Hz, 1 H), 6.21 (dd, *J* = 17, 17 Hz, 1 H), 3.66-3.77 (m, 4H), 3.36-3.40 (m, 1 H). ¹³C NMR (D₂O) δ 144.6 (*J*_{PCC} = 5 Hz), 129.3 (*J*_{PC} = 172 Hz), 99.8 (*J*_{PCCC} = 18 Hz), 76.4, 76.3, 72.2, 64.6. HRMS (FAB) calcd for C₇H₁₃O₈P (M+Na⁺) 279.0246, found 279.0250.

1-Deoxy-1-phosphonomethyl-L-sorbose (74). Intermediate **84** (0.26 g, 0.67 mmol) was dissolved in CH₃OH (10 mL), and hydrogenated over 10% palladium on

carbon for 4 h. The suspension was filtered through a pad of Celite, and the filtrate was concentrated. The residue was dissolved in CH_2Cl_2 (15 mL) at 0 °C under Ar, and TMSBr (1.0 g, 6.7 mmol) was added. The reaction was stirred for 1 h and concentrated to a light yellow paste, which was then stirred with water (5 mL) for 15 min. Dowex 50 (H^+) (10 mL suspension in water) was added and stirred at 65 °C for 12 h. The reaction mixture was filtered, neutralized with aqueous NaOH, and purified by AG1-X8 anion exchange chromatography eluted with a linear gradient (250 mL + 250 mL, 100-300 mM) of $\text{Et}_3\text{NH}^+\text{HCO}_3^-$ (pH 7.2). Fractions containing organic phosphate were combined, passed through Dowex 50 (H^+) column, degassed, and neutralized with dilute aqueous NaOH. Concentration under vacuum afforded disodium salt of **74** (0.16 g, 79%). ^1H NMR (D_2O) δ 3.55-3.80 (m, 4 H), 3.30-3.40 (m, 1 H), 1.84-2.10 (m, 2 H), 1.50-1.82 (m, 2 H). ^{13}C NMR (D_2O) δ 101.5 ($J_{\text{PCCC}} = 14$ Hz), 76.6, 76.2, 72.4, 64.5, 34.7, 24.5 ($J_{\text{PC}} = 131$ Hz). HRMS (FAB) calcd for $\text{C}_7\text{H}_{15}\text{O}_8\text{P}$ ($\text{M}+\text{Na}^+$) 281.0402, found 281.0405.

Enzymology

Purification of MIP synthase From *E. coli*

Assays

Assay solutions (2 mL) consisted of deionized, glass-distilled water containing 50 mM Tris HCl, pH 7.7, 2 mM NH_4Cl , 0.2 mM DTT, 1 mM NAD, and 5 mM D-glucose 6-phosphate. After incubation at 37 °C for 10 min, enzyme was added and aliquots (0.2 mL) were withdrawn at timed intervals (3 min) and quenched with 20% aqueous trichloroacetic acid (0.05 mL). Precipitated protein was removed by centrifugation. The quenched aliquots (0.1 mL) were incubated with aqueous NaIO_4 (0.2 M, 0.1 mL) at 37 °C for 1 h. After destroying excess NaIO_4 with aqueous Na_2SO_3 (1 M, 0.1 mL), the inorganic phosphate released was determined by the colorimetric method of Ames.⁷² Meanwhile, phosphatase activities were assayed by the same procedure except that NaIO_4 was replaced

by water. Progress curves were generated by plotting OD versus time, and linear regression analysis was performed with the computer program Kaleidagraph 2.0. The specific activity of MIP synthase preparations was calculated with the following equation:

$$\text{Specific Activity } (\mu\text{mole min}^{-1} \text{ mg}^{-1}) = \frac{\text{slope (OD min}^{-1}) \times 10^6 (\mu\text{mole mole})}{\epsilon (\text{OD L mole}^{-1})}$$

$$\times \frac{V_s (\text{mL})}{V_c (\text{mL})} \times \frac{V_a (\text{mL}) \times V_q (\text{mL})}{V_a (\text{mL})} \times \frac{V_t (\text{ml}) \times 10^{-3} (\text{L mL}^{-1})}{\rho (\text{mg mL}^{-1}) \times V_\rho (\text{mL})}$$

where:

- slope is the slope obtained from linear repression of progress curve
- ϵ is the extinction coefficient (26,000 OD L mole⁻¹),
- V_s is the volume of final visualization solution,
- V_c is the volume of aliquot taken for visualization,
- V_a is the volume of aliquot withdrawn from the assay solution,
- V_q is the volume of trichloroacetic acid used to quench the aliquot,
- V_t is the total volume of the assay solution,
- ρ is the enzyme concentration,
- V_ρ is the volume of enzyme added.

Enzyme Purification.

Cells (100 mL) were grown from a single colony of *E.coli* BL21 (DE3)/pT-7-7/MIPSYN in LB medium containing ampicillin (10 g tryptone, 5 g yeast extract, 10 g NaCl, and 75 mg ampicillin in 1 L water) at 37 °C to OD₅₅₀ = 0.5 - 0.6. Large-scale growth in LB medium containing ampicillin (9 x 1 L) were then inoculated from the starter cultures (10 mL each), and grown at 37 °C to OD₅₅₀ = 0.5 - 0.7. IPTG (0.06 g for each flask) was then added and growth was continued for 5 h. Cells were harvested by centrifugation at 6000 g and resuspended in buffer A (20 mM Tris HCl pH 7.7, 10 mM NH₄Cl, 10 mM β -mercaptoethanol, and 0.5 mM PMSF). Cell lysate was prepared by

French press disruption of the cells at 16,000 psi. After centrifugation (18,000 g, 4 °C, 25 min), the supernatant was fractionated with ammonium sulfate. The 45% - 70% fraction was dissolved in buffer A (50 mL). After dialysis against buffer A, the lysate was loaded onto a DEAE column (30 cm x 5 cm) equilibrated with buffer A and eluted with a linear gradient (1500 mL + 1500 mL, 0.01-0.25 M) of NH₄Cl in Buffer A. Fractions with MIP synthase activity were combined and concentrated (PM-10 Diaflo membranes from Amicon). The concentrate (about 5 mL) was then loaded into a Bio Gel A 0.5 size exclusion column (80 cm x 2.5 cm) and eluted with buffer A (500 mL). Fractions containing MIP synthase were combined, concentrated, and stored at -80 °C. To remove the contaminating D-glucose 6-phosphate dehydrogenase, an enzyme solution was passed through a Blue A affinity column (2 mL) and eluted with buffer A. The eluted fractions (0.5 mL) with high concentration of protein were combined and concentrated with a Centricon concentrator (from Amicon).

Enzyme Kinetics

Determination of the Association Rate Constant (k_{on}) for Inhibition of DHQ Synthase.

Assay solutions consisted of 50 mM 4-morpholinepropanesulfonate (MOPS) buffer at pH 7.5, 0.25 mM cobalt (II) chloride, 0.25 mM NAD, and 0.025 - 0.2 mM DAHP in deionized, glass-distilled water. After incubating the inhibitor with the assay solution for 10 min at 15 °C, DHQ synthase (0.2-0.4 units) was added and aliquots (0.15 mL) were removed at time intervals and quenched with 20% aqueous trichloroacetic acid (0.05 mL). Precipitated protein was removed by centrifugation. Inorganic phosphate released was quantitated by the Ames's procedure.⁷² The resulting progress curves were fitted to the equation: $OD_{820} = at - be^{-kt} + c$ where t is elapsed time, and a, b, c, k are the adjustable parameters). The association rate constant (k_{on}) was calculated from :

$$k_{on} = (k - k_{off})(1 + [S]/K_m)/([I])$$

Using $K_m = 1.8 \times 10^{-5}$ M, the calculated k_{on} values for inhibitor did not vary with substrate concentration [S] and inhibitor concentration [I].

Determination of the Dissociation Rate Constant (k_{off}) for Inhibition of DHQ Synthase.

A solution of inhibitor (3.75 - 10 μ M) and DHQ synthase (0.75 - 1.2 μ M) in a buffer, containing 50 mM MOPS, pH 7.5, 0.25 mM cobalt (II) chloride, and 0.25 mM NAD, was incubated at 15 °C for 30 min. An aliquot (40 μ L) of the solution was then added to a solution of DAHP (0.7 mM, 4 mL) in the same buffer at 15 °C. The progress of the reaction was followed by the amount of phosphate released as above. The resulting progress curves were fitted to a equation: $OD_{820} = at + be^{-kt} + c$. where k obtained equals to k_{off} . The calculated k_{off} values for a the inhibitor did not vary with enzyme or inhibitor concentrations.

Determination of the Inhibition Constant (K_i) of MIP Synthase.

Determination of K_i employed Hanes-Woolf analysis of enzyme velocities obtained from assays with varying concentrations (0.4, 0.8, 1.2, 1.6, 2.0 mM) of D-glucose 6-phosphate and varying concentrations (0 - 1 mM) of inhibitor. After incubation of substrate and inhibitor in assay buffer (50 mM Tris HCl pH 7.7, 2 mM NH_4Cl , 0.2 mM DTT) at 37 °C for 10 min, MIP synthase (0.01-0.02 units) was added and aliquots were withdrawn at timed intervals over a 30 min period. The enzyme activities were determined as described earlier. Velocities of reactions were obtained from linear regression of the resulting progress curves. Plots of [S]/V versus [S] (Hanes-Woolf plot) gave [S]/V intercepts of K_{mapp}/V_{max} . Replot of K_{mapp}/V_{max} versus [I] gave an [I] intercept that equal to $-K_i$.

Determination of MIP Synthase-Bound NADH in the Presence of Substrate or Substrate Analogues.

A solution of MIP synthase (15 μM , 0.7 mL) in a buffer containing 25 mM Tris HCl, pH 7.2, 2 mM NH_4Cl , 0.2 mM DTT, and 1 mM NAD was placed in a quartz cuvette and kept at 25 °C for 10 min. The enzyme solution was then scanned to set the baseline absorbance. A small aliquot of a substrate or substrate analogue solution was added and mixed to make the final concentration to 1 mM. Scans were made at timed intervals until there was no further changes in absorbance. Absorbances at 340 nm were then read from the spectra and plotted versus time.

BIBLIOGRAPHY

BIBLIOGRAPHY

- 1 Frey, P. A. In *Pyridine Nucleotide Coenzymes*; Wiley: New York, 1987; part B, Chapter 13.
- 2 (a) Haslam, E. *The Shikimate Pathway*; John Wiley and Sons: New York, 1974. (b) Weirs, U.; Edwards, J. M. *The Biosynthesis of Aromatic Compounds*; Wiley-Interscience: New York, 1980. (c) Ganem, B. *Tetrahedron* **1978**, *34*, 3353.
- 3 (a) LaRossa, R. A.; Falco, S. C. *Trends Biotech.* **1984**, *2*, 158. (b) Hardy, R. W. F.; Giaquinta, R. T. *Bioassays* **1984**, *2*, 152. (c) *Synthesis and Chemistry of Agrochemicals*; Baker, D. R.; Fenyves, J. G.; Moberg, W. K.; Cross, B., Eds.; American Chemical Society: Washington, D. C. 1987; p 1-8. (d) Kishore, G. M.; Shah, D. M. *Ann. Rev. Biochem.* **1988**, *57*, 627. (e) Shaner, D. L. In *Plant Nitrogen Metabolism*; Poulton, J. E.; Romeo, J. T.; Conn, E. E., Eds.; Plenum: New York, 1989: Chapter 7.
- 4 (a) Grossbard, E.; Alkinson, D., Eds.; *The Herbicide Glyphosate*; Butterworths: Boston, 1985. Devine, M. E.; Duke, S. O.; Fedlke, C. F. In *Physiology of Herbicide Action*; Prentice Hall: New Jersey, 1993; Chapter 13.
- 5 (a) Srinivasan, P. R.; Rotchschild, J.; Sprinson, D. B. *J. Biol. Chem.* **1963**, *138*, 3176. (b) Rotenberg, S. L.; Sprinson, D. B. *J. Biol. Chem.* **1978**, *253*, 2210.
- 6 (a) Frost, J. W.; Knowles, J. R. *Biochemistry* **1984**, *23*, 4465. (b) Frost, J. W.; Bender, J. L.; Kadonaga, J. T.; Knowles, J. R. *Biochemistry* **1984**, *23*, 4470.
- 7 (a) Bender, S. L.; Mehdi, S.; Knowles, J. R. *Biochemistry* **1989**, *28*, 7555. (b) Bender, S. L.; Willanski, T.; Knowles, J. R. *Biochemistry* **1989**, *28*, 7560. (c) Willanski, T.; Bender, S. L.; Knowles, J. R. *Biochemistry* **1989**, *28*, 7572. (d) Knowles, J. R. *Aldrichim. Acta* **1989**, *22*, 59.
- 8 Rotenberg, S. L.; Sprinson, D. B. *J. Biol. Chem.* **1978**, *253*, 2210.
- 9 Adlersberg, M.; Sprinson, D. B. *Biochemistry* **1964**, *3*, 1855.
- 10 Maitra, V. S.; Sprinson, D. B. *J. Biol. Chem.* **1978**, *253*, 5426.
- 11 Willanski, T.; Bender, S. L.; Knowles, J. R. *J. Am. Chem. Soc.* **1987**, *109*, 1873.
- 12 (a) Bartlett, P. A.; Satake, K. *J. Am. Chem. Soc.* **1988**, *110*, 1628. (b) Bartlett, P. A.; McLaren, K. L.; Alberg, D. G.; Fassler, A.; Nyfeler, R.; Lauhon, C. T.; Grissom, C. B. *BCPC monogr.* **1989**, *2*, 155. (c) Bartlett, P. A.; McLaren, K. L.; Marx, M. A. *J. Org. Chem.* **1994**, *59*, 2082.

- 13 Willanski, T.; Bender, S. L.; Knowles, J. R. *J. Am. Chem. Soc.* **1989**, *111*, 2299.
- 14 Pieler, L. T.; Montchamp, J.-L.; Frost, J. W.; Manly, C. J. *Tetrahedron* **1991**, *47*, 2423. (b) Montchamp, J.-L.; Pieler, L. T.; Frost, J. W. *J. Am. Chem. Soc.* **1992**, *114*, 4453.
- 15 (a) Morgan, N. G. *Cell Signalling*; Openg University Press: Mitlon Keynes, 1989. (b) Billington, D. C. *The Inositol phosphates*; VCH: New York, 1993. (c) Potter, B. V. L.; Lampe, D. *Angew. Chem. Int. Ed. Engl.* **1995**, *34*, 1993. (d) Findley, J. *Chemistry in Britain* **1991**, 724.
- 16 (a) Berridge, M. J. *Biochem. J.* **1984**, *220*, 345. (b) Berridge, M. J.; Irvine, R. F. *Nature* **1984**, *312*, 315. (c) Berridge, M. J. *Ann. Rev. Biochem.* **1987**, *56*, 159. (d) Mato, J. M. *Phospholipid Metabolism in Cellular Signalling*; CRC: Boca Raton, 1990. (e) *Inositol Phosphates and Derivatives*; Reitz, A. B., Ed.; ACS Symposium Series 263; American Chemical Society: Washington, D. C. 1991.
- 17 (a) Margolis, R. V.; Press, R.; Altsuler, N.; Stewart, M. A. *Brain Res.* **1971**, *28*, 535. (b) Sherman, W. R. In *Inositol Lipids in Cell Signalling*; Michell, R. H.; Drummond, A. H.; Downes, C. P., Eds.; Academic: New York, 1989, p 39.
- 18 (a) Atack, J. R.; Brouton, H. B.; Pollack, S. J. *TINS*, **1995**, *18(8)*, 343. (b) Drummond, A. H. *Trends Pharm. Sci.* **1987**, *8*, 129.
- 19 (a) Hallcher, L. M.; Sherman, W. R. *J. Biol. Chem.* **1980**, *155*, 10896. (b) Shute, J. K.; Baker, R.; Billington, D. V.; Gani, D. *J. Chem. Soc., Chem. Commun.* **1988**, 626.
- 20 (a) Loewus, F. A.; Loewus, M. W. *Ann. Rev. Plant Physiol.* **1983**, *34*, 137. (b) Wong, Y.-H. H.; Sherman, W. R. *J. Biol. Chem.* **1985**, *260*, 11083.
- 21 Charlampous, F. C.; Chen, I.-W. *Methods Enzymol.* **1966**, *9*, 698.
- 22 Donahue, T. F.; Henry, S. A. *J. Biol. Chem.* **1981**, *256*, 7077.
- 23 Maeda, T.; Eisenberg, F. Jr. *J. Biol. Chem.* **1980**, *255*, 8458.
- 24 Mauck, L. A.; Wong, Y.-H.; Sherman, W. R. *Biochemistry* **1980**, *19*, 3622.
- 25 Naccarata, W. F.; Ray, R. E.; Wells, W. W. *Arch. Biochem. Biophys.* **1974**, *164*, 194.
- 26 (a) Pittner, F.; Fried, W.; Hoffmann-Ostenhof, O. *Hoppe-Seyler's Z. Physiol. Chem.* **1974**, *355*, 222. (b) Pittner, F.; Hoffmann-Ostenhof, O. *Monatsh. Chem.* **1976**, *107*, 793.
- 27 Barnett, J. E. G.; Corina, D. L. *Biochem. J.* **1968**, *108*, 125.
- 28 Escamilla, J. E.; Contreras, M.; Martinez, A.; Zentella-Pina, M. *Arch. Biochem. Biophys.* **1982**, *218*, 275.
- 29 Pittner, F.; Torarora, I. I.; Kornitskaya, E. Y.; Khoklor, A. S.; Hoffmann-Ostenhof, O. *Mol. Cell Biochem.* **1979**, *25*, 43.